

N 7 1 - 3 5 0 3 4

N 7 1 - 3 5 0 5 1

NASA TECHNICAL  
MEMORANDUM

NASA TM X-58063  
Volume II

NASA TM X-58063  
Volume II

CALL FILE  
COPY

PROCEEDINGS OF THE SPACE SHUTTLE INTEGRATED  
ELECTRONICS CONFERENCE

NASA Manned Spacecraft Center  
Houston, Texas  
May 11-13, 1971

1. Report No. <b>TM X-58063 - Volume II</b>	2. Government Accession No.	3. Recipient's Catalog No.	
4. Title and Subtitle <b>PROCEEDINGS OF THE SPACE SHUTTLE INTEGRATED ELECTRONICS CONFERENCE</b>		5. Report Date	
		6. Performing Organization Code	
7. Author(s)		8. Performing Organization Report No.	
		10. Work Unit No.	
9. Performing Organization Name and Address		11. Contract or Grant No.	
		13. Type of Report and Period Covered <b>Technical Memorandum</b>	
12. Sponsoring Agency Name and Address <b>National Aeronautics and Space Administration Washington, D. C. 20546</b>		14. Sponsoring Agency Code	
		15. Supplementary Notes <b>Held at the NASA Manned Spacecraft Center, May 11-13, 1971</b>	
16. Abstract  <p>The symposium encompassed five specific categories within the general category of space shuttle integrated electronics. The five categories are published in three volumes as follows:</p> <p>Volume I - Electronics Overview and Guidance, Navigation, and Control  II - Instrumentation and Power Distribution and Communications  III - Data Systems</p>			
17. Key Words (Suggested by Author(s))		18. Distribution Statement  <b>Unclassified - unlimited</b>	
19. Security Classif. (of this report) <b>Unclassified</b>	20. Security Classif. (of this page) <b>Unclassified</b>	21. No. of Pages <b>375</b>	22. Price*

## FOREWORD

As a follow-up of the Space Transportation System Technology Symposium held at the NASA-Lewis Research Center, Cleveland, Ohio, July 15-17, 1970, a series of discipline-oriented conferences was planned, with the Office of Advanced Research and Technology/Office of Manned Space Flight (OART/OMSF) Space Shuttle Integrated Electronics Technology Conference being held at the NASA Manned Spacecraft Center, Houston, Texas, May 11-13, 1971. The Conference goal was to present a timely review of the status of Space Shuttle technology in the major areas of electronics and power systems for the benefit of the industry, Government, university, and foreign participants considered to be contributors to the program. In addition, the Conference offered an opportunity to identify the responsible individuals already engaged in the program. The Conference sessions were intended to confront each presenter with his technical peers as listeners, and this was substantially accomplished.

Because of the high interest in the material presented, it is being published essentially as it was presented, utilizing mainly the illustrations used by the presenters along with brief words of explanation. The document is unclassified, and each of the authors has determined that his paper can be published in this manner. This publication is aimed at revealing the substance and significance of the work in this manner now, rather than in a more refined form much later.

# CONTENTS

Page

## INSTRUMENTATION AND POWER DISTRIBUTION

### AIR DATA SENSING FOR SPACE SHUTTLE

- Delroy J. Sowada, Frederick A. Moynihan, and Ronald G. Bailey,  
Honeywell Incorporated; and Alex Hafner, NASA-Marshall Space Flight  
Center . . . . . 3

### ZERO-G PROPELLANT GAUGING OF CRYOGENICS

- R. G. Morrison, TRW Systems Group . . . . . 37

### ZERO-G RADIO FREQUENCY GAGING SYSTEM FOR SPACE SHUTTLE PROPELLANT TANKS

- H. E. Thompson, NASA-Marshall Space Flight Center; and N. E. Stanley,  
B. J. Shebler, and W. Ott, Bendix Corporation . . . . . 53

### SHUTTLE SENSORS

- Vernon C. Melliff, Jr., Manned Spacecraft Center; and Arthur T. Linton,  
The Boeing Company . . . . . 73

### SOLID STATE POWER CONTROLLERS

- Jack C. Boykin and William C. Stagg, Manned Spacecraft Center; and  
Donald E. Williams, Marshall Space Flight Center . . . . . 105

### AN AUTOMATIC ELECTRICAL DISTRIBUTION SYSTEM

- Dr. M. A. Geyer, Westinghouse Electric Corporation . . . . . 133

### SPACE SHUTTLE CONNECTOR DEVELOPMENT

- B. J. McPeak and W. J. Shockley, NASA-Marshall Space Flight  
Center . . . . . 143

### SPACE SHUTTLE ELECTRIC POWER DISTRIBUTION CONSIDERATIONS

- J. L. Welch, NASA-Marshall Space Flight Center . . . . . 177

### A SOLUTION FOR THE SPACE SHUTTLE HIGH TEMPERATURE ANTENNA PROBLEM

- E. A. Kuhlman, McDonnell-Douglas Corporation . . . . . 185

### ANTENNA TECHNOLOGY — MATERIALS FOR ANTENNA PROTECTIVE COATINGS

- M. C. Gilreath, NASA-Langley Research Center . . . . . 203

### ANTENNA TECHNOLOGY — ANTENNA DESIGN AND SCALE MODEL TECHNIQUES

- W. F. Crowell, NASA-Langley Research Center . . . . . 223

	Page
<b>AUTOMATIC ANTENNA SWITCHING TECHNIQUES</b>	
H. Dean Cubley, Manned Spacecraft Center . . . . .	243
<b>SPACECRAFT INTEGRATED PARAMETRIC AMPLIFIER DEVELOPMENT</b>	
P. H. Dalle Mura, NASA-Goddard Space Flight Center . . . . .	279
<b>LOW-RATE COMMUNICATIONS UTILIZING DIGITAL CODING AND MODULATION</b>	
B. H. Batson, C. K. Land, and R. W. Moorehead, Manned Spacecraft Center . . . . .	291
<b>COMPRESSION AND ERROR CORRECTION FOR TV</b>	
R. B. Blizard, W. A. Stevens, J. L. McKinney, H. M. Gates, W. B. Anthony, D. L. Manion, and C. C. Korgel, Martin Marietta . . . .	311
<b>INTEGRATION OF RF FUNCTIONS FOR NAVIGATION, VOICE AND DATA COMMUNICATION</b>	
T. S. Bettwy, TRW Systems Group . . . . .	329
<b>MICROWAVE TRAVELING WAVE TUBE AMPLIFIERS FOR SPACE COMMUNICATIONS SYSTEMS</b>	
Bruce M. Kendall, NASA-Langley Research Center . . . . .	363

**INSTRUMENTATION AND POWER DISTRIBUTION**

AIR DATA SENSING FOR SPACE SHUTTLE

Delroy J. Sowada, Frederick A. Moynihan, and Ronald G. Bailey  
Honeywell Inc.  
St. Paul, Minnesota

and

Alex Hafner  
NASA-Marshall Space Flight Center  
Huntsville, Alabama

## FOREWORD

The presentation provides interim results of work by the authors on Contract NAS 8-26326 since August 1970. Monitoring and direction were provided by Alex Hafner, John Hamlet, and Tom Marshall of NASA-MSFC, Huntsville.

Acknowledgment is given for numerous helpful contacts with personnel at NASA, North American Rockwell, McDonnell Douglas, General Dynamics/Convair, and Honeywell. Also, many sources in the literature were drawn upon.

## AUTHORS' INTRODUCTION

Under direction of K. E. Floren, Project Engineer, the Honeywell authors provided the following functions under the contract NAS 8-26326.

D. J. Sowada - System Integration and Analysis  
F. A. Moynihan - Aerodynamics and Sensor Design  
R. G. Bailey - Installation Design and System Definition

Alex Hafner was primary NASA Monitor, leading the design reviews.

## PRESENT STATUS

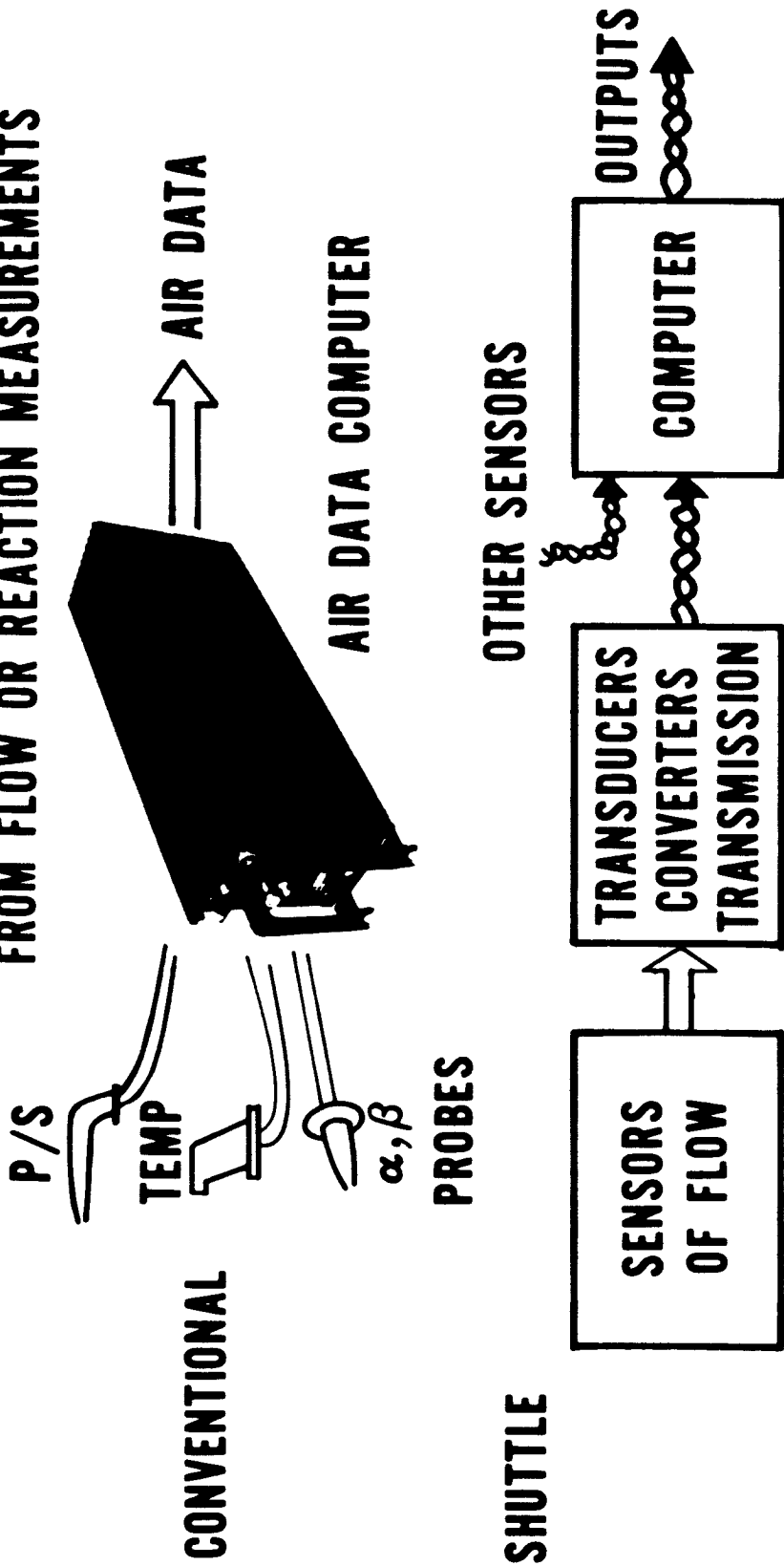
Currently proceeding to a refined mechanization of the selected sphere nose sensor plus pitot/static probe concept in terms of sensor installation on current Shuttle vehicles, selection among available pressure transducers, assessment of expected performance, and detailing of associated electronics units.

## ABSTRACT

This Technology Study Report describes the feasible and useful air data sensing alternatives in terms of potential uses, practical mechanization, and primary impact related to the current configuration of the Space Shuttle vehicle and avionics. Recommendations are made to provide a baseline air data measurement (ADM) system for integration into the Shuttle vehicles. The state-of-the-art feasibility of the recommended system is substantiated by flight experience, wind tunnel tests, and simulation studies.



# AIR DATA: ATMOSPHERIC FLIGHT PARAMETERS FROM FLOW OR REACTION MEASUREMENTS



## MEASUREMENTS

- CALIBRATION
- AIR DATA CONVERSION
- BLENDING
- USE OF AIR DATA

## ATMOSPHERIC FLIGHT PHASES

The listed flight phases are those when flying through the sensible atmosphere. Needs are those functions essential to vehicle piloting and guidance, navigation, and control. For convenience, these can be divided into subsonic flight and re-entry/transition flight, combining later return and ferry phases.

The boost phase is short, timewise, and determined by guidance and control, rather than air data sensing. Special pressure sensing could be employed to alleviate loads; however, the special nature is best handled by integration with the special problem rather than the ADM system.

Subsonic and re-entry flight operation determine needs of the air data kind.

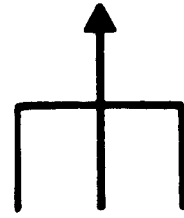
# ATMOSPHERIC FLIGHT PHASES

COMBINED BOOST

BOOSTER RETURN

ORBITER RETURN

ABORT RETURN



(RE-ENTRY TRANSITION CRUISE  
OR GLIDE LANDING)

ORBITER FERRY



(TAKEOFF, CLIMB, SUBSONIC  
CRUISE, DESCENT, LANDING)

## AIR DATA NEEDS

Thanks to many, after several iterations of what's needed?, what can be provided?, what's already aboard?, is it really needed?, etc., the listed needs survived the test of being essential. In the following list:

1, 3, and 5 are parameters that can be provided only by air data means; the need for near zero sideslip control during later phases of re-entry is critical for vehicle survival. Winds cause inertial navigation system (INS) determination of airspeed and flow direction to have serious error at the slower speeds.

2 and 9, altitude data, are useful for INS divergence clamping and for altimetry needs during subsonic flight; non-air-data sensing methods are possible.

∞

6 and 8 provide for better guidance and control performance, if obtained by air data means.

The critical boost-loading problem (4) is solved better by non-air data means; direct monitoring of skin temperatures (7) is an intimate part of thermal protection system design, not air data. Skin temperature sensing has been pursued (e.g., ASSET program) as a form of air data sensing; these concepts need further development not consistent with 1972 technology base goal.

Can these needs be satisfied?

## AIR DATA NEEDS

### SUBSONIC FLIGHT

- \* 1. AIRSPEED (OR MACH)
- 2. PRESSURE ALTITUDE
- \* 3.  $\alpha$  &  $\beta$
- \*\* 4. HI-Q BOOST LOADING

### RE-ENTRY & TRANSITION

- \* 5. SIDESLIP STABILIZATION
- 6.  $\alpha$  REFERENCE
- \*\* 7. CRITICAL SKIN TEMP'S.
- 8. FLIGHT INTENSITY (q)
- 9. ALTITUDE REFERENCE

\* MUST BE AIR DATA ..... FOR SURVIVAL

\*\* NON-ADM

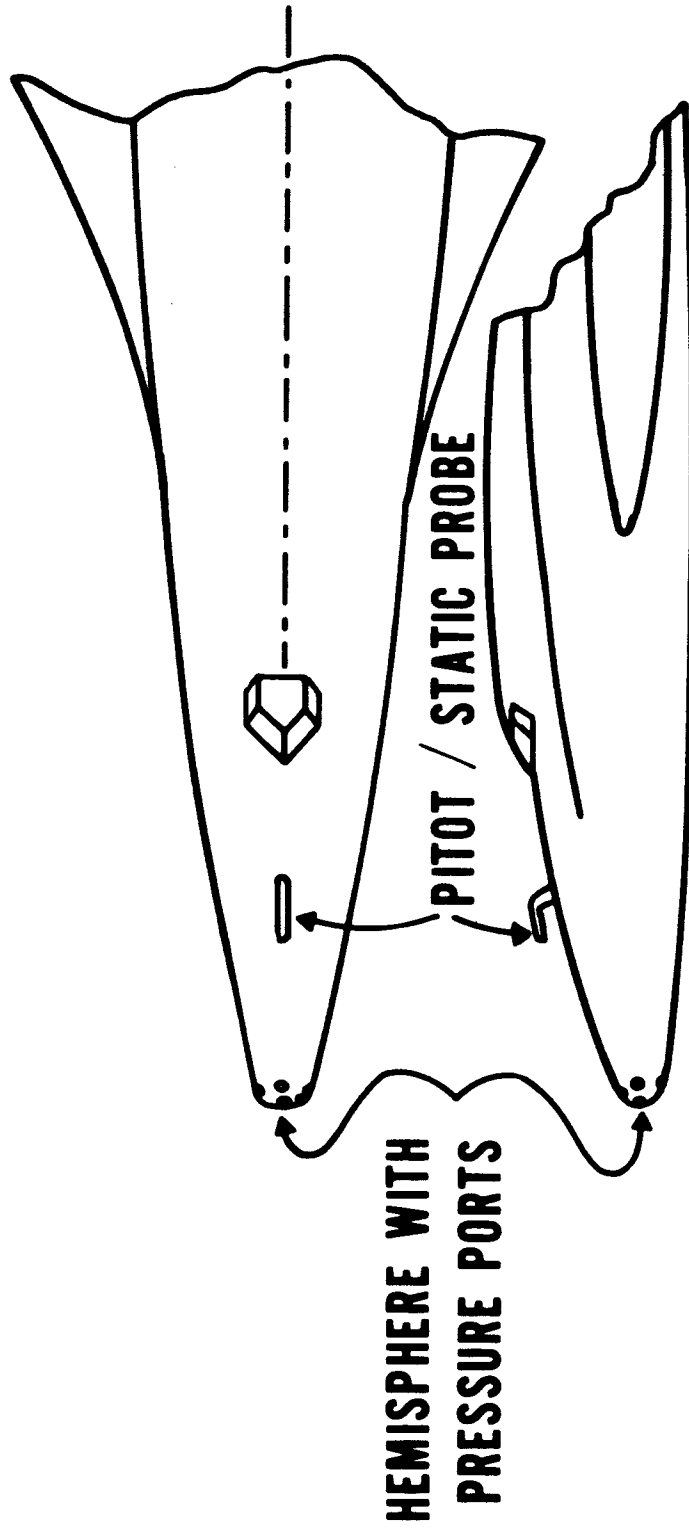
### CONCEPTUAL SKETCH OF ADM SENSORS

The solution consists of a spherical nose with small pressure ports and a conventional subsonic pitot/static probe mounted permanently at a cool place on the vehicle.

Measurement of  $\alpha$  and  $\beta$  by pressure ports on a sphere is an established technique but with movable spheres and only over a limited Mach number range. The Space Shuttle requirement of a large  $\alpha$  range, along with use over a large Mach number range, from re-entry to landing, using a fixed sphere was shown to be possible. The spherical nose shape is more compatible with structure and heating problems than, for example, a nose boom.  $\alpha$  and  $\beta$  can be determined, independent of Mach number and altitude, using a sphere.

The conventional pitot/static tube is for subsonic flight and landing where it would provide better accuracy of air-speed and pressure altitude than possible with the nose taps. Without vehicle shock waves, the subsonic probe can be mounted away from the nose area.

# CONCEPTUAL SKETCH OF ADM SENSORS



## ADM FUNCTIONS

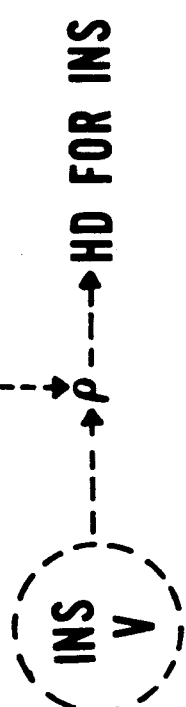
Differential pressures from port pairs on the nose provide means to determine sideslip,  $\beta$ , and angle of attack,  $\alpha$ , for all speeds after dynamic pressure,  $q$ , exceeds 15 PSF or 720 newtons/m<sup>2</sup> (near the point where sensible decelerations are evident in re-entry).

Addition of an absolute pressure measurement enables determination of stagnation pressure. At the higher speeds ( $M > 2$ ), simple correlation provides dynamic pressure,  $q$ , for control scheduling. In turn, INS velocity can be used to determine ambient air density,  $\rho$ , which allows determination of density altitude for INS vertical channel clamping.

At subsonic speeds, the P/S probe enables the conventional determination of pressure altitude and forms of air-speed. The clamped, vertical INS channel is the best source of vertical speed.



# ADM FUNCTIONS

<u>MEASUREMENTS</u>	<u>OUTPUTS</u>	<u>CONDITION</u>
SPHERE NOSE	$\beta$ - SIDESLIP $\alpha$ - ANG. OF ATT.	$q > 15$ PSF ALL SPEEDS
PORT PRESSURES	$P_{t2}$ - STAG. PRESS.	$q > 15$ PSF $M > 2$
STATIC PRESSURE	$q$ - DYN. PRESS.	
TOTAL OR IMPACT PRESSURE		SUBSONIC
P/S PROBE	$H_p \rightarrow INS \rightarrow \dot{H}$	

## FEATURES OF APPROACH

The approach is very attractive. Using flight proven concepts, clamping and blending improve the INS approach. The vehicle's thermal protection, structural, and aerodynamic characteristics are unchanged (compare with supersonic boom ahead of nose). Without deployment mechanisms, the approach is simple, reliable, and available throughout flight. Zero pressures of outer space provide opportunity for transducer offset calibration. With redundancy to survive in-flight failures, failure isolation is easy. The concept allows degraded gain, but good-null sideslip sensing backup, and needs no between-flight refurbishing.

Of course, it provides the necessary functions.

The spherical concept has flown on the X-15, Apollo, and various small probes. Currently produced transducers satisfy accuracy needs. The extension to entry usage has been shown on basis of analyses and wind tunnel tests over the past 10 years.

## **FEATURES OF APPROACH**

- **USES FLIGHT-PROVEN ELEMENTS**
- **AUGMENTS ON-BOARD INS AUTONOMY**
- **MINIMUM VEHICLE COMPROMISE**  
(THERMAL PROTECTION, STRUCTURAL, AERODYNAMIC)
- **AVAILABLE DURING ENTIRE FLIGHT**
- **CALIBRATION, FAILURE ISOLATION, & BACKUP OPTIONS**
- **NO MOVING PARTS - SIMPLE, RELIABLE**
- **NO BETWEEN-FLIGHT REFURBISHING**
- **PROVIDES NECESSARY FUNCTIONS**

### BASIC AND REDUNDANT CONFIGURATIONS

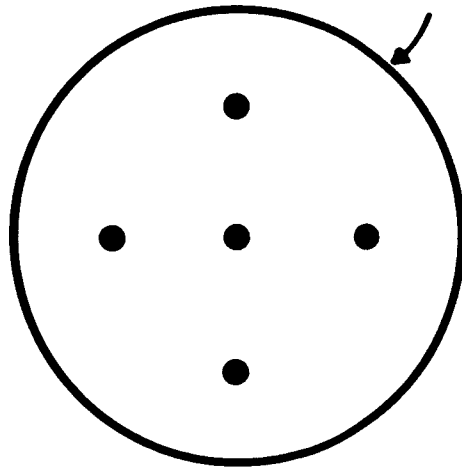
With five holes in the spherical nose, three differential transducers, and one absolute transducer,  $\alpha$ ,  $\beta$ , and  $P_{t2}$  are determined. By adding holes and transducers, the measurements are made redundant. With 13 holes and three identical sets of transducers, triple redundancy is provided. Accuracy is improved by scheduling the best of the redundant sets as function of angle of attack.

The pitot/static tube with transducer pair is made redundant with multiple transducer sets and multiple tubes.

After detailed vehicle installation, the failure probabilities (of blockage, line breakage, transducer failures, and electronic failures) together with means to avoid single-point failures and maintain identical transducer/electronics assemblies will need analysis to arrive at the best redundant configuration. The possibility of backup sideslip control sensing should allow less than full 3-channel redundancy.

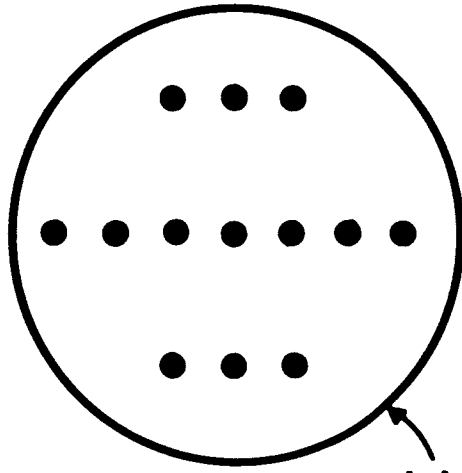
# CONFIGURATIONS

ESSENTIAL



5 TAPS

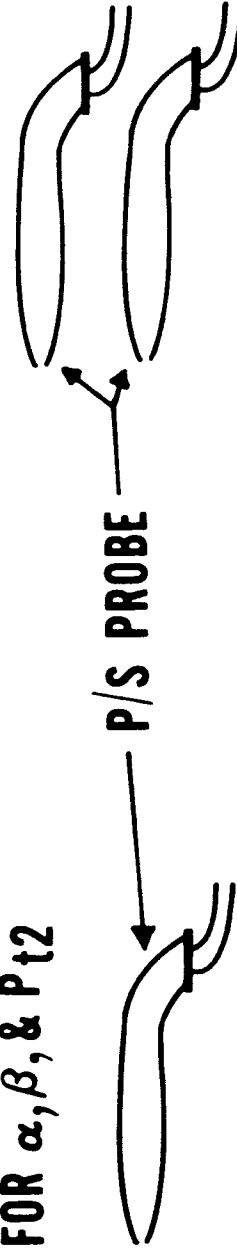
REDUNDANT



13 TAPS

HEMISPHERE NOSE  
(FRONT VIEW)

FOR  $\alpha$ ,  $\beta$ , & P t2



ALTITUDE/VELOCITY TRAJECTORIES (RE-ENTRY)

Now that we have reviewed the ADM measurement concept, let us take a closer look at how it is integrated into the Shuttle vehicle and avionics. First we consider integration of ADM and INS for performance benefit; then the added ADM hardware will be reviewed; finally the computational aspect will be reviewed.

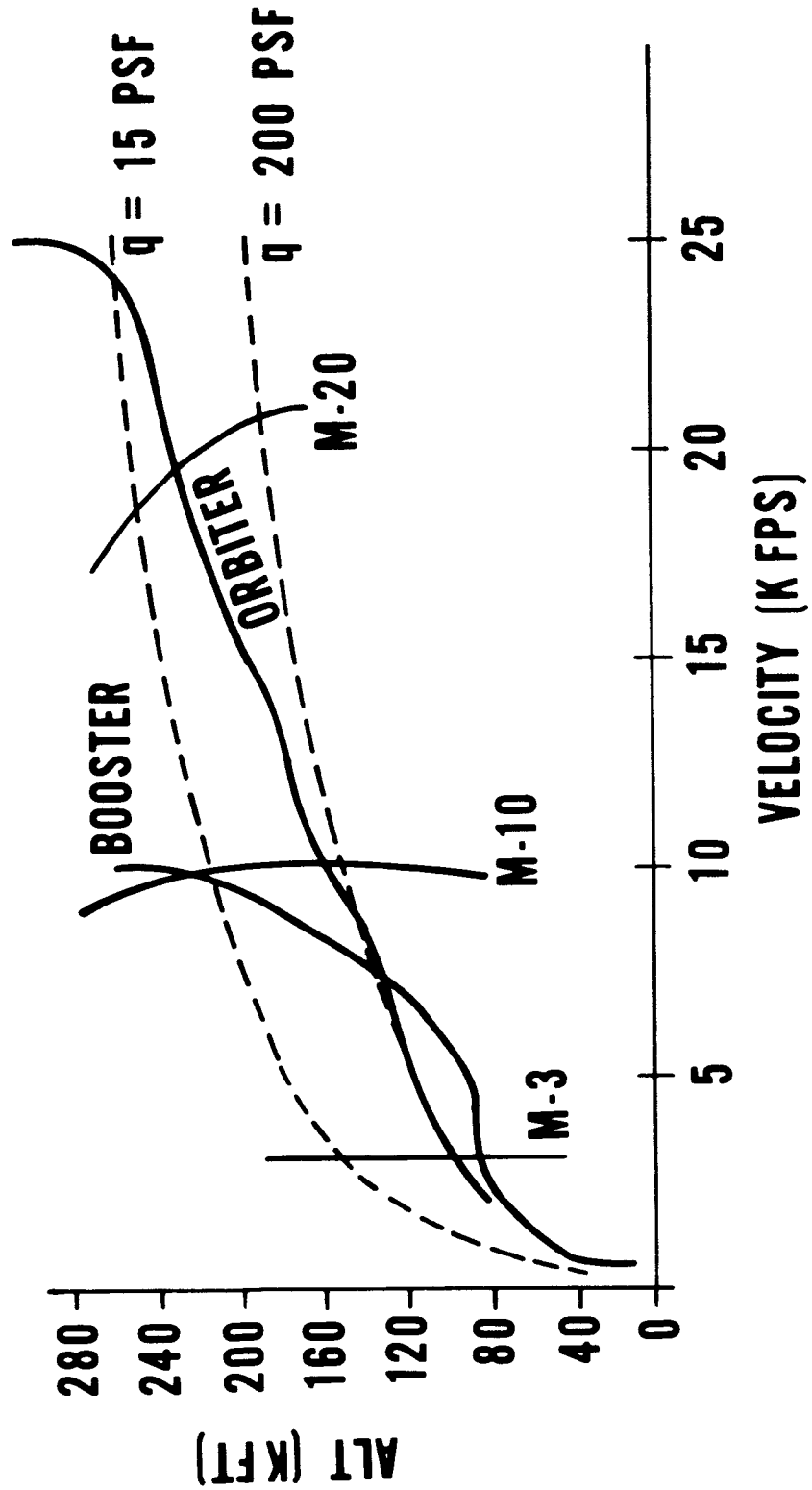
Notice that significant decelerations occur near the  $q = 15 \text{ PSF}$  or  $720 \text{ newtons/m}^2$  curve and that dynamic pressure,  $q$ , varies primarily with altitude at high speeds. Once decelerations are underway, dynamic pressure grows significantly higher than  $15 \text{ PSF}$ .

In brief, the INS will be shown to have significant increase in derived-air-data-parameter errors as speed decreases, during descent, because the INS cannot measure wind. On the other hand, the ADM becomes more sensitive as dynamic pressure increases. With such complementing of characteristics, blending is the obvious conclusion.

For International units:

KFT	40	80	120	160	200	240	280
KM	12	24	36.5	49	61	73	85
KFPS	5	10	15	20	25		
KMPS	1.5	3	4.6	6.1	7.6		
PSF	15	200					
Newtons/m <sup>2</sup>	720	9576					

# ALTITUDE/VELOCITY TRAJECTORIES (RE-ENTRY)



WINDS

The following slide merely references wind magnitudes (mean and maximum) at various altitudes used in deriving data on the next slide. The expected mean winds above 30K feet are large.

Converted into International units:

Altitude (Meters)	Mean (MPS)	Maximum (MPS)
6K	24	38
9K - 14K	90	128
30K - 79K	73	104

Reference: Handbook of Geophysics, Revised Edition - 1960  
United States Air Force  
Air Research and Development Command  
Air Force Research Division  
Geophysics Research Directorate



# WINDS

**MEAN  
(FPS)**

**MAX  
(FPS)**

**ALTITUDE  
(FEET)**

80	125
300	420
240	340

**20K**

**30-45K**

**100-260K**

### INS WIND ERRORS

Without vertical clamping, errors would be larger at the transition point, about the same early in entry, and gross in subsonic flight. Thus, clamping should start during entry.

Early in entry, the INS provides the best available measurements; at transition, sideslip error becomes intolerable. For subsonic flight, INS measurement of air data parameters is not meaningful.

At transition, the altitude is about 100K feet or 30 KM, while the velocity is about 4 KFPS or 1.2 KMPS. The mean wind of 240 FPS or 73 MPS is about 6 percent of the vehicle velocity while the maximum wind is 8.5 percent of the velocity. If winds were from the side, either an  $\alpha$  or  $\beta$  error, depending on bank angle, of 60 milliradians (mean wind) or 85 milliradians (maximum wind) would be caused. These angles correspond to  $3.4^\circ$  to  $4.9^\circ$ .

The values on the following slide are thus possible error magnitudes, including INS and mean wind errors.

With some manipulation of random-direction probabilities, these errors at transition could be converted to smaller probable errors that in turn justify another ADM solution. A supersonic/subsonic probe with pitot/static,  $\alpha$ , and  $\beta$  capability could be deployed at transition and be used through landing.

# INS WIND ERRORS (VERTICAL CLAMPED)

PARAMETER	SUBSONIC	TRANSITION	EARLY BOOSTER ENTRY	EARLY ORBITER ENTRY
H < 45K FT V < 1K FPS	H ≅ 100K FT V = 4K FPS	H = 200K FT V = 10K FPS	H = 250K FT V = 25K FPS	
$\alpha/\beta$	5-20°	4°	1°	0.4°
RELATIVE WIND	10-30%	7.5%	2%	<1%

### ERROR CHARACTERISTICS OF SPHERE/NOSE SENSOR

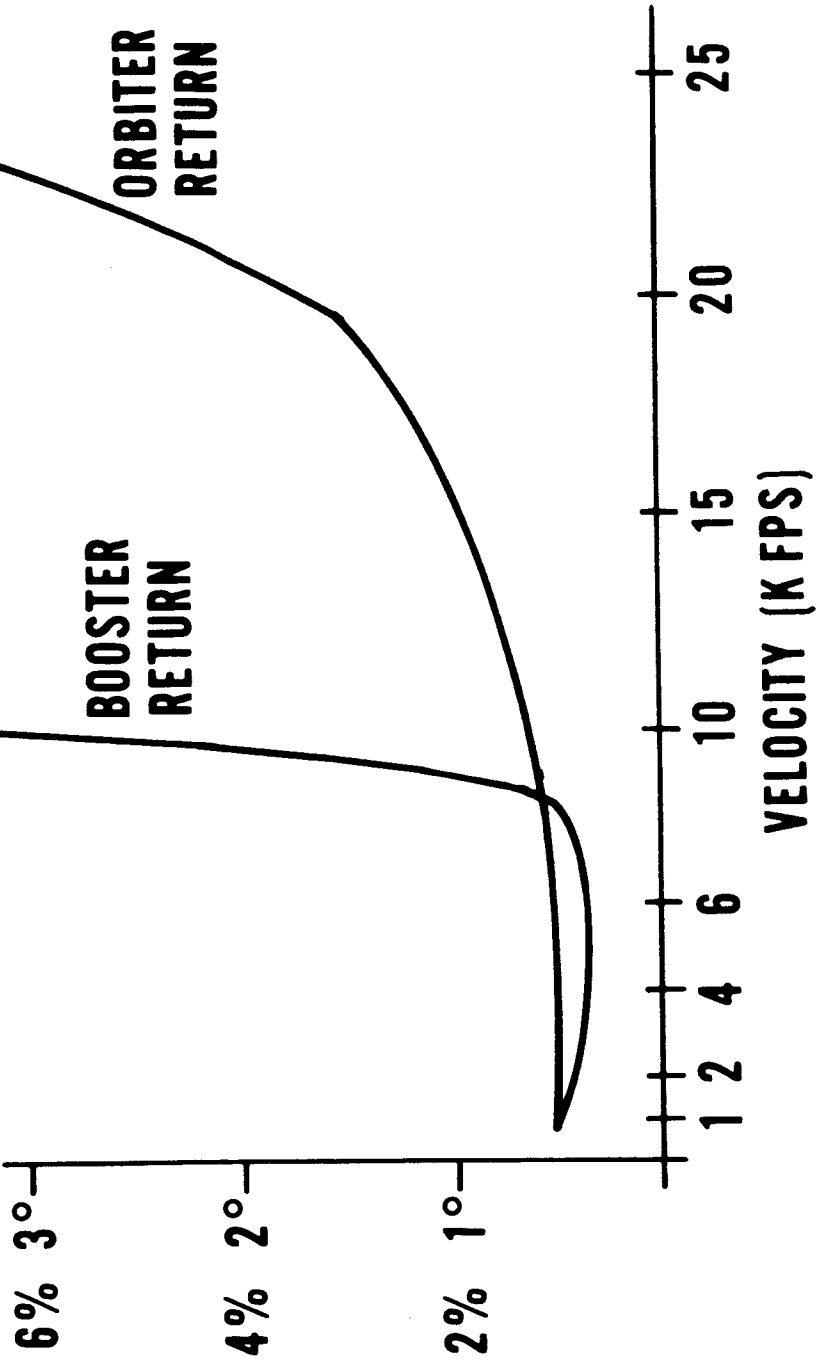
The flow direction sensor errors include misalignments of the nose section and imperfections of spherical pressure distributions which are partly calibratable for a given vehicle. The effects of vehicle bending and distortion of the spherical shape result in  $\alpha$  and  $\beta$  measurement errors that need to be controlled to about one degree (17.5 mrad).

The remaining errors decrease with increasing flow intensity. Replotting as a function of velocity for the entry trajectories, these errors are seen to decrease with velocity, during descent.

Since INS wind errors increase during descent, blending of measurements from ADM and INS is indicated.

# ERROR CHARACTERISTICS OF NOSE SENSOR

- MISALIGNMENTS
- SPHERICAL FLOW MODEL
- FLOW INTENSITY  $\propto \frac{1}{qB}$



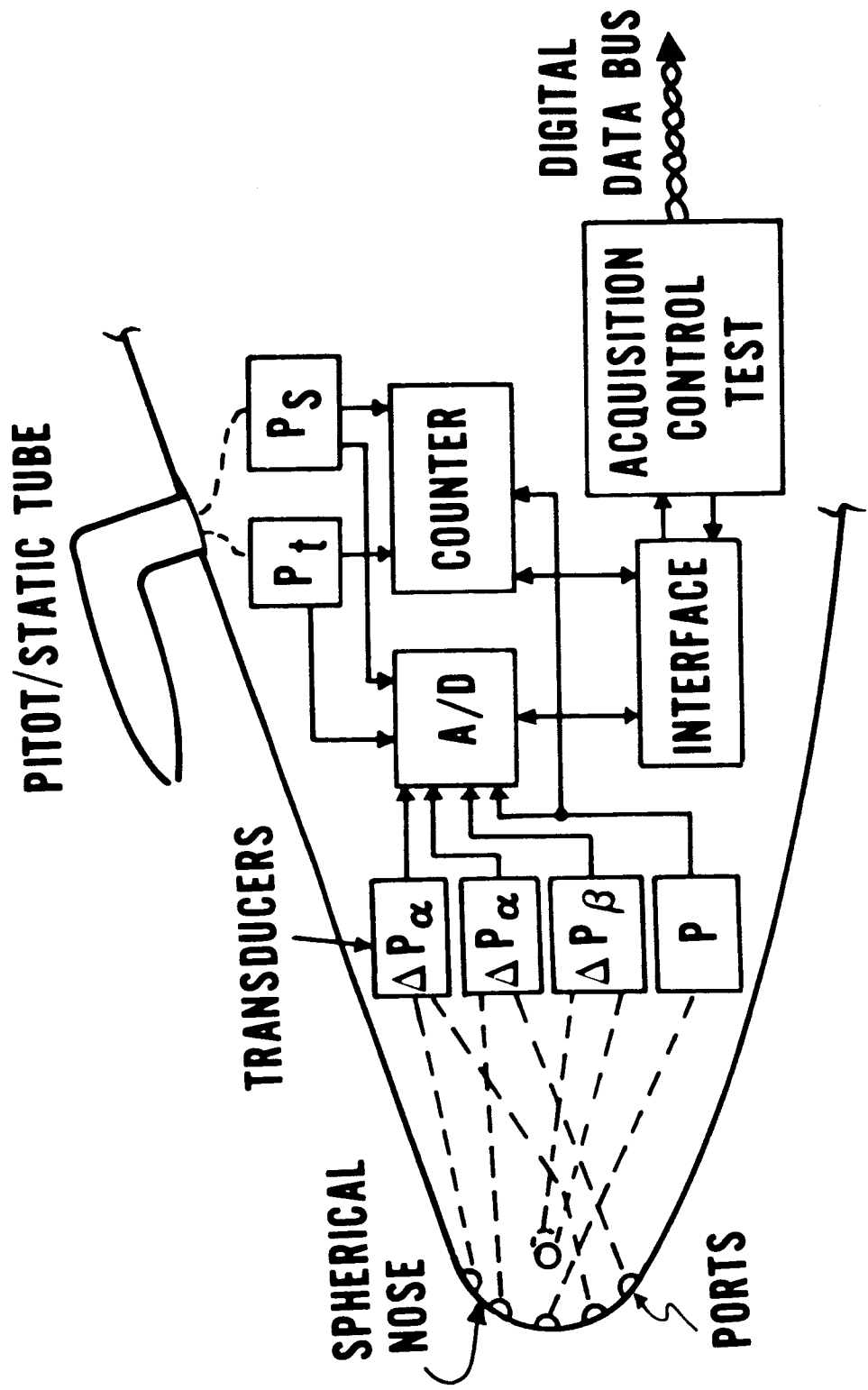
## ADM HARDWARE

The ADM provides digital measurements of absolute and differential pressures to the data bus. The transducers and electronics can be located in a forward avionics bay with short pneumatic lines to minimize line-lag and thermal exposure. Such transducers require normalization to standard scale and temperature compensation; thus, correction constants and measurements of temperatures are additional items of data sent to the computer for processing.

Selection from available transducers is underway; design of electronic assembly can then be defined. Preliminary coordination with vehicle contractors established feasibility of spherical nose shape and means to attach plumbing.

Numerous combinations of number of ports, number of transducers of each type, and number of electronic units and types are possible. Specific installations can be optimized to suit performance and redundancy objectives in view of needs.

# ADM HARDWARE



### COMPUTATION FLOW

The computation of air data parameters  $\alpha$ ,  $\beta$ , and  $P_{t2}$  proceeds by using two pressure differences  $\Delta P_1$  and  $\Delta P_2$  to determine  $\alpha$  and a pressure intensity function  $F$ . This approach does not require knowledge of flight conditions (like Mach number and altitude).

The third pressure difference,  $\Delta P_3$ , is zero when  $\beta = 0$  with sensitivity (gain) maximized but varying with angle of attack and flight intensity. For sideslip control (to null),  $\Delta P_3$  times a scheduled gain could be used. For  $\beta$  in angular units,  $\alpha$  and  $F$  are used.

The absolute pressure measurement,  $P$ , at a particular point on the spherical nose is used to compute stagnation pressure,  $P_{t2}$ , using computed values of  $\alpha$ ,  $\beta$ , and  $F$ .

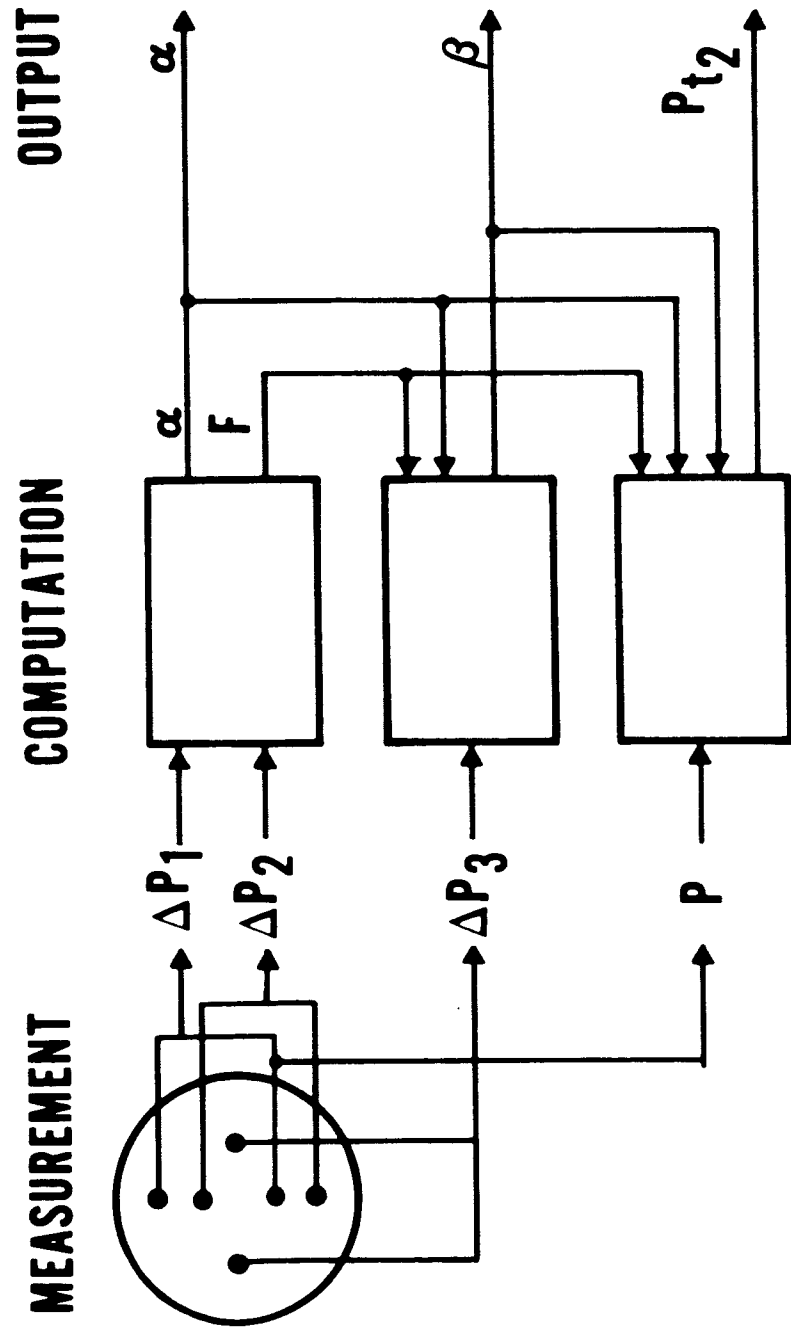
Correction constants are employed to compute the pressure values from transducer outputs. Improved system accuracy could be realized by automatically calibrating for zero output when above the sensible atmosphere.

UNCLASSIFIED

UNCLASSIFIED



# COMPUTATION FLOW

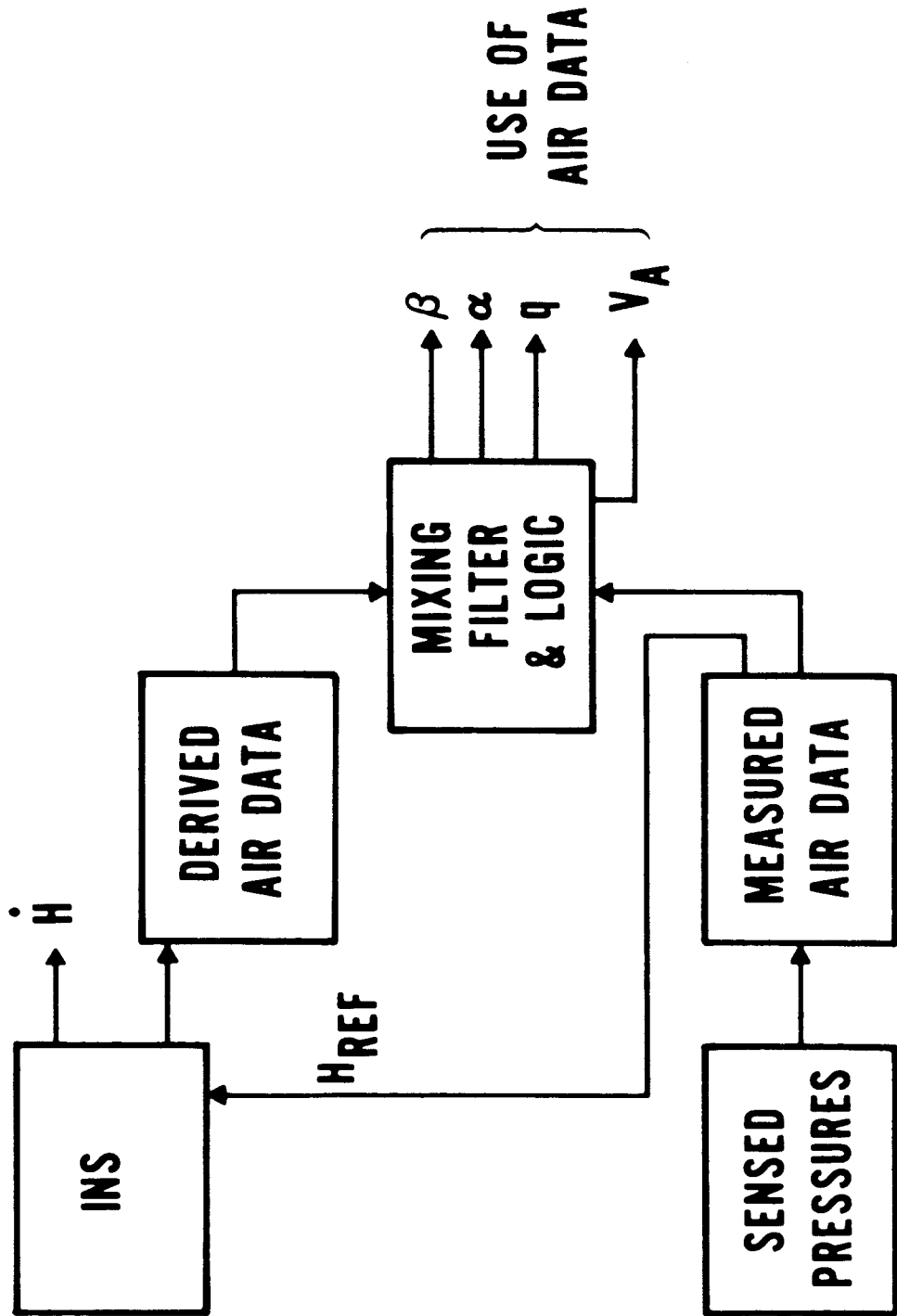


### BLENDING OF MEASUREMENTS

To complete the description of computations, this slide illustrates the blending of INS and ADM measurements. The altitude reference clamps the vertical channel of the INS to improve its performance and provide altitude rate,  $\dot{H}$ .

The mixing filter provides an improved estimate, or a logic chooses the best available source, thus providing digital words for air data use (by other programs or subsystems).

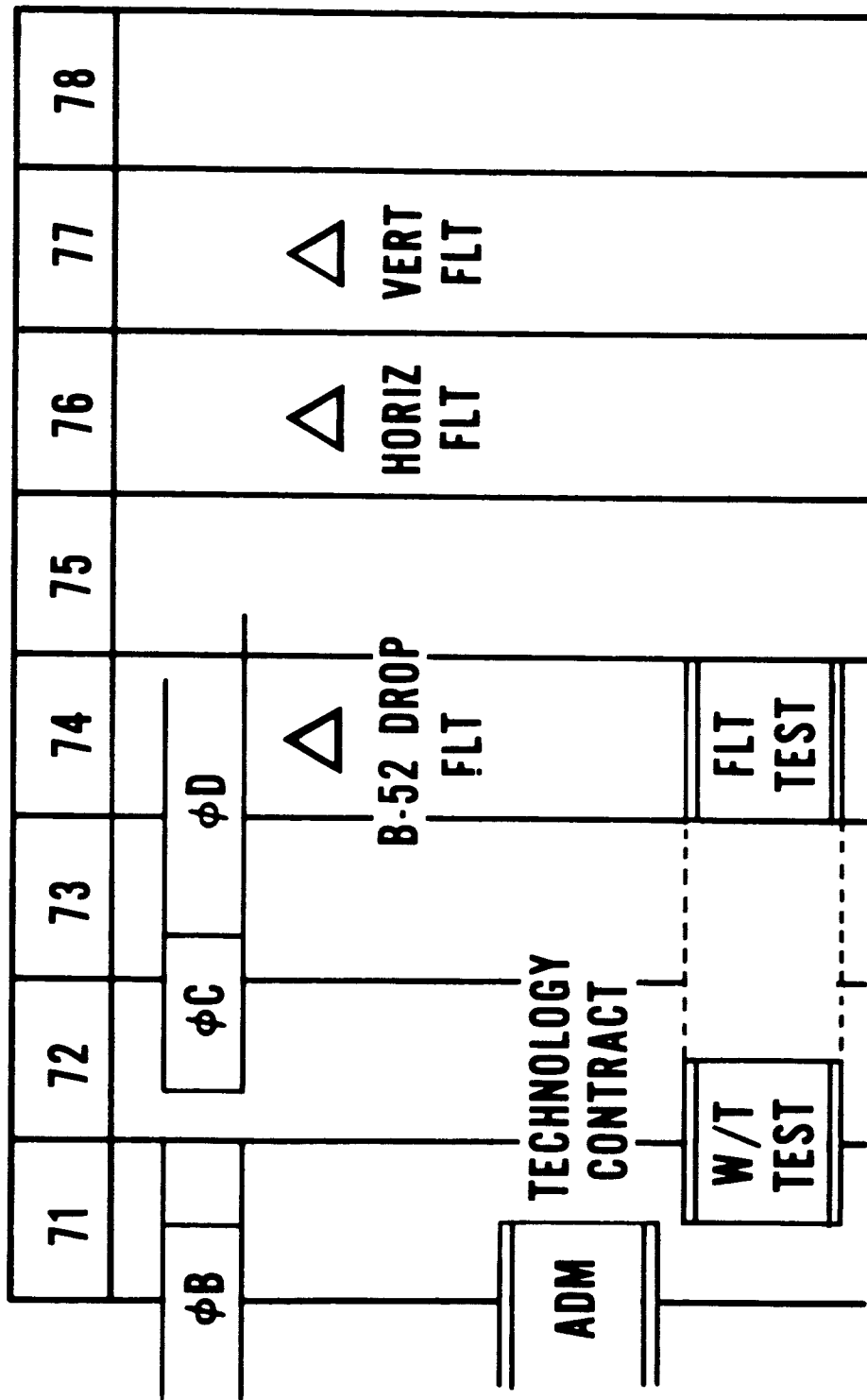
# BLENDING OF MEASUREMENTS



### SPACE SHUTTLE SCHEDULE

To influence vehicle design meaningfully, the ADM Technology Contract is currently providing supporting information to the Phase B Studies. It is expected that the sphere nose concept can be integrated into upcoming wind tunnel tests on vehicle models to give increased confidence in this approach for incorporation into vehicles.

# SPACE SHUTTLE SCHEDULE



### REMAINING WORK

To summarize, the sphere nose plus subsonic probe approach is feasible, useful, and attractive when compared to other approaches like supersonically deployed booms and subsonic probes only. Implementation depends on decision to do so and specifics of vehicle and avionics configurations.

The first three items are underway to the extent of preliminary design definition, under the ADM Technology Contract. The last three are extended Phase B and Phase C efforts.

## **REMAINING WORK**

- **INTEGRATION OF SPHERICAL NOSE**
- **INSTALLATION DESIGN**
- **TRANSDUCER SELECTION & ASSESSMENT**
- **PROOF - TESTING & SIMULATION**
- **INTEGRATION INTO VEHICLE & AVIONICS**
- **DESIGN & DEVELOPMENT**

ZERO-G PROPELLANT GAUGING OF CRYOGENICS

R. G. Morrison

TRW Systems Group  
Redondo Beach, California



## MISSION REQUIREMENTS

In the zero-g environment for the Space Shuttle, the measurement engineer is faced with two significant problems in determining the amount of propellant remaining. These are the temperature of the liquid, and just where the liquid mass might be.

Zero-g propellant quantity measurements are required as "status quo"; i.e., no knowledge of prior usage or venting is available since the measurement must determine the amount of fuel remaining. In the event that the vehicle is docked for a long period of time, an absolute quantity measurement must be made before the mission can proceed.

When the propellant is preferentially positioned, more conventional measurement techniques will, in all probability, be satisfactory.

When the propellant experiences a relatively small change in temperature during the life cycle of the mission, several mass measurement techniques offer a relatively simple measurement method. That is, unfortunately, not the case for cryogenics where liquid is introduced at one temperature and is gradually rising to the vapor temperature.

## PROPELLANT CONDITIONS

The temperature of the cryogenics and the surrounding structure emerges as one of the most important parameters in determining propellant quantity.

Since the temperature of the liquid is gradually rising, zero-g stratification conditions are in all probability quite unpredictable. Some form of mixing is desirable, and devices to control the location of the liquid are needed.

An accurate measurement of temperature will aid in predicting the degree of thermal stratification, surface tension, and inviscidness present in the liquid. This measurement must represent an average temperature of the ullage or liquid. Point sensors may give improper indications since small amounts of liquid clinging to the sensor would indicate a temperature somewhere between the ullage or wall condition and a representative liquid temperature.

In all gauging techniques, temperature has a pronounced effect on the gauging mechanism. A few important changes brought about by varying temperature are:

- Density
- Dielectric Constant
- Sound Velocity
- Electrical Resistivity
- Specific Heat
- Viscosity
- Surface Tension

## CANDIDATE SYSTEMS OTHER THAN RF

Two systems, aside from the RF work reported by Bendix, appear to offer a method of determining propellant quantity of specific cryogenes.

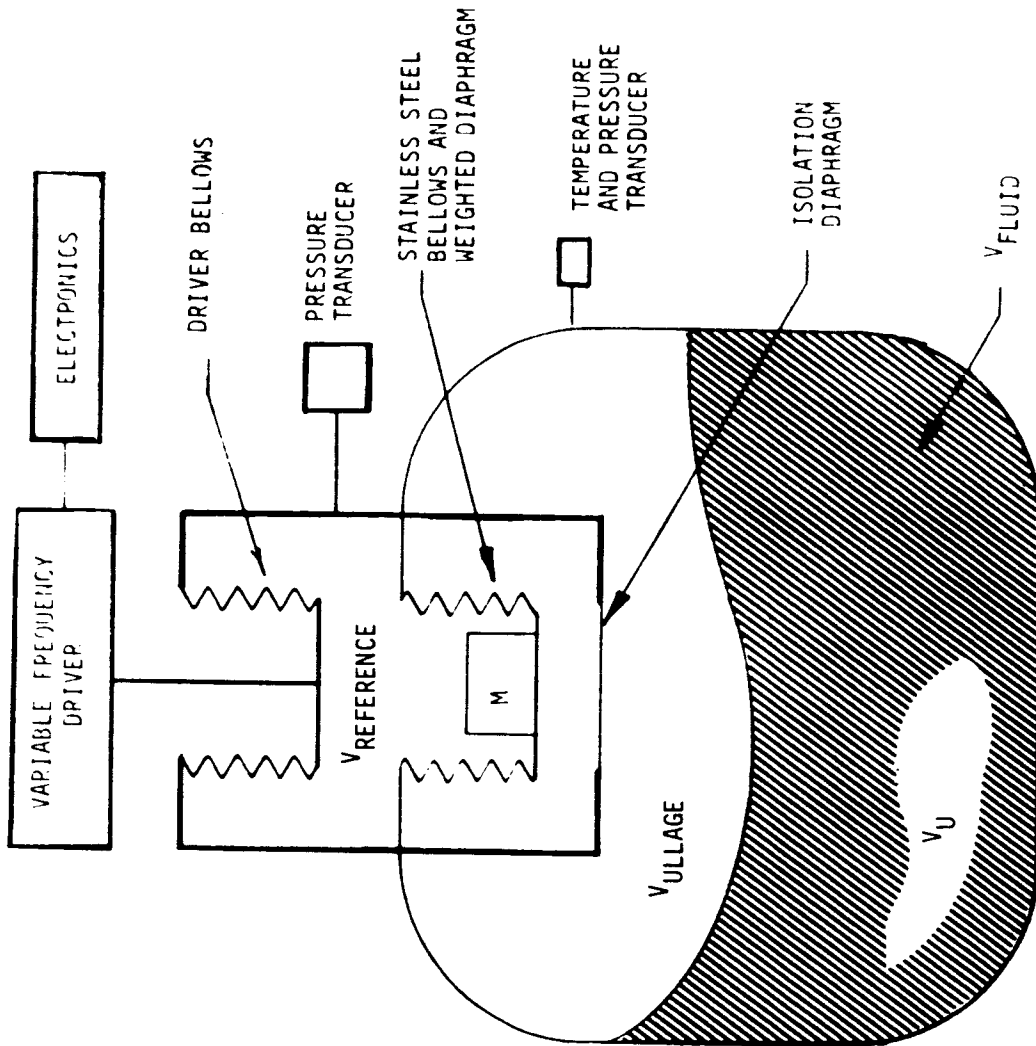
These are the Resonant Infrasonic Gauging System and the Nucleonic Gauging System.

The RIGS is essentially a low frequency ( $\sim 10$  Hz) loudspeaker. The key element is a weighted diaphragm which is driven at resonance. This resonance is determined by observing the pressure oscillations measured in a small reference volume. The observed resonant frequency is typically very low ( $\sim 1.0$  to  $0.5$  Hz for large tanks). It can be shown theoretically and experimentally that for low frequencies, the wave transmission through the ullage gas is a function of the specific heat ratio and ullage pressure. For storable propellants, the technique has been shown to measure propellant quantity accurately, provided the ratio of ullage compressibility to liquid compressibility is very high ( $\sim 1000:1$ ). The measurement of average ullage temperature is extremely critical since it determines the specific heat ratio.

RIGS requires three moving parts: i.e., the driver bellows, the resonant bellows, and the isolation diaphragm.

For gauging LOX, the system may be satisfactory provided a flexible isolation diaphragm can be obtained. A newly developed fluorastomer, AF-E-124D, is presently being tested in LN for flexural performance.

For LH<sub>2</sub> the system offers very little promise, since the compressibility of LH<sub>2</sub> and the establishment of a reliable gas gamma from an average temperature measurement introduce variables which make the overall system accuracy unacceptable.



RIGS GAUGE

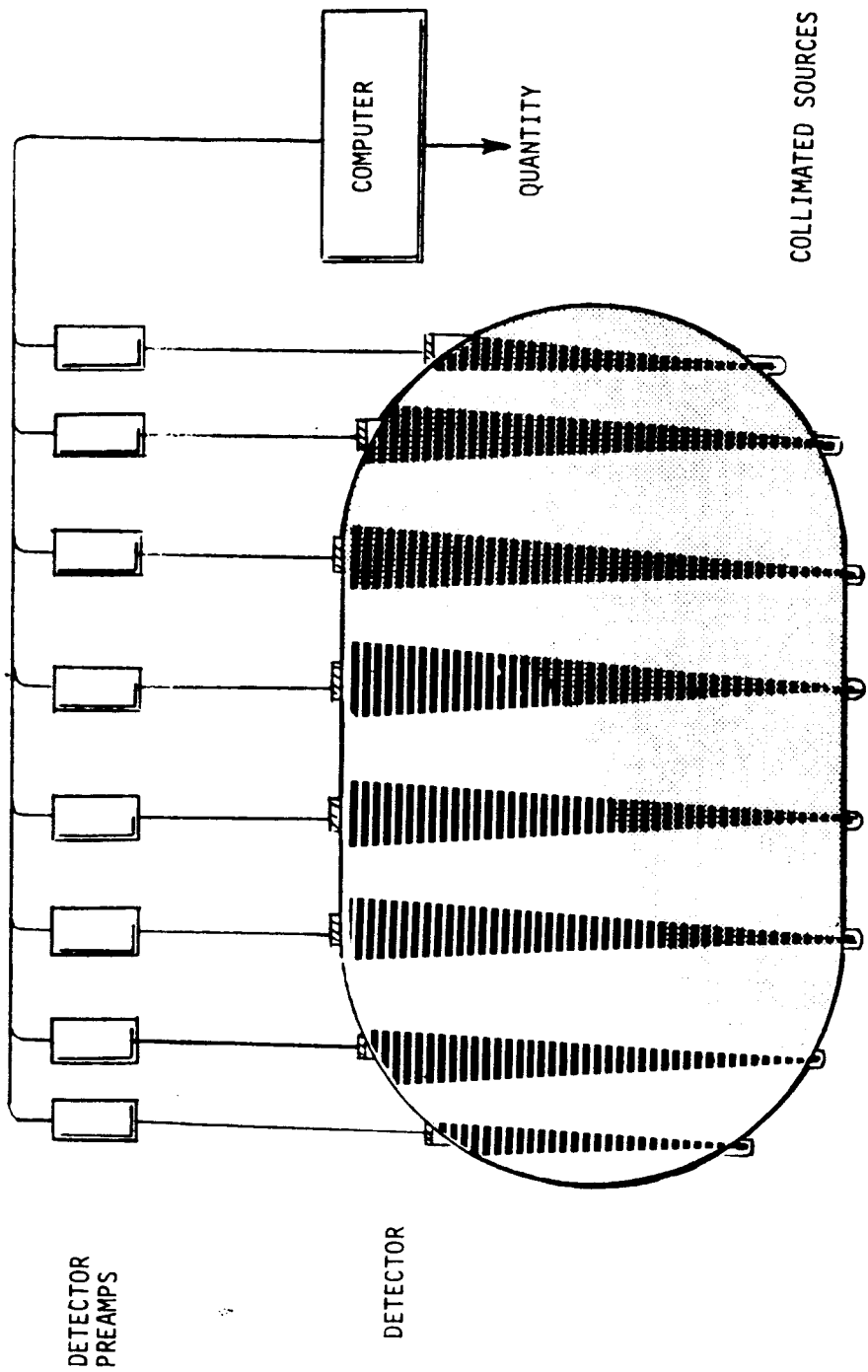
FIGURE 1

The nucleonic gauging technique employs a number of radioactive sources accompanied by a like number of detectors. In effect, each source/detector pair measures a discrete column from which a mass measurement is determined. Since the measurement is one of total mass between the source and detector, a minor correction must be made for fluid phase. This can be determined from a temperature measurement of either the vapor or liquid.

For low density propellants such as  $LH_2$ , the system requires very low strength sources. For high density liquids such as  $LOX$ , the required source strength must increase. If the present concept of twin tanks for  $LH_2$  and  $LOX$  holds, it appears that a nucleonic gauge can be developed to measure propellant in both cryogenes.

TRW is presently developing a nuclear zero-g gauging system, and the progress of that contract is currently reported in monthly and quarterly publications.\*

\* "Development of a Zero-G Gauging System," Contract F04611-71-C0010 AFRPL, Edwards AFB, California.



NUCLEONIC GAUGING SYSTEM

FIGURE 2

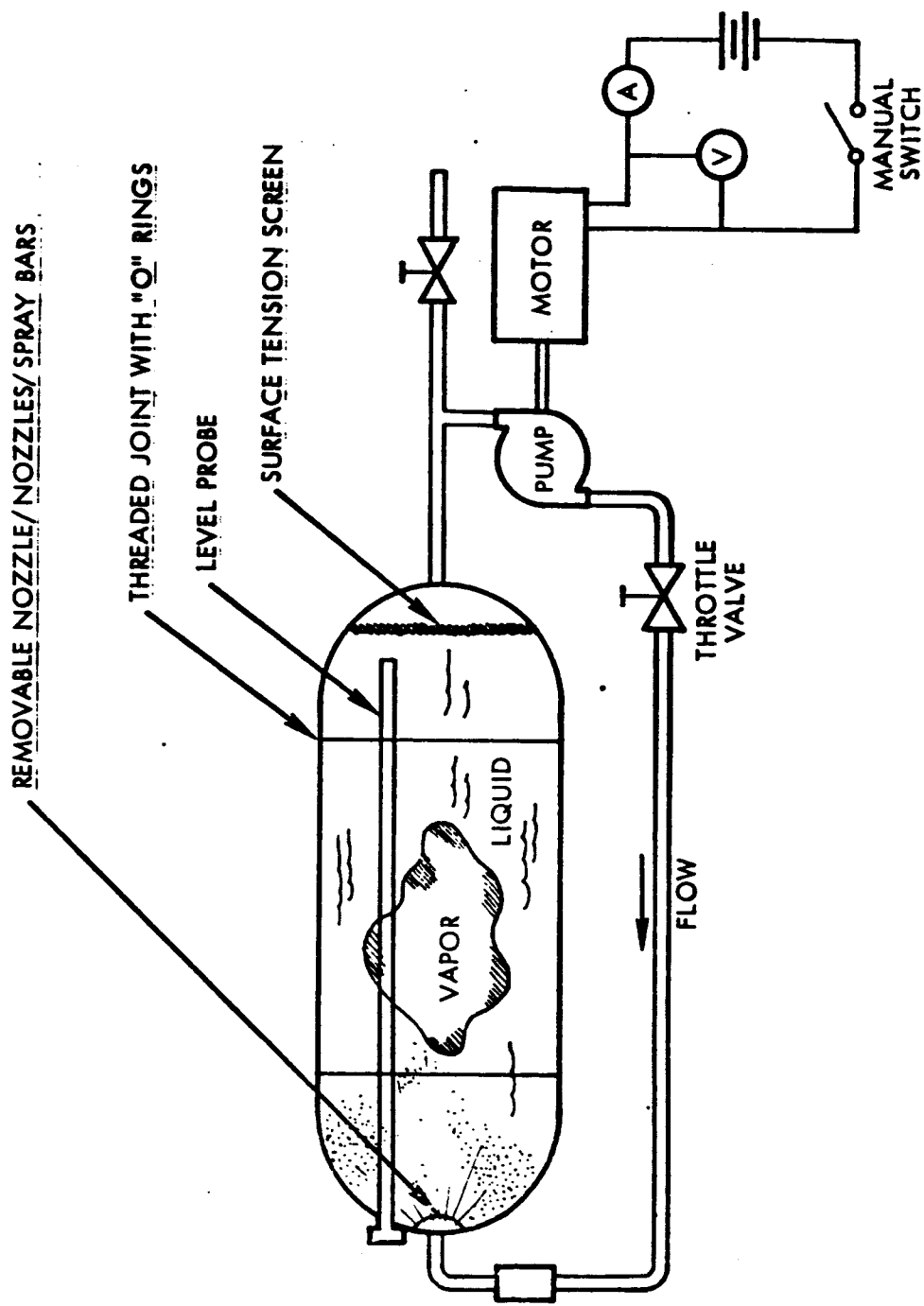
## PROPELLANT POSITIONING

Under the current study of possible zero-g gauging systems, an evaluation of several propellant positioning techniques was undertaken.

Since the amount of energy required to position the liquid under absolute zero-g is small ( $\sim 10^{-5}$  g), fluid injection systems appear to have merit.

Propellant mixing systems employing nozzles to break up thermally stratified layers of the liquid are being considered. If a vapor piston could be established or if enough momentum could be imparted into the liquid to position it preferentially, all measurement techniques are made much easier.

To establish whether or not the injection approach has merit, a test series utilizing spray injection is under consideration. The design of the nozzle is not trivial, since the pressure must be accurately distributed to prevent geysering of the fluid mass or amplifying of the tank wall meniscus.



PROPOSED PROPELLANT POSITIONING EXPERIMENT

FIGURE 3

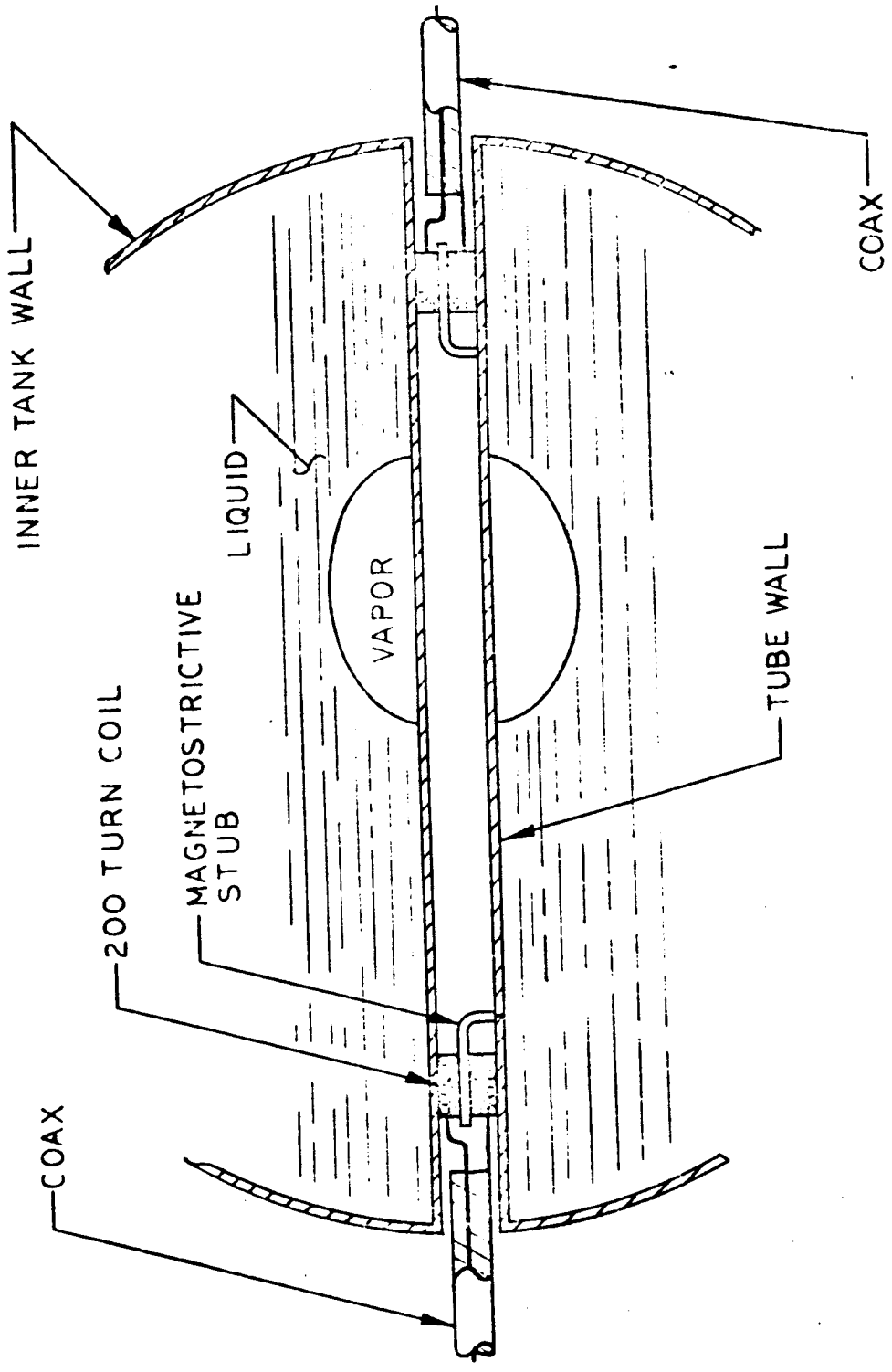


## ULTRASONIC GAUGING

Under this current zero-g study contract, a close look has been taken at the potential use of a pulsed ultrasonic system. This technique has the unique advantage of being able to obtain an average temperature measurement and measure the density of the liquid. It can extract the density measurement independent of propellant position, provided the ullage can be maintained in a single location.

The sensing hardware is extremely simple and actually displays improved performance in cryogenic temperatures. A copper wire is wrapped around a magnetostrictive core. The core is then attached to a sensing bar, and a measure of the attenuation of the induced shear or flexural wave determines the quantity of liquid in contact with the sensing bar. The time it takes the shear wave to travel from the transmitter to the receiver is an excellent measure of the average temperature of the sensing bar.

At first glance, the technique appears complicated; however if the liquid can be preferentially positioned, the advantages are significant. The transceivers can be mounted externally on the tank wall or on internal piping, and one can obtain two critical measurements (temperature and quantity) with the same measurement tool.

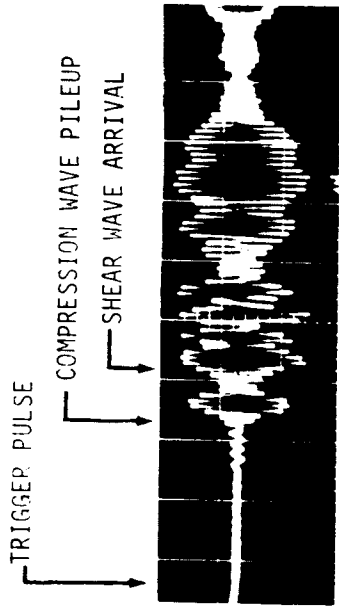


BASIC ULTRASONIC LIQUID QUANTITY GAUGE

FIGURE 4

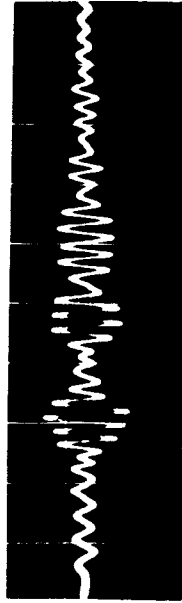
The data shown in Figure 5 are taken from an ultrasonic system in a cryogenic environment. The instrument consists of an aluminum bar with the receiver coil submerged in liquid nitrogen. To extract the desired signal, a gating circuit is designed to isolate a chosen cycle of the shear wave oscillation. By measuring the amplitude of the received signal, the amount of liquid between the sensing coil and driver coil can be obtained. By measuring the time shift of the signal from a given reference (i.e., the input pulse to the receiver coil), the average temperature of the bar can be established.

Preliminary lab tests in liquid nitrogen have confirmed the basic performance of the ultrasonic hardware. The discrete frequency shown in the illustration is a predictable characteristic of the detector. The dimensions of the stub determine the natural oscillation frequency, which in this case is approximately 180 KHz. Since the frequency domain has been established, all unwanted signals can be easily filtered and the desired time window established to extract the two variables (temperature and liquid level).



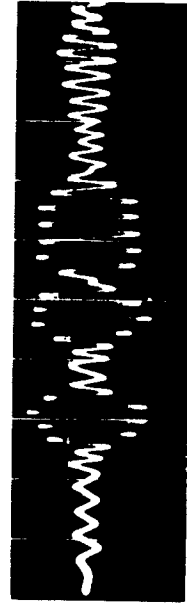
TYPICAL RECEIVED SIGNAL ON  
24" ALUMINUM BAR IN LIQUID  
NITROGEN

SWEEP SPEED 50 SEC  $\text{cm}^{-1}$   
AMPLITUDE 200 MV  $\text{cm}^{-1}$



RECEIVED SIGNAL WITH BAR  
55% SUBMERGED IN LIQUID  
NITROGEN

SWEEP SPEED 20 SEC  $\text{cm}^{-1}$   
AMPLITUDE 200 MV  $\text{cm}^{-1}$



RECEIVED SIGNAL WITH BAR  
35% SUBMERGED IN LIQUID  
NITROGEN

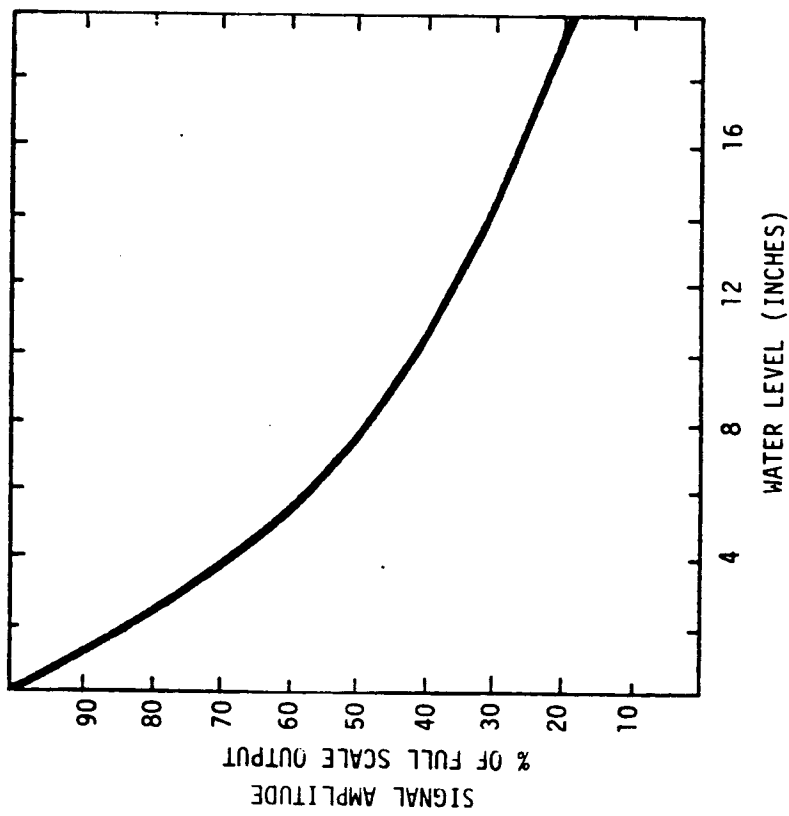
SWEEP SPEED 20 SEC  $\text{cm}^{-1}$   
AMPLITUDE 200 MV  $\text{cm}^{-1}$

ULTRASONIC SHEAR WAVE DATA (ALUMINUM 6061-T6)

FIGURE 5

The fact that the amplitude of the received signal increases with decreasing propellant is significant. This means that the quantity remaining can be gauged more accurately as the fuel is expended.

Figure 6 illustrates a calibration of the ultrasonic gauge in water at room temperature. Preliminary analysis of cryogenic data indicates that the behavior of the transducer performs in the same manner.



ULTRASONIC CALIBRATION CURVE

FIGURE 6

## CONCLUSIONS

The nucleonic system offers a distinct advantage in measuring propellant quantity since it requires no electrical penetration of the cryogenic tank.

RIGS has many unanswered questions regarding cryogenic applications. It is not a candidate for LH<sub>2</sub> systems; however it may be adapted to LOX.

If a system can be designed which will preferentially position the liquid, ultrasonic systems may prove to be the simplest and least expensive.

ZERO-G RADIO FREQUENCY GAGING SYSTEM  
FOR SPACE SHUTTLE PROPELLANT TANKS

H. E. Thompson

NASA-Marshall Space Flight Center  
Huntsville, Alabama

and

N. E. Stanley, B. J. Shebler, W. Ott

Bendix Corporation  
Davenport, Iowa

ABSTRACT

This paper presents the progress of RF Gaging and its applicability to Space Shuttle propellant gaging systems. Included are basic theory, analysis, test results to substantiate theory and analysis, along with test data from systems built and tested to date. Also included are tank and fluid orientation data with characteristic performance curves, repeatability and system accuracy. Some problem areas and their solutions as applicable to space shuttle mission capability enhancement are also presented.



## INTRODUCTION

A Radio Frequency mass quantity gaging system is presently being evaluated for application in space vehicle propellant systems. Analysis and substantiating tests have been carried out with various hydrocarbon fuels, liquid oxygen, and liquid nitrogen to determine system performance characteristics over various frequency ranges, fill levels and tank orientations.

Presented in this paper is fundamental description of the principle of operation for RF gaging, along with mathematical formulas and supporting data. Also included are system block diagrams, photographs of hardware and some test setup arrangements. The data presented depicts loading data characteristic curves for various fluids and system gaging accuracy as applicable to Space Shuttle.

## BACKGROUND

In 1966 Bendix funded a study program at Iowa State University to determine what basic principles could be used to gage fluids in a Zero-g environment. From this study the Radio Frequency resonant cavity technique was selected as having the best potential.

During early RF gaging development, the technology of microwave and low frequency integrated circuits was not sufficiently advanced to allow use of suitable off-the-shelf components. Therefore, laboratory test equipment and specially designed circuits were relied upon. As components needed to fabricate the necessary circuitry have become state-of-the-art in the last year or so, significant improvements have evolved.

During development of this system, the fundamental relationships between propellant mass and mode count were investigated, including a means for exciting the modes in a more optimum manner. The mode patterns observed as the oscillator frequency was swept over selected frequency ranges, provided experimental data for low-loss and high-loss propellants that could be used to support theoretical analysis. Theoretical Mathematical expressions have advanced that provide a means for calculating the needed operating fre-

quency and the expected number of observable resonant modes in a propellant tank as a function of liquid mass in the tank.

Under the sponsorship of MSFC, further experimental verification and the refinements of theoretical predictions have been recently carried out with good success, and have provided a basis for developing scaling correlations and improved system performance predictions.

#### PRINCIPLE OF OPERATION

The Radio Frequency (RF) quantity gaging concept envisions the introduction of microwave energy into a tank so as to illuminate it by setting up electromagnetic fields throughout the entire volume of the tank. The tank interior is a dielectric region completely surrounded by conducting walls. There exist electromagnetic field solutions of certain frequencies and spatial configuration that satisfy the boundary conditions and correspond to the storage of electromagnetic energy over time intervals that are long compared with the period of the resonant frequencies. Such a system is commonly called a cavity, and the resonant solutions are the normal theoretical modes of the cavity. Each cavity has a different set of normal modes, differing both in frequency and in spatial configuration. All such sets have an infinite number of members.

If the set of normal modes is ordered with respect to increasing resonant frequency, there is always a lowest resonant frequency, but, in general, no highest resonant frequency. In the direction of higher frequencies, the normal modes increase in complexity and in density, becoming infinitely dense at infinite frequencies. For a given frequency range above the lowest resonant frequency, mode density increases with average dielectric (real part of the complex permittivity) of the cavity.

The number of observable (detectable) modes will be equal to or less than the number of theoretical modes dependent on the following factors:  $Q$  of the tank and antenna assembly, complex permittivity of the

average dielectric of the tank, mode detector and the characteristic impedance of the RF source and coupling elements, including RF cables.

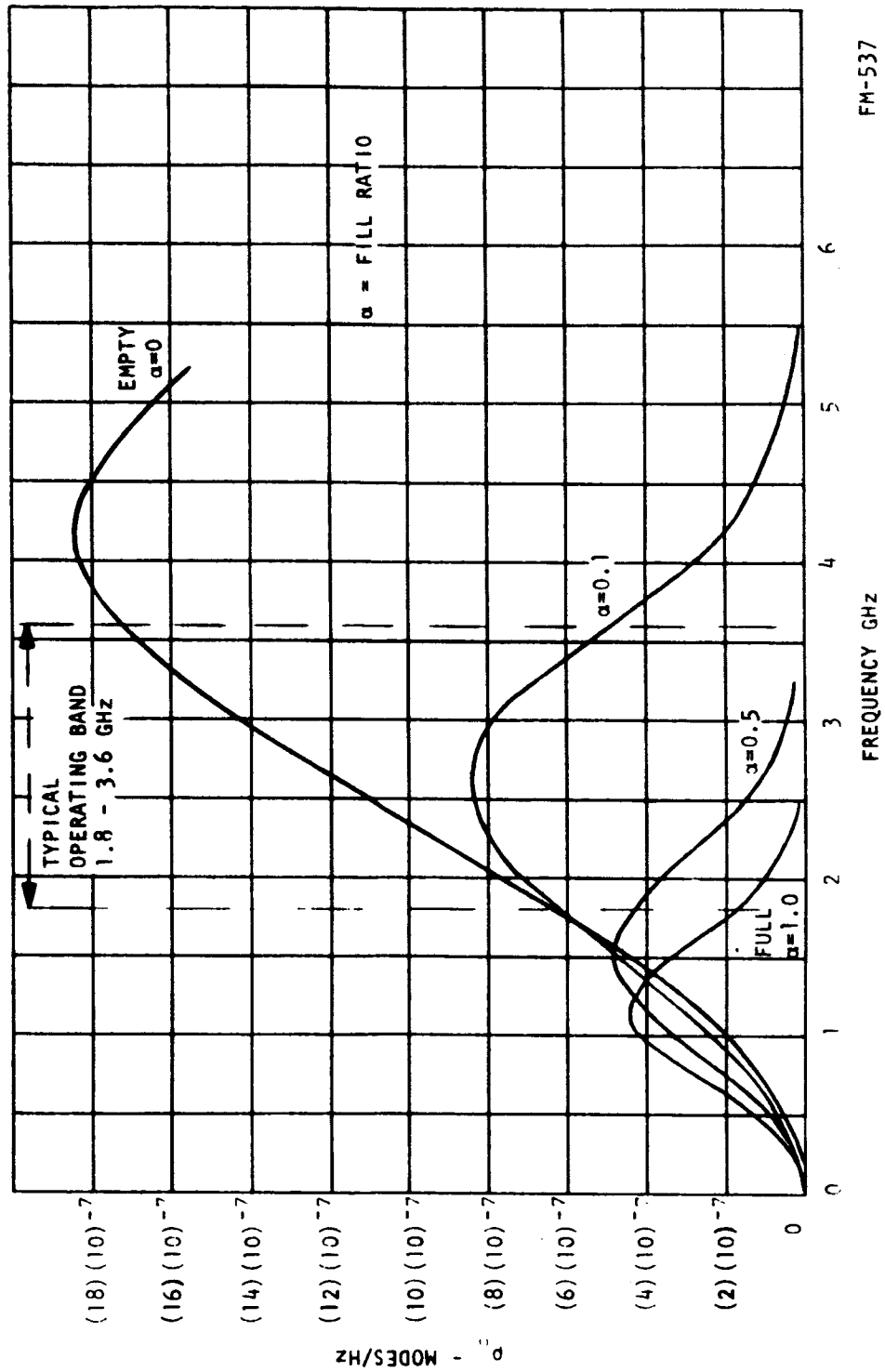
If the average dielectric and the walls of the tank were ideally lossless, the density of detectable modes would always increase with frequency. However, due to tank wall losses, even with an ideal lossless dielectric, the density of detectable modes eventually reaches a peak with increasing frequency and then falls off. This is due to normal modes merging when the system Q is less than infinity.

If a low loss dielectric is added to the tank interior, the density of detectable modes will increase at a higher rate with frequency due to the increased real part ( $\epsilon'$ ) of the complex permittivity; however, the peak density will now occur at a lower frequency due to additional loss contributed by the imaginary part ( $j\epsilon''$ ). With higher loss dielectrics, this phenomena is amplified so that the peak density may occur at relatively low frequencies in the microwave spectrum.

Based on the statistical probability of "observing", or detecting, a mode, an equation has been developed which predicts this type of behavior. Figure 1 is a plot of densities for a high loss dielectric calculated using the equation and plotted versus frequency for several different filling factors. Because the relatively low frequency at which the peak occurs when the tank is full, it is evident that high loss dielectrics should be gaged on the high frequency "tail" of the density curves where the number of modes will be decreasing with increasing frequency. In contrast with this, low loss dielectrics are more conveniently gaged on the low frequency side where the number of modes increases with increasing frequency.

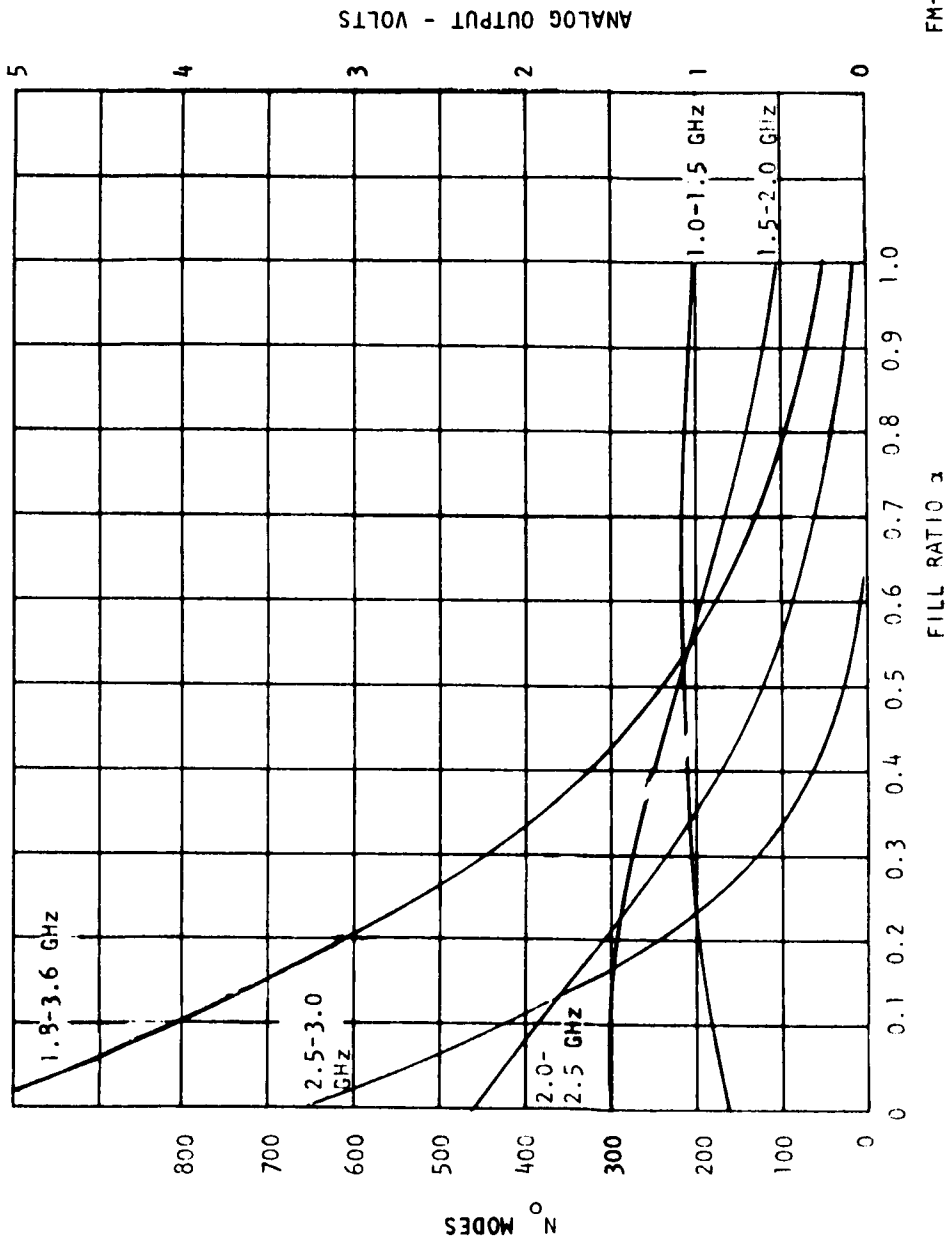
Integration of the mode density curves of Figure 1 over a fixed frequency band produces the number of observable modes in that band. Figure 2 shows the number of modes which exist in selected frequency bands as the tank is filled with RP-1. Also shown is the output voltage which would exist if the number of modes is converted directly to an analog signal.

To obtain a system with detectable modes that are nearly independent of the location of the fluid in the tank, the number of cubic wavelengths at the lowest frequency is made as large as possible by increasing the lower band-edge frequency.



FM-537

Figure 1.- DENSITY OF OBSERVABLE MODES IN A 1/10-SCALE S-1VB TANK LOADED WITH RP-1



FM-538

Figure 2.- OUTPUT CHARACTERISTICS OF A RF GAGING SYSTEM  
ON A 1/10-SCALE S-1VB TANK FILLED WITH RP-1

Figure 3 shows the RF Gaging System in block diagram form. The RF section consists of a voltage tunable RF Sweep Oscillator, an attenuator, a low-pass filter which cuts off at the maximum desired output frequency, and a directional coupler which provides a sample of the RF power level. This level is held constant by detecting it at the directional coupler and using the detected power level to control a power leveling circuit. The power leveling circuit controls the DC bias of the RF sweep oscillator.

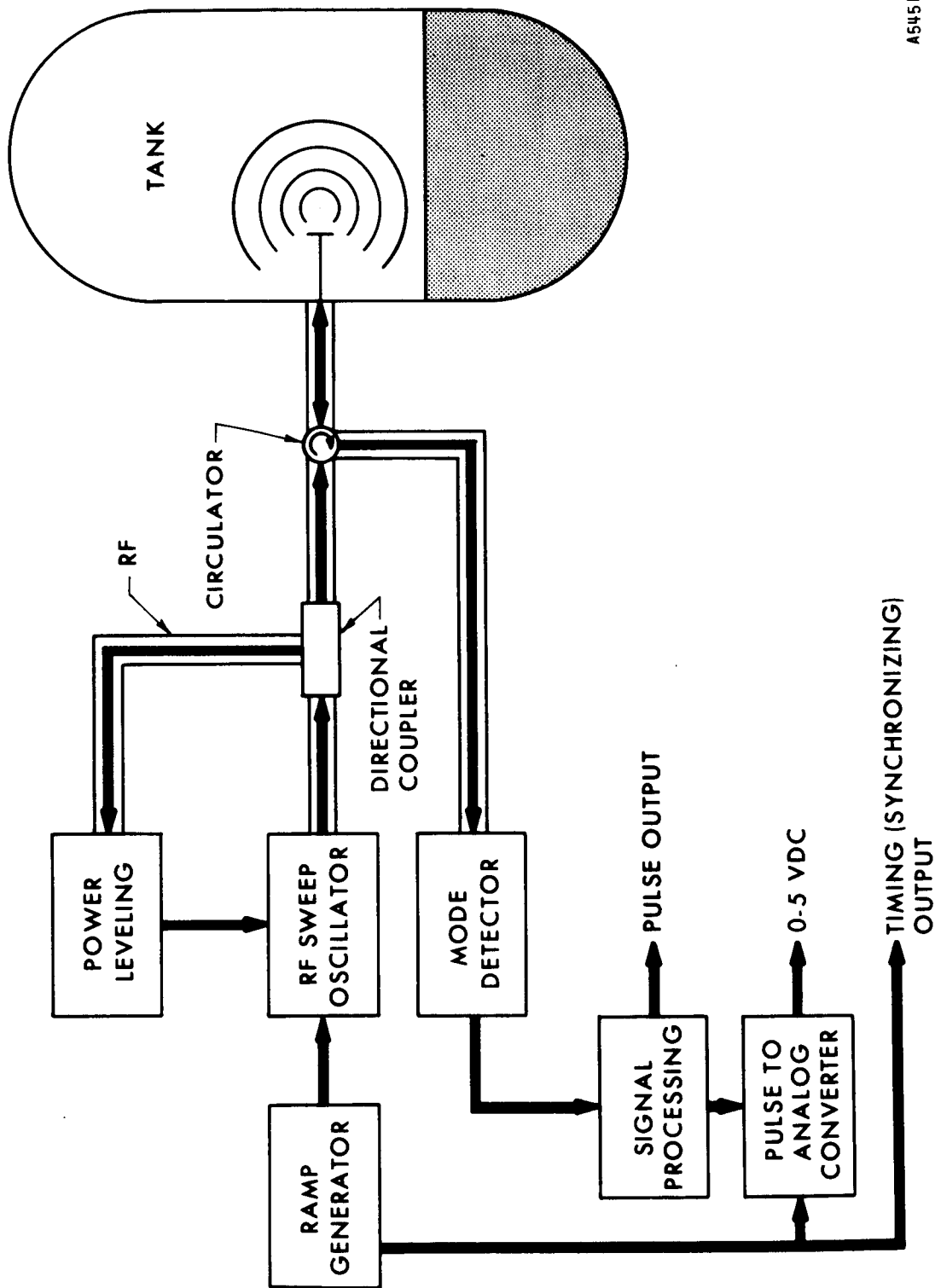
The RF oscillator frequency is controlled by a ramp voltage which is generated in the Ramp Generator. The ramp voltage causes the oscillator to sweep over a frequency  $f_1$  to  $f_2$ .

The RF energy is coupled into the tank probe through a circulator and coaxial cable. The tank probe is a wide band spiral antenna. The RF energy reflected from the probe is detected at the third port of the circulator using a Mode Detector (crystal diode). This detected energy contains the mode information.

The Signal Processing circuit produces a constant-width, constant-amplitude pulse for each detectable mode. This provides a train of pulses which can be counted electronically by using the timing pulse from the ramp generator, or fed into a Pulse to Analog Converter to obtain an 0-5 VDC analog voltage.

#### PROGRESS TO DATE

Recent efforts to experimentally evaluate the latest RF gaging refinements have been very successful. Much progress has been made in correlating analytical predictions with experimental results. The calculated operating RF frequency band, and the subsequent number of modes observed for a given tank and fluid can now be made with a greater degree of confidence. Data obtained with laboratory test tanks and test fluids has been shown to be very repeatable on a day-to-day basis, regardless of whether laboratory or prototype RF sources are used.



A5451-250

Figure 3.- RF MODE COUNTING SYSTEM

### Theoretical Analysis

The theoretical maximum number of modes which may be established for a given empty tank over a fixed frequency band can be expressed mathematically. Over the frequency band bounded by  $f_1$  and  $f_2$ , the number of modes that can be excited is given by:

$$N = \frac{8\pi V}{3c} \left[ f_2^3 - f_1^3 \right] \quad (1)$$

where

$V$  = volume of the tank

$c$  = velocity of light

When the tank is partially filled with a dielectric material, the theoretical mode count loading dependence is a linear relationship given by the following expression:

$$N = \frac{8\pi V}{3c} \left\{ f_2^3 - f_1^3 \right\} + \left[ (\epsilon')^{3/2} - 1 \right]^\alpha \quad (2)$$

where

$\epsilon'$  = the dielectric constant of the material (real part of permittivity)

$\alpha$  = fractional fill ratio

Equation (2) describes the ideal case. In practice it is impossible to excite, detect, and count all the theoretically possible modes in any given tank due to mode degeneracies and mode merging. Mode degeneracy is a condition where more than one mode exists at a given frequency, and is therefore detected and counted as one. Mode merging is defined as the merging of neighboring modes caused by a low system Q. In the case of high Q systems (tanks whose internal surfaces are good electrical conductors, and where the material to be gaged has a low electrical loss factor) Equation (2) can be used to predict the maximum number of excitable modes. Since this number is the maximum possible, not including mode degeneracies, the actual observable mode count falls below this predicted maximum. An empirical modification of Equation



(2) can be made to reflect the effects of mode degeneracy.

A generalized theoretical treatment derived from Equation (2) that takes into account low Q systems in which mode merging is evident has been formulated, and is given by:

$$\rho_0 = 3Kf^2 \exp\left(-\frac{2\beta}{Q_L} Kf^3\right) \quad (3)$$

where

$\rho_0$  = frequency - density of observable modes

$$K = \frac{8V}{3C} \left\{ 1 + \left[ \left( \frac{1}{3} \right)^{3/2} - 1 \right] \right\}$$

$\beta$  = experimental factor

$Q_L$  = quality factor, or Q of system

Equation (3) is based on the statistical probability of mode detection.

The actual number of observable modes, ( $N_0$ ), in a frequency band from  $f_1$  to  $f_2$  may be obtained by integrating Equation (3) between these limits. This gives:

$$N_0 = \frac{1}{C} \left[ \exp(-CN_1) - \exp(-CN_2) \right] \quad (4)$$

where

$$C = \frac{2\beta}{Q_L}$$

$$N_{1,2} = K(\alpha) f_{1,2}^3$$

The system Q;  $Q_L$ , can be calculated using the formula

$$\frac{1}{Q_L} = \frac{1}{Q_d} + \frac{1}{Q_u} + \frac{1}{Q_i} + \frac{1}{Q_e} \quad (5)$$

where  $Q_d$  ( $\alpha$ ) relates to the dielectric,  $Q_u$  relates to the empty tank,  $Q_i$  relates to internal thermal insulation if present, and  $Q_e$  relates to the external source and RF probe. The quality factor  $Q_d$

is a function of the fractional fill ratio,<sup>s</sup> and dependent on both the real and imaginary parts of the complex permittivity ( $\epsilon' - \epsilon''j$ ) of the material to be gaged.

The value of  $Q_L$ , as determined from Equation (5), may be used in conjunction with Equation (4) to establish the optimum frequency limits,  $f_1$  and  $f_2$ , for a high loss, descending curve of  $N_0(\infty)$ .

Table I contains the computed optimum frequency bands for several tanks and fluids. Empirical substantiation of these predictions to establish system scaling law methods is currently being achieved under a NASA MSFC contract.

### Test Results

During the past few years a large amount of experimental data has been gathered in which the intended purposes were:

- 1) To correlate theoretical predictions of loading dependence as determined by Equations (2) and (4) with experimental results and verify scaling relationships.
- 2) To verify the prediction that the mode count remains essentially invariant with redistribution of the tank contents.
- 3) To evaluate the RF gaging system under operating conditions that could not be determined theoretically; that is, propellant out-flow, and dynamic situations as simulated by slosh and bubbling conditions.

Testing of the RF gaging system concept to the above objectives has been performed successfully on several scale model spacecraft tanks and with several simulated fuels. Safety and cost considerations have limited testing with LOX and  $LN_2$  to static tests; however, with cryogenics there is presently no reason to believe that orientation sensitivity should be any greater than that of the non-cryogenic fuel simulates.

Fuel simulates such as Benzene and RP-1 have been used for orientation sensitivity tests with data as shown in Figures 4 and 5 repeated several times, indicating very little orientation sensitivity.

TABLE I  
FREQUENCY RANGE FOR VARIOUS TANK & FLUID ELECTRICAL PROPERTIES

TANK	FREQUENCY RANGE GHz	LIQUID	VOLUME [m <sup>3</sup> ]	SURFACE AREA [m <sup>2</sup> ]	ε'	ε''	tanδ	N <sub>oe</sub>	N <sub>of</sub>
General Space	2.3 to 3.6*	RP-1	0.133	1.55	2.08	(190)(10) <sup>-5</sup>	(91.5)(10) <sup>-5</sup>	1,182	149
1/10 Scale S-IVB	2.0 to 3.0	RP-1	0.220	2.65	2.08	(190)(10) <sup>-5</sup>	(91.5)(10) <sup>-5</sup>	1,107	20
1/20 Scale S-IVB	4.0 to 5.0	RP-1	0.0256	0.628	2.08	(190)(10) <sup>-5</sup>	(91.5)(10) <sup>-5</sup>	438	24
Spherical Al	1.60 to 2.8	RP-1	0.164	1.45	2.08	(190)(10) <sup>-5</sup>	(91.5)(10) <sup>-5</sup>	791	50
Spherical Al	1.5 to 2.4	Transil Oil	0.164	1.45	2.18	(610)(10) <sup>-5</sup>	(280)(10) <sup>-5</sup>	504	7
General Space	4.2 to 5.0	Benzene	0.133	1.55	2.28	(13.1)(10) <sup>-5</sup>	(5.75)(10) <sup>-5</sup>	1220	245
1/10 Scale S-IVB	3.5 to 4.2	Benzene	0.220	2.65	2.28	(13.1)(10) <sup>-5</sup>	(5.75)(10) <sup>-5</sup>	1,256	277
1/20 Scale S-IVB	5.5 to 6.5	Benzene	0.0256	0.628	2.28	(13.1)(10) <sup>-5</sup>	(5.75)(10) <sup>-5</sup>	681	608
1/10 Scale S-IVB	3.0 to 3.8	Styrofoam	0.220	2.65	1.2	(30)(10) <sup>-5</sup>	(25)(10) <sup>-5</sup>	1,314	271
1/20 Scale S-IVB	5.0 to 6.0	Styrofoam	0.0256	0.628	1.2	(30)(10) <sup>-5</sup>	(25)(10) <sup>-5</sup>	604	312
1/10 Scale S-IVB	4.6 to 5.1	Paraffin	0.220	2.65	1.65	(3.43)(10) <sup>-5</sup>	(2.08)(10) <sup>-5</sup>	850	288
1/10 Scale S-IVB	4.7 to 5.2	LN <sub>2</sub>	0.220	2.65	1.428	(4.28)(10) <sup>-5</sup>	(3)(10) <sup>-5</sup>	581	154
1/10 Scale S-IVB	2.0 to 3.0	LOX	0.220	2.65	1.51	(136)(10) <sup>-5</sup>	(90)(10) <sup>-5</sup>	1,052	68
Spherical Al	1.6 to 3.0	LOX	0.164	1.45	1.51	(136)(10) <sup>-5</sup>	(90)(10) <sup>-5</sup>	1,010	243
Full Scale S-IVB	0.5 to 1.0	LH <sub>2</sub>	300	320	1.23	<(1)(10) <sup>-7</sup>	<(1)(10) <sup>-7</sup>	1,780	1020

\*Based on Actual Test Data. All other Ranges Calculated from Equations Given in Appendix A.

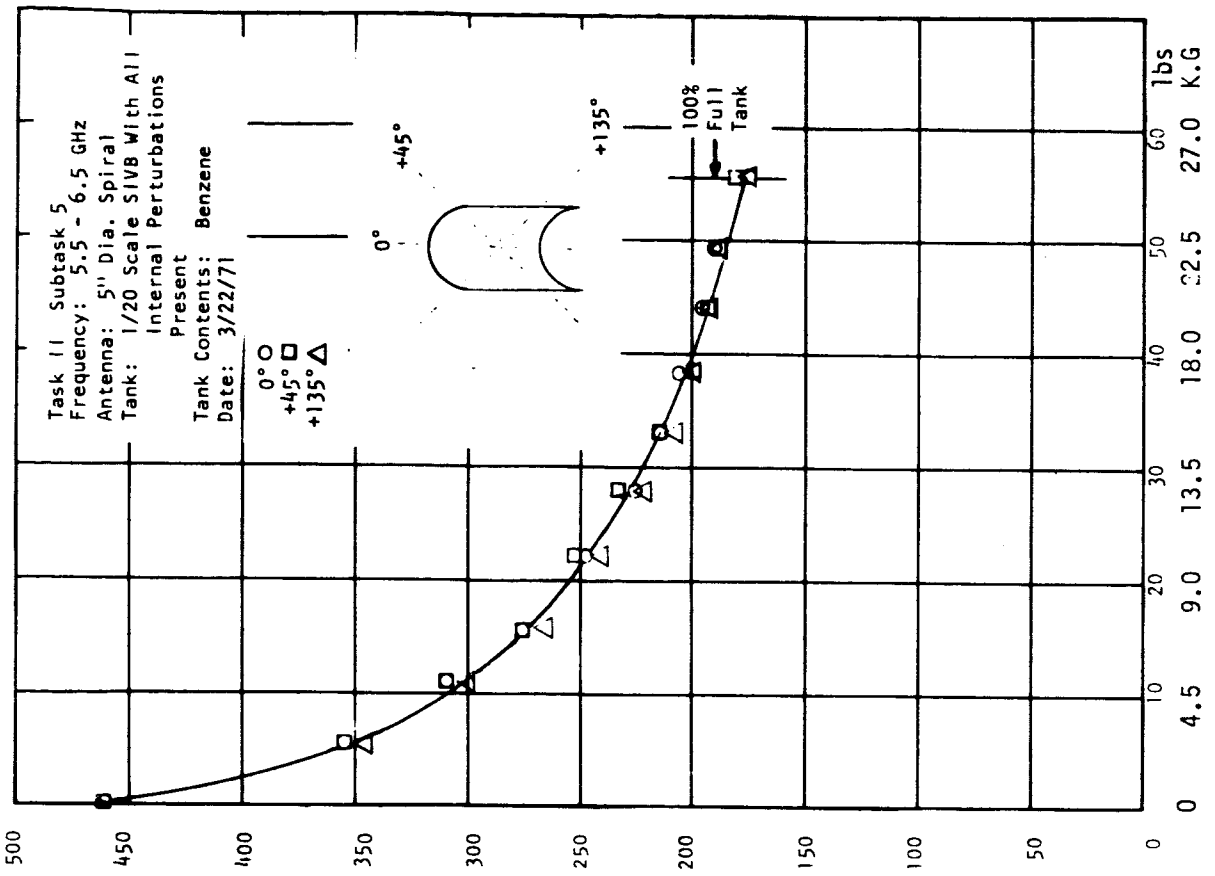


Figure 5.- BENZENE MASS

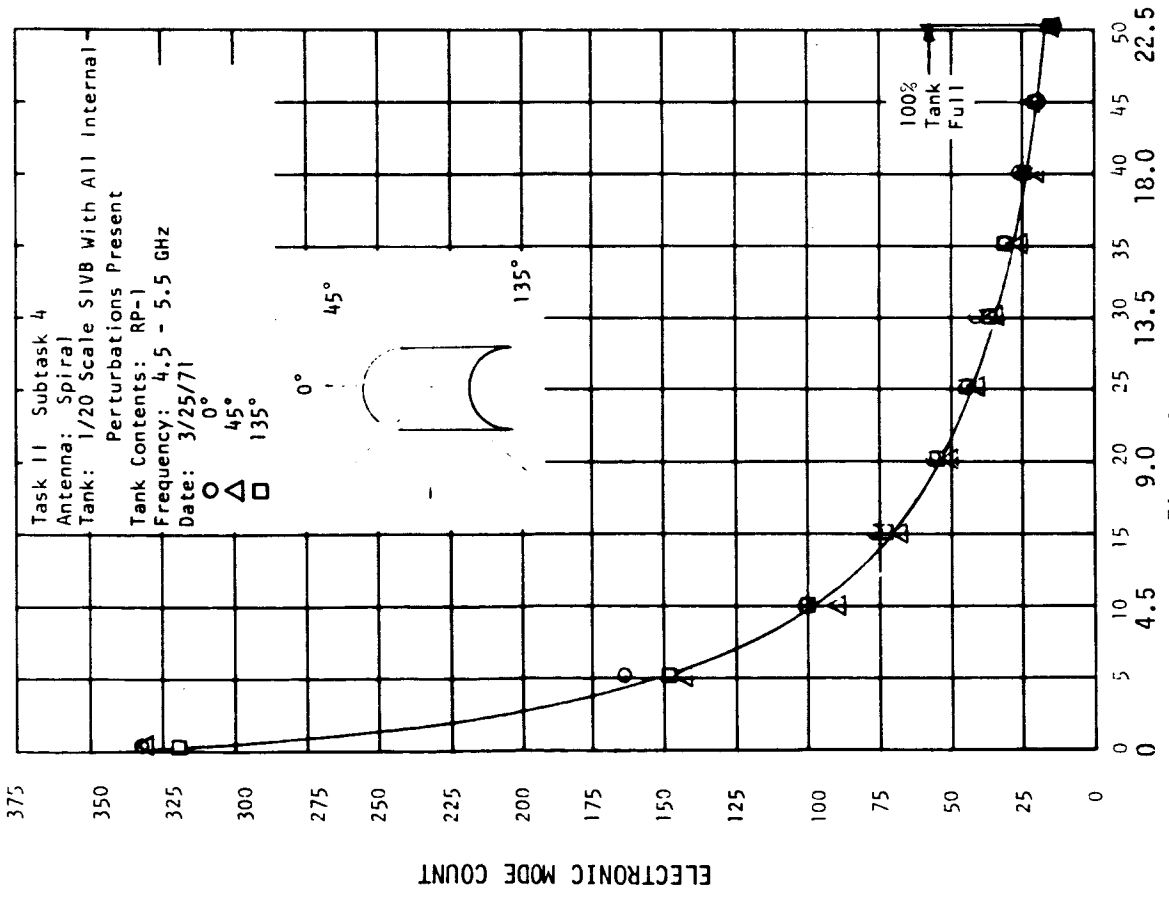


Figure 4.- RP-1 MASS

LOX loading data can be seen in Figures 6 and 7 for two different tank geometries and Liquid Nitrogen loading data can be seen in Figure 8, and LOX data of a different frequency in Figure 9. The low loss characteristics of LN<sub>2</sub> make it more suitable to gaging with an ascending mode count as the quantity increases. High loss fluids are generally more suitable to decreasing slope or decreasing mode count with increasing mass.

The tank probe used to gather the Benzene data can be seen in Figure 10. The tank, a 1/20 scale LH<sub>2</sub> tank can be seen in Figure 11 with the top dome shown in Figure 12.

The top dome of a 1/10 scale SIVB LH<sub>2</sub> tank, used for LOX and LN<sub>2</sub> tests can be seen in Figure 13 with RF probe installed. The tank probe ready for installation can be seen in Figure 14. Figure 15 shows the packaged electronics (RF section at the left and electronic processor section at the right) for a recent breadboard system.

#### Error Analysis

With the present state of low level sophistication in the prototype systems tested, the repeatable accuracy of the spiral antenna and breadboard electronics is as follows:

0 - 30% fill	± 1%
30 - 50% fill	± 1.5%
50 - 70% fill	± 1.8%
70 - 100% fill	± 2.7%

This accuracy is based on using 99% of the data points taken during testing of the latest breadboard system and compares the electronic processor output signal with the reading on the weighing scales 24 inch dial.

Methods are being studied to improve the accuracy at the full end by mode count feedback loops to change the RF input frequency to improve the full end sensitivity. The objective is 1.5% maximum error (% of full reading) from empty to full.

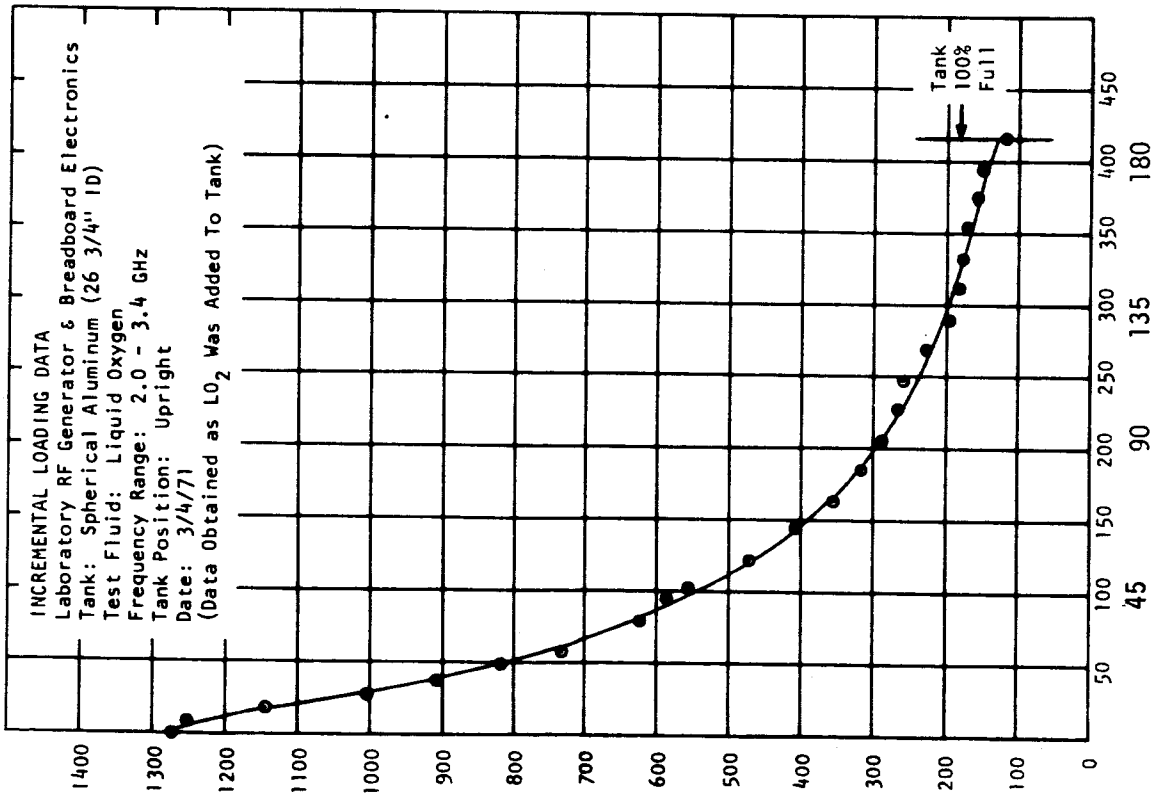


Figure 6.- LOX MASS

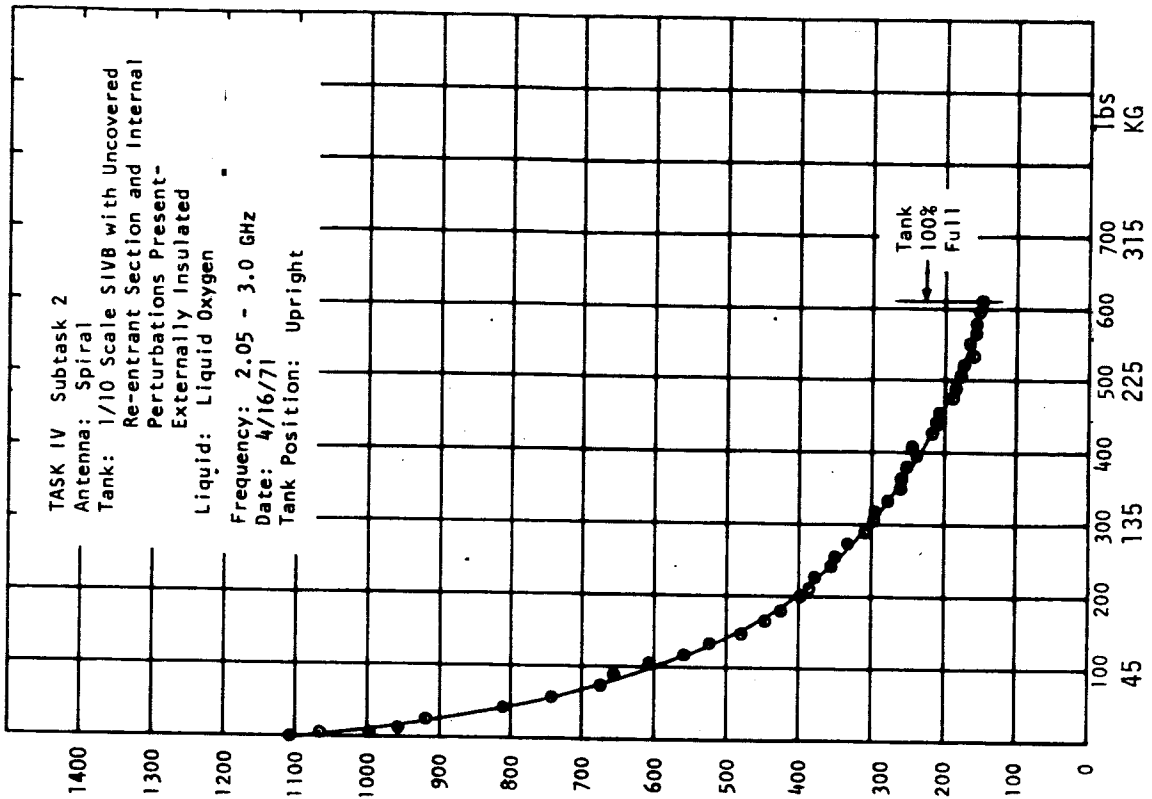


Figure 7.- LOX MASS

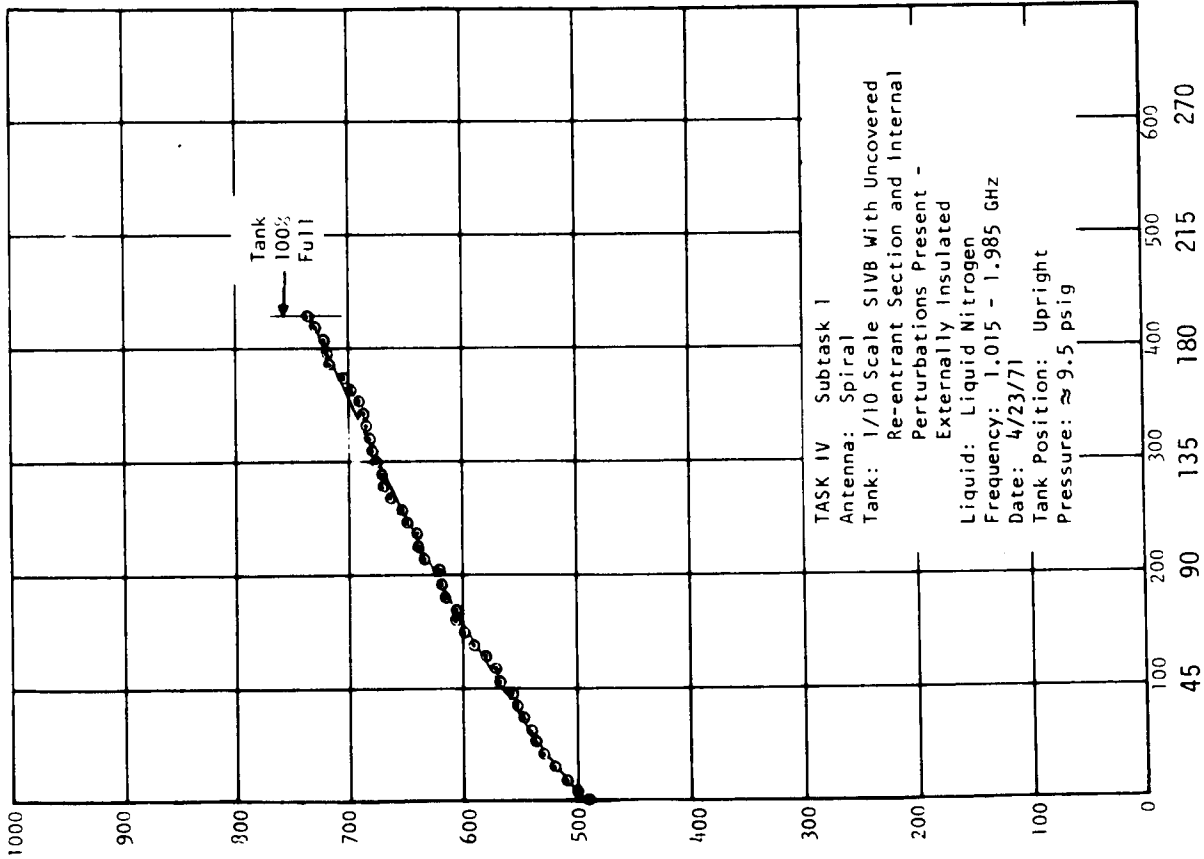


Figure 8.- LH<sub>2</sub> MASS

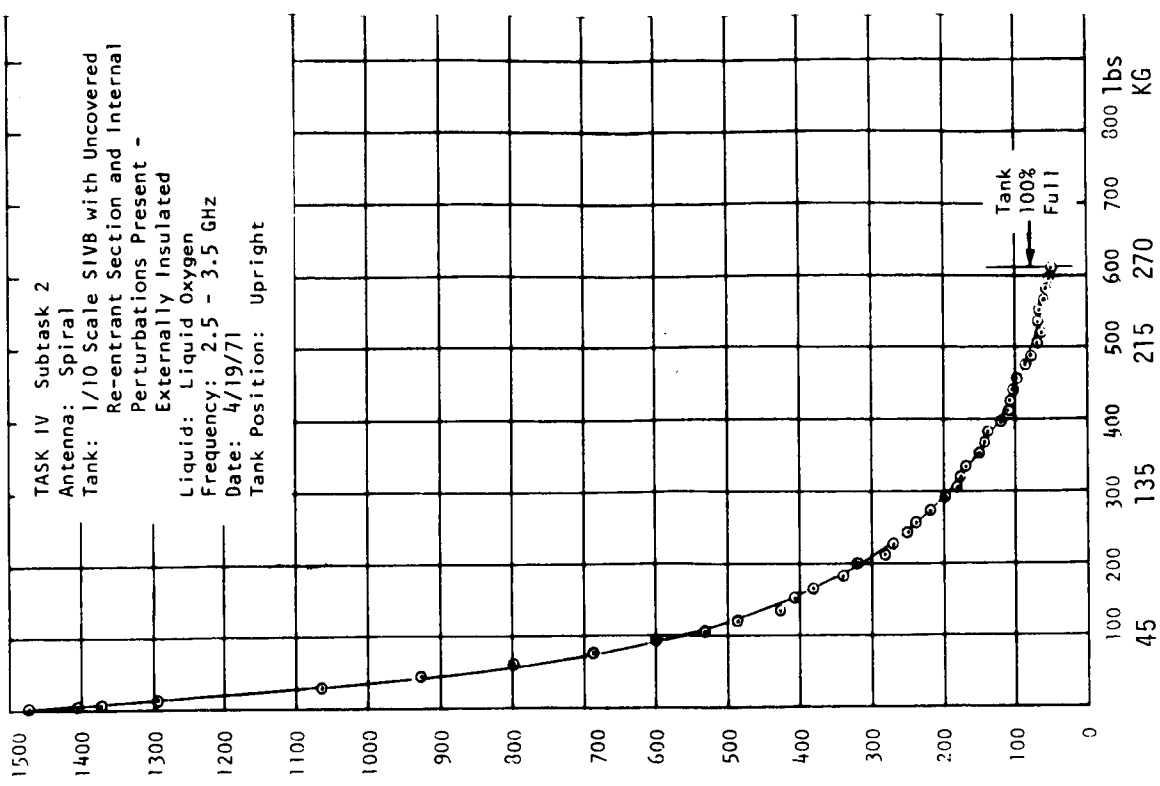


Figure 9.- LOX MASS



Figure 10.- RF GAGING PROBE COMPLETED READY FOR INSTALLATION IN THE 1/10 SCALE SIVB TANK



Figure 11.- 1/20 SCALE SIVB TANK USED FOR RF GAGING STUDIES WITH J-2 TEST STAND INTERNAL HARDWARE





71453CC116-1

Figure 13.- 1/10 SCALE SIV<sub>B</sub> TANK TEST  
SETUP FOR BENZENE  
GAGING TESTS



71453CC500-5

Figure 12.- 1/20 SCALE TANK DOME WITH  
PROBE INSTALLED

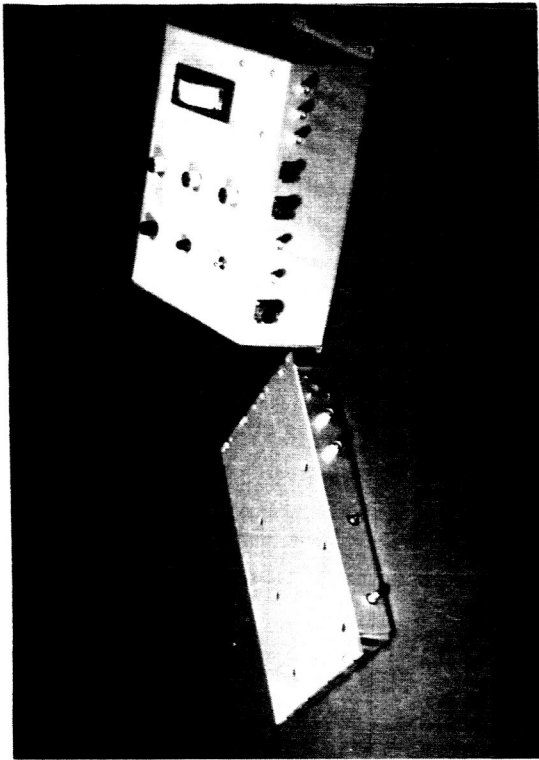


Figure 15.- PACKAGED ELECTRONICS (BREADBOARD)  
TYPICAL FOR 1/10 SCALE SIVB SYSTEM



Figure 14.- RF GAGING PROBE USED FOR 1/10  
SCALE SYSTEM CRYOGENIC TEST

## CONCLUSIONS

Test Results and Analytical Data now available lead to the following conclusions:

- 1) The RF Gaging technique has been proven feasible for both cryogenic fluids such as LOX, and for various non-cryogenic dielectric fluids.
- 2) RF Gaging technology has advanced to a point where the performance of the system can be predicted for most types of spacecraft tanks and fluids. Scaling laws have been developed which permit the prediction of operating characteristics of the RF Gaging System when used with full-size shuttle vehicle type tanks.
- 3) Solid state RF hardware is now available for construction of ground test and flight test systems and allows more direct fabrication and tests of breadboard systems for performance and accuracy evaluations.

# **SHUTTLE SENSORS**

**VERNON C. MELLIFF, JR.**

**MANNED SPACECRAFT CENTER  
HOUSTON, TEXAS**

**AND**

**ARTHUR T. LINTON**

**THE BOEING COMPANY  
HOUSTON, TEXAS**

## SUMMARY

The typical Shuttle environments that constrain the performance of the required Shuttle sensors are described. The maximum environmental temperatures for sensors are expected to be  $-300^{\circ}\text{F}$  to  $+650^{\circ}\text{F}$  ( $-184^{\circ}\text{C}$  to  $+344^{\circ}\text{C}$ ) for large portions of the wing area and fuselage. The new high temperature materials present many unique sensor design problems with regard to sensor installation and calibration. Operational requirements of the Shuttle sensors are much more stringent than of previous spacecraft — life expectancy is 10 years, 100 missions between major repair work, and rapid turn-around time between missions (2 weeks limit).

With consideration of the Shuttle requirements, this paper discusses pressure, temperature, strain, acceleration, vibration, and acoustic transducers; their inherent design deficiencies; and suggested methods and approaches for solution of these deficiencies.

## INTRODUCTION

This paper will address some of the more significant constraints on sensor technology relative to the Space Shuttle Program. No attempt will be made to cover all of the constraints on the Shuttle sensors, nor will the paper discuss all the required types and their applications.

The sensors referred to in this paper are the types which are required to verify the vehicle performance during the flight test phase and also to provide information for the operational control of the vehicle. These sensors will be required to perform for many missions over a relatively long period of time and under very severe environmental conditions.

This paper is a summary of the preliminary requirements for Shuttle sensors; and the quantity, location, and temperature environment limitations are indicated.

Next, we will discuss the significant constraints that will influence the need for sensor development, such as high temperature, advanced materials, and program requirements. Following that, I will discuss five or six sensors most commonly used, their limitations, and some possible solutions. Finally, we will present some overall conclusions.

# **OUTLINE**

- **SUMMARY REQUIREMENTS**
- **SIGNIFICANT CONSTRAINTS**
  - **HIGH TEMPERATURE SHUTTLE ENVIRONMENT**
  - **SHUTTLE MATERIALS**
  - **PROGRAM REQUIREMENTS**
- **SPECIFIC SENSOR CONSIDERATIONS**
- **CONCLUSIONS**

### SHUTTLE SENSOR REQUIREMENTS

The following chart is shown to give you an understanding of the magnitude of the problem. We have shown three general vehicle locations with the expected quantity of transducers in each location. You will note that the majority of the sensors will be in the moderate to severe environments, such as the wing, fuselage areas, and the surface.

The Shuttle may use off-the-shelf sensors for approximately one-half these requirements, providing they are judiciously selected and evaluated with respect to their installation. Furthermore, technology does exist to support the other sensor requirements, but the application of the technology to the specific sensor hardware will require development.

The sensor cost is a concern. An average sensor may cost \$1,000; however, with the addition of wiring, signal conditioning, installation effort, calibration, test, checkout, maintenance, and documentation, the cost may well run to 10 times this amount. The total cost for Apollo measurements was over \$100 million, and with the Shuttle preliminary requirements projected four times larger than on Apollo, costs could be significant.

# PRELIMINARY SHUTTLE SENSOR REQUIREMENTS

SENSOR TYPE	CABIN 0° TO 200° F	WING/FUSELAGE -300° TO 650° F	SURFACE -300° TO 3000° F
PRESSURE	28	567	
TEMPERATURE	98	2078	856
STRAIN		60	146
VIBRATION & ACCELERATION	2	178	40
ACOUSTICS	2	120	
FORCE	4	8	
DEFLECTION		6	
SPEED (RPM)	12	10	
RADIATION	2		
HUMIDITY	3		
PARTIAL PRESS	5		
QUANTITY	6	10	
FLOW	8	8	
PH	4		
TOTALS	<u>174</u>	<u>3045</u>	<u>1042</u>



# SENSOR CONSTRAINTS

- HIGH TEMPERATURE SHUTTLE ENVIRONMENT
- SHUTTLE MATERIALS
- PROGRAM REQUIREMENTS

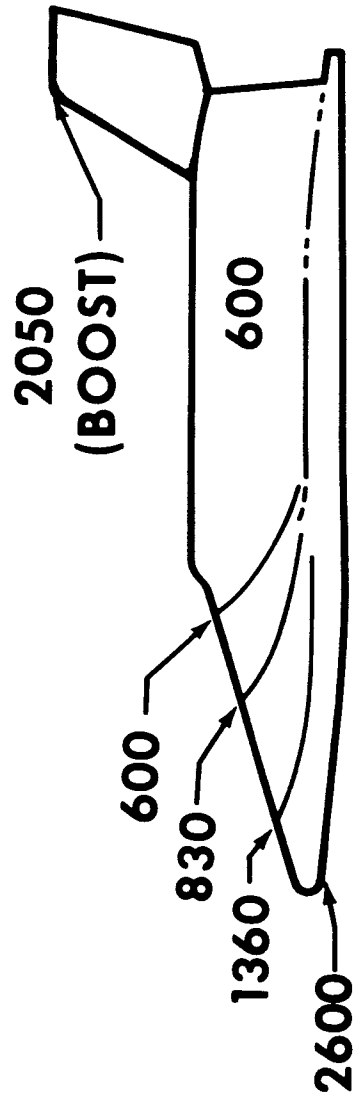
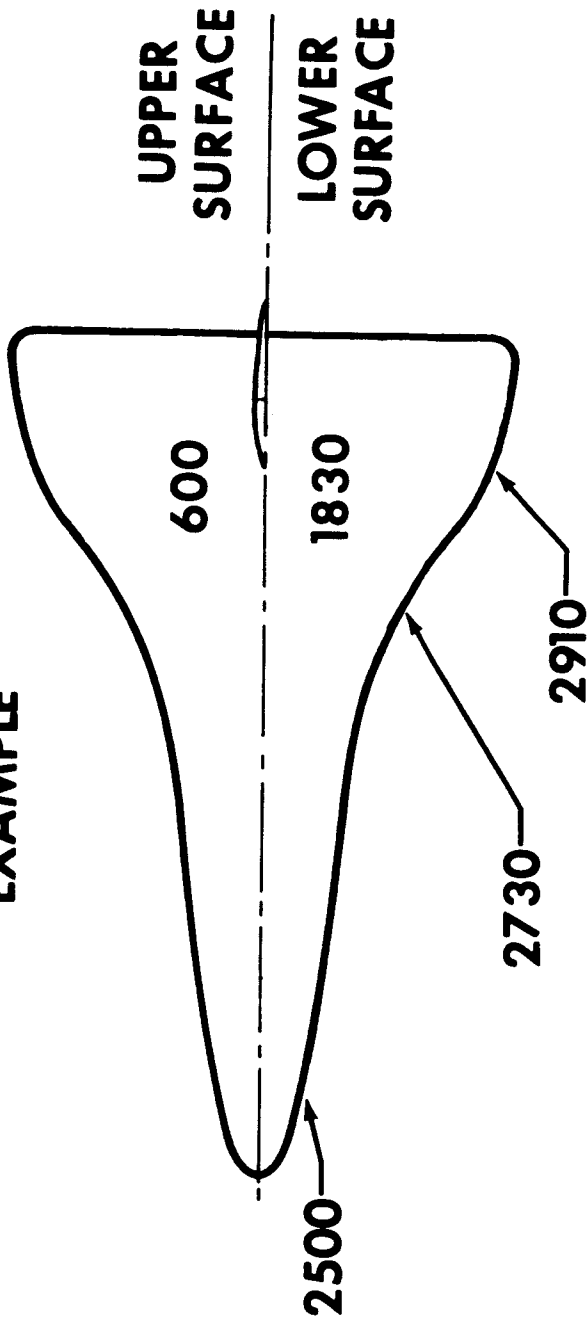
## MAXIMUM SURFACE TEMPERATURES

The maximum expected surface temperatures shown are proposed by one of the contractors for the Shuttle's study phase. Although the temperatures may deviate from this, it does provide an example of probable conditions.

You will note the upper surface will be near 600°F (316°C) and the bottom surface near 1830°F (999°C) for the entry phase of the mission. The nose stagnation temperature reaches 2600°F (1404°C) and the leading edge a maximum of 2910°F (1599°C). During the boost phase, the vertical fin tip reaches a peak of 2050°F (1121°C).

# MAX SURFACE TEMPERATURES °F

## EXAMPLE



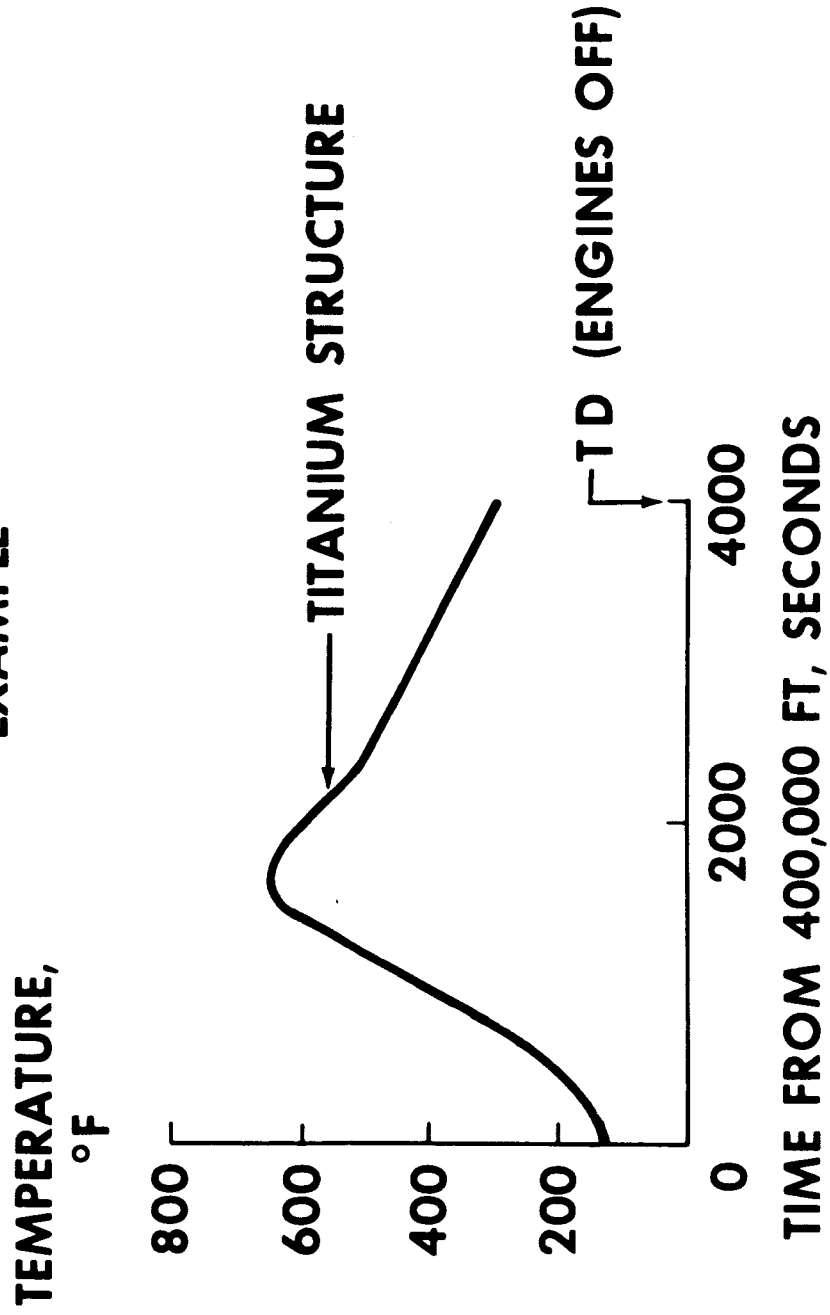
SUBSTRUCTURE TEMPERATURE RESPONSE

The following slide represents the internal responses due to the upper surface thermal environment during entry. The response from the lower surface is almost identical, or should be if the thermal design is correct, even though the temperatures are much more severe.

The prime data are required during the first 15 to 20 minutes of entry, which is in the area of the the most rapid environmental change, and thus have the greatest impact on the transducer accuracy. Pressure measurements, for example, will be affected because of unequal thermal conductivity within the sensor producing mechanical distortion.

# SUBSTRUCTURE ENTRY TEMPERATURE RESPONSE

## EXAMPLE

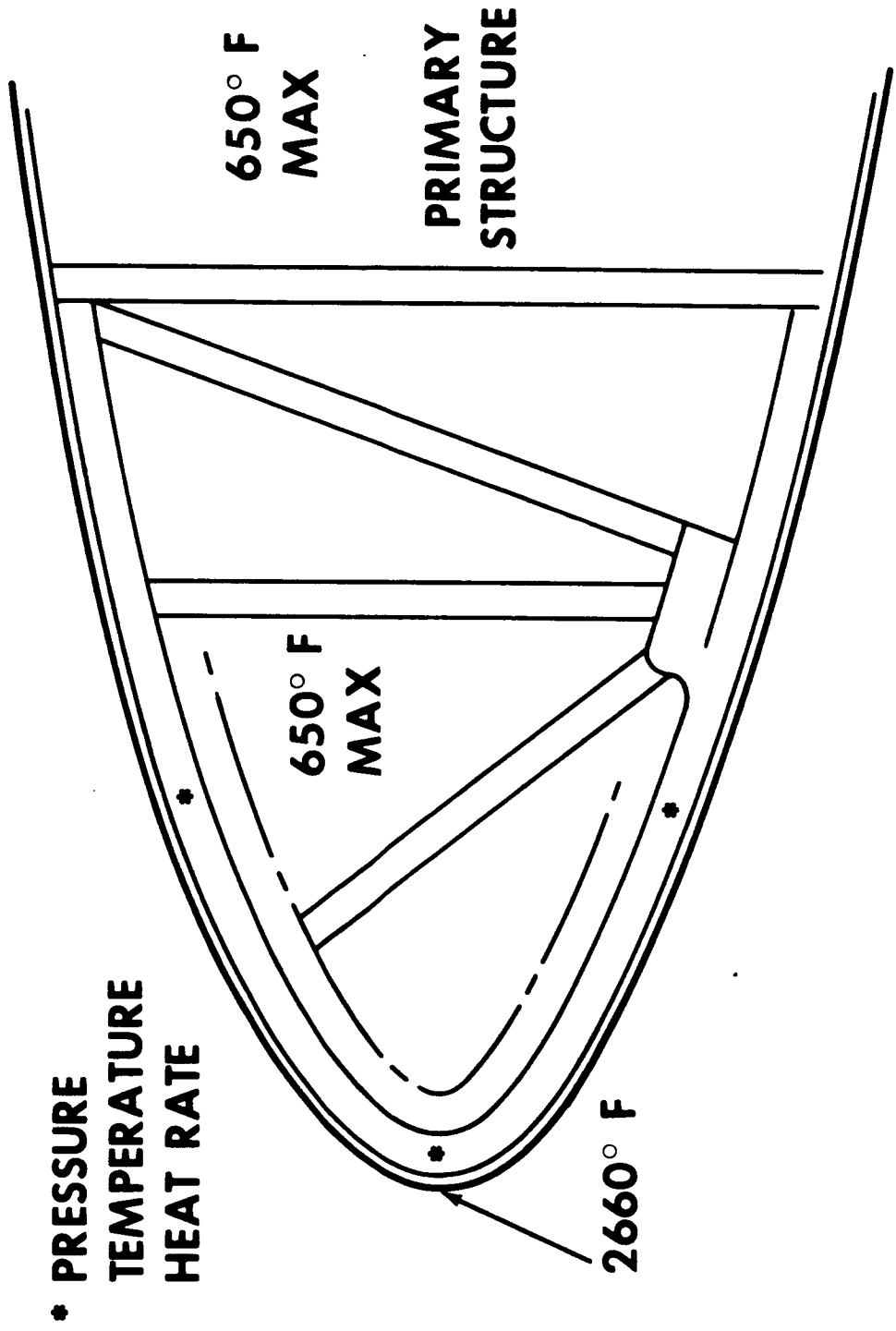


#### WING LEADING EDGE

Indicated by the following slide are typical sensor locations as may be required by aerothermal engineering. The internal structure design is presently being based upon a maximum of 650°F (343°C), not only at the leading edge, but throughout the entire wing area.

The major problems are, again, the method, process, and procedures to install sensors such as pressure transducers, thermocouples, and calorimeters into these new high temperature materials. The integrity of the instrumentation must be verified in that it will not weaken or destroy the basic structure. Also, the effect of the instrumentation mass and weight must be determined with respect to the materials, such as titanium or columbium. Another concern is that signal conditioning cannot be integrally installed with transducers in the wing unless a means is developed to operate solid-state devices at these temperatures. This is a big change from the Apollo transducers, which primarily had signal conditioning with or adjacent to the transducer.

# WING LEADING EDGE

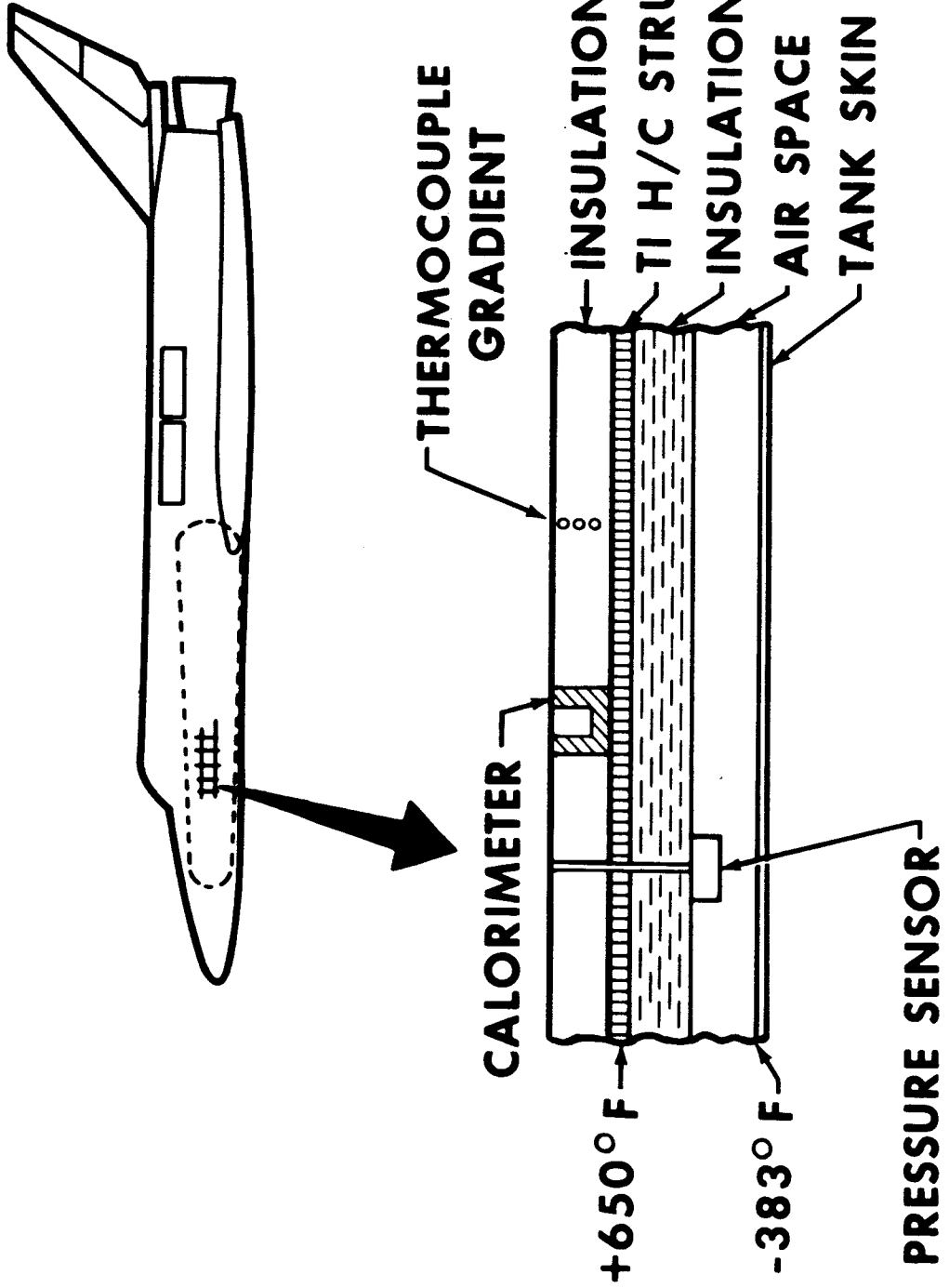


#### FUSELAGE TANK AREA

The following slide shows some examples of sensor locations in the fuel tank area which are in a most severe environment. These temperatures represent the best available information with the configuration presently defined.

During the boost or launch phase, the tank surface is expected to be  $-300^{\circ}\text{F}$  ( $-184^{\circ}\text{C}$ ) before launch, with the titanium honeycomb structure going to  $+150^{\circ}\text{F}$  ( $66^{\circ}\text{C}$ ) in 200 seconds after launch. Before entry, the tank skin could be as low as  $-383^{\circ}\text{F}$  ( $-231^{\circ}\text{C}$ ), with the titanium structure going to  $650^{\circ}\text{F}$  ( $343^{\circ}\text{C}$ ) about 1500 seconds after the initiation of the entry phase.

# FUSELAGE TANK AREA



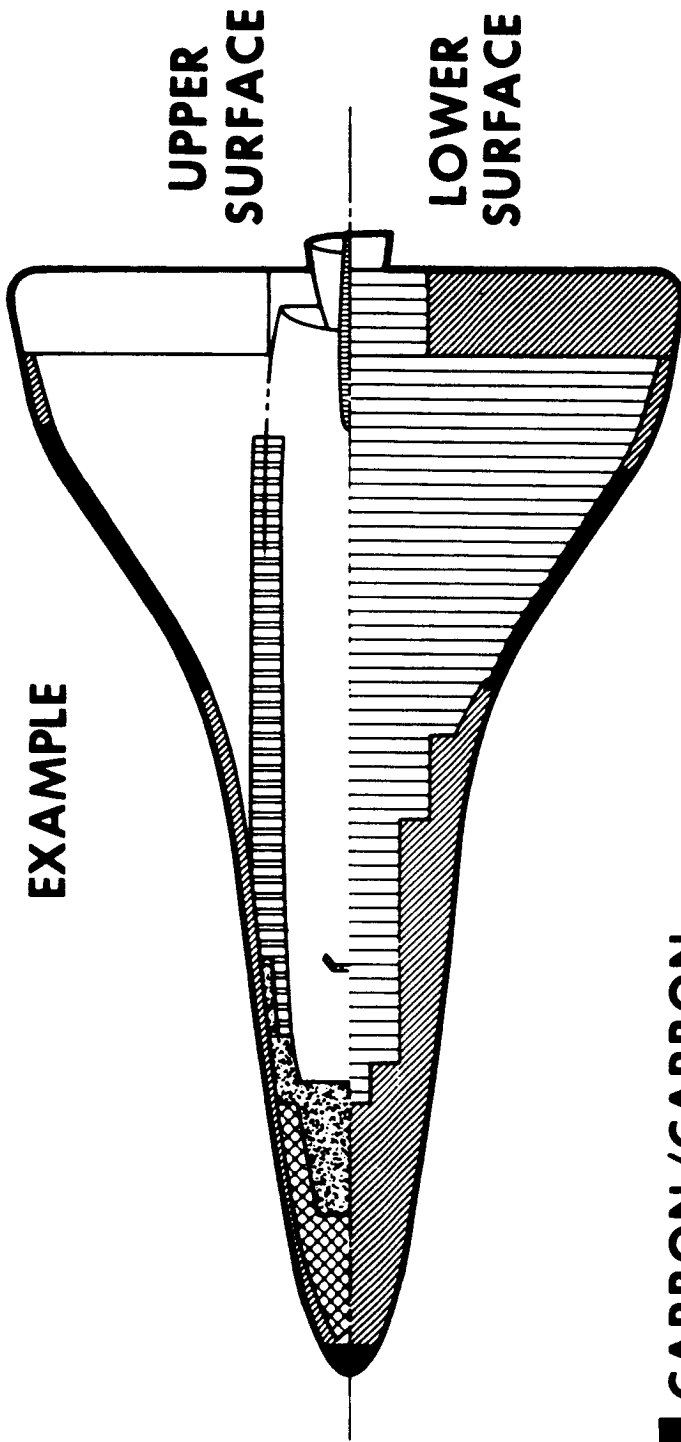


#### PROPOSED SURFACE MATERIAL DISTRIBUTION

The instrumentation designer on the Shuttle is faced with a large variety of exotic materials. Problems of how to install thermocouples, strain gauges, and calorimeters in, on, and through these materials present challenging installation designs. Many of these metals are coated with materials that cause additional problems, such as the columbium metal which has a chromic oxide coating. Each of these new materials will undoubtedly require a careful design and verification test program to insure proper instrumentation performance. These surface materials imply another problem for the instrumentation people in that each material may require sensors matched to the material characteristics, which will further multiply the sensor types. This is not a happy thought when we are trying hard to promote commonality and cost effective design.

# SURFACE MATERIAL DISTRIBUTION

EXAMPLE



- |   |                            |   |                           |
|---|----------------------------|---|---------------------------|
| ■ | CARBON / CARBON            | ■ | INCONEL 718-SHINGLES      |
| ▨ | COLUMBIUM (FS-85) SHINGLES | ▨ | RENE' 41-HOT STRUCTURE    |
| ▧ | HASTELLOY X SHINGLES       | □ | TI (6AL-4V)-HOT STRUCTURE |
| ▩ | RENE' 41-SHINGLES          | ▩ | TI (6AL-4V)-SHINGLES      |

## PROGRAM REQUIREMENTS

The program requirements establishing a 10-year operational life for a vehicle is extremely difficult for the Shuttle sensors. With multiple flights over an extended period of time, many failures of sensors will occur unless adequate preventive measures are taken. Although sensors have been used on experimental aircraft during their test programs, in most cases the operational life of these units has been relatively short (under 5 years) and not required to meet the unique environments anticipated for the Shuttle. The present flight test plans establish a 2-year period for the horizontal test phase (in atmosphere) and a 2-year period for the vertical test phase (orbital). Since most of the sensors are for the test phase, the flight test plans dictate a 2-year life for these sensors. Also, the 100-mission requirement implies about a 2-year period between major maintenance work on the Shuttle. Therefore, accessible sensors could be replaced during these periods if it were mandatory for the mission. Some sensors will be inaccessible and will require special attention for design life, stability, and calibration. Strain gages have a definite operational life limit and require consideration in flight test planning. For example, based upon X-15 flight test experience, it is estimated that over 20 percent of the Shuttle strain gages (5000 micro-strain type) will fail before 2 years of operation; therefore, a concept of excess measurements for strain must be considered.

Downtimes during a flight test program are costly and unproductive because essentially the program is waiting for the data to verify the design. Range changes to measurements are the most common, usually because the initial selection is an approximation. The designers should accept this challenge to develop transducers with multiple ranges, selectable at the transducer or preferably at the signal conditioner, with no increase in cost. Of course, this would add to the complexity of the system, but on some critical Shuttle measurements, it may not only be desired but mandatory. Also, there will be areas of critical measurements that will be inaccessible. In these areas, it would be desirable to install redundant transducers to insure results in the event of a transducer failure.

The 2-week turn-around time between landing and launch will stress simplicity and efficiency in performing calibration, minor modification, and repair of sensors. There appears to be no clean-cut and cost effective method of performing the Shuttle sensor calibration. There will probably be many different calibration procedures based on the type of sensor, location, criticality, and design stability.

Accuracy requirements should be very carefully reviewed because unnecessarily severe requirements could be a significant cost driver. Most measurements are required during a relatively short span of the mission. The accuracy tolerance should be specified for that period and verified to that environment.

## **PROGRAM REQUIREMENTS**

- **LIFE - 10 YEARS**
- **100 MISSIONS - MINIMAL REPAIR**
- **RAPID TURN-AROUND BETWEEN MISSIONS**

## PRESSURE TRANSDUCERS

Most of the pressure measurement requirements for Apollo have been met by utilization of the strain gage diaphragm type pressure transducer with integral or separate signal conditioner and power supply. Other test programs have utilized variable reluctance, linear variable differential transformers, and piezoelectric principles in the basic transducer.

Strain gage types, specifically vacuum-deposited thin-film strain gage transducers, and deposited semi-conductor gages appear to offer the most potential. The major problems are caused by temperature changes resulting in uncompensated diaphragm deflections and changes in lead wire resistance. There are methods for reducing the effect of resistance changes. These include utilization of constant current excitation sources and the installation of additional wiring to record the actual voltage at the transducer. These methods will provide very accurate data over the temperature range expected in the Shuttle interior; however, when temperatures are rapidly changing, as during boost and entry, unacceptable errors may result. Recent developments in quartz diaphragms indicate that little development may be required to provide transducers for higher temperature environments with more rapidly changing temperatures than presently available.

Also, consideration should be given to using transducer thermal control to minimize measurement errors due to rapidly changing temperatures. Approaches that might be considered are:

- a. Providing individually controlled heating to maintain temperatures at maximum operating temperatures.
- b. Design of individual or small group evaporative type coolers operating on the water boiler principle. This would consume a considerable quantity of water and be subject to human error.
- c. Cooling by means of latent heat of fusion. This method requires use of a material having a suitable low melting point so that it absorbs heat without appreciable temperature increase until all of the material melts.

Very low range pressure transducers will experience diaphragm damage when exposed to the ambient pressure. A limited diaphragm displacement transducer is, therefore, required.

The presently available pressure transducers will operate satisfactorily up to a temperature of about 650°F (344°C). But where it is necessary to monitor pressure at the skin surfaces, a source tube must be used to separate the transducer from the severe thermal environment. Shock tube calibration will then be required to determine the measurements transient response. The transient response of a diaphragm transducer depends upon the cavity volume of the transducer and the diameter and length of tubing which connects the transducer to the pickup point in the system being measured. This latter factor is an additional source of error. The sensor manufacturer will have to work closely with the vehicle design engineers to develop an optimum mechanical configuration to achieve the response required in particular applications.

# PRESSURE

- RANGE
  - 0 TO 1600 PSIA
- IMPACT
  - MOST REQUIREMENTS SATISFIED  
WITH OFF-THE-SHELF SENSORS
  - PRESENT CAPABILITY 650° F (STATIC)
- PROBLEM AREAS
  - RAPID TEMPERATURE CHANGE
  - OVERSTRESS OF DIAPHRAGM AT LOW RANGE
- POSSIBLE SOLUTIONS
  - INTERNAL HEATERS
  - LIMIT DIAPHRAGM DISPLACEMENT

## TEMPERATURE

The skin temperature sensors will be subjected to the most severe thermal environment on the vehicle. Therefore, this section will concern itself primarily with the design of sensors to meet this severe environment. Design selection will favor thermocouples since development problems of thermocouples are considered to be more amenable to solution than for resistance element surface sensors, because the resistance element sensor utilization would require the solution of the problems of bonding to exotic materials and thermal insulation resistance degradation.

Skin surface temperatures on the Shuttle orbiter are expected to reach temperatures in the order of 3000°F (1480°C) during boost and/or entry. Similar thermal conditions were anticipated on the X-20A (Dyna-Soar) vehicle. Temperature measurements were performed on the Apollo Command Module heat shield using thermocouples at temperatures in excess of 3000°F (1480°C).

The Dyna-Soar initial thermocouple design consisted of a tungsten/tungsten-26% rhenium (W/W-26 Re) thermocouple insulated with compacted magnesium oxide and clad with 0.065-inch OD tantalum. The junction was formed by swaging a molybdenum plug into the end of the sheath between the thermocouple wires. The installation was performed by first swaging a molybdenum rivet into a dimpled hole in the skin. The rivet was then drilled, the transducer inserted, and the rivet crimped to hold the thermocouple in place. For oxidation protection, the rivet and the transducer were individually disilicide coated before installation and then the complete assembly was coated after installation.

It was found that the pure tungsten leg of W/W-26 Re became brittle after heating. Tests made with samples of W-5 Re/W-26 Re showed poor ductility repeatability from batch to batch, in addition to discontinuities in the wires. As a result of these evaluations, Pt/Pt-13 Rh was selected as the prime material. The Pt/Pt-13 Rh combination was chosen because it has a higher thermoelectric output than Pt/Pt-10 Rh, although it is slightly under the minimum specified output of 20 millivolts at 3000°F (2968°C).

The Apollo Program employed W/W-26 Re thermocouples also. No problems were encountered because of the relatively short temperature cycle time.

From the foregoing discussion, it is evident that extensive development effort has been expended on high temperature thermocouples. No difficulty should be encountered in the selection of a thermocouple to be compatible with the expected Shuttle environment. A temperature measurement system accuracy of 5 percent may be attained by thermocouple calibration prior to installation. The measurement channel characteristics are then adjusted to match that of the thermocouple calibration. One area which may require development is the installation techniques of thermocouples on the Shuttle skin. However, because of industry experience in thermocouple installation, this is not believed to be unsolvable.

## **TEMPERATURE**

- **RANGE**
  - **-440° TO +2700° F**
- **IMPACT**
  - **MEASUREMENTS ON HEAT SHIELD SURFACES**
- **PROBLEM AREAS**
  - **MOUNTING IN MATERIAL**
  - **INTEGRITY OF STRUCTURE**
  - **SENSOR DISTURBANCE ON NATURAL ENVIRONMENT**
- **POSSIBLE SOLUTION**
  - **DESIGN AND FABRICATE AS AN INTEGRAL PART OF HEAT SHIELD ASSEMBLIES**



## STRAIN

The measurement of structural strain is complicated by the high temperature environment and the limited industrial experience in the installation of strain gages on exotic materials.

Conventional high temperature strain gages are limited to approximately 600°F (316°C) for static strain measurements, and 1500°F (816°C) for dynamic measurements. For dynamic measurements, a higher temperature may be tolerated because the temperature induced drift is of low frequency compared to the data and may then be filtered out. The upper temperature limit is primarily determined by the loss of insulation resistance of the leads to each other and to ground. For example, the insulation resistance of a high temperature, weldable sheathed gage (Microdot SG 425) has a resistance to ground of 50 megohms at 1210°F (655°C) but drops to 8000 ohms at 1470°F (795°C).

During development of the X-20, several gages were investigated for operation at 1600°F (872°C). They included a weldable gage, free filament ceramic bonded gage, fiber glass backed gage, and a sprayed-on gage. None were able to withstand the temperature environment.

Present state-of-the-art gages can be used up to 1500°F (816°C). However, for higher temperatures, development work is required. Also, investigation is required in gage bonding on exotic materials. Gage bonding to exotic materials is probably the single most significant problem which must be solved before strain gages can be used on the Shuttle.

An alternate approach to measuring strain in the high temperature areas is the use of displacement transducers between two fixed reference points. The problem of gage bonding is thereby eliminated. The displacement transducer may be mounted a finite distance from the skin, which places the transducer in a less severe thermal environment. Typical candidate transducers are potentiometric, capacitive, or variable inductance. Further trade studies are necessary to determine which of these alternates provides the most cost-effective, accurate, and reliable approach to Shuttle structural strain measurement.

The problem of gage life is another factor for consideration. It has been industry's experience to expect large numbers of strain gage failures during a flight test program. However, failure mode examinations reveal the failures to be usually due to bond or lead failure for low range strain gages --- rarely gage fatigue. For high range gages, fatigue failure is quite common. This again points to development required in the art of gage installation or the use of displacement transducers to measure strain.

## **STRAIN**

- **RANGE**
  - **±5000 AND ±100,000 MICRO-STRAIN**
- **IMPACT**
  - **±5000 MICRO-STRAIN CAPABILITY**
    - 600° F STATIC**
    - 1500° F DYNAMIC**
  - **±100,000 MICRO-STRAIN CAPABILITY 150° F**
- **PROBLEM AREAS**
  - **GAGE BONDING TO EXOTIC MATERIALS AT HIGH TEMPERATURE**
  - **BASIC MATERIAL ELASTIC LIMIT**
- **POSSIBLE SOLUTION**
  - **EXPAND TEMPERATURE CAPABILITY OF DISPLACEMENT SENSOR**

#### LINEAR ACCELEROMETERS

A large number of low frequency accelerometers will be required to conduct the flutter analysis program in the several flight regimes. For measurements inside the environmentally controlled areas, the presently used servo-type accelerometers will provide the required accuracy of  $\pm 2$  percent full scale from 0 to 50 Hz. Some development effort will be required to achieve 2 percent accuracy below 2 Hz. These transducers at cabin temperatures are capable of excellent static and low frequency accuracy, and the main source of uncertainty will be in calibration.

For measurements outside the environmentally controlled areas, the situation is different because of the temperature environment and, again, calibration limitations which in this case will have to cover frequencies up to 20 Hz or higher for flutter tests. The presently used servo-type transducers will not survive the expected temperature environment in their current configuration.

For low frequency measurements, the servo-type accelerometer offers a possible solution, using some form of temperature conditioning. Several approaches were suggested in relation to the pressure transducer problem. Here again, development effort will be required to meet performance requirements.

# **LINEAR ACCELEROMETERS**

- **RANGE**
  - **±20 g (0 - 20 Hz)**
- **IMPACT**
  - **PRESENT CAPABILITY 325° F**
- **PROBLEM AREAS**
  - **ELECTRONIC THERMAL LIMITS**
  - **MATERIAL THERMAL CHARACTERISTICS**
- **POSSIBLE SOLUTIONS**
  - **THERMAL CONTROL**

### VIBRATION

For high frequency vibration measurements, the piezoelectric transducer appears to be the most promising. In the past, the maximum temperatures for piezoelectric transducers have primarily been limited by ferroelectric Curie temperatures and crystal phase changes. Quartz, which is often used, is limited to about 500°F (260°C). High piezoelectric strain constants are extremely important to provide adequate transducer output and small size. Accelerometers must be small and light to minimize their affect on structure motion. High bulk resistivity is also critical since the resistance of insulating materials decreases exponentially with temperature increase. A general rule is that resistance drops by a factor of 10 for each 212°F (100°C) increase. Thus, with a temperature increase from 70°F (20°C) to 1330°F (720°C), the resistance would drop by a factor of 10 million.

Present day calibration methods limit vibration sensor calibration to approximately 10 KHz. Experimental methods exist for calibrating in excess of 10 KHz, but refinements will be required to adapt these methods for use in industry.

Recently developed materials show promise of meeting the requirements for Shuttle vibration transducers. For example, PIEZITE P-15 piezoelectric material has a Curie temperature above 1750°F (954°C). Charge sensitivity varies little from room temperature to at least 1500°F (816°C), and the output is equivalent to those materials now used in accelerometers at lower temperatures. It is anticipated that further developments with this and other types of materials will permit development of suitable accelerometers for specific Shuttle requirements.

# VIBRATION

- RANGE
  - 20 Hz TO 16 KHz
- IMPACT
  - PRESENT CAPABILITY TO 650° F
  - MEASUREMENTS NEAR HEAT SHIELD SURFACES 1500° F
- PROBLEMS
  - HIGH TEMPERATURE EFFECTS ON PIEZOELECTRIC MATERIALS
  - INSULATION RESISTANCE DECREASE
  - HIGH FREQUENCY CALIBRATION
- POSSIBLE SOLUTION
  - HIGH TEMPERATURE PIEZOELECTRIC MATERIAL BEING DEVELOPED

### ACOUSTICS

Acoustic sensors are available which will adequately measure the sound level in the cabin. A capacitance type sensor may be used over the frequency range of 50 to 10,000 Hz with a required dynamic amplitude range of 40 dB.

However, acoustic measurements are also required in areas outside the cabin for structural fatigue studies. This imposes very severe temperature and differential pressure requirements on the sensor. Current technology dictates the use of a piezoelectric transducer with active cooling to satisfy the severe environmental condition, but the cost and weight penalty would be great. It is evident that considerable effort will be required to develop a sensor which will be compatible with the Shuttle environment. Recently developed high temperature piezoelectric material may be candidate for use in advanced high temperature acoustic sensors.

The calibration of an acoustic system is a complex procedure. The system must be calibrated prior to vehicle installation over the required frequency range at multiple sound pressure levels. Calibration must also be performed at representative operating temperature and pressure. A pressure-sensing feedback loop may be required to be incorporated in the sensor to provide pressure compensation.

# ACOUSTICS

- RANGE
  - UP TO 140 dB CABIN
  - 140 - 170 dB STRUCTURE
- IMPACT
  - CAPACITIVE TYPE SUITABLE FOR CABIN
  - PIEZOELECTRIC TYPE FOR STRUCTURES
- PROBLEM AREAS
  - VARYING AMBIENT PRESSURE
- POSSIBLE SOLUTION
  - PRESSURE SENSING FEEDBACK



### CONCLUSIONS

This paper has attempted to highlight the state of present technology in providing selected sensors capable of operating in the Shuttle environment. Some of the measurements may be implemented by using presently available sensors. However, the Space Shuttle presents certain temperature and materials problems which require continued developmental effort.

On the skin and adjacent internal areas, high temperature levels and high temperature rates of change are predicted. Sensors in these areas must withstand an environment exceeding the experience of any previously flown vehicle. Within this environment, the sensors must provide accurate data, be reliable, and be cost effective.

Thermocouples exist which will operate satisfactorily in the high temperature environment, but development effort is required to adapt strain gages, acceleration and vibration sensors, pressure transducers, and acoustic sensors to the Shuttle environment. The trend of development indicates that these problems are solvable. High Curie point piezoelectric material is being developed for use in accelerometers and acoustic sensors. Quartz diaphragm pressure sensors are being developed for extreme temperature applications. Many possible methods of measuring strain are under study. Near-term development will yield an acceptable system.

The second major problem is posed by the exotic materials to be used in construction of the vehicle. There is minimal industry experience in bonding instrumentation to proposed Shuttle materials. This is a very challenging problem, but cooperation between materials engineers and instrumentation engineers of NASA and industry will result in a satisfactory solution.

## **CONCLUSIONS**

- **SENSOR HARDWARE WILL REQUIRE DEVELOPMENT**
- **INSTALLATION TECHNIQUES MUST BE DETERMINED**

# **SOLID STATE POWER CONTROLLERS**

**JACK C. BOYKIN**

**AND**

**WILLIAM C. STAGG**

**MANNED SPACECRAFT CENTER  
HOUSTON, TEXAS**

**AND**

**DONALD E. WILLIAMS**

**MARSHALL SPACE FLIGHT CENTER  
HUNTSVILLE, ALABAMA**

SOLID-STATE POWER CONTROLLERS

Jack C. Boykin

and

William C. Stagg

NASA-Manned Spacecraft Center  
Houston, Texas

and

Donald E. Williams

NASA-Marshall Space Flight Center  
Huntsville, Alabama

SUMMARY

A spacecraft PDC (power distribution and control) subsystem utilizing solid-state switching elements and capable of being computer controlled offers many potential advantages over systems using conventional electromechanical switching devices. These include higher reliability, longer life, a more rugged system, more flexibility, and an inherent compatibility with other advanced avionics subsystems. The trend in spacecraft design is toward larger, more sophisticated vehicles with correspondingly larger and more complex systems requiring electrical power. This trend has resulted in increasing numbers of power distribution paths and power-switching functions, in addition to requirements for cleaner (transient-free) electrical power to supply the complex avionics systems. This paper addresses one of the potential improvements in the PDC subsystem which is being strongly considered for these program and system interface requirements, the SSPC (solid-state power controller). The paper presents the basic functions of the SSPC, some of the basic design concepts thus far evolved for performing these functions, and some of the considerations involved in both the design and application of these devices. Spacecraft systems requirements as well as the potential results of applying SSPC's in an approach to meeting these requirements are presented. Finally, this paper presents the development status of SSPC's to date, along with the requirements for further development of the devices, systems, and concepts necessary to take full advantage of this technology.

## INTRODUCTION

Spacecraft system designs and component applications have always drawn heavily on aircraft program experience. The Space Shuttle will be no exception, and may increase the dependence on aircraft experience due to its aircraft modes of flight. In the area of PDC (power distribution and control), relatively few improvements have been generated by aircraft systems in the last 20 years. However, as interfacing subsystems become more complex and payload delivery requirements increase, the PDC subsystem must be improved or it will become a significant burden on other systems.

## POWER CONTROLLER FUNCTIONS

The SSPC will provide four basic functions or capabilities in an advanced PDC subsystem: (1) switch power ON and OFF to a load from a bus, (2) provide circuit overload protection, (3) provide remote control and monitoring of these functions, and (4) provide current limiting during overload conditions.

All of these functions except current limiting have been provided in the past by various combinations of toggle switches, circuit breakers, fuses, relays, and motor switches. In addition to the obvious advantages of replacing several types of devices with one single device to perform the many functions required by a system, the SSPC has the added advantage of reducing the total number of switching elements required since each load circuit of a conventional system normally employs a circuit breaker and one or more of the other switching devices in order to provide full functional capability. The current limiting function is not only advantageous from a safety hazard viewpoint, but also will offer great improvements to the entire electrical power system by reducing the transients normally generated during switching and fault conditions.

- **POWER CONTROLLER FUNCTIONS**
- **SWITCHES POWER ON AND OFF BETWEEN A BUS AND A LOAD**
- **PROVIDES CIRCUIT OVERLOAD PROTECTION**
- **REMOTE CONTROL CAPABILITY**
- **SHOULD PROVIDE CURRENT LIMITING DURING OVERLOAD CONDITIONS**

## BASIC SSPC DESIGN

The SSPC's envisioned for Shuttle application suffer from a problem common to programs implementing advanced technology; i.e., theory and breadboard knowledge far outweigh flight applicable hardware production. A major contributor to this condition is, of course, the lack of funds for manufacturers to pursue flight packaging development. This is a condition beyond the control of the power systems designer. Another major factor contributing to the situation is the lack of detailed system requirements presented to the SSPC designer to provide the real requirements on the SSPC. This problem is being studied by the power systems designers for the Shuttle; however, until sufficient details of the Shuttle system designs and requirements are generated, the limited availability of funds forces power systems designers to be hesitant in hardening detailed requirements. These circumstances have led to varying design concepts by manufacturers of a solid-state, current sensing switching device. The next portion of this paper will deal in more detail with several design approaches and the advantages and disadvantages of each.

To better understand the differences in the designs to be presented, a review of the basic design concepts pursued in early SSPC programs is in order. Figure 1 shows the basic building blocks of a d.c. SSPC. The power switching transistor must have sufficient voltage and power dissipation rating to be compatible with the system transients and the overload and circuit protection modes of operation. The regulator is used to provide a buffer effect so that the voltage to the internal circuitry is relatively independent of bus-voltage variations. The driver circuit must put the power transistor into deep saturation to provide low voltage drop and power dissipation. A d.c. to d.c. converter can be used to provide this drive power and at the same time provide the signal-to-load isolation required by computer control systems such as the Shuttle proposes. The overload circuit protection interfaces with the current sensing element and the drive circuitry to provide the circuit breaker function with the added improvement of an actual current limiting capability. A current fold-back is allowed for increased voltages to hold the power dissipation of the semiconductor within limits and help prevent the semiconductor junction from rising above its rated value during the worst case conditions of a high voltage transient on the input and a short circuit on the output. In order to protect the SSPC and optimize the PDC subsystem operation, a trip-out circuit is provided to turn off the power switch and indicate with a trip signal that the action has occurred. Reduced tripping times for higher voltages are designed to allow MIL-STD-704 transients without nuisance tripping and still allow the designer to give as much protection as possible to the semiconductor switch.

# DC POWER CONTROLLER

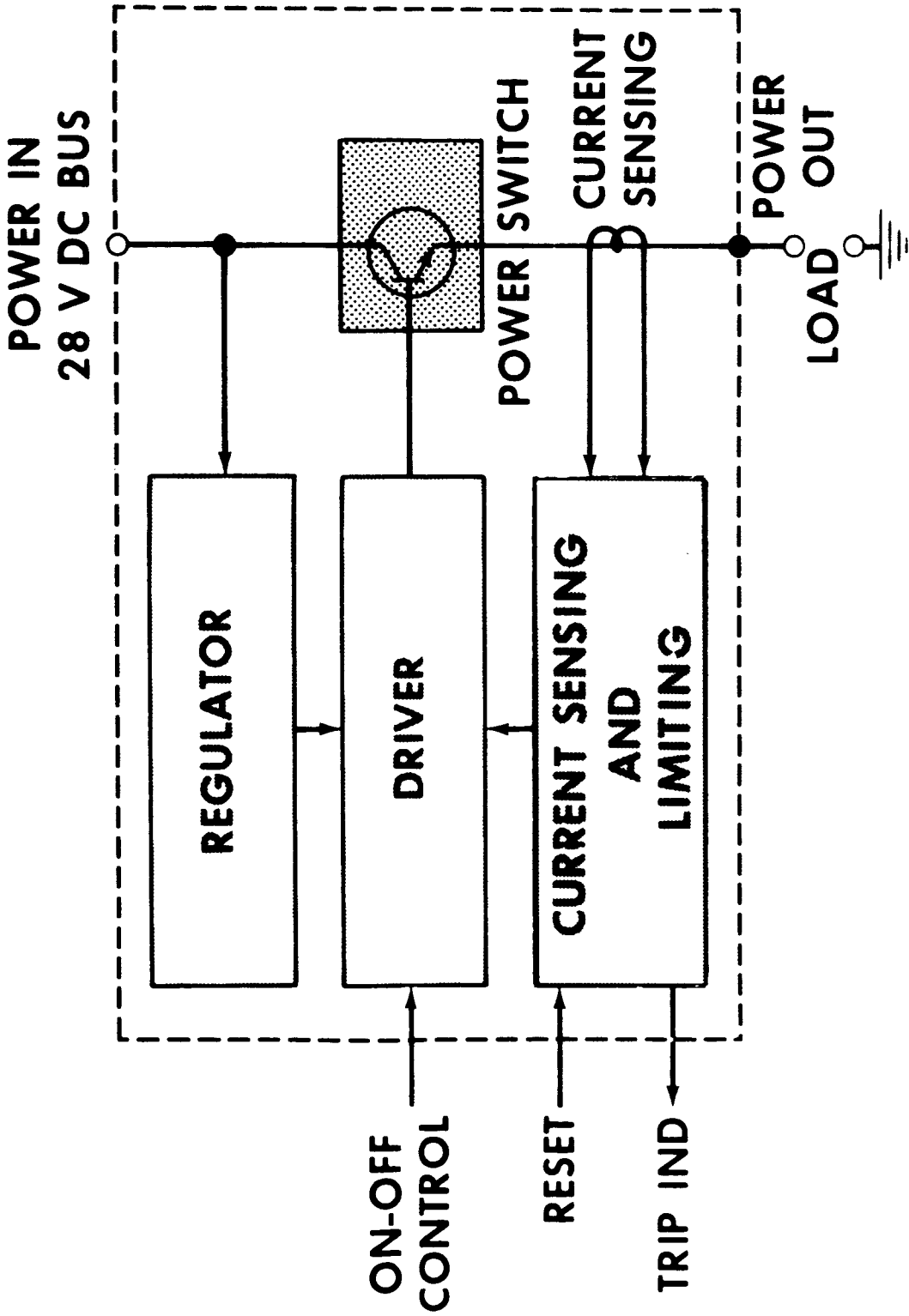


FIGURE 1

## DESIGN CONSIDERATIONS

It should be evident from the previous discussion that SSPC's are not simple components such as the electromechanical components (relays, circuit breakers, etc.) used in conventional PDC subsystems. They are indeed very complex, multi-technology semiconductor devices employing not only power semiconductors, but also thin and thick film integrated circuits. This complexity, along with PDC subsystem requirements, leads the SSPC designer to consider five important points in his design and to attempt to optimize all of these.

- a. Low Dissipation and Voltage Drop. Low dissipation in both the "ON" and current-limiting modes is important from the standpoint of obtaining maximum efficiency in the PDC system and from the standpoint of minimizing the thermal stresses to which the power semiconductor device is subjected. Designing for the lowest dissipation possible also has a profound effect on the maximum SSPC current rating achievable with current state-of-the-art power semiconductors. Low voltage drop across the SSPC is also very important both because it affects the dissipation in the device and because of the effect it has in minimizing the wire gauge required in order to maintain acceptable voltage limits at the load equipment.
- b. High Current Capability. As discussed previously, the degree of success which the SSPC designer achieves in minimizing the power dissipation within the device plays a major role in determining the current rating of the device and consequently the maximum current rating obtainable with state-of-the-art semiconductors.
- c. Current Limiting. Current limiting is a very desirable feature in SSPC's because of its effect in minimizing transients on the power bus due to overloads and faults. Various parameters, such as system voltage, power semiconductor ratings, and SSPC design techniques affect the degree of current limiting available with any particular SSPC design. In some cases, power dissipation in the current-limiting mode goes so high as to render that mode of operation impractical.
- d. Control/Output Isolation. Isolation between the control input circuitry and the power handling output circuitry is important because of the possibility of inducing EMI from the power bus into the data bus control system and adversely affecting its operation. Because of the fact that the solid-state circuits, unlike their electromechanical counterparts, do not offer inherent isolation, special consideration must be given to this requirement. Two techniques commonly used to provide isolation are solid-state optically coupled devices and transformer coupling between the control input and the drive stage.
- e. Low Leakage in the "OFF" State. This characteristic is important because of its effect on the overall efficiency of the PDC subsystem and generally restricts the designer to the use of silicon rather than germanium power semiconductors.



## **DESIGN CONSIDERATIONS**

- **LOW DISSIPATION AND VOLTAGE DROP**
- **HIGH CURRENT CAPABILITY**
- **CURRENT LIMITING**
- **CONTROL/OUTPUT ISOLATION**
- **LOW LEAKAGE IN 'OFF' STATE**

### DESIGN APPROACHES

Figures 2 to 5 present various design approaches which have been put forward thus far. Accompanying each figure is a brief discussion of the advantages and disadvantages of each approach. As will be seen, in some cases, optimization of one design consideration leads to compromises in other areas.

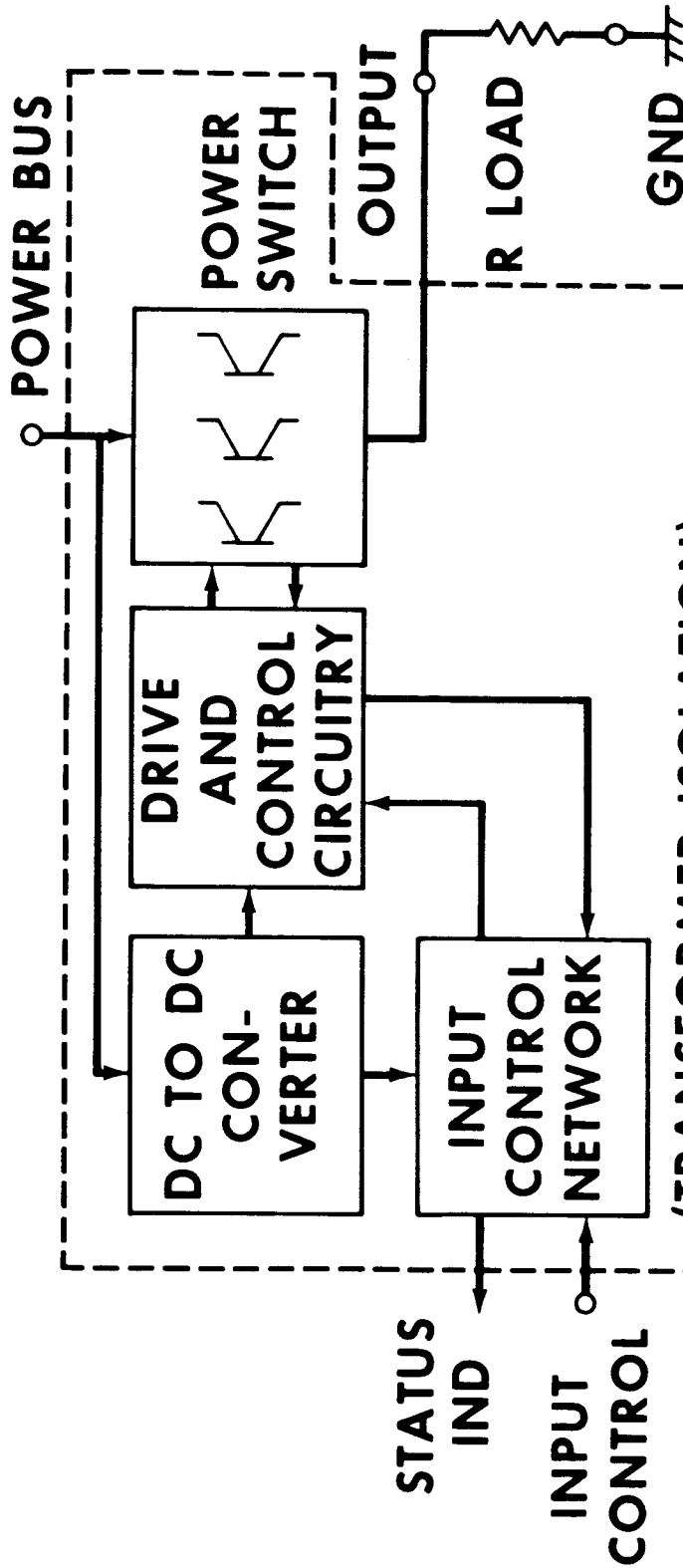
Figure 2 illustrates a design which uses a transistor in deep saturation as the power switch for normal operation. When an overload exists, the base drive to the power output transistor is decreased so that the transistor now operates in its active region to achieve current limiting. For SSPC ratings up to 5 amps, a single power transistor is employed; for higher ratings, two or more power transistors may be paralleled in order to maintain the power dissipation in each transistor within acceptable limits during all modes of operation. This particular design uses transformer coupling to achieve isolation between the control input and power circuitry.

This design has two distinct advantages. During normal operation, the single transistor in deep saturation provides a low voltage drop and consequently low power dissipation in the SSPC. This design also provides a current limiting mode of operation which is a very desirable feature because of its effect in minimizing transients on the power bus.

One disadvantage of this design is the fact that its internal power supply for the control electronics continues to draw power in the "Off" state which, when added to the leakage of the power transistor, decreases the efficiency of the FDC subsystem. A possible additional disadvantage is that if parallel power transistors are used for higher current ratings, some complexity may need to be added to the drive circuitry to insure that the power transistors turn on and off at the same time. Also, matching impedances may need to be added in series with each power transistor, thus increasing the voltage drop across the SSPC.

# SATURATED OUTPUT

## ACTIVE CURRENT LIMITING



### ADVANTAGES

- (1) LOW OUTPUT VOLTAGE DROP
- (2) CURRENT LIMITS

### DISADVANTAGES

- (1) LOW EFFICIENCY IN 'OFF' STATE

FIGURE 2

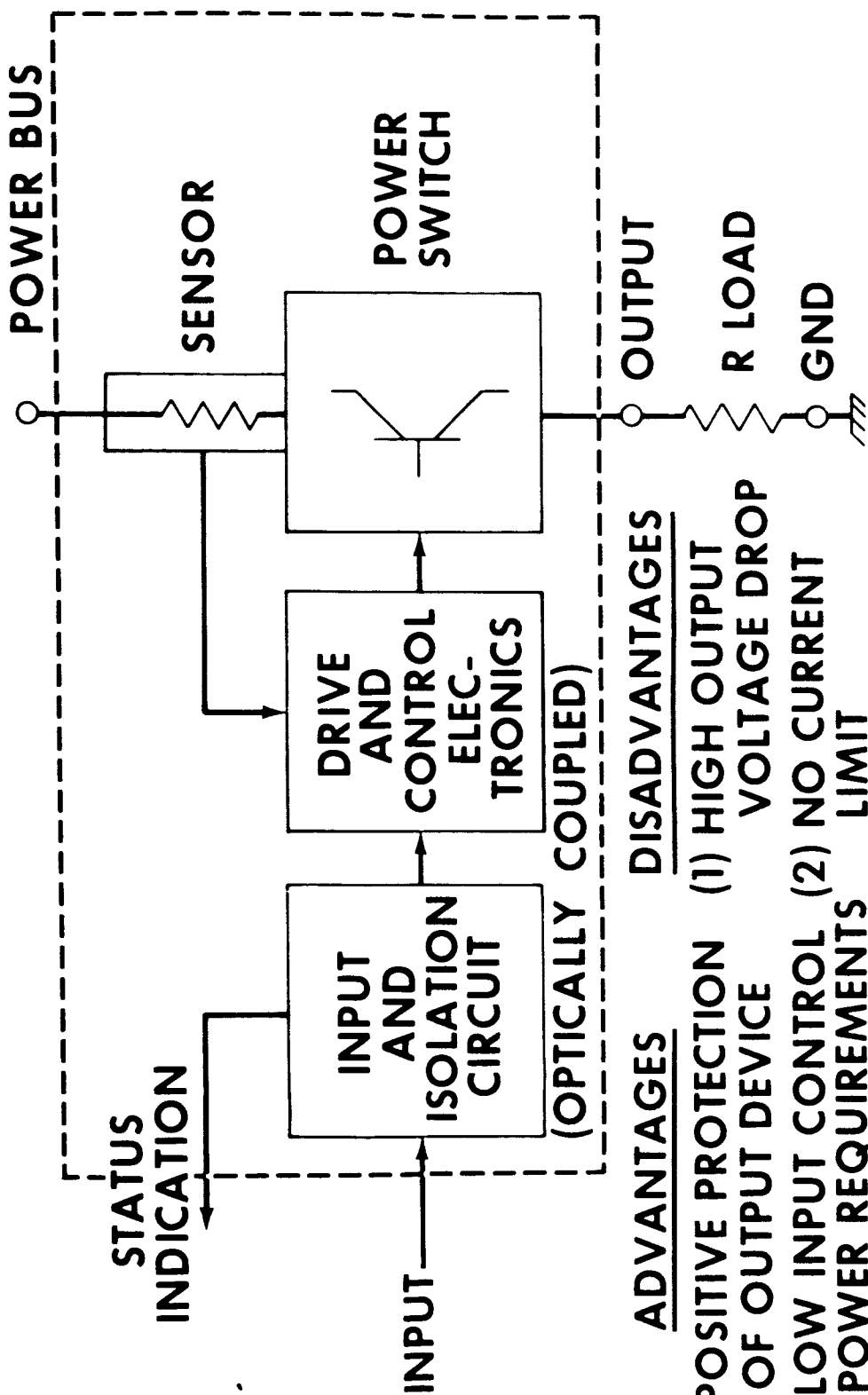
Figure 3 shows another design which employs a deeply saturated transistor as the power switch for normal operation. It differs from the previous example, however, in that overload sensing is accomplished by sensing the actual temperature of the power semiconductor chip. When an overload causes the temperature of the chip to rise to a predetermined critical value, typically 170°C, base drive to the power semiconductor is cut off, thus interrupting the overload current. With such a thermal sensing scheme, the SSPC can be made to be the equivalent of a mechanical "trip-free" circuit breaker. Another difference in this design is that it uses optically coupled semiconductor devices to achieve isolation between the control input and power circuitry.

The thermal sensing scheme offers some advantages and some disadvantages. It offers positive protection for the power semiconductor since the overload sensing method utilizes the parameter most critical to the semiconductor, i.e., the junction temperature. On the other hand, thermal sensing makes the overload trip point and time dependent upon the temperature of the surrounding environment and the heat sink to which the SSPC is mounted.

Some disadvantages to this particular approach are the fact that it does not provide a current limiting mode and it is possible that the combined voltage drop of the power semiconductor and the thermal sensing device may be excessive.

# SATURATED OUTPUT THERMAL SENSING

NO CURRENT LIMIT



## ADVANTAGES

(1) POSITIVE PROTECTION OF OUTPUT DEVICE

(2) LOW INPUT CONTROL POWER REQUIREMENTS

## DISADVANTAGES

(1) HIGH OUTPUT VOLTAGE DROP

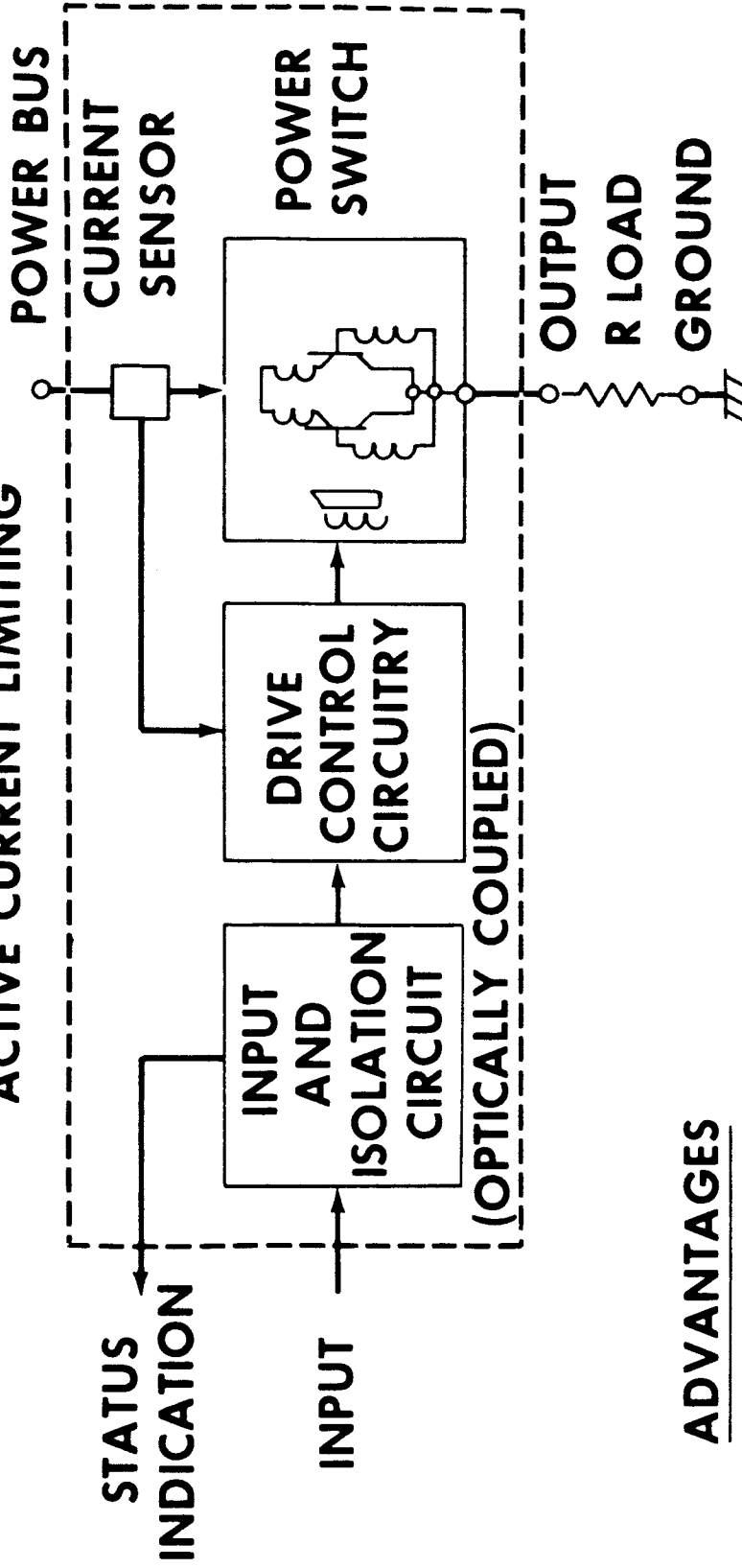
(2) NO CURRENT LIMIT

FIGURE 3

The design outlined in figure 4 is radically different from the first two presented and employs basically a saturated switching transformer driving the power output transistor and is similar in approach to a switching oscillator. By using this switching technique, the designer can accomplish time sharing of the load current between the two output transistors. Time sharing at a frequency below the thermal time constant of the output transistor can reduce the thermal stress of the transistor by allowing a finite cooling time between power pulses during normal and overcurrent conditions. This switching concept could be limited due to output noise generation and/or EMI-RFI generated by the current transformers. This problem could be severe enough that large and complex filtering networks might counter the advantages of the switching device.

This design uses optically coupled semiconductor devices to achieve control input isolation similar to figure 3.

# CURRENT SWITCHING OUTPUT ACTIVE CURRENT LIMITING



## ADVANTAGES

- (1) SELF-REGULATING
- (2) LOW INPUT POWER
- (3) HIGH EFFICIENCY  
IN 'ON' STATE

## DISADVANTAGES

- (1) POSSIBLE NOISE ON  
OUTPUT LINE
- (2) RFI-EMI GENERATION

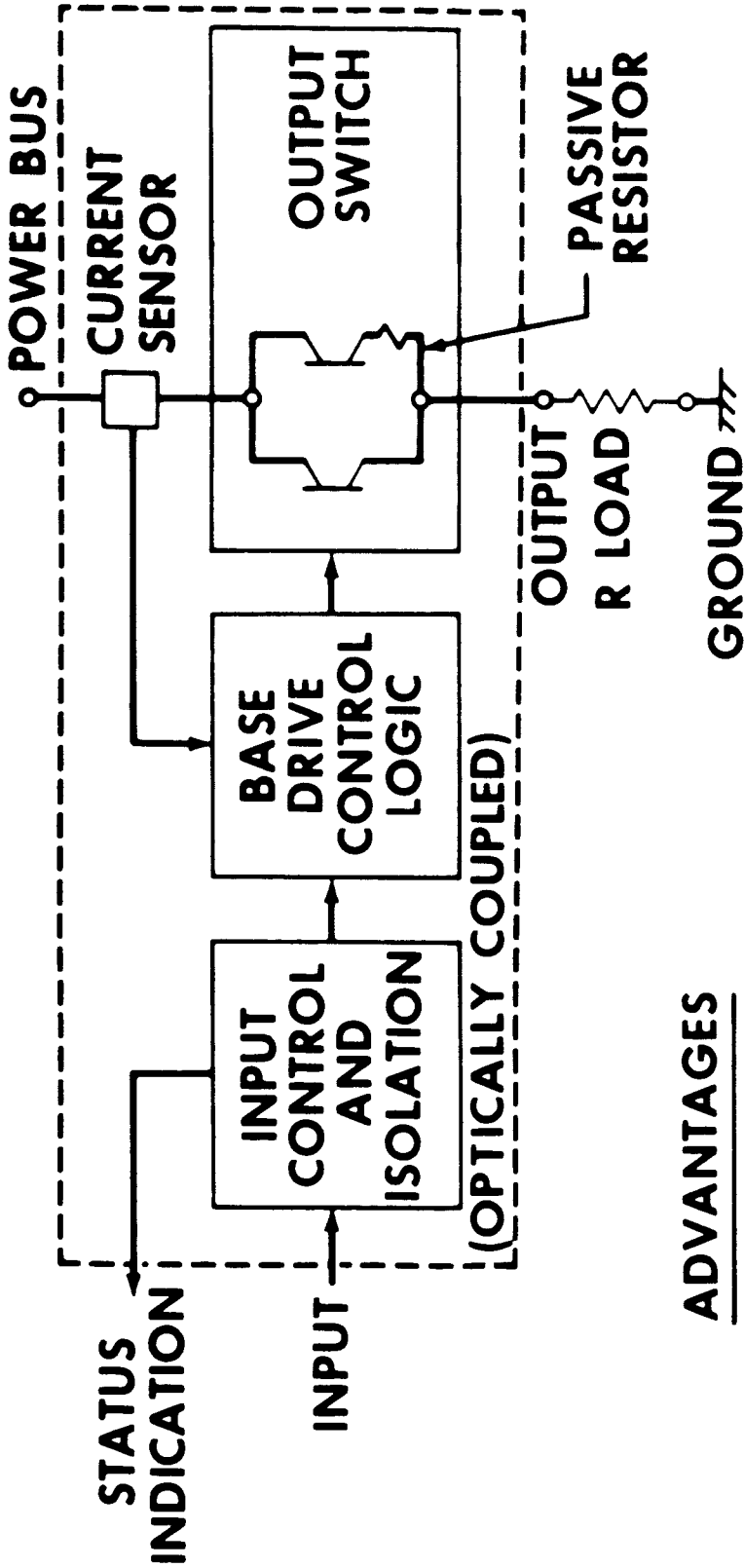
FIGURE 4

Figure 5 illustrates another concept different in basic philosophy from those previously presented. This approach proposes current limiting by a means other than high power dissipation in the output transistor. Using a dual output power stage, the first path is active during normal load conditions and a separate path is used for overload conditions. The first stage uses a single power transistor which is operated in a deep saturation state, thus allowing the low voltage drop characteristic. Under overload conditions, the first stage is turned off and the second stage is turned on. This stage consists of an output transistor (also operated in a saturated mode) in series with a power resistor which provides current limiting and a relief element for the main power switch during overload conditions in which high power dissipation is required. The major problem with this design is the complexity of the circuitry involved in switching from one stage to the other.

The examples presented here show only a few of the many possible circuit designs which could fulfill the Shuttle switching requirements if development is carried to completion. The technologies involved in these designs appear to be fully capable of meeting Shuttle requirements, leaving the designer with the prime task of hardening a concept and producing a candidate flight packaged unit for test and evaluation.



# PASSIVE CURRENT LIMITING



## ADVANTAGES

- (1) CURRENT LIMIT
- (2) LOW INPUT POWER
- (3) LOW OUTPUT VOLTAGE DROP
- (4) LOW POWER DISSIPATION IN OUTPUT TRANSISTORS

## DISADVANTAGES

- (1) INCREASED COMPLEXITY
- (2) RFI-EMI GENERATION

FIGURE 5

### ADVANCED SPACECRAFT TRENDS AFFECTING THE POWER DISTRIBUTION AND CONTROL SUBSYSTEM

The overall Shuttle Program requirements emphasize the shortcomings of a conventional PDC subsystem and point out the three basic trends in spacecraft design which make PDC subsystem improvements mandatory: (1) automation, (2) reuseability, and (3) system size.

#### Automation

The advances in electronic technology in recent years have made digital computer capability a realistic flight item which has been utilized by individual avionics subsystems to improve upon their capabilities. This has resulted in increased sophistication and capability of these systems. This has allowed the use of automated functions for not only increasing the accuracy and speed of the functions, but also reducing man's workload. The effectiveness of this automation is presently reduced somewhat due to the unavoidable interfaces with the conventional PDC subsystem. Presently applied solutions to this problem involve complex and heavy hardware such as the Apollo sequencer system to allow even a minimal number of automated functions. The interfacing **subsystems implementing** the advanced electronic capability available to them are also more susceptible to the transients generated by the conventional PDC systems interfaces. Their circuits must usually suffer reliability, weight, and simplicity penalties to counter this transient susceptibility.

#### Reuseability

Typical Shuttle planning calls for mission cycles in the hundreds and program life of up to ten years. Present PDC subsystem components are not regarded as suitable for spacecraft application under these conditions due to the normal degradation processes of mechanical wear and tear. Solid-state devices substituted for these components offer a potential for approaching an unlimited life component.

#### System Size

Perhaps the driving function in the requirement for an improved PDC subsystem is the trend towards a larger system. The vehicle being designed is on the order of 200 feet in length, with electrical power requirements higher than ever before on a space vehicle. A conventional PDC subsystem to service this type of system involves extremely heavy, complex and inflexible wire harnesses, as well as large quantities of power handling electromechanical devices which are subject to wear and limited cycle life.

# **ADVANCED SPACECRAFT TRENDS AFFECTING THE PDC SUBSYSTEM**

- **AUTOMATION**
  - **REMOTE CONTROL**
  - **COMPUTER COMPATIBILITY**
- **REUSEABILITY**
  - **10 YEAR, MULTI-MISSION SYSTEMS**
- **SYSTEM SIZE**
  - **PHYSICAL DIMENSIONS**
  - **POWER REQUIREMENTS**
  - **DISTRIBUTED BUSES**

### DISTRIBUTED POWER BUS SYSTEM

In order to optimize the PDC subsystem in a Shuttle with the aforementioned characteristics, the basic change from conventional systems to a distributed power bus system with remote control is mandatory. A typical Shuttle distributed bus arrangement is shown in figure 6. The main power control stations are located as nearly as possible to the prime power sources and have remote control capability. Remote PDU's (power distribution units) are located in various other strategic areas according to the location of the individual loads themselves. The PDU's feed power directly to the users through SSPC's which are controlled from the data bus system. The greatest advantage of this concept is the weight savings in wiring no longer required to be routed through the manual control elements in the crew area. Wire weight savings are also gained in removing the many individual wires required to carry power from central buses to each user in a remote area and replacing these with the one larger power feeder to a PDU. Individual wires must still distribute power from the PDU to each user, but over a relatively short distance. The major portion of the numerous individual wires is replaced by a single feeder larger than any one of the original wires, but much lighter than the sum of the wires replaced.

# ELECTRICAL EQUIPMENT LOCATION

## EXAMPLE

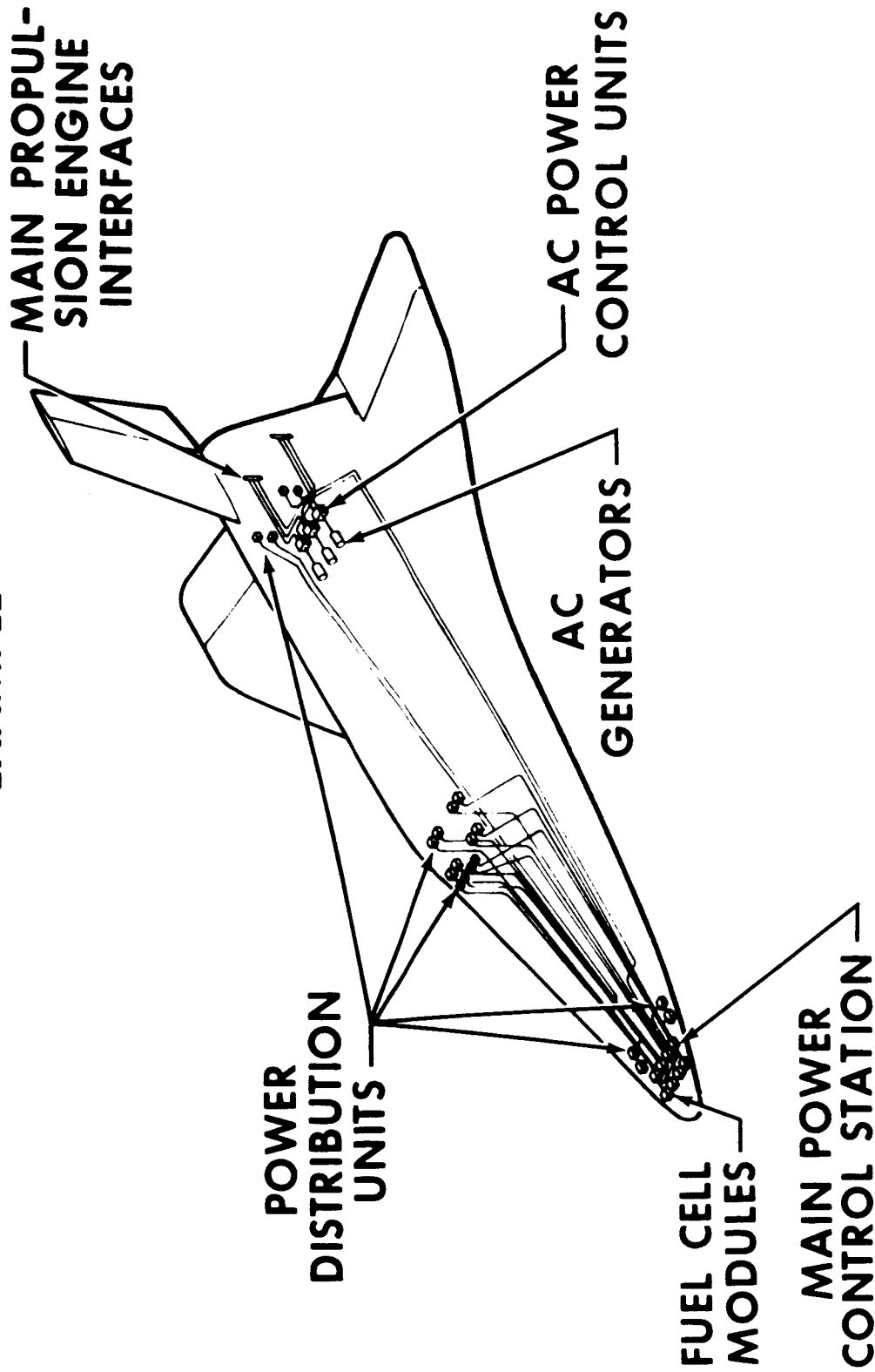


FIGURE 6

#### WEIGHT TRADE-OFF STUDIES

The potential weight savings previously discussed may be very significant for payload critical aircraft and spacecraft such as the Shuttle. The magnitude of this potential savings, however, is dependent on the system to which the concept is applied. Two systems which have received detailed trade studies in this area are the A-7 Aircraft and the Phase B Space Shuttle. As shown in table I, the potential savings are of significant magnitude to warrant further investigation into application of the SSPC concept. There are other areas of potential weight savings in the PDC subsystem which are receiving special study in conjunction with the SSPC concepts; for example, preliminary results indicate possible weight savings on the order of 15 percent with the application of flat conductor cable in the Shuttle.

# WEIGHT TRADE-OFF STUDIES

APPLICATION	SYSTEM WEIGHT		REDUCTION, PERCENT
	CONVENTIONAL	SOLID-STATE	
A-7 AIRCRAFT	576 LB	315 LB	45
PHASE B SHUTTLE	2516 LB *	1998 LB *	21

\* WITH FLAT CONDUCTOR  
CABLE THESE FIGURES  
WOULD BE 15 PERCENT  
LOWER

TABLE I

#### ADVANTAGES OF SOLID-STATE POWER CONTROLLERS

All of the improvements to the PDC subsystem previously discussed have depended on the application of a remote control power switch. Some of the inherent problems of mechanical contacts were mentioned earlier, and are well known to power system designers. Recent semiconductor technology advancements have provided us with a design concept which lessens, if not completely eliminates, the bulk of these problems while offering other system improvements at the same time.

One of the most important advantages the SSPC has over the electromechanical device is the inherent compatibility with a data bus control system. Low level control and monitoring of these solid-state devices establish the control system/power device interface with common hardware, whereas conventional power devices must undergo significant modification in order to accomplish this interface. Potential higher reliability, longer life, reduced EMI levels, and greatly improved overload protection accuracy are other examples where inherent mechanical limitations are alleviated by the SSPC. Another possible advantage of the SSPC is the capability of the solid-state device to current limit for fault protection. This capability offers many potential system improvements such as reduced transients, decreased generator fault capacity requirements, and perhaps even additional weight savings.



# **ADVANTAGES OF SOLID-STATE POWER CONTROLLERS**

- **COMPATIBILITY WITH DATA BUS CONTROL SYSTEMS**
- **REMOTE CONTROL (ON-OFF-RESET)**
- **TRIP INDICATION**
- **POTENTIALLY HIGHER RELIABILITY WITH LONGER LIFE**
- **PC CAN REPLACE CONVENTIONAL BREAKER  
AND ASSOCIATED SWITCH**
- **CURRENT LIMITING (DC UNITS)**
- **REDUCED EMI**
- **PROTECTION ACCURACY GREATLY INCREASED**

#### DEVELOPMENT STATUS

The basic concept of a PDC subsystem design employing computer control and solid-state switching devices was developed about ten years ago by LTV aircraft designers. This effort has progressed to a design and test simulator associated with the Navy and Air Force programs involving the A-7 Aircraft. This program has developed a basic systems application concept, a candidate control and monitoring system, and a flight configuration component designed with most of the basic electrical characteristics required of an SSPC. An extensive test program is planned for evaluation of this simulator, both as a system and on a component level.

A very substantial program has been carried on by Westinghouse Electric Corporation in both systems and components design. This program has resulted in control and interface hardware production as well as various breadboard power controller fabrications. Testing and demonstration programs are presently being performed with this hardware. Many programs are being performed by industry in systems analysis, such as Grumman Aerospace Corporation studies on the F-14 Fighter Aircraft, and all of these efforts should aid in the development of the technology involved.

The Manned Spacecraft Center has undertaken an evaluation program as a result of a feasibility study accomplished by LTV Aerospace Corporation indicating great potential improvements in spacecraft PDC subsystems applying SSPC's. Present efforts at this Center involve systems integration and interface requirements investigations being accomplished with the integrated avionics breadboard program. A limited amount of component evaluation has been accomplished to date on hardware purchased for the integration program, and although it must be kept in mind that these SSPC's are themselves breadboard units, initial test results indicate electrical characteristics equalling or surpassing expected values.

Future Manned Spacecraft Center plans include more component evaluation and systems integration, but the immediate efforts will be concentrated on flight packaging development in order to meet the demanding Shuttle time frame. Marshall Space Flight Center is also supporting and will continue to support component evaluation and development, especially in the area of high voltage semiconductor switches. Lewis Research Center will also support the National Aeronautics and Space Administration efforts in this field, presently concentrating on development of high voltage designs and components.

## **DEVELOPMENT STATUS**

- **PREVIOUS APPLICABLE WORK (LTV, W, GAC, ...)**
- **MSC INVESTIGATIONS (SYSTEM INTERFACE REQUIREMENTS, COMPONENT EVALUATION)**
- **FUTURE**
  - **MSC (PACKAGING AND COMPONENT EVALUATION)**
  - **MSFC (COMPONENT EVALUATION AND HIGH VOLTAGE DEVELOPMENT)**
  - **LRC (HIGH VOLTAGE COMPONENT DEVELOPMENT)**

CONCLUDING REMARKS

The studies discussed here, as well as numerous unmentioned efforts in both system and component development, have precipitated great interest in the application of solid-state power controllers in the Shuttle PDC subsystem. The subsystem weight criticality and complex interfacing problems of the proposed Shuttle concepts present a difficult design task to the PDC subsystem designer, while the SSPC presents him with a very promising method of meeting both of these areas of concern.

Due to the potential advantages of a PDC subsystem applying SSPC's, development will surely continue both through Government and industry funding. There are numerous areas of SSPC development required for universal application, but the Space Shuttle application requires a qualified component within the next few years. In order to meet this requirement, system designers may limit themselves to a maximum rating SSPC, or compromise some electrical characteristics presently envisioned. However, even if design development is slowed temporarily in order to flight package and qualify today's candidate SSPC's, the potential improvements to the Shuttle PDC subsystem could provide the first major step in utilizing this technology to its fullest.

## **CONCLUDING REMARKS**

- **SOLID-STATE POWER CONTROLLERS ARE A PROMISING APPROACH TO SATISFYING THE SHUTTLE POWER CONTROL REQUIREMENTS**
- **PRESENT TECHNOLOGY OFFERS VARIOUS APPROACHES TO ELECTRONIC DESIGN**
- **SOME DEVELOPMENT WORK STILL NEEDED**

## AN AUTOMATIC ELECTRICAL DISTRIBUTION SYSTEM

Dr. M. A. Geyer

Westinghouse Electric Corporation  
Aerospace Electrical Division  
Lima, Ohio

The Automatically Controlled Electrical System (ACES) is a new method of distributing and controlling electrical power. It utilizes remotely controlled power switching and circuit protective devices. Control is exercised through a small general purpose computer using multiplexed control signals. This computer directs the control signals to and from the appropriate system control devices. In addition, it is programmed for automatic control, sequencing and self-checkout functions.

The system offers numerous potential benefits such as:

- Reduced wiring weight and complexity
- Reduced manual supervision
- Lower overall cost
- Less susceptibility to human error
- Fewer bulkhead penetrations
- Simplified maintenance
- Programming of load availability under conditions of low power availability
- Greatly simplified means for system growth and modification

ACES is currently being developed for aircraft and spacecraft applications, but use on submarines and surface ships is also foreseen. The concept may eventually find application in office buildings and industrial plants, particularly continuous process industries.

In an aircraft or spacecraft, the flight crew must be able to exercise control over the electrical system. They must be able to turn loads on and off, and have quick access to the thermal circuit breakers which protect the electrical busses, load switches and thermal circuit breaker panels in the cockpit. In a large aircraft such as a commercial airliner, this requires running heavy electrical power feeders from the generators—located on the engines—to the cockpit, a run of 150 feet or more.

Only 25 percent of the electrical power is used in the cockpit area. The other 75 percent is used in other parts of the vehicle. This power is distributed to the loads by running electrical wires from the electrical busses in the cockpit to each of the loads. This requires many miles of electrical wire. For example, the Concorde (the European-built supersonic transport) has 150 miles of electrical wiring for distribution, control and indication purposes.

A conventional electrical distribution system is shown schematically in Figure 1. Compare this to a system which uses a means of remotely controlling the 75 percent of the power which is not used in the cockpit area. Such a system is shown

in Figure 2. Here the electrical power feeders are routed to electric power busses located at electrical "centers of gravity" for various portions of the vehicles. Remotely controlled circuit breakers (RCCBs) are located on the rearward busses. RCCBs are thermal circuit breakers which contain solenoids to open and close them. They are remotely controlled by applying 28 volt power to the control terminals. This requires running a small electrical wire to the cockpit for each RCCB. Since the status of each RCCB must also be known, it is necessary to run a second wire to the cockpit to indicate if the RCCB has tripped. Since these are power carrying wires, they must also be protected by small thermal circuit breakers.

Westinghouse performed a comparative study of the conventional distribution system and the remotely controlled system just described. An airframe company provided information on aircraft loads, load location, wire size and weight, and circuit breaker size and weight for a new transport aircraft design. The results of this study are given in Table 1. Despite the fact that more feet of wire and more thermal circuit breakers were used in the remotely controlled system, there was an overall weight savings of approximately 160 pounds from the use of much smaller wire.

Additional studies were performed to determine what other savings and advantages might be possible from applying other concepts to an electrical distribution system. Multiplexing has long been recognized as a way of reducing the amount of wire required for control purposes. Since remote control was a desirable feature of the system, multiplexing appeared to be a viable concept for further reduction of wire weight.

TABLE I

	<u>Thermal</u>		<u>RCCB</u>	
	<u>Weight</u> <u>Pounds</u>	<u>Cost</u> <u>Dollars</u>	<u>Weight</u> <u>Pounds</u>	<u>Cost</u> <u>Dollars</u>
Load Wire	445.7	28,550*	421.2	29,032*
Thermal Breakers	86.9	7,397	51.2	4,474
RCCBs	—	—	128.7	13,200
Galley Feeder	57.0	1,296**	38.3	1,116**
Bus Feeder	342.0	11,002**	135.0	6,266**
<b>TOTALS</b>	<u>932.4</u>	<u>48,245</u>	<u>774.4</u>	<u>54,088</u>

\*An installed load wire cost of \$.50 per foot was used.

\*\*An installed feeder wire cost of \$2.00 per foot was used.

### THERMAL BREAKER AND RCCB SYSTEM WEIGHTS AND COSTS

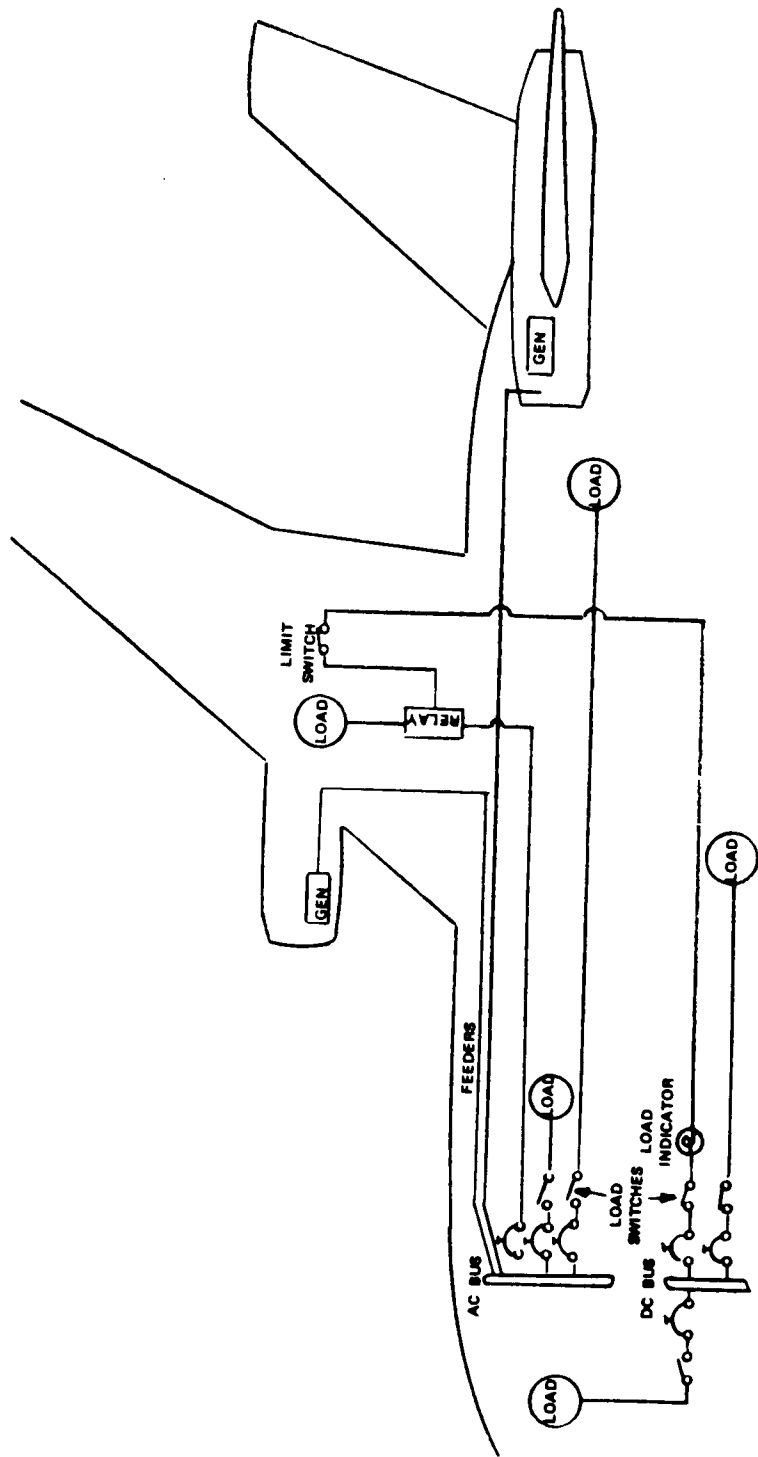
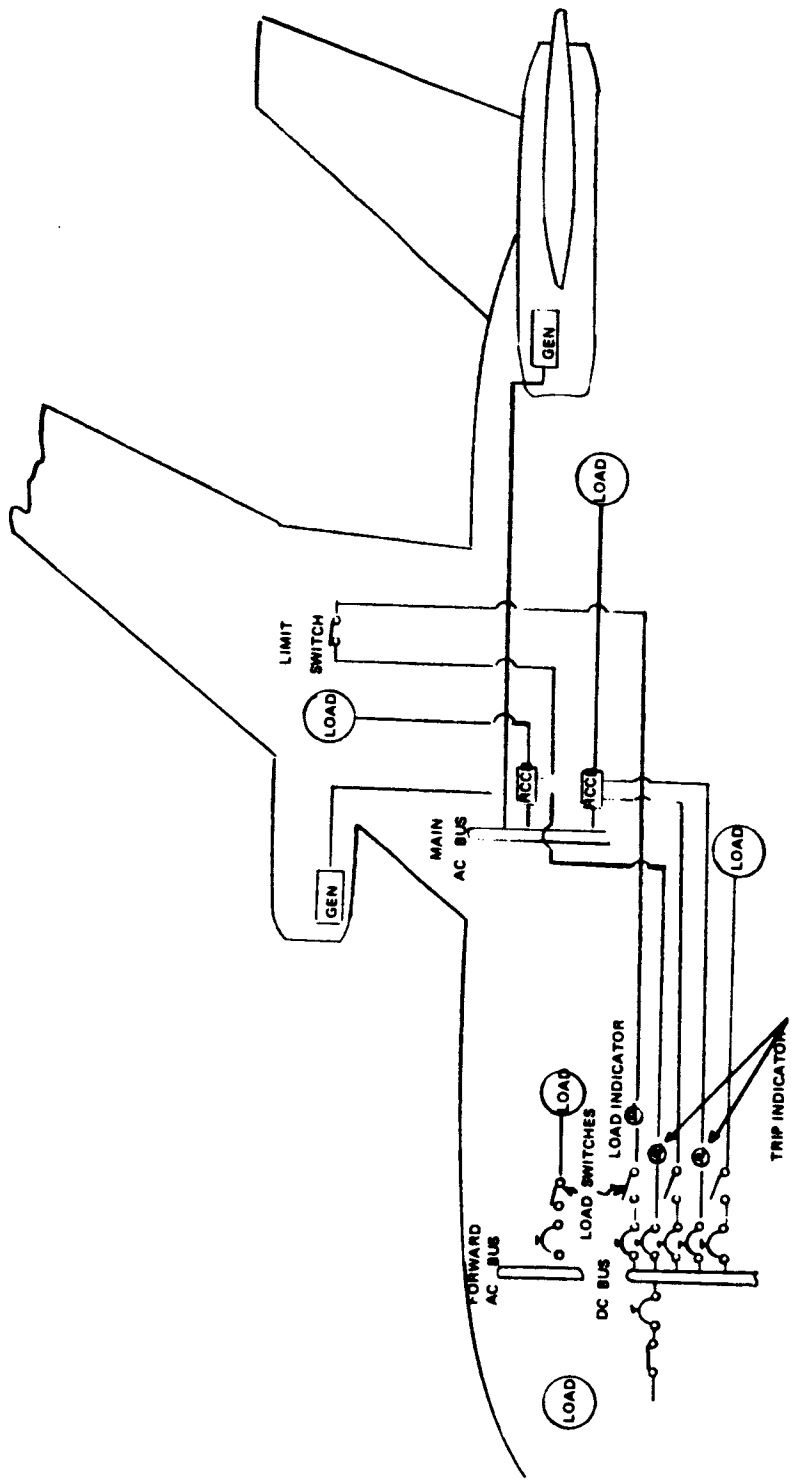


FIGURE 1  
CONVENTIONAL ELECTRICAL  
DISTRIBUTION SYSTEM



**FIGURE 2**  
**RCB ELECTRICAL**  
**DISTRIBUTION SYSTEM**



The U.S. Navy's Solid State Electrical Logic (SOSTEL) concept was also considered. In this concept, mechanical electric-power-switching devices such as thermal circuit breakers, relays and limit switches are replaced by solid state electric-power-switching devices and solid state transducers. As a result, the relay logic conventionally employed for such load control and sequencing functions as extending and retracting the landing gear can be replaced by much more reliable solid state logic. The SOSTEL concept also encompasses the use of solid state remote power controllers which perform both remote load switching and circuit protection functions similar to an RCCB. The transducer signals and control and indication signals for the remote power controllers (RPCs) readily lend themselves to multiplexing.

System features such as self-checkout, sequencing of high inrush current loads and load programming also appeared to be important considerations.

Studies of these concepts and techniques led to the definition of an electrical distribution system concept called the "Automatically Controlled Electrical System", or ACES.

ACES embodies the use of solid state RPCs and solid state transducers insofar as it is economically and technically practical to do so. The use of mechanical switching devices is not precluded since many power levels encountered in aircraft applications cannot yet be practically handled by solid state devices.

A control system schematic is shown in Figure 3. This schematic is somewhat misleading in that the Distribution Control Center (DCC) and the data bus are really in triplet as is shown in Figure 4. The Remote Input/Output (RIO) unit is internally triplicated. Such a configuration allows each computer to be dedicated to its own system and still be capable of assuming the overall computing load if the others fail. Thus, the control system can withstand, at a minimum, two failures without any noticeable effect.

The logic required for load control and sequencing, self-checkout, and load management is contained in the DCC. Signals from transducers and switch/indicator modules (SIMs) are transmitted to the DCC on a multiplexed data bus via RIO units. Logic equations are solved by the computer, and command signals are transmitted on the multiplexed data bus specifying which RPCs are to be turned on or off. The RIOs, which provide the interface between the data bus and the RPCs, "decode" the command signals and route them to the appropriate RPCs which provide the desired load switching functions.

If an overload condition is sensed by an RPC, it provides the circuit protection function by tripping open to prevent damage to the circuit. When it trips open, the RPC transmits an open indication signal to the DCC via an RIO and the data bus. After a pre-programmed time delay, the DCC automatically transmits a reset signal to reclose the RPC. If the fault has cleared, the RPC remains closed and power is restored to the load. If the fault persists after a pre-programmed number of automatic reclosures, the DCC transmits a trip indication signal to the cockpit indicating which RPC has tripped. The RPC remains tripped until manual action is taken to reset. The number of automatic reclosures which may be as few as zero is programmed in the DCC computer for each of the RPCs it controls. So the number of automatic reclosures may be varied depending upon load criticality and other criteria.

Turn-on and turn-off commands are manually provided to

the system by SIMs located on the craft's subsystem control panels. The indicator portion of a SIM may be used to indicate if the RPC which that SIM controls has tripped from an overload condition, or to indicate any other occurrence or condition in the system. Manual reset is accomplished by switching the SIM to the "OFF" then back to the "ON" position.

An additional man-system interface is also provided by a data entry and display panel (Figure 5) which is intended to substitute for the capability currently provided by the large thermal circuit breaker panels. This panel provides single point entry and display capability with greatly reduced space and weight requirements.

If a portion of the electrical generating capacity is lost, the system will automatically shed load in accordance with a pre-programmed load priority schedule. This prevents overloading the electrical source. Different load priority schedules are likely to be required for different flight modes. The system software has been designed to handle up to four different load priority schedules which can be selected according to four flight modes.

No analog signals are to be transmitted on the data bus. If analog comparisons are to be made, they will be made on an analog basis in the transducer. Only the fact that a limit has been reached will be transmitted. This, of course, is binary information identical to a switch. Analog control—such as voltage regulation—will be done on an analog basis at the location of the controlled device. Such controllers can actually be smaller and cheaper than A/D-D/A converters. For instance, Figure 6 is a photograph of a voltage regulator for a 90 KVA, 400 Hz, aircraft generator. The logic of the generator control unit is in the DCC. This lack of a requirement for analog transmission on the data bus dramatically lowers data bus rates and alters the word format.

The self-checkout is under software control. Any malfunction of a line replaceable unit is found during control system power up and the location of the unit is indicated on the data entry and display panel. This built-in test is activated every time power is applied to the DCC or upon command of a switch.

Sequencing is accomplished by software control. Simultaneous switching of loads can be restricted to a time sequence of application under software command as to the order and time intervals of application. This sequence also holds for reset of tripped RPCs.

The DCC is a small general purpose military type computer of modular design (Figure 7) and uses standard transistor-transistor-logic (TTL) integrated circuit devices of medium scale integration (MSI) complexity to maximum advantage. It is composed of control, arithmetic, memory and input/output units.

The DCC input/output unit contains a serial data transmission capability for multiplexed communication with the RIOs, a real time clock, and additional input/output mode control. The unit can withstand a data bus short to ground on any one or two busses without damage.

DCC physical specifications are in Table II.

A piece of ground support equipment is the test console which is used to service the DCC. Such a console is shown in Figure 8 with a paper tape program loader. The loader is

required for a DCC with an electrically alterable memory, such as plated wire.

The DED, Figure 5, contains a 10 digit keyboard, a numerical display and several switches and indicating lamps. An operator can open or close an RPC by keying in the appropriate RPC address and pressing the "open" or "close" switch. The DCC can be programmed to permit keyboard control of only selected RPCs. If an incorrect address or an address of an RPC not subject to keyboard control is keyed in, the "invalid address" lamp will light.

If an RPC trips, the "RPCs tripped" lamp lights. The addresses of the tripped RPCs can be displayed by switching to the "RPCs trip" mode and pressing the "clear/update" switch.

If the system goes into an automatic load shedding mode, the "loads shed" lamp will light. The addresses of the RPCs controlling the shed loads can be displayed in a manner similar to that for tripped RPCs by switching to the "loads shed" mode.

Each RIO will accommodate up to 64 transducers, SIMs, RPCs, or any combination thereof. Each has 64 command output and 64 status inputs. The control outputs provide signals which activate an RPC or the indicator portion of a SIM. The status accept signals from transducers, limit switches, the switch portion of a SIM and the status indicator output of an RPC.

The key to system operation is the software. The software program is the means of directing the computer hardware and peripheral equipment to accomplish the required control function. Creation of the software is likely to be more closely related to the application than design of the hardware and generally requires a deeper and more extensive understanding of the application. The efficiency of the software, the clarity of use, ease of modification and versatility for new insights into the application is as significant an indication of the extent to which the application is understood as is the design, complexity and size of the hardware.

The software has been written and need not be changed, no matter what the application. Thus, the major portion of the appropriate software has been developed.

This paper has presented a quick look at an automatically controlled electrical system as envisioned by the Aerospace Electrical Division of Westinghouse. It is designed for, but not restricted to, aircraft and spacecraft electrical distribution systems. The modularity, reliability, redundancy, and software make it a leading contender for any automatically controlled electrical system requiring zero-error operation.

TABLE II

	Power (Watts)	Weight (Lbs.)	Size (Cu. In.)
DCC (Military) 8K Memory	68	12	864
DCC (Space) 5.5K Memory	6	4	85
Console (With Tape Reader)	—	—	—
RIO (Including Connectors)	24	5.1	293

DISTRIBUTION CONTROL CENTER SPECIFICATIONS

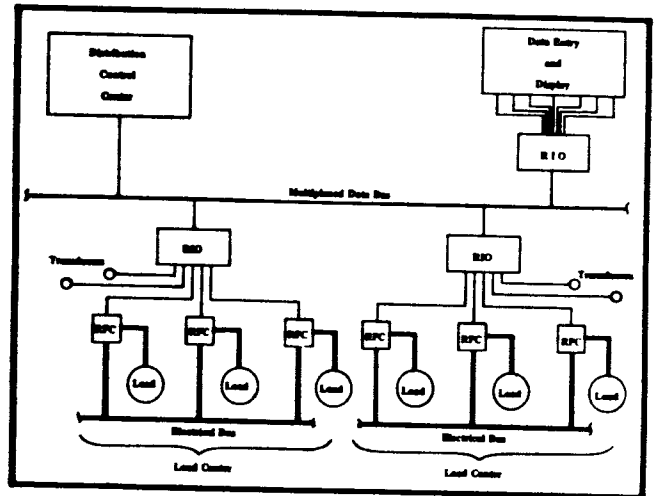


FIGURE 3  
SYSTEM SCHEMATIC

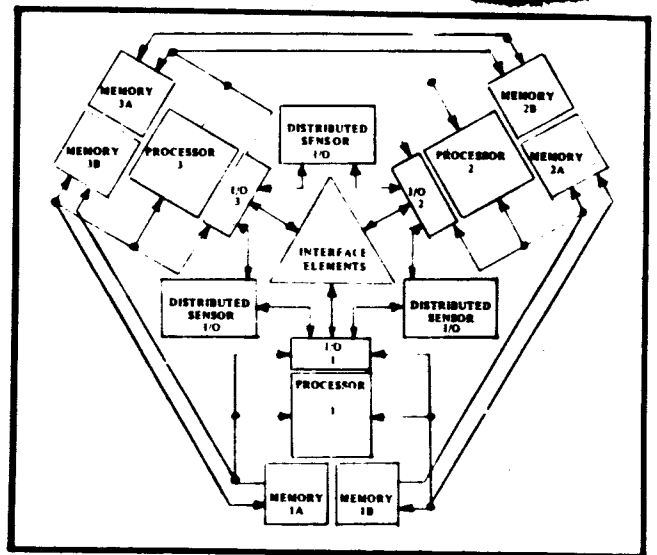


FIGURE 4  
ULTRA RELIABLE CONFIGURATION

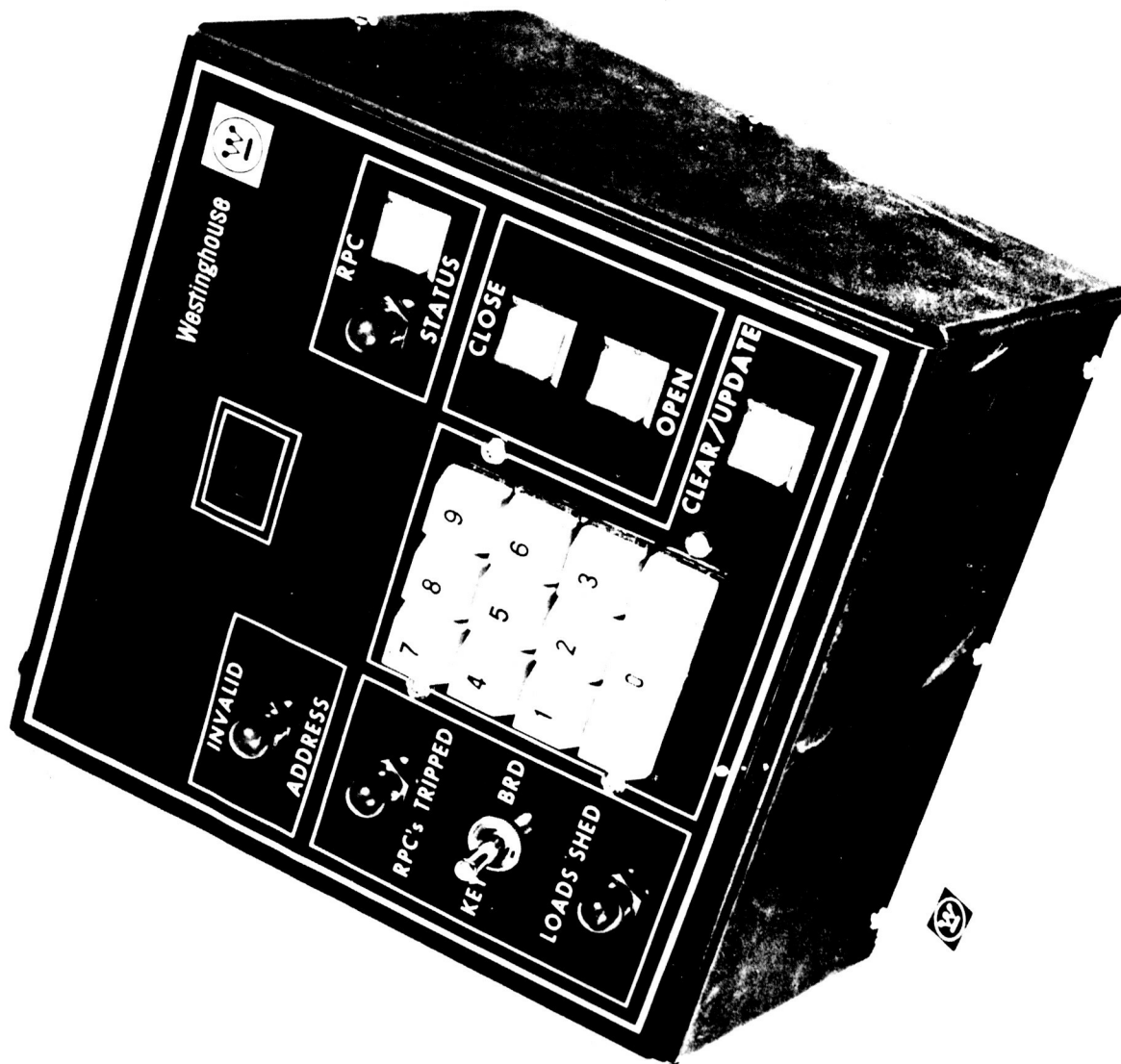


FIGURE 5  
DATA ENTRY AND DISPLAY PANEL

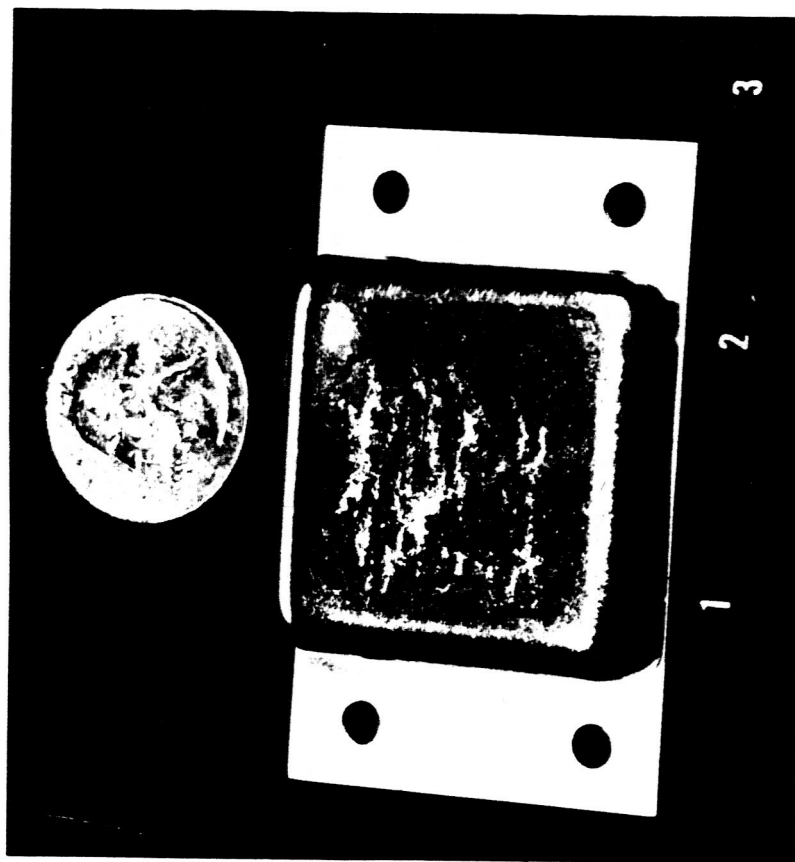


FIGURE 6  
HYBRID VOLTAGE REGULATOR

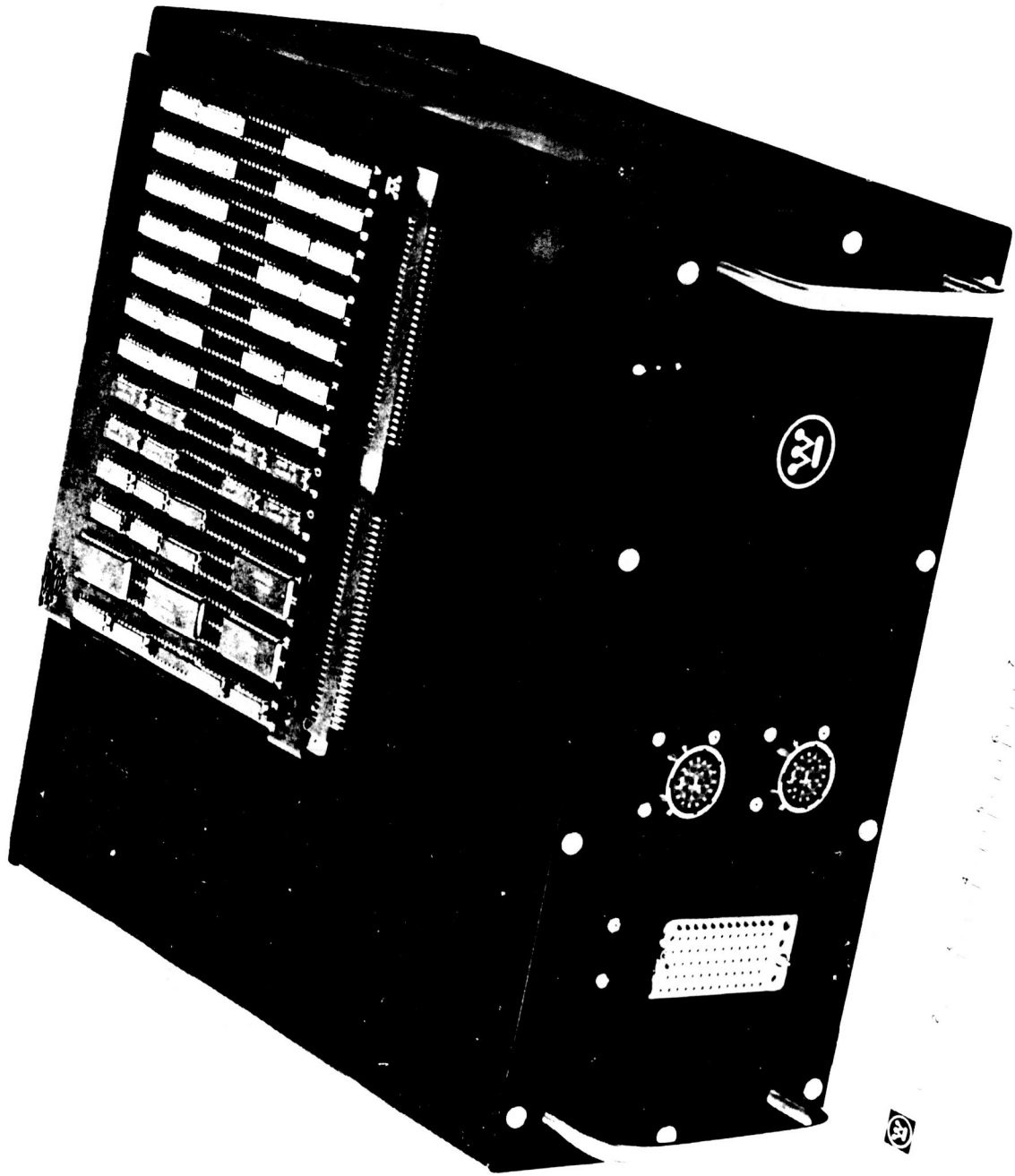


FIGURE 7  
DISTRIBUTION CONTROL CENTER  
(COMPUTER)

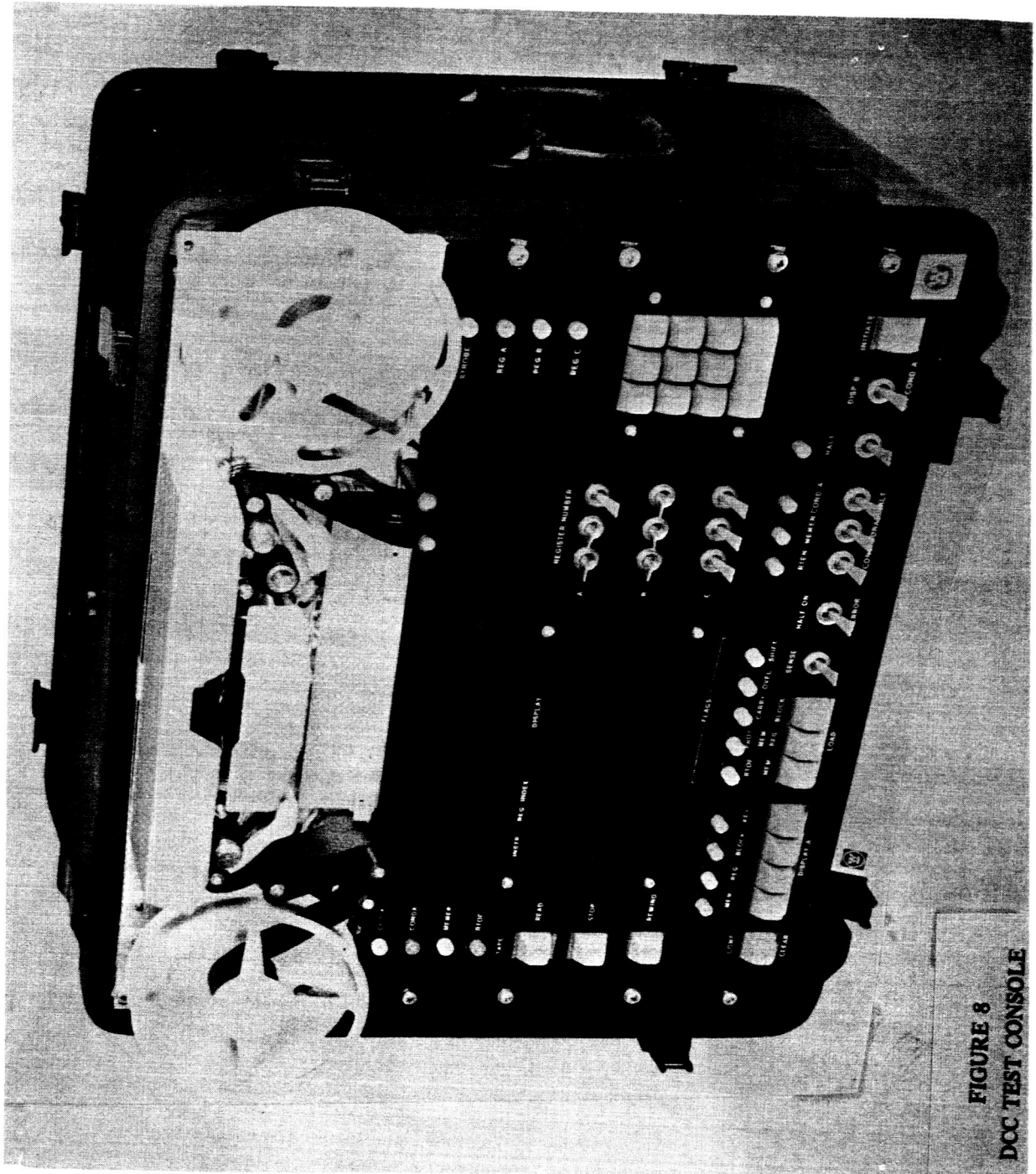


FIGURE 8  
DCC TEST CONSOLE

## **SPACE SHUTTLE CONNECTOR DEVELOPMENT**

**B. J. McPeak and W. J. Shockley**

**NASA-Marshall Space Flight Center  
Huntsville, Alabama**

### **I**

Standard and upgraded MIL-C-26482 and MIL-C-5015 connectors were the workhorses for the Saturn launch vehicle, Mercury, Gemini, and Apollo spacecraft. All of these were relatively successful space vehicles. However, they were not free from exasperating day to day problems. It has often been said that problems with the electrical wiring harness and its component parts were one of the more serious concerns with all of these vehicles. Electrical connectors presented more than their appropriate share of these troubles. Some of these problems are delineated below:

- Recessed contacts
- Recessed inserts
- Bent pins
- Torn or cracked grommets
- Dinged contacts
- Corroded contacts
- Intermittent socket contacts
- Cracked contacts (due to crimping)
- Scratched or scarred pins
- Scratched or chipped or corroded finish
- Coupling ring spring failures
- Loose threaded parts
- Splayed contacts

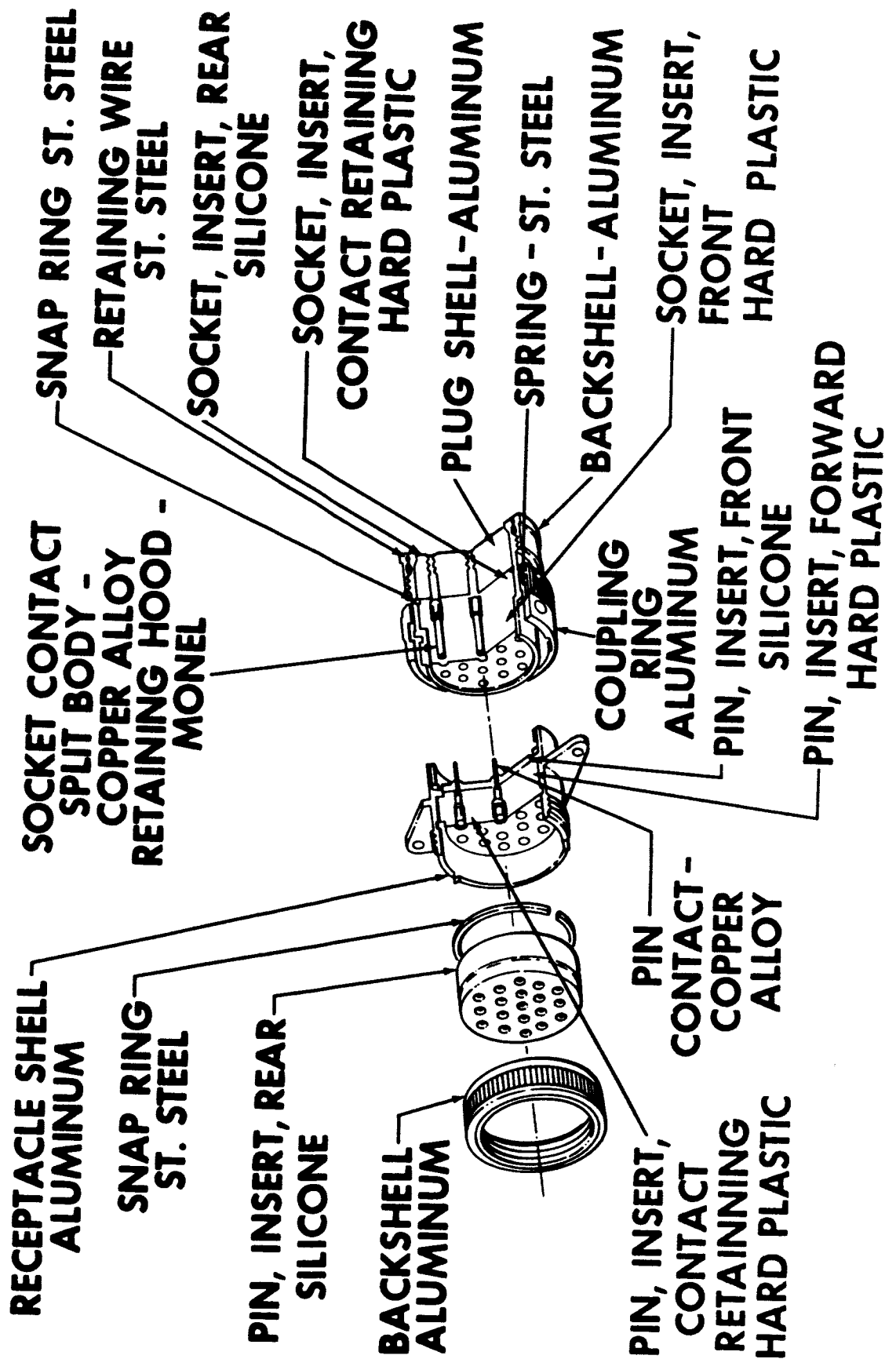
## II

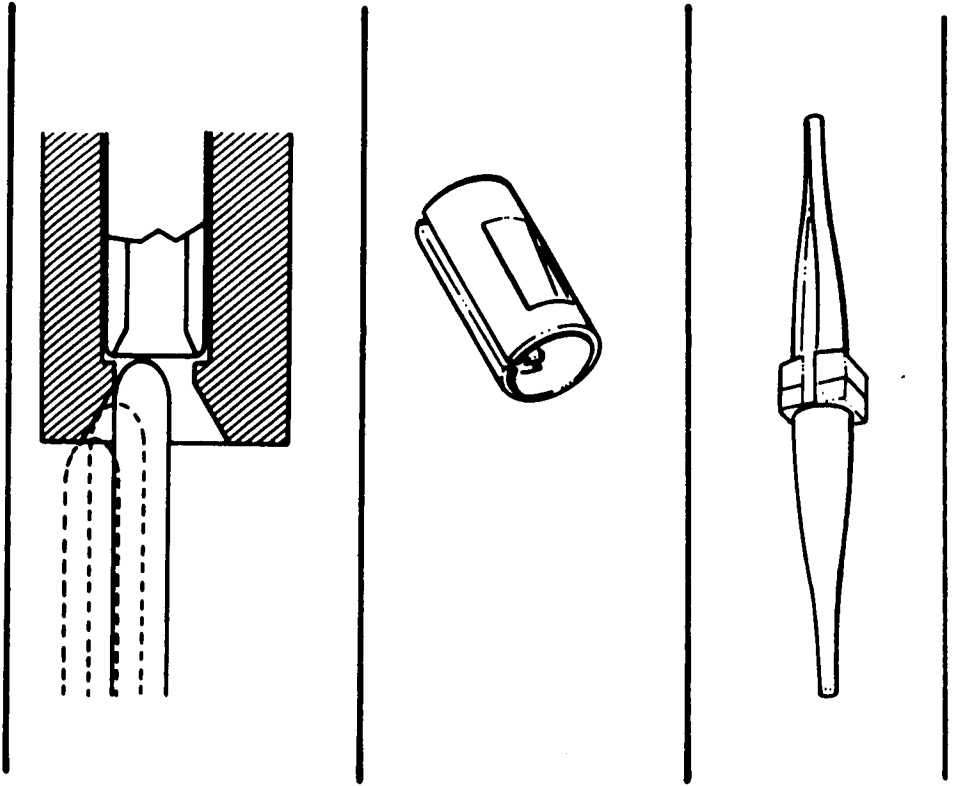
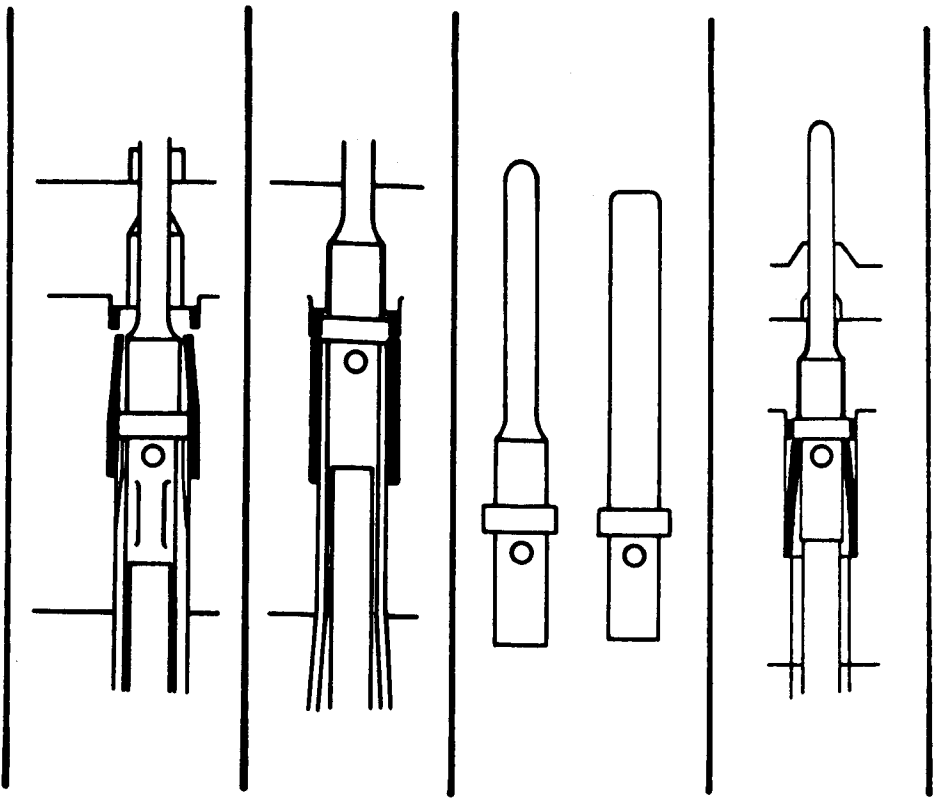
MSFC Specification 40M39569 type connectors are the mainstream or workhouse connectors for the Skylab space vehicle. These connectors are an upgraded NAS1599 type, selected and modified by NASA/MSFC to meet the more stringent and peculiar requirements of Skylab. This connector has solved many of the recurring problems that were common during the Saturn program. Design features of this connector and some of the problems solved are presented below:

- Silicone rubber instead of neoprene rubber for extended temperature and sealing capabilities.
- Insert retained by snap ring and bond between shell and insert.
- Rear contact release system has a stamped metal retaining clip captivated by molded-in shoulders in the hard plastic insulator. This method of contact retention prevents recessed contact problems.
- A rear-inserted plastic tool expands the lines beyond the contact shoulder, releasing the contact.
- The expendable plastic insertion/extraction tool is supplied with each connector. This flexible tool minimizes damage to contact, insulator or grommet.
- Simpler, stronger contact design offers greatly improved resistance to bending or damage. Contacts have a single holding shoulder and no undercuts. Probe-proof sockets have chamfered entry to aid in mating.
- Interfacial seal on pin insert is bonded to hard dielectric. Tapered raised barriers around each pin contact interlock into lead-in chamfers on socket insert, assuring individual contact sealing.
- Hard dielectric closed entry socket insert has lead-in chamfers, providing for realignment of any bent or misaligned pin contacts. For example, a #20 pin bent approximately one diameter from the position will be realigned to mate with the socket. If the pin is severely bent, the hard plastic will stop the pin and prevent mating instead of allowing puncture and uncontrolled pin contact to the outside of the socket barrel.
- Reduced clearance between contact and hard plastic insulator wall provides contact stability and prevents splayed contacts.
- Wire moisture sealing is accomplished by multiple riser design in rear silicone grommet.
- Simplified socket contact design eliminates intermittent circuit problem inherent with multipiece socket contact configurations.
- Meets Skylab outgassing requirements.



# MSFC 40M39569 (MODIFIED NAS1599) CONNECTOR



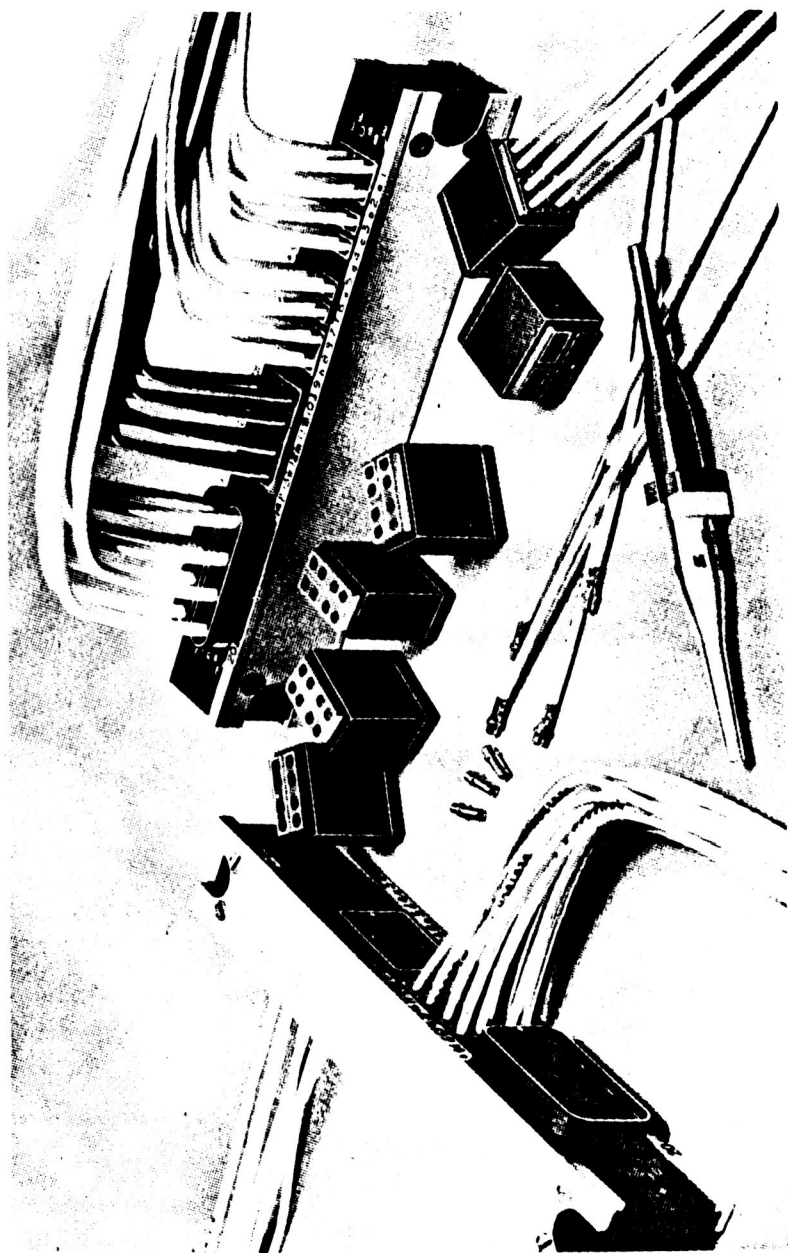


### III

Termination devices meeting MSFC Specification 40M39589 for distribution, bussing, and interconnection are used on Skylab. These devices are a tremendous improvement over the terminal strips, solder terminals, and junction boxes formerly used and offer:

- Enclosed, environmentally protected busses and junctions.
- Removable crimp contacts.
- Standard contact crimp dimensions common with 40M39569 (Mod. NAS1599) connector.
- Standard crimp tools.
- Standard contact insertion and removal tools.
- Easy assembly with fewer tools.
- Meets extended temperature range common with 40M39569 connector.
- Meets stringent Skylab vacuum outgassing requirements.
- Minimized system weight.
- Easy installation in confined areas.
- Circuit design modifications easily accomplished.

# DISTRIBUTION AND BUSSING TERMINATION DEVICES



#### IV

The Zero-G Electrical Connector is also used in addition to the 40M39569 (modified NAS1599) type on Skylab. MSFC Specification 40M39580 defines this connector. The Zero-G Connector is the first electrical connector of major usage specifically designed to meet NASA's needs. Other major NASA connector types evolved from standard or modified connector designs such as MIL-C-26482, MIL-C-5015, or NAS1599 which were established to meet general purpose military and aerospace requirements. The Zero-G Connector was developed by the Bendix Corporation working with Marshall Space Flight Center and McDonnell Douglas Astronautics Company, Western Division. The Zero-G Connector is a handle operated, over-center lock, environmentally sealed unit with removable crimp type contacts. The development of the Zero-G Connector design was aimed to most effectively accomplish the following objectives:

##### A. Environmental

The connector must be capable of withstanding the hostile environments of space. It must give reliable service and operation in a space cabin atmosphere of humidity and oxygen. The connector materials and finishes must withstand effects of such corrosive contaminants as might be present in earth or space cabin atmospheres.

##### B. Performance

The design of the connector was selected to satisfy the following performance requirements:

Ignition-proof operation under electrical load conditions in a highly combustible atmosphere.

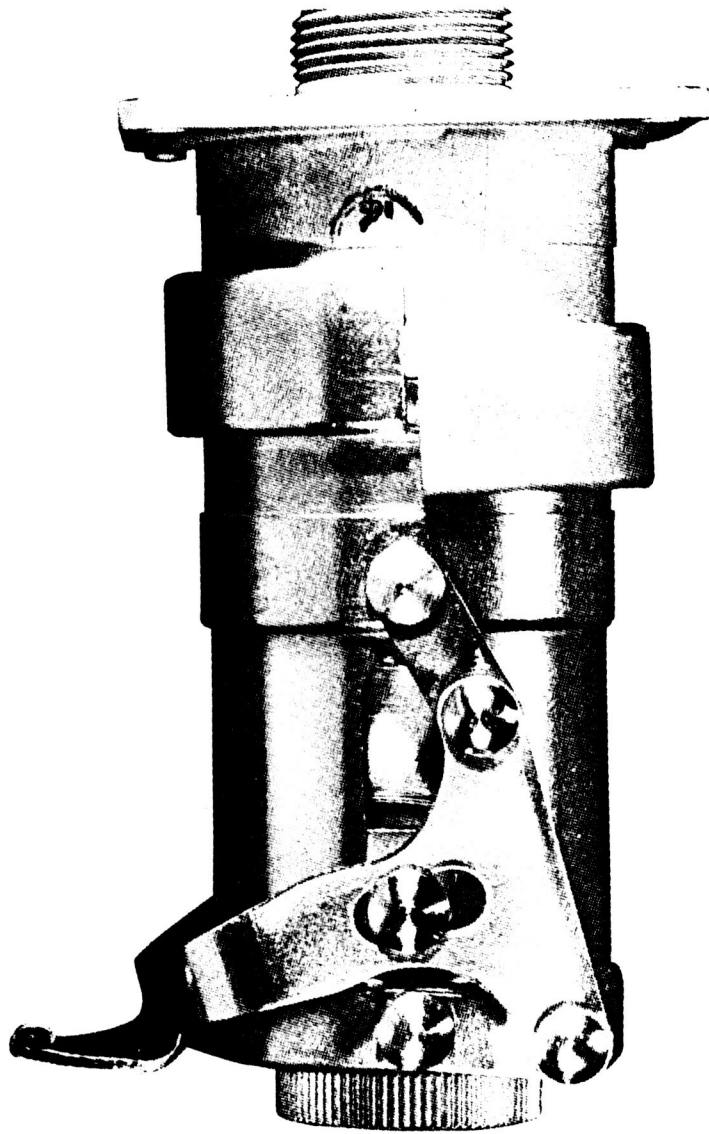
The connector materials must not support combustion in an oxygen rich atmosphere nor outgas toxic or other objectionable matter in a space cabin environment.

Reliable, maintenance-free service over its intended lifespan, making maximum use of proven design concepts and minimum use of complicated mechanisms.

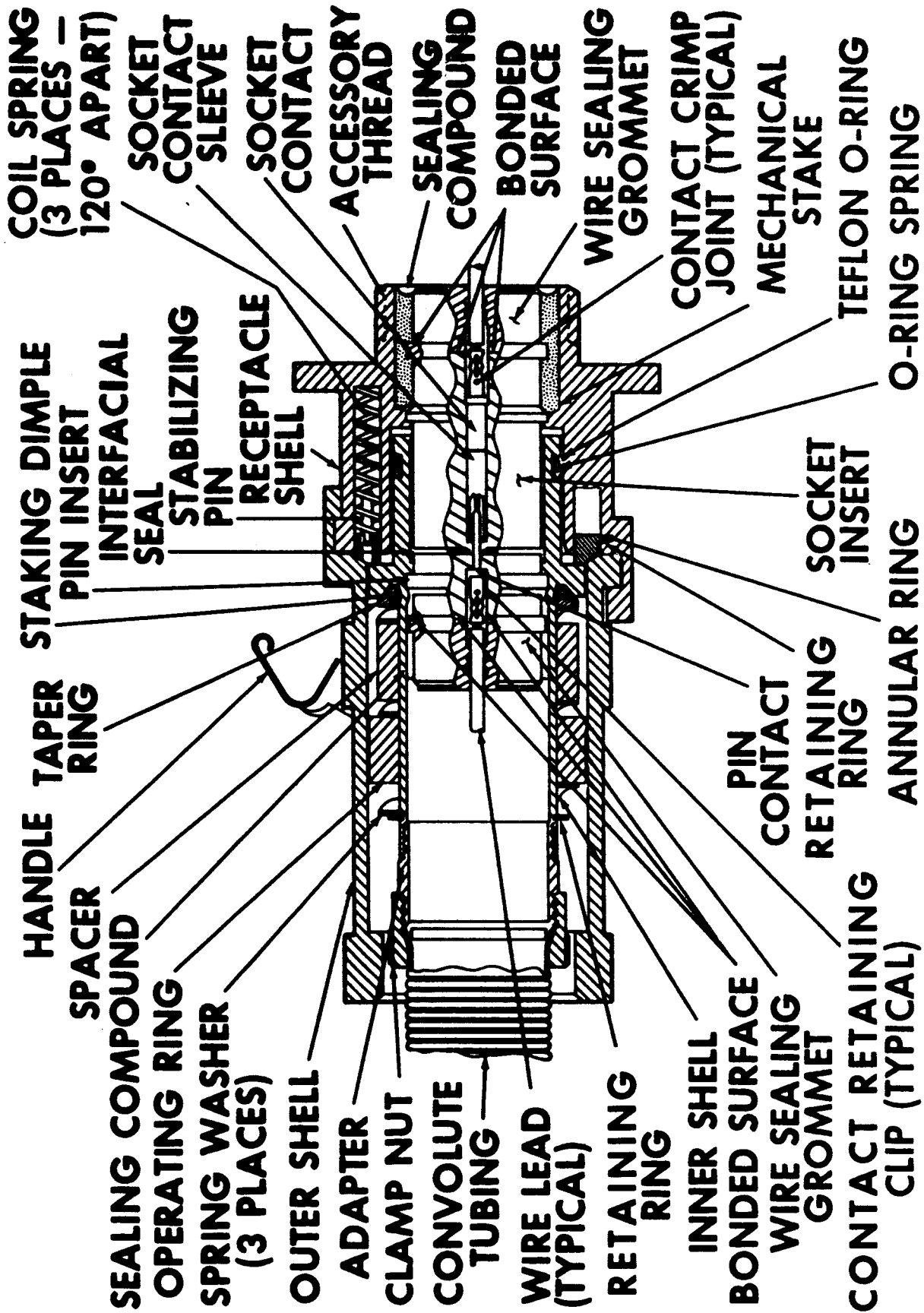
##### C. Astronaut Operation

The design was selected to achieve a simple one, two, three, one-handed mating or unmating sequence. The "hook-and-lip" method of shell engagement (see detail design section) and the handle operated locking feature (see mating sequence and configuration section) enables the astronaut to achieve connector engagement and disengagement with minimum effort. The Zero-G Connector design eliminates the 90° rotation and initial alignment search of conventional circular connectors; the design is especially adapted for operation in a space suit where physical movement and vision are limited.

# SKYLAB ZERO-G CONNECTOR



# SKYLAB ZERO-G CONNECTOR DESIGN FEATURES



#### D. Detail Design

To utilize already proven concepts of connector design, the insert assembly (insulator, contacts, retention clips and grommet seals) utilizes the same physical design as MIL-C-38999 for LJT connectors. The deep barrel, short contact concept gives the desired contact protection and enhances the ignition-proof characteristics of the connector.

#### E. Contact Retention

The contact retention system is the rear insertable, rear release, clip retained method developed by industry for the NAS1599 connector. The rear release method of contact removal increases alignment stability in that broad clearances around the contact periphery at the mating interface is not required for entry of a front release tool.

#### F. Insert Dielectric

The hard dielectric insulation material of the insert assembly is a glass fiber filled epoxy resin (Epiall 1288-BX) well known for its superior strength, low moisture absorption, nonoutgassing, nontoxic, and nonflammable characteristics. The chamfered lead-in feature of the hard face socket insert aligns and guides the entering pin contact into its mating socket. It also provides the "Cork-in-bottle" individual contact seal when the interfacial seal with the raised donuts surrounding each pin contact is compressed between the interface of the mated pin and socket inserts.

#### G. Contacts

The electrical contacts are a high conductive copper alloy, plated with 100 microinches of hard gold over an underplate of soft gold. This type of plating eliminates the undesirable features of silver or nickel underplates, improves plating adhesion and porosity, decreases contact resistance, and results in a longer contact life over an extended operating temperature range. Size 20 and 16 socket contacts are the one piece slotted segment design for improved reliability. The size 12 socket contact utilizes a discrete spring member of substantial size and securely attached within the socket barrel. The spring member portions of all socket contacts are enclosed in a stainless steel sleeve for protection of the contact springs and exclusion of oversize diameter pins or probes.

#### H. Seals

The wire sealing grommets and interfacial seals are a silicone rubber compound for extreme low temperature use, which enables the connector to remain environment resistant.

It further precludes the need for potting operations and greatly enhances connector maintainability.



The main gland seal (O-ring) is a U-shaped circular seal of virgin TFE teflon with an internal spring member to maintain constant seal between male and female shells and still allow pressure relief when mating or unmating. The teflon seal further retards the rapid escape of burning gases should ignition occur within the confines of the connector.

#### I. Shells and Housings

The connector shells are an aluminum alloy which exhibits excellent stability over the temperature extremes, has good strength characteristics, and is readily available to the manufacturer.

The plating of all shells and aluminum parts is chromium over nickel. This results in a tough, durable, electrically conductive finish with superior resistance to corrosion from salt spray and other contaminants present in earth or space cabin environments.

#### J. Operating Mechanism and Springs

The operating handle and linkage are corrosion resistant stainless steel for strength and improved wear characteristics. All spring members are either stainless steel or beryllium copper alloys with proven capabilities to operate over the required temperature range.

The annular ring is a circular spring loaded metal ring located in the shell interface of the connector receptacle. Its purpose is to provide friction to hold the plug and receptacle shells together in alignment until the operator pushes the handle mechanism forward to engage the contacts and latch the connectors.

#### K. Ignition-Proof Design

The ignition-proof design of the connector is achieved by (1) the outer shells of the plug and receptacle being mechanically interlocked around the entire connector periphery (by two 180° concentric hook-and-lip configurations), (2) the movable male shell of the plug extends into the fixed female shell of the receptacle approximately 1/2 inch; this forms a labyrinth of overlapping metal parts which slows the escape of burning gases and at the same time exerting a tremendous quenching, or cooling, effect to dissipate energy before reaching the outside atmosphere. An arc can occur at the connector contacts should they be engaged or disengaged in a power-on condition; however, before the atmosphere outside the connector would ignite, the following chain of events must occur. Assuming the atmosphere internally and externally of the connector is an explosive mixture and an arc occurs at one or more contacts, then:

1. The energy level of the arc must be sufficient to offset the quenching effect of the surrounding electrodes (male and female contact) and ignite the gas in the minutely small chamber formed by the contacts and the insulator (approximately  $1.6 \times 10^{-8}$  in<sup>3</sup> volume).
2. The energy from the initial detonation must then escape into the main chamber of the connector formed by the separation of the contact interfaces (approximately  $8.9 \times 10^{-3}$  in<sup>3</sup> volume, worst condition) with a sufficient energy level to offset the quenching effect of all the surrounding contacts and metal shells and ignite the gaseous mixture of this chamber. Should this event occur then:
3. The energy from the second detonation must be sufficient to force burning gases through the labyrinth of metal baffles formed by the connector shells, offsetting their quenching effect and have sufficient energy to ignite the external mixture.

To obtain the required data for discrete calculation of all the variables encountered in the operation of the Zero-G Connector would require a lengthy and expensive laboratory study program; therefore testing has been performed under worst case conditions to verify the ignition-proof design.

This has been successfully accomplished in the laboratories of McDonnell Douglas.

#### L. Mating Procedure

The mating interfaces of the plug and receptacle shells are identical (i.e. morph-riditic) with a 180° lip extending around the outer periphery of the shell and continuing into a hook around the remaining half of the shell periphery. To engage the connectors, the plug and receptacle are brought together such that they physically meet with the hook on the plug resting in a position above the lip on the receptacle.

Next the connector halves are moved together with the hooked lips engaging until the opposing hooks on the outer periphery butt and the connector halves are concentric. At this point, the connectors are in proper alignment for engaging the contacts and are held in this position by pressure from the annular ring.

Then the handle is brought forward by thumb action, which moves the inner shell of the plug forward into the receptacle shell, first locking the connector halves together and forming a peripheral O-ring seal. Finally, the inner shell comes to rest with the insert interfaces butting together to compress against the interfacial seal to form an individual seal around each mating contact. To unmate the connectors, the handle is moved back until it locks in the "rear lock" position. The connector halves are then moved apart by a slight twisting action to override the annular ring pressure at the mating shell interfaces. The handle mechanism has two over-center lock positions; one at the extreme rear position to lock the movable plug insert in its full unmated position to prevent its interference with the initial engagement of the outer shells; the other over-center lock at the extreme forward position locks the connector halves together.

Spring pressures for the lock positions are derived from 3 wave spring washers surrounding the inner shell. The wave washers also provide constant spring pressure against the mating insert interfaces to compress the interfacial seal and maintain environmental resistance.

The environmental seal at the rear of each connector plug and receptacle is achieved by compression of the sealing glands in the wire sealing grommet against each individual wire. If all wire holes are not used, then teflon sealing plugs of the same nominal diameter as the wire are inserted into the unused holes and the entire connector is sealed.

#### **M. Astronaut Compatibility**

Crew Systems analysis for astronaut performance has been implemented into the design and development of the Zero-G Connector.

The prime considerations were that the connector be operated by an astronaut in a pressurized suit under a zero-g environment, while exerting a minimum amount of physical effort and movement.

The configuration of the handle, the length of travel, the operating forces involved, and the length and diameter of the connector shells were included in the analysis.

Polarizing pins and grooves have been included in the design to prevent cross-plugging where such a requirement might exist. Large letters denoting polarizing positions are stamped on each side of the hook and lip such that a quick glance at the letters during the mating sequence will confirm if the plug and receptacle are identically polarized.

The connector shells are so designed that by sliding the two halves of the Zero-G Connector together until the shells form a concentric circle, automatic alignment is assured. No rotational search to locate alignment keys is required.

Recent investigations have been in the area of electrical connector basic materials. Some of the areas being studied are:

- Electrical contact materials and platings
- Connector shell and housing materials and platings
- Structural dielectric materials
- Elastomeric seal materials

One of the more significant studies is that of elastomeric seal materials.

The applications of elastomers for use as sealing members in basic connector designs normally fall into two categories. All connectors suitable for exposure in harsh environments require a main seal to keep that environment from penetrating between the two halves of the connectors. In its simplest form, this is an O-ring or a flat gasket. It is placed in compression when the two halves are mated, forming a barrier for moisture, air, or contaminants.

The second critical sealing area is the rear of the connector where the wires are soldered or crimped to the contacts. Here a seal must be maintained around each wire as well as to the back face of the insert to isolate the contacts from each other and from the metal shell. This has been accomplished in the past either by potting with a liquid resin or elastomer or by use of a molded grommet. This study has been limited to materials for the latter.

The basic properties required for these applications are the same; low compression set at all temperatures, high resilience, and adequate resistance to the mechanical and thermal conditions encountered.

The difference is largely that of fabrication of a simple item compared with a complex one. While O-rings, despite their simple shape, provide unique problems in manufacture, they certainly in no way approach the difficulties innate to connector grommet designs. Quite obviously, the material which produces a completely acceptable O-ring can be a dismal failure in a grommet mold with its thin walls and severe undercuts.

A major improvement in connectors was accomplished when silicone elastomers were developed to replace neoprene elastomers. However, with new and more stringent requirements, the capabilities of silicone are being stretched to the limit.

Present and anticipated requirements seem to indicate the need for a change from silicone to some new elastomeric compound for connector seals. Flammability requirements in oxygen environments, vacuum outgassing requirements, and expected severe temperature extremes, when considered along with all other requirements,

emphasize the need to **develop new compounds**. Many of the methods used in the Skylab program to meet crew area flammability requirements impose a tremendous penalty. Development of connector materials and electrical wire that will meet the flammability requirements without the massive coverings used in Skylab will bring about a tremendous weight, volume, cost, and time savings.

Therefore a major goal was established to find an elastomer or elastomers which would be suitable for use in electrical connector main joint seals and wire sealing grommets with particular attention to the following:

- Temperature extremes of  $-200^{\circ}\text{C}$  to  $+200^{\circ}\text{C}$ .
- **Nonflammable or self-extinguishing in oxygen atmosphere.**
- Negligible outgassing in space environments.
- Manufacturable, reasonable priced, readily available material.
- Other characteristics typical of general connector requirements.

Compounds based on fluorocarbon rubbers such as du Pont Viton or 3M Fluorel provide chance of overall compliance with requirements because of their proven flame resistance in oxygen atmospheres.

At the same time the fundamental shortcomings of these materials also have now become evident, notably poor moldability, poor resilience, cold temperature weakness, and recent indications of susceptibility to moisture degradation.

Further investigation into the fluorocarbon rubbers available indicated two more Fluorel materials worthy of study. These are Mosites #1087-JJ and Raybestos Manhattan L-3583-2. Both these materials are in the 55-60 durometer range necessary for grommets. Data is incomplete, but they appear comparable with du Pont's Viton VS 2001.

An abbreviated study confirmed suspicions relative to moldability. Molding was confined to simple molds and still there was difficulty in obtaining acceptable samples. Greatest problem seemed to be from inability to get a proper cure as parts were inclined to be porous and contain blisters. More familiarity with the material might overcome this as far as simple moldings **such O-rings or gaskets are concerned**. The material is much too hard for use in connector grommets. Earlier parts were molded with Fluorel L-2231 from Raybestos Manhattan with no difficulty encountered on simple parts but with tearing of webs on standard grommets.

The whole fluorocarbon elastomer family as represented by 3M's Fluorel and du Pont's Viton have been rapidly improving. Disregarding flame resistance for the moment, the major impetus has been in compression set. Both companies have been able to reduce compression set at all temperatures. For example, Viton E-60C has about the same set after 1000 hours at  $392^{\circ}\text{F}$  as the original Viton A had after 70 hours. Fluorel 2160 is comparable. **As a result of these achievements, new**

specifications have been issued specifically to cover these materials. These are MIL-R-83248 and AMS 7280 and mark a major advance in state-of-the-art recognition.

Du Pont also has a modified Viton designated LD-487 having lower temperature characteristics than the standard materials. Brittle point is  $-60^{\circ}\text{F}$  approximately and TR-10 is  $31^{\circ}\text{F}$ , compared with  $-40^{\circ}\text{F}$  and  $-5^{\circ}\text{F}$  for Viton A. These are still a long way from  $-200^{\circ}\text{C}$  but do represent a substantial improvement.

Because there has been so much progress in these materials, including success in developing Viton connector insert and grommet materials, it seems logical that they could be further improved in those directions considered advisable. This would be a main effort suggested for further investigation.

The alternatives to these materials are unsuitable in one area or another when compared with present guidelines. The organic rubbers as a whole are all unsatisfactory from a temperature standpoint. Temperature resistance also eliminates the CNR or Nitroso rubbers developed by Thiokol which appear to be equal to the fluorocarbons in flame resistance in oxygen atmospheres. However, CNR is also listed in NASA 50M02442 "ATM Material Control for Contamination Due to Outgassing" as an "unacceptable material".

The Dexsil materials developed by Olin Matheson appear to have the heat resistance required but difficulties in manufacture have pretty well curtailed their progress to production status. These materials are reported capable of withstanding temperatures considerably higher than the silicone. Outgassing in hard vacuum was reported minimal, tests for 72 hours at  $155^{\circ}\text{C}$  yielding only 49 ppm total organics and less than 5 ppm carbon monoxide. The materials was also self extinguishing in air, and flash and fire points are extremely high. Flammability tests conducted by NASA showed the samples tested were not **self-extinguishing in 16.5 psia oxygen**.

Both of the above materials had a further disadvantage, price, with the CNR rubbers at approximately \$600 per pound and Dexsil at \$100 per pound. No chance of their utilization in connectors at their present status is anticipated.

Beyond these lie even newer polymers in various stages of development such as the perfluoroalkylene triazines and copolymers of tetrafluoroethylene and prefluoro (methyl vinyl ether), the former under investigation by Hooker Chemical and the latter by du Pont. These are materials of the future, warranting close observation as they progress but hardly likely for serious consideration at this date.

The materials most commonly used in high performance electrical connector grommets and seals have been silicone rubber compounds. Both fluorinated oil resistant silicones, non-fluorinated silicone, and blends of both have been used.

Properly formulated silicone rubbers are capable of long life at  $200^{\circ}\text{C}$  with minimum effects on mechanical and electrical properties. In general, they are also low in outgassing in vacuum or air at these temperatures. However, it is still necessary to

assure absence of low molecular weight fractions and other volatiles which may be characteristic of specific compounds. As a rule this can be accomplished by high temperature curing, in extreme cases under vacuum.

At sub-zero temperatures, they range in brittle point from  $-90^{\circ}\text{F}$  ( $-68^{\circ}\text{C}$ ) for the fluorinated stock to  $-178^{\circ}\text{F}$  ( $-116^{\circ}\text{C}$ ) for the best low temperature materials. While this is still well above the  $-200^{\circ}\text{C}$  requirement, it is considerably below the best temperature recorded for the fluorocarbon rubbers. The brittle point does not by itself categorize the material as unsatisfactory at  $-200^{\circ}\text{C}$ . Tests on actual connectors employing both Viton and certain silicones in liquid helium and liquid nitrogen have failed to cause any permanent damage although some fluorinated silicones have cracked during this exposure.

The main obstacle to use of silicone rubbers remains flame resistance in oxygen atmospheres. While the basic polymers, even the fluorinated ones, have no inherent flame resistance, progress is being made through the use of additives. Prompted by Boeing Specification BMS 1-59 and McDonnell-Douglas DMS 2012, Dow Corning, General Electric, and Union Carbide have all produced rubbers which are flame retarding and quickly self-extinguishing in air.

Dow Corning Silastic 2351 and related compounds and General Electric CE5537 are not only flame resistant in air but also have other properties important to connector grommet design. These materials are not fluorosilicones and consequently have no substantial resistance to common oils and fuels.

Most recently Arthur D. Little, Inc., in a NASA development program has succeeded in producing silicone formulations having oxygen index ratings as high as 0.60. More usable compounds have oxygen index ratings from 0.40 to 0.50 and were self-extinguishing in NASA tests in 50% oxygen at 10 psia. They were also slow burning in 100% oxygen at 6.2 psia. These compounds utilize decabromodiphenyl (DBDP) as an additive to conventional silicone compounds such as General Electric SE-517. At the present time, this additive is an experimental product, and results are dependent on high purity. Mechanical properties of these flame resistant silicones are reduced some by the additive but, from the limited data now available, might be usable. Tensile strengths over 700 pounds per square inch and elongations over 450% are quite typical and certainly within the parameters needed for grommets. Low temperature resistance does not seem to be affected significantly by the additive, but heat aging data is not sufficient to indicate whether it causes any detrimental effects.

In general, it appears that Arthur D. Little Inc., has made a substantial contribution to flame resistant silicone rubber technology and that considerably more remains to be done before the optimum material is developed. Their work has been limited at

this time to one basic silicone reinforced gum, GE SE517, and one catalyst, 2,4-dichlorobenzoyl peroxide. Other gums and catalysts could be expected to provide improvements in some of the other properties which appear to be borderline with the present compounds incorporating DBDP.

These materials do not appear to be nearly as flame resistant as the Viton and Fluorel materials but are substantially better than the silicones now in use. They warrant a very serious consideration for use in grommets.

One other very feasible approach would be provision of a flame resistant face on the exposed surface of a silicone rubber grommet. This face would most logically be one of the Fluorel or Viton formulations. Such a combination could give us the best of both material systems at some sacrifice in size and cost.

The various Viton and Fluorel compositions could be further investigated. This would be largely a study of design adaptability with moldability being the chief factor. Web design of the grommet holes is expected to be crucial because of the low elongation of these materials.

At the same time a formulation program should continue to provide an improved grommet material. This would be a two directional study, on one hand attempting to improve the shortcomings of the fluorocarbon materials while retaining their flame resistance, and on the other hand improving the flame resistance of the silicones without losing their desirable attributes.



**Digital Efficiency:**

Investigation is presently being conducted concerning digital efficiency or the effects of interconnect systems on the transfer of high speed digital signals.

The digital pulse is the controlling parameter in such digitized equipment as computers, guidance systems, and multiplexing systems as to their ability to receive, store, retrieve, and display information in large quantities at rapid rates within reasonable equipment physical size and weight limitations.

An effort has been made to determine if present or future digital pulse information is or will be deleteriously affected by interconnects, such as cable-connector combinations, in the following parameter areas:

- A. Wave Form Distortion With Respect to:
  - Rise Time Characteristics
  - Pulse Width
  - Fall Time Characteristics
  - Repetition Rate
  - Phase Shift
  - Amplitude Changes
- B. Signal Change Due to Short Term Discontinuities
- C. Circuit to Circuit Crosstalk
- D. Limitations on Integrated Circuit Fan-out Capabilities

Through literature searches and information obtained from digital equipment suppliers, it has been established that to increase the capabilities of digital controlled systems, efforts are being made to shorten the rise time and width of the digital pulse. At the same time efforts are being made to increase the repetition or clock rate pulse chains to meet future needs.

The losses in transmission lines and electrical interconnecting mechanisms affect the fidelity of transmitted pulses, and these losses increase with increasing frequency. In particular it is evident that as pulse rise times and widths continue to decrease, the conventional pin and socket multipin connectors will prove to be too lossy to serve as digital system interconnects.

At the same time it is evident that presently available test methods are marginal for test work in the sub-nanosecond and picosecond time range.

Thus the limitations of an electrical connector and its suitability for a specific digital application cannot now be determined in advance with certainty.

The conclusions derived from the study reported here indicate that further consideration is needed in the following specific areas:

- Development of test methods suitable for establishing the limits of operation for interconnects in digital systems.
- Measurement of multi-channel connector impedances in circuits handling fast digital pulses.
- Measurement of pulse rise time, duration, and repetition rate capabilities of multi-channel connectors currently in use in circuits dealing with fast digital pulses.
- Evaluation and determination of acceptable levels of cross-talk in multi-channel connectors currently being used.
- Determination of ageing effects on the parameters determined in above statements.

At the completion of this task, if so dictated by the work outlined above, further effort should be directed toward the development of specific multi-channel connectors which are capable of dealing with anticipated rise times, signal levels, and pulse repetition rates in future applications.

A continued effort in the investigation of digital interconnects should:

- Determine if interconnect problems exist in present system pulse transfer techniques.
- Determine if interconnect pulse transfer problems will be aggravated in future systems.
- Outline a detailed follow-on program for actual measurement and evaluation of connectors in use on present digital systems.
- Outline an evaluation of proposed connector materials for their electrical properties as to their future application in improved design digital connectors.

The ability of a particular digital system to originate a defined pulse shape. Transfer the pulse shape, and receive the pulse shape, meanwhile maintaining the pulse's integrity, can be defined as the digital efficiency of the system. The origination, transfer, and receive functions within a system will repeat many times during operation so that a loss of digital efficiency, though minor in nature on a one time basis, could, if repeated often enough, result in a complete degradation of the pulse shape to the point where system error or malfunction would result.

In order to increase the capabilities of digital controlled systems, designers have been attempting to shorten the rise time and the pulse width of the digital pulse, while at the same time increasing the repetition or clock rate of pulse trains.

Prior to the advent of the present integrated circuit (IC) technology, pulse generation was limited in the 1930's to 1940's by inherent properties of vacuum tubes, mechanical switches and relays, and their related discrete component circuitry. The digital pulse in most cases was defined as to time parameters in milliseconds. They could be classed as hertz or kilohertz systems with respect to circuit pass band and wave length limitations.

The transistor and diode-resistor networks began to replace the earlier vacuum tube and mechanical devices by the mid-1950's. As the types of transistors multiplied, their rise time was less limited due to improvement in junction forming technology. The digital pulse generation capabilities had reached the microsecond range and was approaching the nanosecond range by the late 1950's. Most circuits consisted of discrete components. Even with the advent of printed circuit board techniques, the systems could be classified as megahertz systems.

Semiconductor technology continued to improve to the point where frequency generating capabilities within the junction approached a 4 gigahertz gain-pass band property. This made possible pulse rise time in the nanosecond time range. The semiconductors failed to achieve their capabilities consistently due to losses introduced by the hermetic packaging and necessary circuit connecting wires to the various semiconductor junctions. This was undoubtedly the first evidence of interconnect limitations on digital pulse generating systems.

The IC technology which became practical in the middle 1960's aided in reducing junction interconnect limitations by making possible shorter wiring techniques and also better control as to placement of interconnects. Compensation could be designed into the IC circuit to overcome many of the IC interconnect wiring losses and impedance mismatch losses. At the same time tunnel diode pulse generating devices in a chip form gave theoretical performance capabilities of 7 to 10 picosecond rise times. When placed in their operational environment the actual rise times were increased to approximately 20 picoseconds. The above technology improvements made possible a gigahertz generating system.

From the mid 1960's to the present time articles in trade and professional journals began to appear warning of cable-connector problems associated with the transmission of microwave frequencies necessary to assure the integrity of these picosecond or sub-nanosecond pulse rise times.

During this time interval more and more digital functions were being incorporated on a single chip resulting in the use of many medium scale integrated (MSI) systems to make up a complete digital operated system, such as a computer. The shift to MSI systems, has reduced the number of conventional cable-connector system interconnects within a functional digital system, but has not eliminated them. Interconnects will be required until systems such as a complete operational computer can be placed on a single chip,

achieving the ultimate in large scale integration, (LSI). Some authorities feel the practicality of such an LSI system will not be achieved until the 1980's.

The MSI systems of today and in the next decade use the mother-daughter board concept to package the digital circuitry, making necessary the use of some form of cable-connector combination to marry the various board configurations into a complete digital system. In addition, cable-connector combinations are necessary to tie interface hardware such as remote programmers and readout devices to the digital system. The interface hardware cable-connector in some form will undoubtedly always be necessary even with the successful advent of complete LSI digital systems.

The study indicated that there are two areas in a digital system where interconnects will be a problem in the next 10 to 15 years. These areas are:

- A. Where cable-connectors will be necessary to interconnect circuit boards within a system to facilitate function changes, ease of assembly, and serviceability.
- B. Where cable-connectors will be necessary to interconnect a given digital system to its remote interface hardware.

The problems and solutions related to digital pulse transmission will be similar in both areas, with the former being more severe in nature in the immediate future.

A digital pulse whose shape is represented by Figure 1 has a rise time of  $T_1$  to traverse an amplitude change of 10% to 90% of its maximum amplitude. As  $T_1$  approaches zero, the number of frequencies which must be generated and transmitted approaches infinity. Since  $T_1$  has a finite value, a relationship between a particular rise time and its upper frequency component exists.

$$FT_1 = K \tag{1}$$

where  $F$  is the upper frequency in MHz,  
 $T_1$  is the rise time in microseconds,  
 $K = .35$ , where the rise time overshoot must be limited to 2 or 3 percent of the maximum. Table 1 was calculated from equation 1 and shows presently used and future possible digital pulse rise times and their upper frequency components. The electrical length of an interconnect device is,

$$\lambda = \frac{300 \times 10^6}{E_r F} \quad \text{where: } \lambda = \text{wave length in meters} \tag{2}$$

$300 \times 10^6 = \text{velocity of light, in meters/second}$   
 $F = \text{frequency in hertz}$   
 $E_r = \text{relative dielectric constant of medium}$

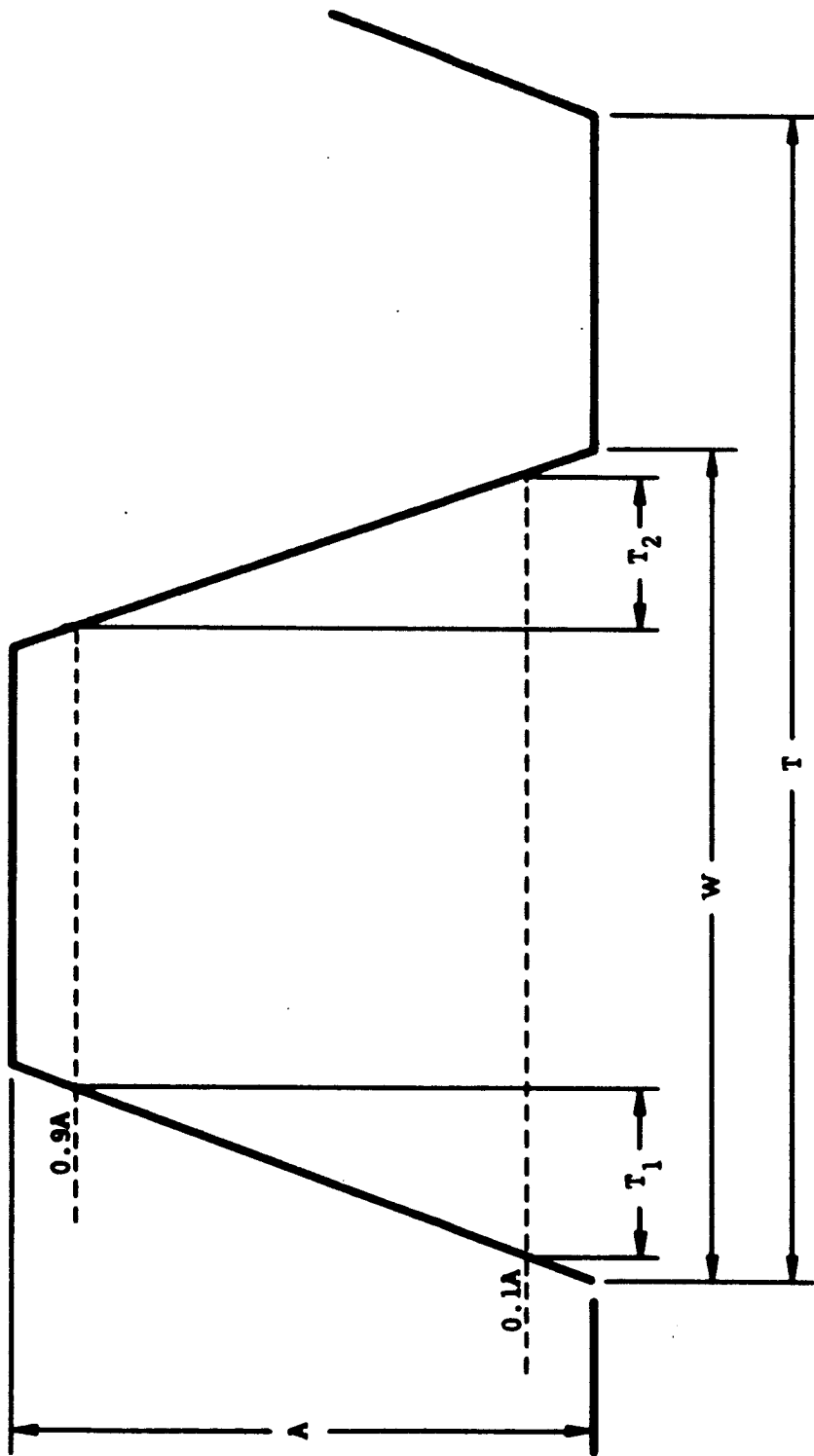


FIG. 1 DIGITAL PULSE DIAGRAM

Table 1

Rise Times Vs. Frequency & Wavelength

Rise Time - $T_1$	Upper Frequency - F	Wave Length $\lambda =$ meters in air (E=1)
10 microseconds	35 khz	8580 meters
1 microsecond	350 khz	858 meters
100 nanoseconds	3.5 mhz	85.8 meters
10 manoseconds	35 mhz	8.58 meters
1 nanosecond	350 mhz	.858 meter
100 picoseconds	3.5 ghz	.0858 meter
10 picosecond	35 ghz	.00858 meter
1 picosecond	350 ghz	.000858 meter

Present digital rise times appear to fall between a maximum of 5 microseconds to a minimum of 10 nanoseconds. This means the upper frequency which must be transmitted undisturbed is from 70 KHz to 35 MHz.

The present average relative dielectric constant in most transmission mediums is 4.0. (See Table 2 for various dielectric material parameters.) This means the wavelength, or one electrical length, for transmission interconnects will be between 214 to 4.18 meters, or 700 to 13.7 feet. If cable-connector lengths have had physical lengths which were much less than one quarter of these electrical lengths (175 to 3.4 feet), then degradation of digital pulses due to influences introduced by mismatch and changes in velocity constant would have been minimal. Also the effects of capacity loading due to interconnects would be less a factor at the above 35 MHz frequency limit. When rise times approach 1 nanosecond and less, then cable-connector electrical lengths decrease to fractional parts of an inch, and the effects on pulse shape with respect to velocity constant and electrical parameters, such as distributed capacity, inductance, and AC resistance of the interconnect must be considered.

The future rise time goals within the next 5 to 10 years show that rise times are expected to be between 3 nanoseconds to 1 picosecond. The 1 picosecond goal is from one company who is presently achieving 100 picosecond rise times. This same company has performed their own development on connectors for digital pulses, recognizing an existing problem.

As pulse times decrease, the present circuitry now in use appears to limit their amplitude. The normal digital pulse today is 5 to 8 volts in amplitude. Future pulse amplitudes are trending to millivolt and in some cases, microvolt levels. This will undoubtedly place limitations of pulse fanout capabilities assuming complementary improvements in line driver capabilities. Losses or vibration induced noise from connectors would be more noticeable to these low level pulse signals.

### Cables:

The coaxial cable is the preferred way to transmit picosecond-time digital pulses, followed closely by stripline transmission lines. They may in the future be replaced for some applications by laser beam transmissions.

As a point of interest, experimental work with laser beam transmission has progressed to the point where scientists have observed laser pulses as short as 1 picosecond in duration. Their application to digital pulse transmission systems in some form is certain to appear in the future.

The losses in present coaxial transmission lines affect the fidelity of the transmitted pulse. These losses appear as conductor or copper losses and as medium or dielectric losses and are as follows:

$$\text{Copper loss } A_{\text{cu}} = \frac{0.434}{Z_0} \left( \frac{1}{d} + \frac{1}{D} \right) F^{1/2} \quad \text{db/100 FT} \quad (3)$$

$$\text{Dielectric loss } A_d = 2.78 E_r^{1/2} R_p F \quad \text{db/100 FT} \quad (4)$$

Where  $D$  = diameter of inner surface of outer conductor, inches  
 $d$  = diameter of outer surface of inner conductor inches  
 $F$  = frequency, megahertz  
 $E_r$  = relative dielectric constant at frequency  $F$   
 $R_p$  = power factor of dielectric at frequency  $F$   
 $Z_0$  = characteristic impedance of coaxial cable in ohms.

A study of Equations 1, 3, and 4 shows that losses within a coaxial line will increase as pulse rise times decrease and their upper frequency components increase. Both losses increase with increasing frequency. The effects of these losses on pulse shape is to attenuate the higher order of frequency components necessary to form and maintain the rise time slope. The result is a delay in or a longer rise time. For example, one foot of RG-9/u cable will increase an ideal (zero rise time pulse) to 20 picoseconds, while 8 to 10 feet of RG-58/u cable will increase the same ideal pulse to 1 nanosecond. Furthermore, the rise time does not necessarily vary linearly with length.

### Connectors:

The amount of degradation to the digital pulse contributed by the connector in the interconnect system has not been clearly defined by any literature studied or companies contacted in this program. Several reasons for this lack of information on connectors can be advanced, and are as follows:

- A. Some companies have stated that connectors were a problem in their digital circuits, but when questioned further, could not define these problems such that a separation of electrical from mechanical problems could be determined. Most companies do not use methods of test to determine source and cause of component failures. They generally rely on "in circuit" testing and "debugging" on a system by system basis.

B. The connector has not been a culprit on most digital systems to date, as its electrical length has been short relative to the resulting pulse induced wave lengths.

The second reason appears the more valid of the two since the connector, while subject to the same loss factors as the cable, is several orders of magnitude physically smaller than most cable systems in use today. Where connector loss and impedance mismatch problems have been severe, high quality single circuit coaxial connectors are employed. Some typical coaxial connectors in use are the Amphenol precision 7-mm type APC-7, the General Radio GR type 874, and the 3-mm OSM connector.

Multipin connectors are in use in various forms for multi-interconnecting digital circuit boards and also to interface hardware. These connectors consist of the cylindrical MS and Pygmy types, the rectangular printed circuit, rack and panel, flat cable, dip socket, and TJS terminal junction system types. Most have appeared with one or more coaxial contacts installed in place of some of their normal pin and socket arrangements. These have been introduced at specific digital user requests where certain circuits passing through a particular connector must be controlled for losses due to the dielectric or impedance mismatches. The coaxial system also minimizes circuit to circuit crosstalk.

**Multipin Connectors - Pin and Socket:**

As pulse rise times decrease the conventional pin and socket multipin connectors will prove too lossy to serve as digital interconnects. These losses will occur mainly in the form of dielectric losses and pin to pin impedance mismatch losses. These losses will make it impossible to achieve narrower pulse widths and also increased repetition rates when they reach the picosecond rise time range. The common forms of pin and socket arrangements within their dielectric inserts will increase their circuit crosstalk potentialities.

Some typical dielectrics used in connector inserts are shown in Table 2 along with their relative dielectric constants and dissipation factors measured at 1 megahertz.

**Table 2**

**Insert Dielectrics**

Material	Die. Const.	Diss. Factor
Phenolic Mineral Filled	9-15	.07 - .20
Melamine Glass Fiber Filled	6.5-7.5	.013-.015
Alky D Glass Filled	5.2-6.8	.008-.023
Diallyl Phthlate Glass Filled	3.4-4.5	.009-.014
Silicone Glass Fiber Filled	3.2-4.7	.002-.020
Polycarbonate Glass Filled 10-40%	3.0-3.4	.007-.008



As stated in Equation 4, the dielectric loss at a given frequency is a function of the materials relative dielectric constant,  $E_r$  and its power factor or dissipation factor,  $R_p$ . The materials shown in Table 2 are mainly composite or filled materials whose mix proportions can vary. These mix variations are known to affect their electrical properties at the normal low frequency (1 MHz) measurement ranges. Very little is known about their behavior in the microwave frequency range. Physical arrangements of the contacts within the dielectric can give an infinite number of combinations of characteristic impedance for pair arrangements within a connector shell as shown by Equation 5 and Figure 2. A balanced shell shielded contact pair is used for example purposes.

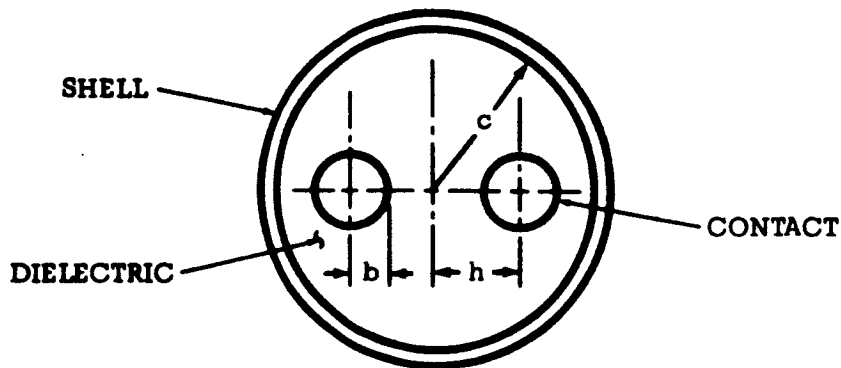


FIG. 2 SHIELD PAIR BALANCED 2 CONTACT CONNECTOR

Equation 5 shows that the characteristic impedance of two contacts within a multipin connector is not only dependent upon the dielectric constant of the insert material, but also upon the contact's diameter, their spacing from each other, and their position distance from the inner diameter of the connector shell.

$$Z_0 = \frac{120}{E_r} 2.303 \text{ LOG } 2V \frac{1 - \sigma^2}{1 + \sigma^2} - \frac{1 + 4V^2}{16V^4} 1 - 4\sigma^2 \quad (5)$$

Where:  $E_r$  = Relative Dielectric Constant of the Insert

$$V = \frac{h}{b}$$

$$\sigma = \frac{h}{c}$$

Variations of Equation 5 for cylindrical and rectangular type connectors versus various pair diameters, spacing, and position could be performed on a computer and would result in a large number of impedance values in today's more common connectors.

This exercise would yield nothing other than their inadequacy if an attempt were made to use them to transmit picosecond pulses where they must be impedance matched into 50, 75, 93, and 300 ohm source and detector pulse circuitry.

Another area where connectors of this type may prove their pulse transfer inadequacy is in the typical physical design areas of a pin and contact arrangement. Equation 5 assumes that radius  $b$  is constant throughout its length. This is not true of most pin and socket contacts. There are diameter undercuts on most, used for contact retention within the dielectric. There are also diameter changes at the mating areas of the pin to socket which vary in length, dependent upon insertion tolerances. These diameter variations can be as long as .250 inch in length for a size 20 contact. A time domain reflectometer (TDR) measurement using a 28 picosecond rise time pulse would show these diameter changes as impedance discontinuities along the length of the contact.

#### Pulse Measurement and Standards:

As this study was pursued several additional factors pertaining to picosecond rise time generation became apparent. These factors were

- lack of a rise time standard for calibrating test equipment, and
- a scarcity of test equipment capable of measuring and displaying picosecond rise time.

The National Bureau of Standards has been working for two years on a rise-time calibration service (Page 43 E. D. N. March 1, 1970). The standard for this service will be a sampling scope whose response has been evaluated in the frequency domain. Its amplitude response was measured to 18 GHz, and its phase response to 9 GHz. Pulse voltage down to 1 volt amplitude will be measured from 20 picoseconds (at about 25 percent uncertainty limit), to 100 picoseconds (at better than 5 percent uncertainty limit) and on up (with 2 to 3 percent uncertainty limit). The pulse width will be limited to 300 picoseconds.

Realtime oscilloscopes such as the Hewlett-Packard model 183A has a band width of 250 MHz, and is the widest gain-band width oscilloscope on the market to date. The rise time of these scopes is 1.5 to 3.5 NS. The rise time measurement ( $T_1$ ) is limited by the square root of the sum of the squares of pulse generated ( $T_G$ ) and the pulse received ( $T_R$ ).

$$T_1 = \sqrt{T_G^2 + T_R^2}$$

For this reason these oscilloscopes would not be adequate for viewing picosecond pulses.

Sampling scopes with band widths in the gigahertz frequency range are available for pulse measurement. A 50 picosecond pulse rise time would have to be measured with a sampling scope whose band width was at least 7 GHz to meet the requirements of Equation 1. The sampling scope is limited by the fact that the pulse must be repetitive, although with some scopes, the repetition need not be periodic. Also, jitter and drift can be limiting factors.

For component evaluation to pulse response, such as interconnects, the time domain reflectometer (TDR) is considered by most authorities in the field as the best instrumentation available today. Present state of the art TDR instrumentation can produce 35 picosecond pulse rise times. They can differentiate circuit impedance discontinuities as short as .250 inch.

### Conclusions:

- A. Connectors have not been a severe source of digital pulse degradation where pulse rise times, pulse widths, fall times and repetition rates have been greater than 1 nanosecond in duration. This is due to the fact that operating wave length has been considerably larger than the connector electrical length.
- B. The losses in pulse forming and receiving circuitry have exceeded those in connectors until the recently new advances in MSI technology which may alter this situation.
- C. Connectors of future digital circuit technology will prove a limiting factor in signal transmission in both the area of circuit interconnects and the area of interface hardware interconnects. These limiting factors are as follows:
  - Slowing the pulse rise times by their losses.
  - Limiting the shorter pulse width capability.
  - Increasing pulse fall time.
  - Limiting faster repetition rates.
  - Pulse distortion may occur due to amplitude changes and jitter caused by contact movement from shock or vibration which may introduce transients or "glitches" on the incoming pulses.
  - Phase shift may occur through the connector due to impedance shifts from reactive impedance changes through the connector.
  - Fan-out of signals may be limited, where connectors introduce excessive losses to low level millivolt or microvolt pulse signals.

## Detailed Recommendation:

### A. Introduction

As a result of the work conducted by the Electrical Components Division of The Bendix Corporation under the sponsorship of the Marshall Space Flight Center on Phase 1 of the Materials Investigation and Tests for the Development of Space Compatible Electrical Connectors, it is evident that problem areas associated with the digital efficiency of connectors are eminent. As the need to deal with digital data at higher speeds increases, the digital efficiency of multi-channel connection mechanisms must also increase. Very little work has been conducted in industry on the problem of the digital efficiency of connectors and, in general, test methods have been confined to "in circuit tests". This approach, although satisfactory for existing needs, does not lend itself to establishing limits of operation in multi-channel connection mechanisms until problems become apparent.

It is, therefore, proposed that the task of developing test methods to define these limits be undertaken. Having established these limits, testing on selected types of connectors will then be conducted to determine where these devices are no longer serviceable with respect to rise time, pulse duration, and pulse repetition rate.

### B. Problem Statement

The final report pertinent to Task V, Phase 1 of the Materials Investigation and Tests for the development of Space Compatible Electrical Connectors indicates that, within the next 5 to 10 years, rise times in the order of picoseconds are expected in digital circuits. Due to this very **fast rise time, pulse amplitudes will be restricted** to 1 volt or less. The ability of existing multi-channel electrical connection mechanisms to deal with these speeds and amplitudes has not been clearly defined due to lack of available information. It also appears to be doubtful if existing connectors are capable of dealing with pulses having such parameters.

In dealing with pulses having sub-nanosecond rise times, small amplitudes and fast repetition rates, test and calibration equipment is extremely scarce. Some manufacturers do, however, sell equipment which is just adequate to observe and test the transmission of these fast pulses through networks.

It is, therefore, felt that further work should be conducted to develop test methods and techniques which can be used to define limiting parameters associated with the digital efficiency of existing connectors.

Although the above referenced report indicates that problems due to mechanical shock and vibration can exist in connectors handling fast digital pulses, it is felt that such problems would, by virtue of the relatively large mechanical masses associated with connectors, exhibit themselves by much longer duration effects such as completely missing portions of the signal for periods of time approaching or

exceeding a millisecond duration. Such absence of signal would be apparent in connectors currently in use. The limitations of existing equipment to measure discontinuities are presently in the nanosecond range and further advances on these capabilities are limited by the state of the art. It is, therefore, felt that any test on these parameters would not provide satisfactory limits and conclusions. For these reasons, it was decided to omit testing in these areas.

In this portion of the work, it is proposed that test methods be established to determine impedances, rise time capabilities and cross talk limitations of existing connectors. It is further proposed that these specific tests be conducted on selected samples of connectors which are currently being used in circuits dealing with fast digital pulses in order to determine their limitations.

As this work progresses, observations will be made concerning the limiting factors and, if necessary, recommendations will be made as to how these frequency limitations can be improved in future connectors.

#### C. Planned Approach:

In this effort, it is planned to reference the work to three areas of testing as follows:

- Impedance measurement which will be accomplished by frequency domain techniques.
- Pulse rise time measurement as indicated by time domain testing.
- Cross talk as determined by signal level detected on inoperative lines.

Having established test procedures and specific connector types, test fixturing and hardware will be designed and manufactured to facilitate the test program outlined above.

During the test portion, each test will be adequately documented. At the completion of all testing, this data will be reduced and evaluated using applicable techniques. From these results, limits of rise time, pulse duration, pulse repetition rate, and cross talk will be established.

Analysis of these results will then be made and further necessary brief tests will be conducted to indicate, in a broad sense, what connector design parameters need to be modified to improve the digital efficiency of multi-channel electrical connection mechanisms.

## VII

### Future R&D Connector Activity:

The shuttle environments as now defined will introduce certain new connector requirements brought about by the combination of aircraft and space type flights. As a result of this, it is envisioned that certain key connector activities will be necessary.

#### A. Material Development

Continued effort is anticipated in electrical connector material development.

#### B. Digital Efficiency

Continued effort is anticipated concerning the effects of interconnect systems on the transfer of high speed digital signals.

#### C. New High Density Connector Approach

An effort is anticipated to establish a family of connectors with extremely high density contact spacing using a new approach to an all dielectric insert. Connectors with all dielectric inserts have exhibited severe problems with contact retention, ease of assembly, inspection and other weaknesses in the past. Many of these problems have been solved by metal clip contact retention devices in connector designs such as the 40M39569 (Modified NAS 1599) connector. However, the presence of the conducting metal retention devices severely restricts the close spacing of contacts in connector inserts. This new family of connectors could possibly include the following types:

1. Circular
2. Rectangular
3. Distribution, Bussing and Termination Devices
4. Zero-G Coupling Version
5. Above connectors to have common features:
  - Standard insert retention design
  - Standard materials
  - Standard contacts
  - Standard contact crimp tools
  - Standard contact insertion-extraction tools

**D. R. F. Connectors**

Explore and establish a family of R. F. Connectors to handle digital pulsing and R. F. applications.

**E. Flat Conductor Cable Connectors and Termination Devices**

Develop a reliable termination system for flat conductor cable usage.

**F. Engine Harness Connectors**

Explore and establish electrical connectors that will meet special or unusual engine area requirements.

**G. Maintenance and Inspection**

Establish connector designs or modifications that will assure ease of maintenance and inspection of assembled, installed connectors.

**H. Umbilical and Remote Access Connectors**

Explore and establish umbilical and remote access connectors.

## BIBLIOGRAPHY

The major sources of information used in the **Zero-G Connector** portions of this paper are:

Final Report, Contract NAS8-21393  
"Development of Advanced Space Compatible Electrical Connectors", Bendix Corporation, Electrical Components Division contract with MSFC.

Design Presentation of Astronaut connector by  
McDonnell Douglas Astronautics Company, Western Division

The major source of information used in the materials development and Digital Efficiency Portions of this paper is:

Final Report for Phase I, Contract NAS8-26054  
"Materials Investigation and Tests for the Development of Space Compatible Electrical Connectors," Bendix Corporation, Electrical Components Division contract with MSFC.



# SPACE SHUTTLE ELECTRIC POWER DISTRIBUTION CONSIDERATIONS

J. L. Felch

Electrical Division  
Astronics Laboratory  
NASA-Marshall Space Flight Center  
Huntsville, Alabama

## ABSTRACT

The development of the Space Shuttle electric power distribution system is examined considering the state-of-technology. A brief review of conventional air and spacecraft electrical power systems is discussed, and the advantages of a new approach are described. The objectives of MSFC's advanced development studies devoted to this technology area are described. A recommended philosophy of approach for the Space Shuttle electric power distribution system is expressed.

## INTRODUCTION

The requirements the Space Shuttle imposes on the electric power distribution system are considerably greater than previously encountered on manned spacecraft or high performance military and commercial aircraft. Advances in the electrical/electronic state-of-technology made during the past decade should be applied to meet these requirements. MSFC and other NASA Centers have been very active in this technology area. This discussion deals primarily with the work done by the Electrical Division at MSFC, presents a philosophy of approach to meet the Space Shuttle requirements, and identifies some of the problems and what can be done to solve them.

## GENERAL

In performance, the functions of the electric power distribution subsystem are to transmit, distribute, switch, condition, control, protect, and monitor the flow of power from source to utilization equipment. In meeting these requirements, the subsystem must evolve in terms of performance and economy of weight, volume, and ownership cost.

The traditional system concept requires the distribution wiring, often of heavy conductors, to be routed from the source through various switches, circuit breakers, and relays located throughout the vehicle and ultimately to the load. The result is complex cabling with inherent weight and bulk.

### REALITY OF THE PROBLEM

The main problem is that the state-of-technology application related to electric power distribution, processing, and control has not kept pace with the rapidly expanding electrical/electronic technology in general.

Contributing to the problem is the accepted industry standard, MIL-STD-704A, which defines aircraft electrical system power quality. This document specifies the voltage levels of 28 VDC and 115/200 VAC, 400 Hz, 1  $\emptyset$  and 3  $\emptyset$ , and provides a rather liberal tolerance for voltage variations.

If significant advantages are to be achieved, the parameters of MIL-STD-704A will have to be changed to values more suitable for today's technology.

### CONVENTIONAL AIR AND SPACE VEHICLE POWER SYSTEMS

In general, aircraft electric power is derived from the propulsion engine driven alternators producing 115/200 VAC, 400 Hz, 3  $\emptyset$  power. This power and 28 VDC produced by rectification are the only power normally distributed. Power of other forms and quality required is usually produced within or in proximity of the utilization equipment.

To date, manned space vehicle electric power has primarily been derived from batteries and fuel cells and distributed at 28 VDC. Other forms of power required have been produced by inversion or conversion as appropriate to supply the demands of specific utilization equipment.

Currently in both aircraft and space vehicles, the conventional concept is to route power from bus to load through separate electro-mechanical devices required to switch, protect, and control the logic, all performed at the load power level. It should be emphasized that the many series contacts and the interconnecting cabling result in voltage drop and power loss which can only be minimized by increasing wire size, resulting in increased weight and volume.

## THE NEW APPROACH

In the development of aircraft and space vehicle electric power systems, the incorporation of solid-state and hybrid techniques to power distribution and management is unquestionably the remedy.

The technical feasibility of solid-state switching, circuit protection, and software control concepts has been demonstrated by such development programs as the Navy "SOSTEL" (Solid State Electric Logic), the Westinghouse "ACES" (Automatically Controlled Electrical System), and the Bendix-developed Airborne Display and Electric Management System.

Advanced systems as such provide the following improvements over today's conventional systems:

- Increased Reliability
  - Reduced Weight and Volume
  - Increased Flexibility
  - Easier Maintenance
  - Software Control
- New components and concepts for the advanced system are being developed as follows:
- Solid-State Power Controllers
  - Multiplexed Control Data Transmission
  - Programmable Control Logic
  - Built-In Test (BIT) Capability
  - High-Voltage DC Systems
  - Automated Onboard Checkout

There are still continuing R&D requirements in the following technological areas:

- Solid-State Physics
- Data Transmission and Processing
- Heat Transfer and Dissipation
- High-Density Microelectronics
- Transducers
- Memory Systems
- Power Management Software

#### MSFC ADVANCED STUDIES

At the MSFC Electrical Division, work is being performed in-house and under contract covering the following electrical power system technology areas:

- Solid-State Switches
- Hybrid Switches
- Circuit Protection
- Power Controllers
- Power Sources
- Standard Power Supplies
- Wire, Cable, Connectors, and Termination Devices
- Power Switching and Control Concepts
- Controls and Displays

In the contract area, one major effort is the "Space Vehicle Power Processing, Distribution, and Control Study" being performed by TRW Systems Group under NASA Contract NAS8-26270. The primary objective of this study is the definition of a practical generalized concept for electric power processing, distribution, and control applicable to manned space vehicles and future aircraft with special emphasis on the needs of the Space Station/Base and Space Shuttle. The additional objectives are the identification of deficiencies in existing power processing, distribution, and control technology and the establishment of specific goals for the development of advanced components, circuits, or related technology. This program started in March 1971 and will be completed in April 1972.

### CONCLUSIONS

The Space Shuttle can be the beginning for a new philosophy of approach for advanced electric power systems. Knowledge will be obtained and shared; application will become more widespread. Problems will develop and be solved. Time does not permit a deep technical discussion of the application of existing technology to the development of advanced power system concepts.

It is believed that a Solid-State/Hybrid multiplexed software managed power distribution and control system will be incorporated in the next generation of aircraft and in the Space Shuttle.

**COMMUNICATIONS**

A SOLUTION FOR THE SPACE SHUTTLE HIGH TEMPERATURE ANTENNA PROBLEM

E. A. Kuhlman

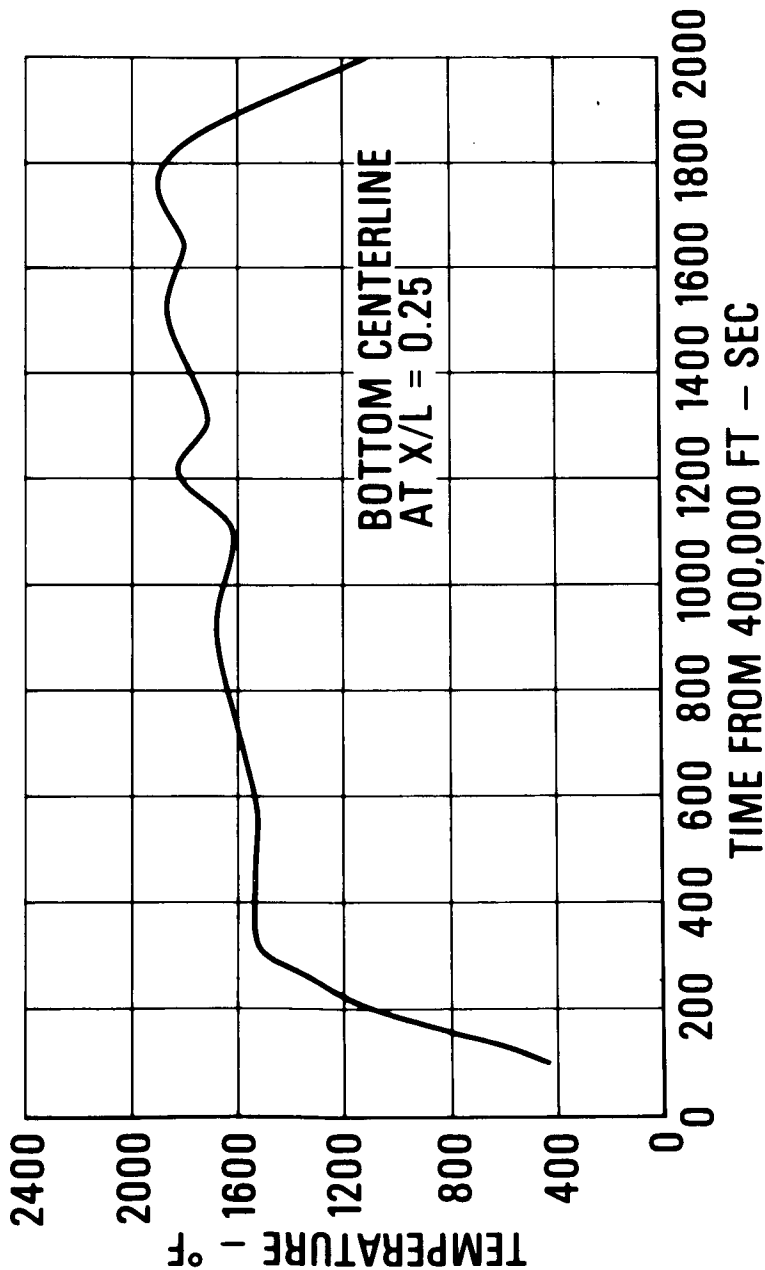
McDonnell-Douglas Corporation  
St. Louis, Missouri

The development of high temperature antennas is one of the more difficult Space Shuttle problems. The avionics systems on-board the Space Shuttle orbiter and booster use frequencies which are used on commercial and military airplanes. The high temperature antennas previously developed for reentry vehicle applications are for other frequencies, and were designed for one shot application. Therefore, the techniques which have been developed for high temperature reentry vehicle antennas may not be directly applicable to the reusable requirements of Space Shuttle. This leaves the designer in the position of applying both new and old techniques to antenna types which have not previously been designed for operation at reentry temperatures.

# SPACE SHUTTLE ORBITER TEMPERATURES

The equilibrium temperature profile on the underside of the Space Shuttle orbiter in an area considered for the location of some of the antennas is shown in this slide. This temperature profile represents the maximum thermal environment expected for the orbiter antenna systems.

## REENTRY EQUILIBRIUM TEMPERATURES Delta Orbiter





## TECHNICAL APPROACH

Two basic technical approaches are possible to solve the Space Shuttle high temperature antenna problems. One is the use of a high temperature antenna which can be mounted directly in the Space Shuttle skin. The other is the use of an off-the-shelf low temperature antenna covered with a dielectric window which provides thermal protection for the antenna and has good RF transmission properties.

- HIGH TEMPERATURE ANTENNA
- LOW TEMPERATURE ANTENNA/HIGH TEMPERATURE WINDOW

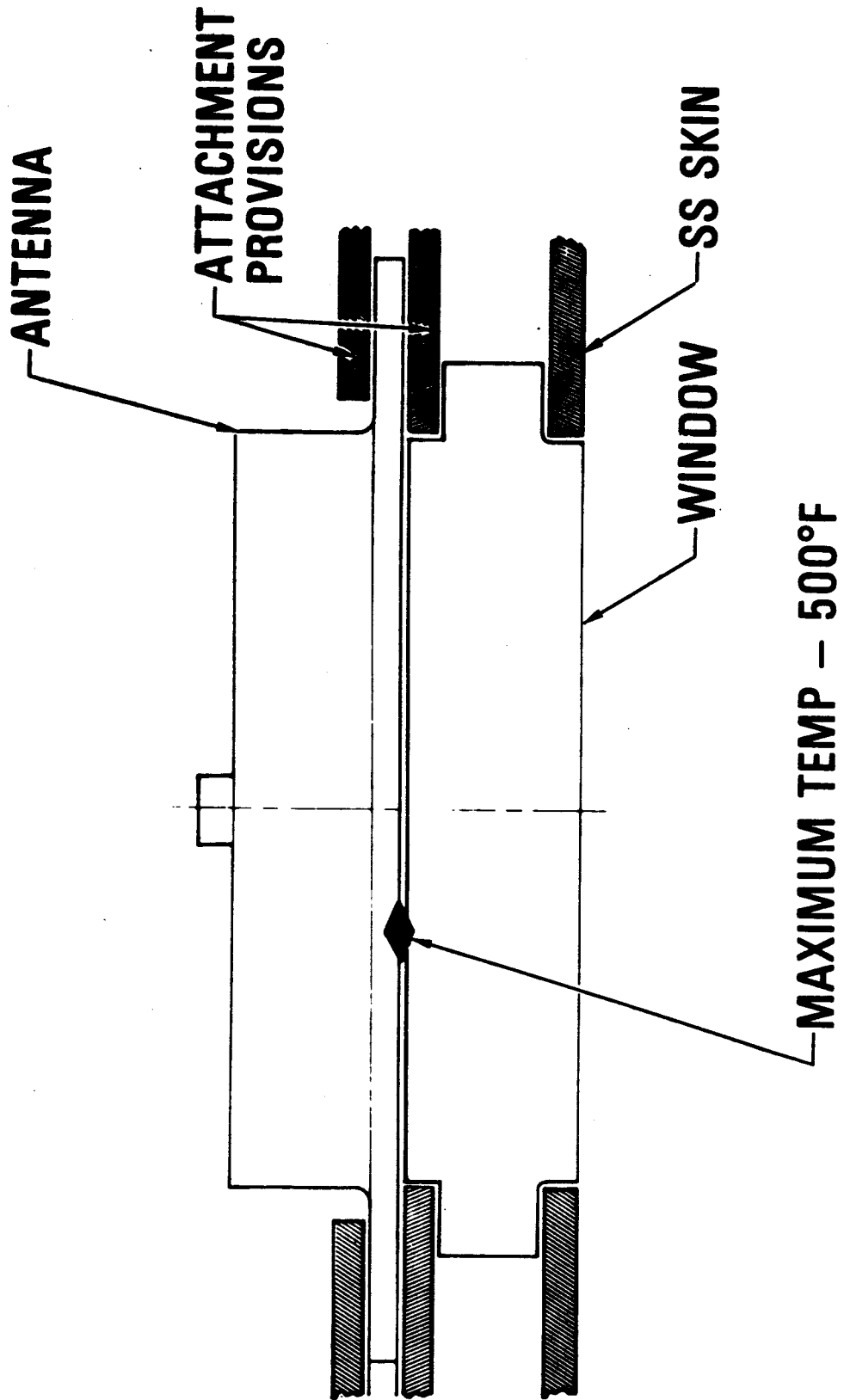
## TECHNICAL APPROACH SELECTION

The primary factors considered in determining which technical approach to take are shown in this slide. After considering each of these items for each of the technical approaches shown on the last slide, the latter off-the-shelf approach was selected for further study. This approach gives a good separation of the electrical and the environmental problems, and does not appear to require state-of-the-art advances in material properties or fabrication techniques in order to solve the problems.

- **DEVELOPMENT AND RECURRING COSTS**
- **DEVELOPMENT STATUS**
- **FUNCTIONAL REQUIREMENTS**
- **MATERIAL REQUIREMENTS AND PROPERTIES**
- **PRODUCIBILITY**
- **SPACE SHUTTLE INTEGRATION**
- **REUSABILITY**
- **PROBABILITY OF SUCCESS**

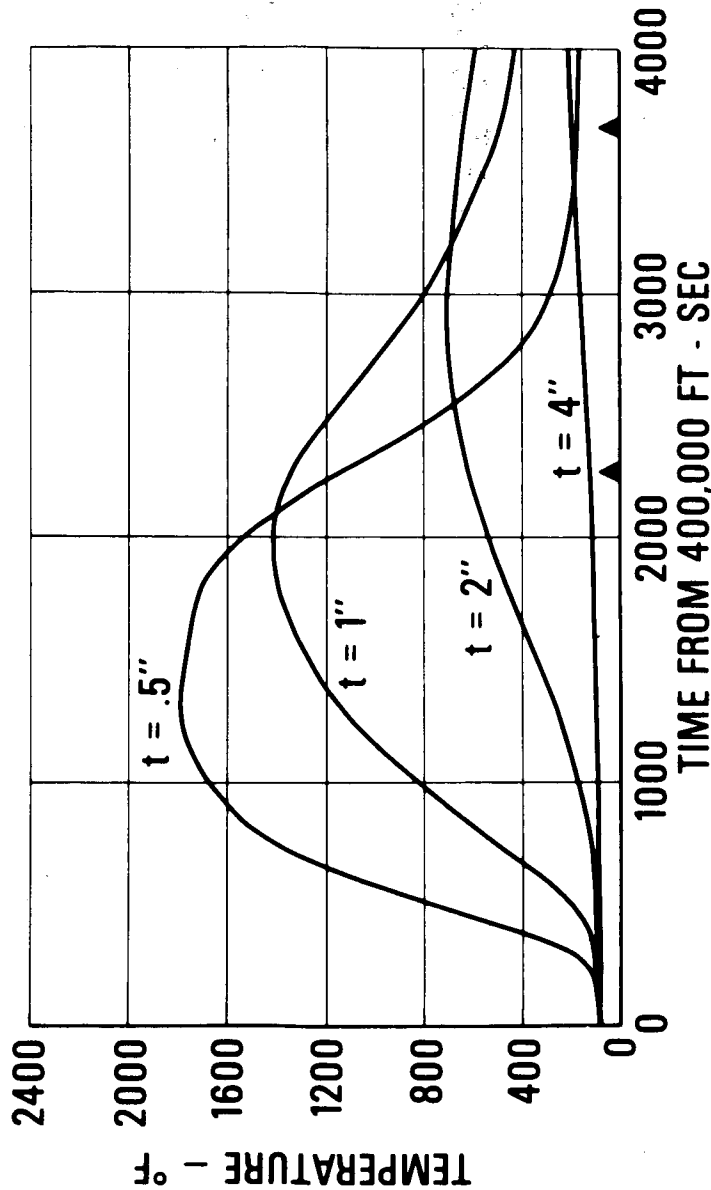
ANTENNA/WINDOW CONFIGURATION

A conceptual design of a typical Space Shuttle antenna installation is shown in this slide.  
The relationship of the antenna and window is shown.



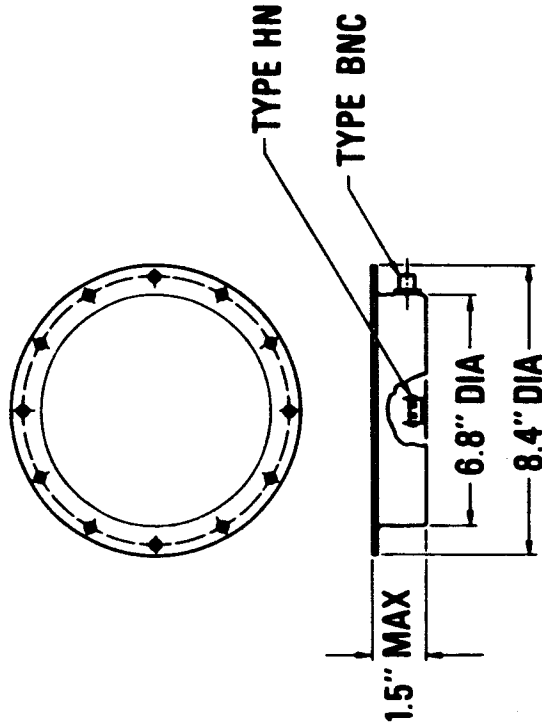
# ANTENNA WINDOW BACKFACE TEMPERATURES

The results of calculations to determine the window thickness are shown in this slide. The results were obtained using shuttle thermal inputs for a typical design trajectory and the thermal properties of slip cast fused silica (SCFC). From these results it can be seen that a window of SCFC 3 to 3-1/2 inches thick will maintain a window backface temperature of 500°F or less. The results would, of course, be different for a different window material.



TEST ANTENNA

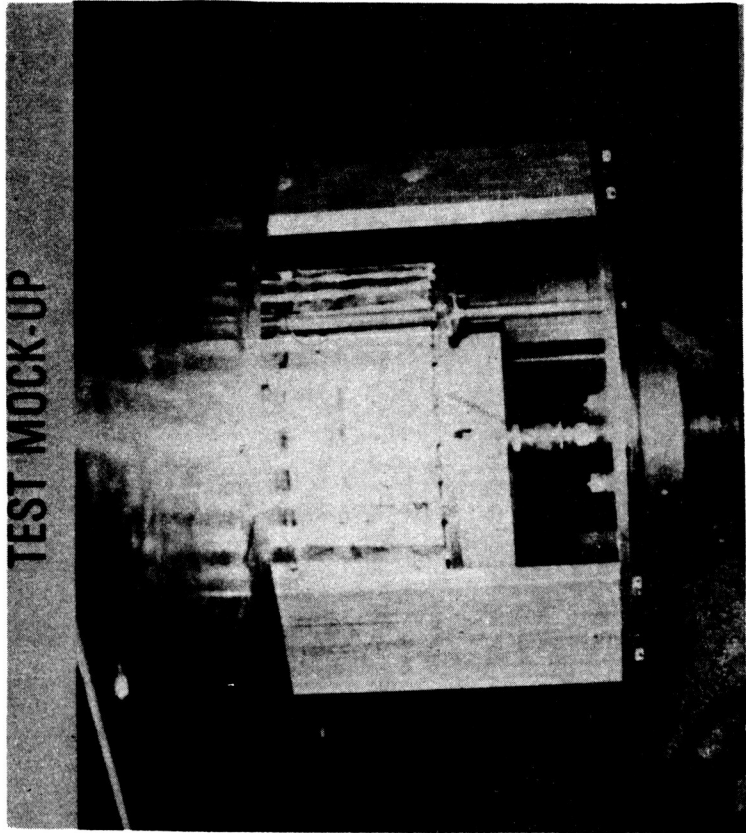
An L-Band annular slot antenna used to obtain the test results to be described is shown in this slide. This antenna is a standard AT-740 and is readily available for operational temperatures of 400°F or less. It has also been designed to operate at a temperature of 500°F. The AT-740 operates at frequencies from 960 to 1220 MHz and is used with DME and ATC systems. The radiation pattern is basically the same as that obtained from a quarter wave stub antenna.



DME/ATC  
L-BAND (960-1220 MHz)

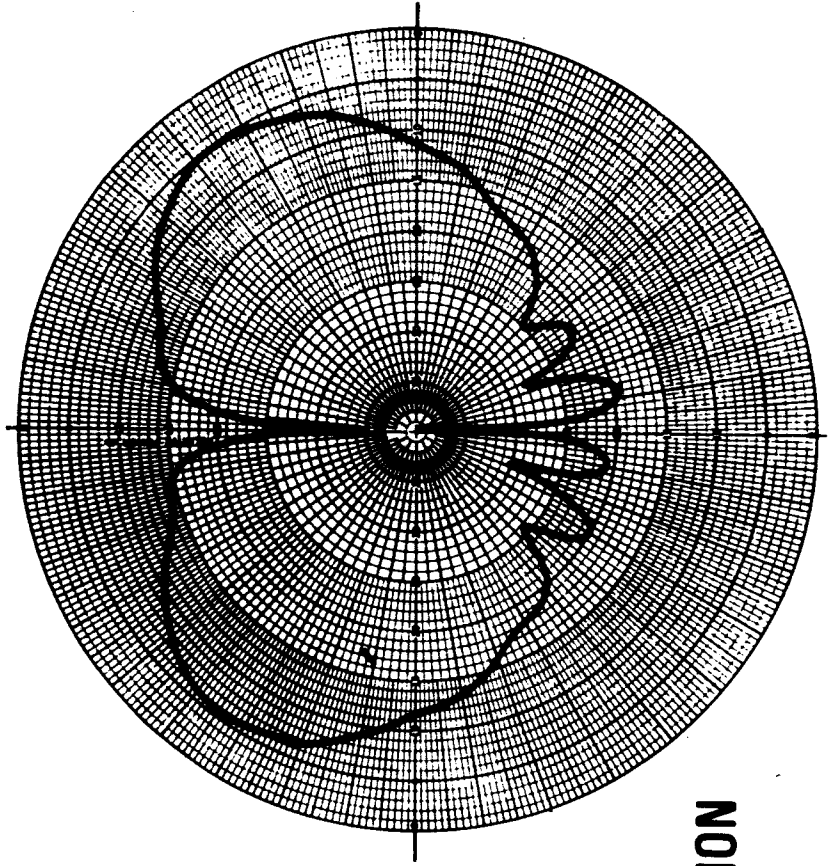
## TEST CONFIGURATION

The test mock-up simulates the essentials of a typical space shuttle orbiter antenna installation. Provisions were made to permit testing with different window thicknesses. The ground plane can also be replaced with a different aperture size to facilitate testing different window diameters. Both radiation patterns and impedance can be measured using this mock-up.



### REFERENCE RADIATION PATTERNS

A typical radiation pattern of the antenna flush mounted in a ground plane is shown for the principal polarization at 960 MHz. The antenna was not covered with an additional window, and the ground plane had the same dimensions as the mock-up described. This pattern serves as a reference for evaluating the degree of degradation attributable to the window in the simulated shuttle installation.

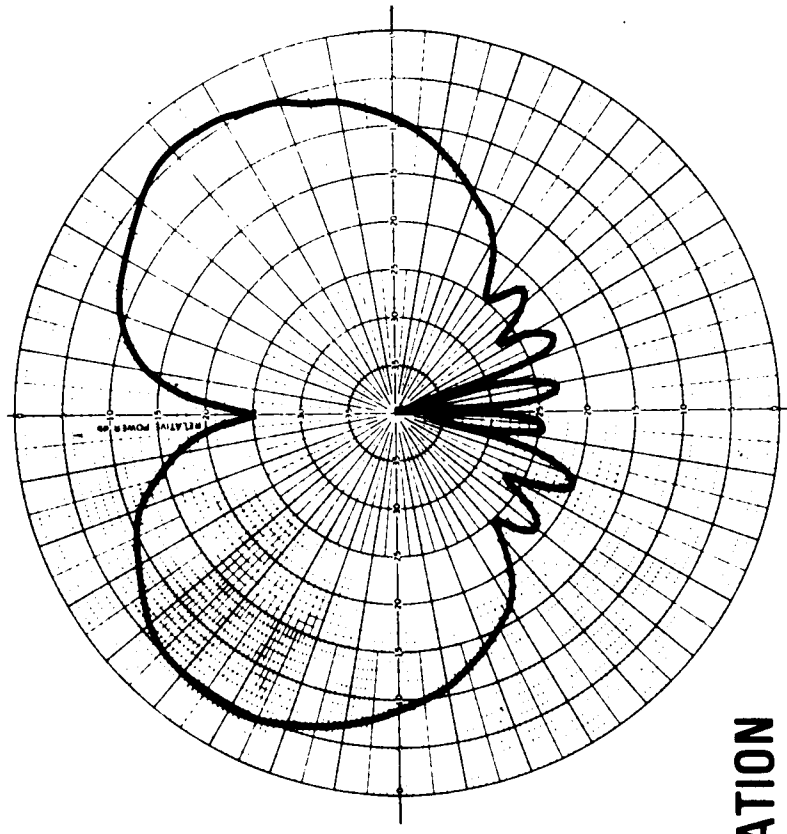


$\theta$  POLARIZATION

f = 960 MHz

REFERENCE RADIATION PATTERNS

A typical radiation pattern is shown for the principal polarization at 1220 MHz. The configuration and conditions were the same as those stated for the previous slide.

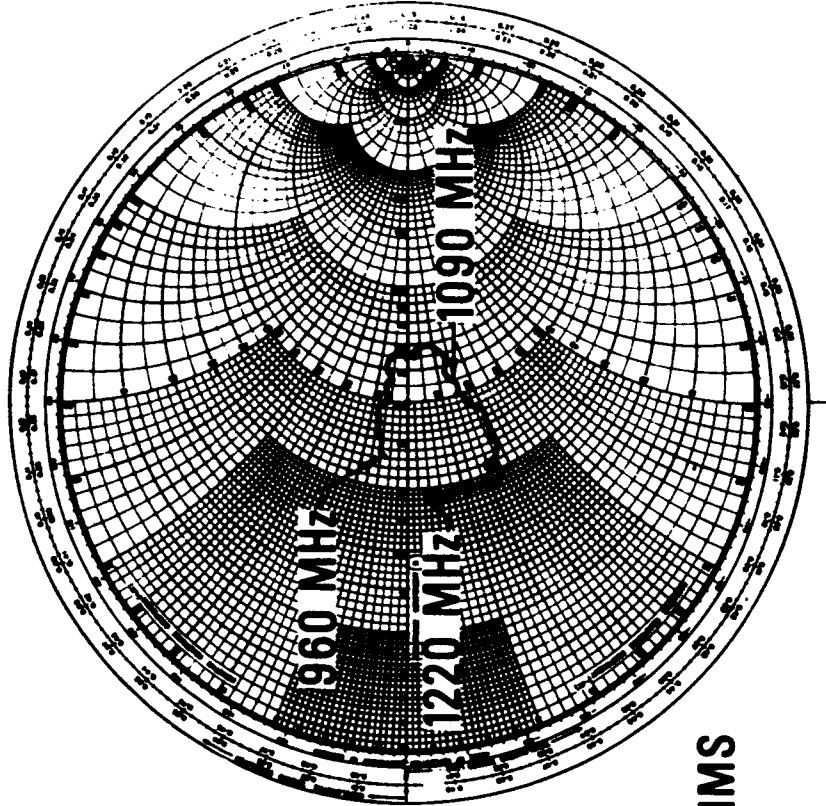


$\theta$  POLARIZATION  
f = 1220 MHz



REFERENCE IMPEDANCE DATA

The impedance characteristics of the antenna for the configuration described for the two previous slides are shown in this slide. The maximum VSWR is 2.05:1.

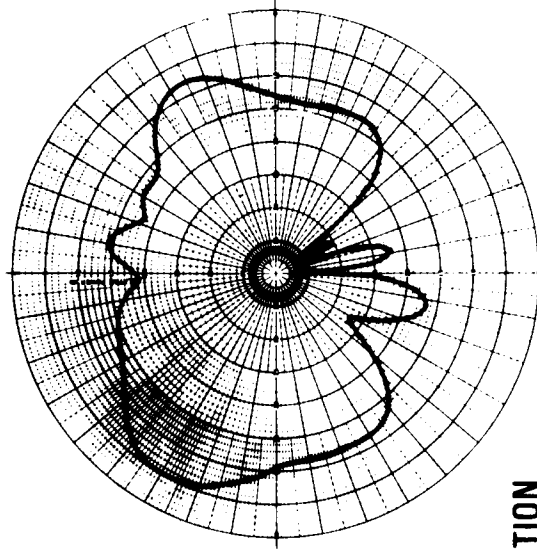


$Z_0 = 50 \text{ OHMS}$

## RADIATION PATTERNS

### WINDOW EDGES OPEN

Radiation pattern measurements with the antenna covered with a window 3.5 inches thick show considerable distortion in the antenna pattern. This was expected since the window edges were not covered with an electrical conductor and energy could be radiated through the window edges behind the ground plane and scattered by the structure supporting the antenna both behind the ground plane and through the window. Therefore, it was concluded that the window edges must be covered with an electrically conducting surface to eliminate the pattern distortion caused by the antenna support structure.

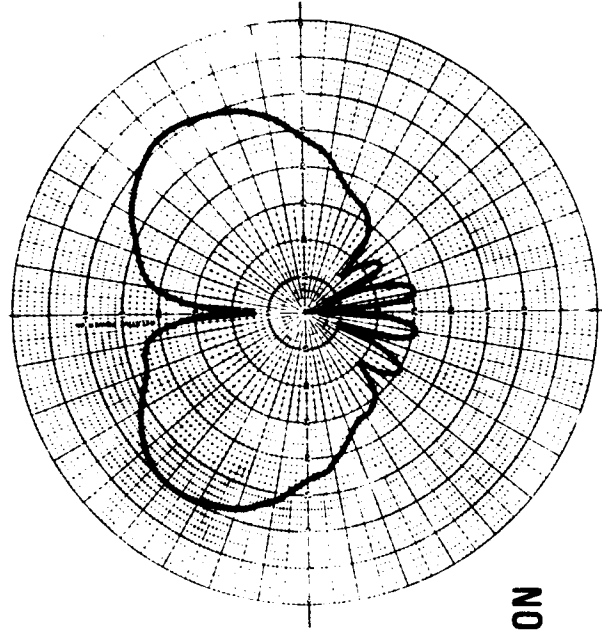


$\theta$  POLARIZATION  
f = 960 MHZ

## RADIATION PATTERNS

### WINDOW EDGES ENCLOSED

Radiation pattern measurements with the window edges entirely enclosed by an electrically conducting material show that the window thickness has very little effect on the shape of the basic antenna pattern. The pattern shown in this slide was measured at 960 MHz. The differences in gain observed are accounted for by considering the transmission characteristics of the window and an increase in the antenna VSWR. This configuration is essentially a dielectrically loaded circular waveguide excited in the  $TM_{01}$  mode with an annular slot antenna. The conductor enclosing the window edges was attached to both the ground plane and the antenna mounting flange.

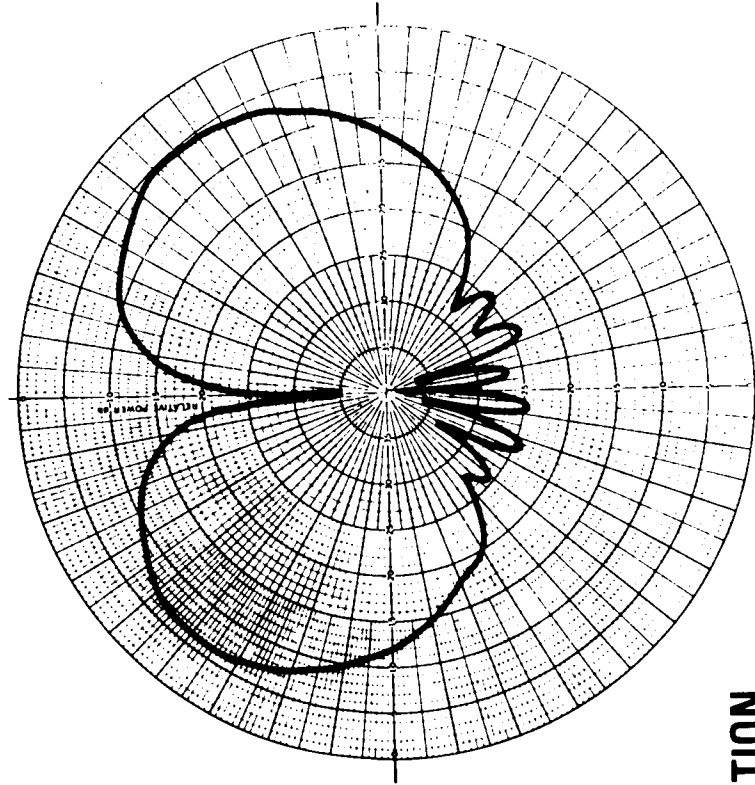


**$\theta$  POLARIZATION**  
**f = 960 MHz**

RADIATION PATTERNS

WINDOW EDGES ENCLOSED

A radiation pattern is shown for the principal polarization at 1220 MHz. The configuration and conditions were the same as those stated for the previous slide.

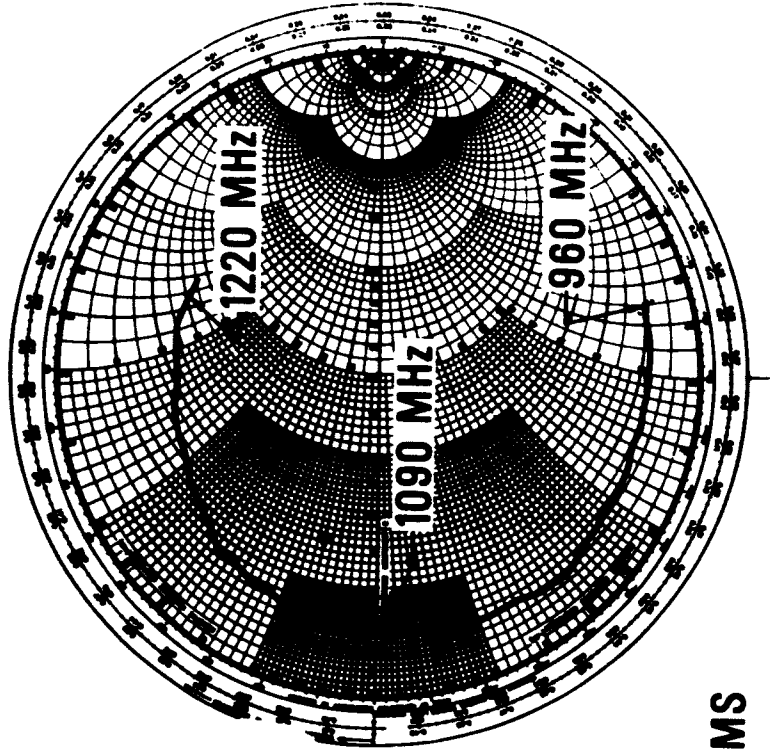


**$\theta$  POLARIZATION**  
**f = 1220 MHz**

ANTENNA/WINDOW IMPEDANCE

WINDOW EDGES ENCLOSED

The impedance for the antenna/window configuration described for the previous two slides is shown in this slide. The VSWR is increased over the entire frequency range. Techniques to obtain an impedance match comparable to the reference condition are being considered. Some revisions in this basic antenna matching network may be required to maximize the system efficiency.

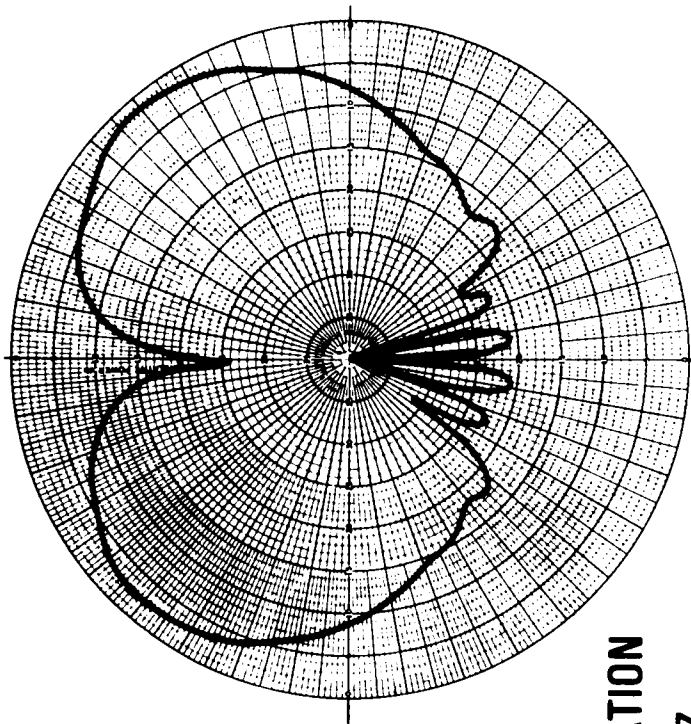


$Z_0 = 50 \text{ OHMS}$

## RADIATION PATTERN

### WINDOW EDGES ENCLOSED WITH PERIODIC STRIPS

Radiation pattern measurements were made with the window edge enclosure changed to 1/2 inch strips spaced approximately 1/2 inch apart to reduce heat conduction paths. The pattern shown in this slide is essentially the same as that obtained with a continuous window edge enclosure. The strips were attached to the ground plane and the antenna mounting flange. This pattern was measured at 1220 MHz. Similar results were obtained at other applicable frequencies.

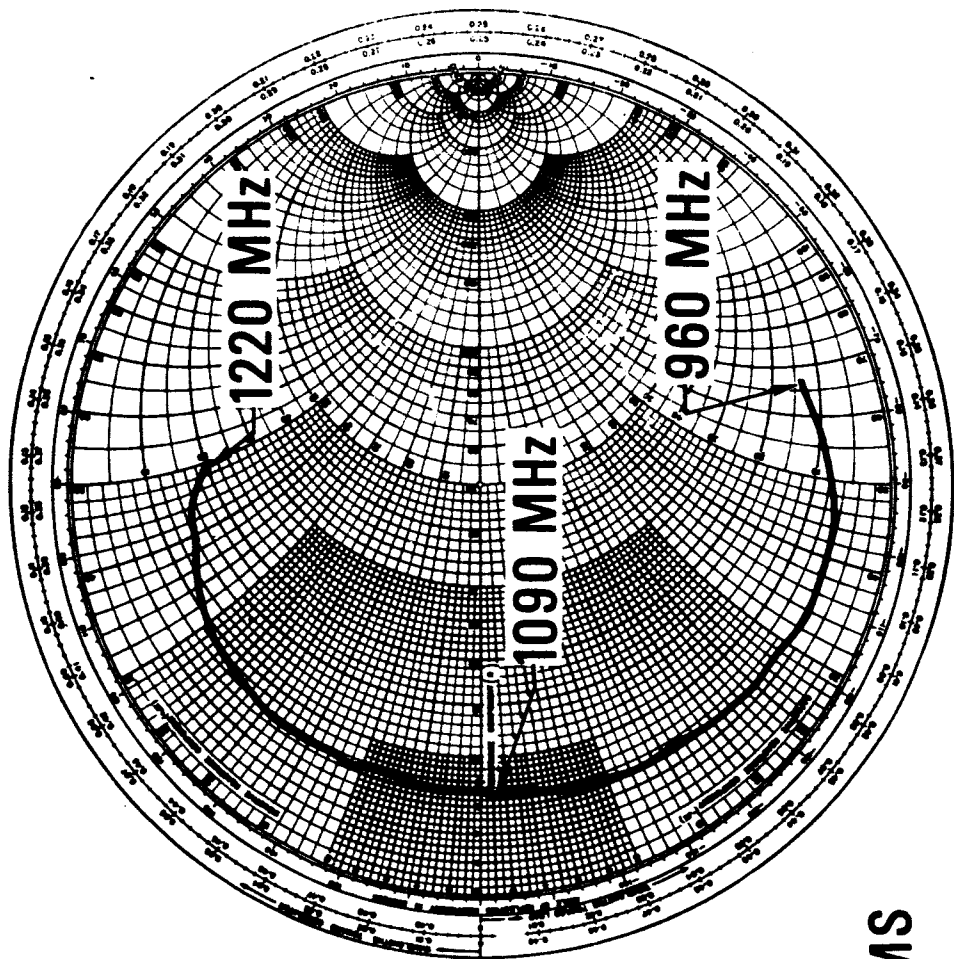


$\theta$  POLARIZATION  
 $f = 1220$  MHz

ANTENNA/WINDOW IMPEDANCE

WINDOW EDGES ENCLOSED WITH PERIODIC STRIPS

The impedance of the antenna/window configuration with the periodic window enclosure is essentially the same as that obtained with the continuous enclosure.



$Z_0 = 50 \text{ OHMS}$

## RESULTS AND CONCLUSIONS

The results given in this slide lead to the conclusion that the antenna/window approach will provide a solution for the Space Shuttle high temperature antenna problem. However, the off-the-shelf antenna may require modification of its matching network to meet the required system impedance match, if future work does not produce a simple and efficient method for obtaining a matched system external to the antenna. At worst, modifying the internal configuration of an existing antenna does not appear to be nearly as difficult as the development of an antenna designed to operate at high temperatures without the benefit of thermal protection.

### RESULTS

- EXCELLENT RADIATION PATTERNS WERE OBTAINED WITH A THICK WINDOW COVERING AN ANNULAR SLOT ANTENNA
- A WINDOW EDGE ENCLOSURE WAS REQUIRED
- THE ANTENNA IMPEDANCE WAS AFFECTED BY THE WINDOW AND WINDOW EDGE ENCLOSURE

### CONCLUSIONS

- THE ANTENNA/WINDOW APPROACH WILL PROVIDE A SOLUTION FOR THE SPACE SHUTTLE HIGH TEMPERATURE PROBLEM
- ADDITIONAL WORK IS REQUIRED TO DETERMINE THE BEST APPROACH TO ACCOMPLISH THE REQUIRED ANTENNA/WINDOW IMPEDANCE MATCH



**ANTENNA TECHNOLOGY -- MATERIALS  
FOR ANTENNA PROTECTIVE COATINGS**

**M. C. Gilreath**

**NASA-Langley Research Center  
Hampton, Virginia**

**MATERIALS FOR ANTENNA PROTECTIVE COATINGS**

**OBJECTIVE: SELECT MATERIALS HAVING SUITABLE THERMAL AND DIELECTRIC PROPERTIES TO COVER FLUSH MOUNTED ANTENNAS ON THE SPACE SHUTTLE VEHICLE**

**APPROACH: • SELECT CANDIDATE MATERIALS**

- **MEASURE DIELECTRIC PROPERTIES OF CANDIDATE MATERIALS AT ROOM TEMPERATURE**
- **AS A FUNCTION OF TEMPERATURE UP TO 20000° F DURING TEMPERATURE RECYCLING TESTS (GEORGIA TECH)**

- **EVALUATE CANDIDATE MATERIALS DURING EXPOSURE TO SPACE SHUTTLE HEATING RATES IN ARC TUNNEL**

- **INVESTIGATE MATERIAL BREAKDOWN DURING SIMULTANEOUS EXPOSURE TO HIGH SURFACE TEMPERATURES AND HIGH RF POWER LEVELS (STANFORD RESEARCH INSTITUTE)**

**CANDIDATE ANTENNA WINDOW MATERIALS FOR THERMAL PROTECTION**

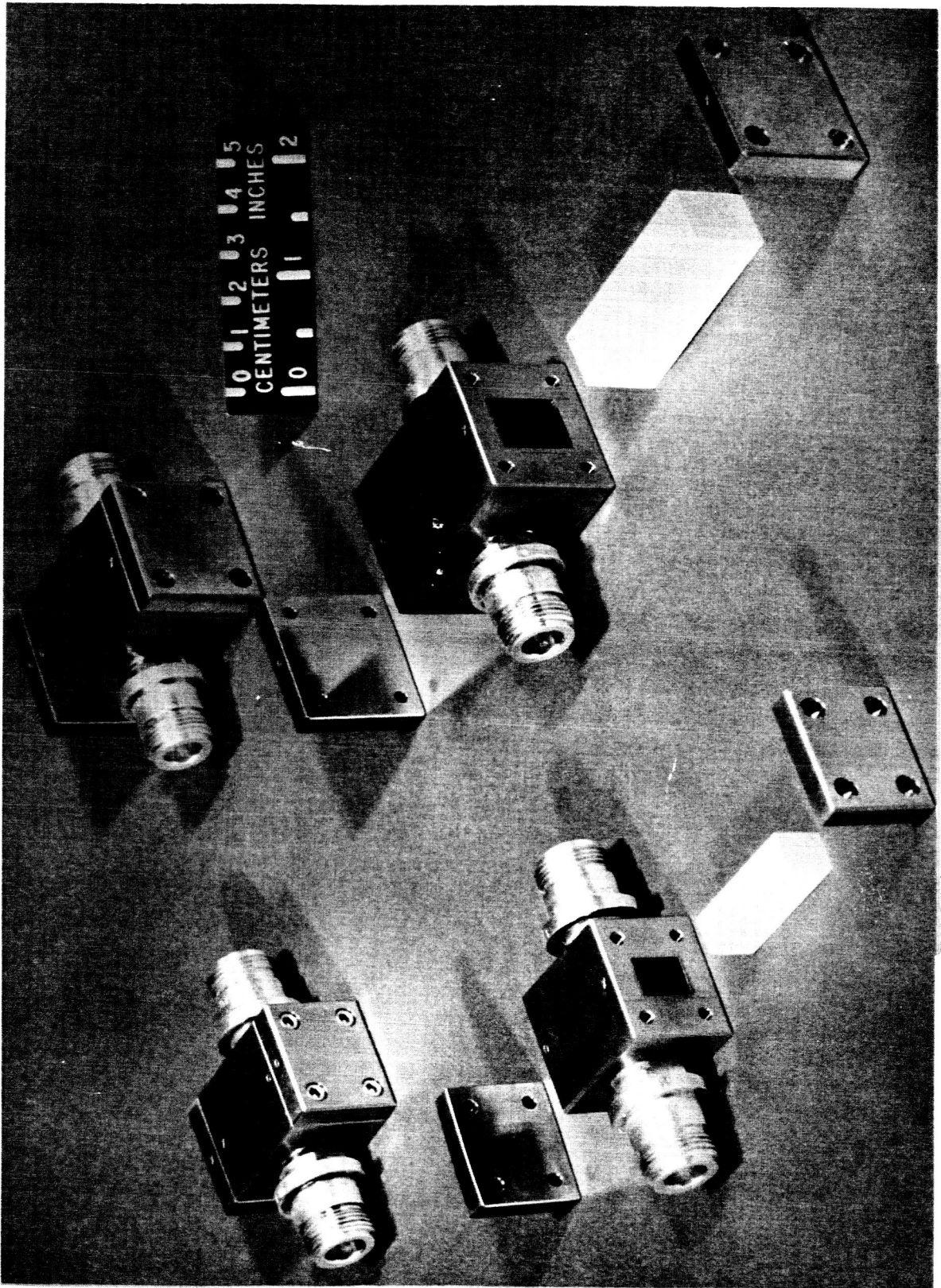
<u>SUPPLIER</u>	<u>NOMENCLATURE</u>	<u>DESCRIPTION</u>
1. PHILCO-FORD CORPORATION	AS-3DX	FUSED QUARTZ - REINFORCED SILICA COMPOSITE
2. RAYTHEON COMPANY	IPBN	ISOTROPIC PYROLYTIC BORON NITRIDE
3. GEORGIA INSTITUTE OF TECH.	-	SLIP CAST FUSED SILICA
4. GENERAL ELECTRIC	MARKITE 3-DQ	FIBER BUNDLE REINFORCED
5. WHITTAKER CORPORATION	-	ALUMINUM PHOSPHATE FOAM (40 - 60 LB./FT. <sup>3</sup> )
6. LOCKHEED MISSILES AND SPACE CO.	LI-1500	SILICA FIBER, RIGIDIZED COATING
7. McDONNELL-DOUGLAS ASTRONAUTICS CO.	MULLITE HCF	RIGIDIZED MULLITE FIBER
8. TETRAHEDRON ASSOCIATES	-	HONEYCOMB, OPEN CELL SILICON COMPOSITE
9. UNION CARBIDE CORPORATION	HD - 0092	HOT PRESSED BORON NITRIDE

TECHNIQUES FOR MEASURING THE DIELECTRIC PROPERTIES  
OF CANDIDATE MATERIALS

- ROOM TEMPERATURE MEASUREMENTS (0.100 - 60 GHz)  
CAVITY PERTURBATION TECHNIQUE (0.100 - 1.0 GHz)  
RESONANT RECTANGULAR CAVITY METHOD (1 - 14 GHz)  
FREE SPACE TECHNIQUE USING FABRY-PEROT INTERFEROMETERS (26 - 60 GHz)
- HIGH TEMPERATURE MEASUREMENTS (TEMPERATURES UP TO 2000° F)  
SHORT CIRCUITED WAVEGUIDE TECHNIQUE (10 GHz)
- HIGH HEATING RATE ARC TUNNEL TESTS  
TRANSMISSION AND REFLECTION MEASUREMENTS (10 GHz)

RECTANGULAR CAVITIES AND TEST SPECIMENS

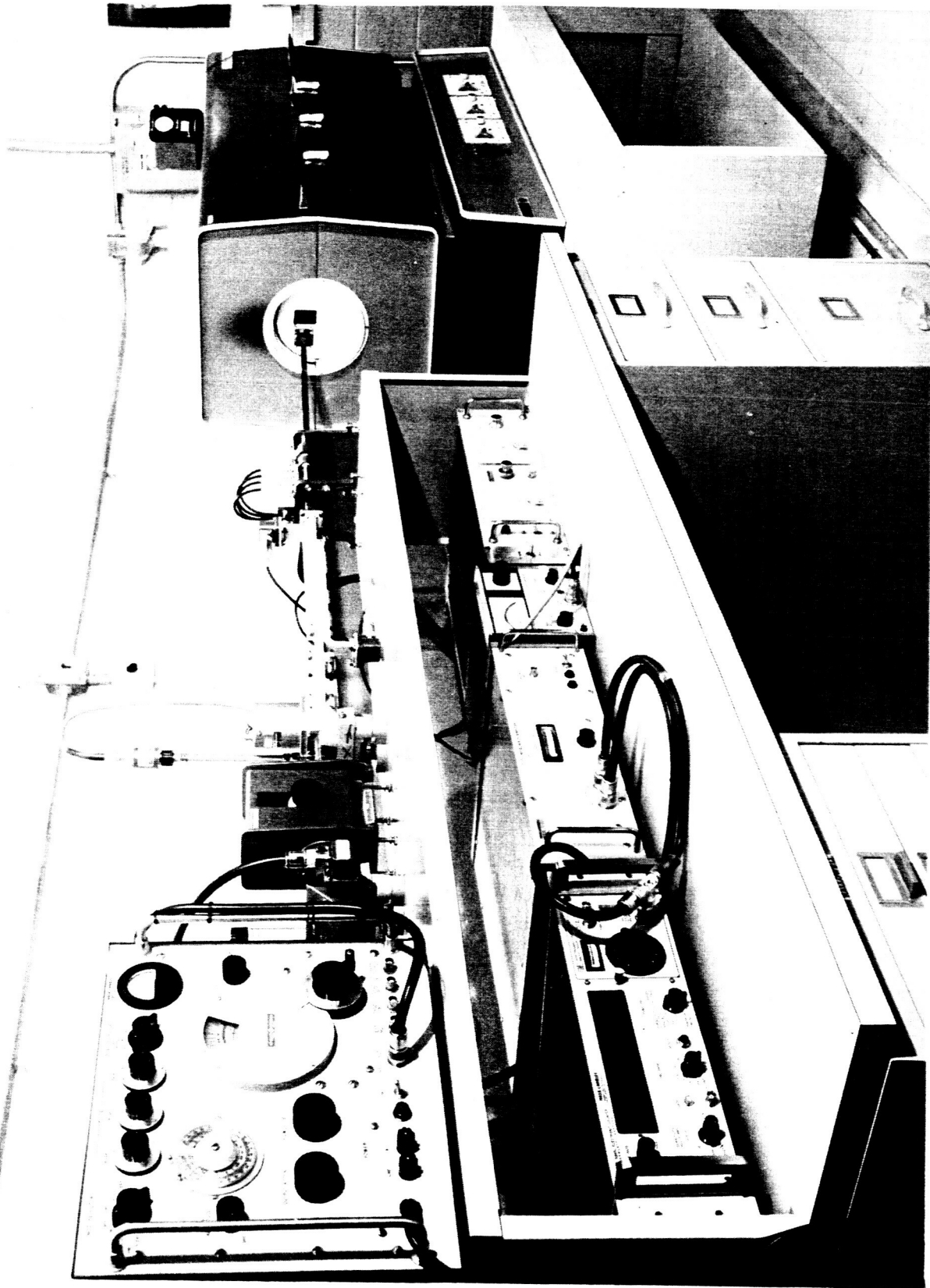
One of the techniques for determining the dielectric properties of candidate materials at room temperature employs the use of resonant rectangular cavities. The dielectric constant and loss tangent values are determined for the candidate materials by comparing the cavity performances with and without the test sample. The interior surfaces of all cavities were gold plated and polished to improve their performance.



RECTANGULAR CAVITIES AND TEST SPECIMENS

### HIGH TEMPERATURE TEST FACILITY

The dielectric properties of most dielectric materials vary as a function of temperature. To determine the changes in the candidate materials being considered here, a short-circuited waveguide technique is being used. Each material will be evaluated from room temperature up to 2000° F. The waveguide test sample holder used in these measurements was constructed from platinum/rhodium material to allow repeated exposure to the high temperatures.

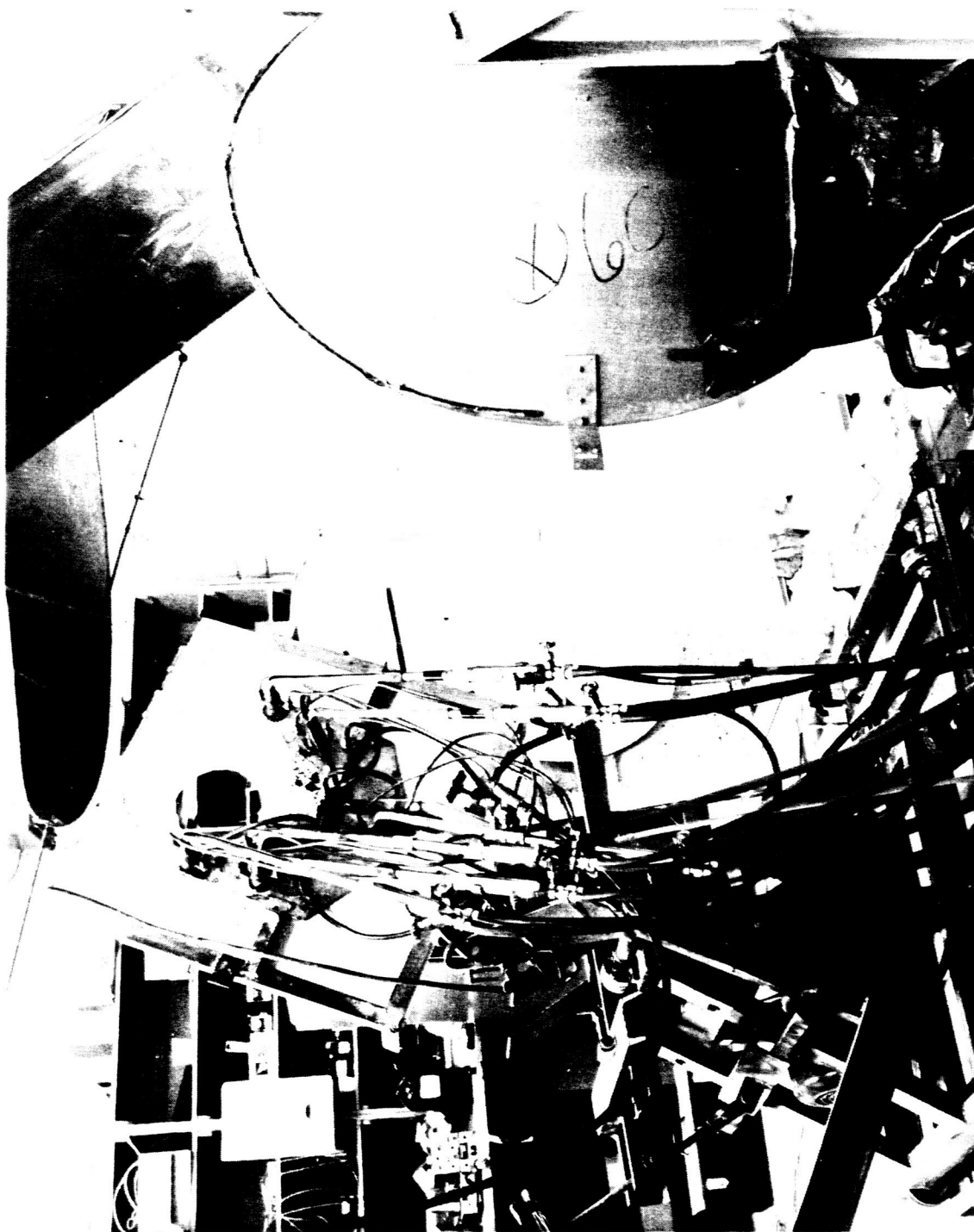


HIGH TEMPERATURE TEST FACILITY

### GEORGIA TECH HIGH TEMPERATURE FACILITY

A test technique has been developed at Georgia Tech for determining the complex permittivity of materials from ambient to greater than 4000° F. The system employs a rotating disk sample which is located at the co-incident focal point between two prolate spheroidal reflectors; the sample is heated on one side by oxyacetylene flames in such a manner that the microwave beam is not affected by the flames. Dynamic measurements are made of the sample insertion phase and insertion loss. A transient heat conduction analysis is used to determine the temperature profiles within the sample, and the electrical transmission data are correlated with the temperature profiles to give dielectric constant and loss tangent as functions of temperature.

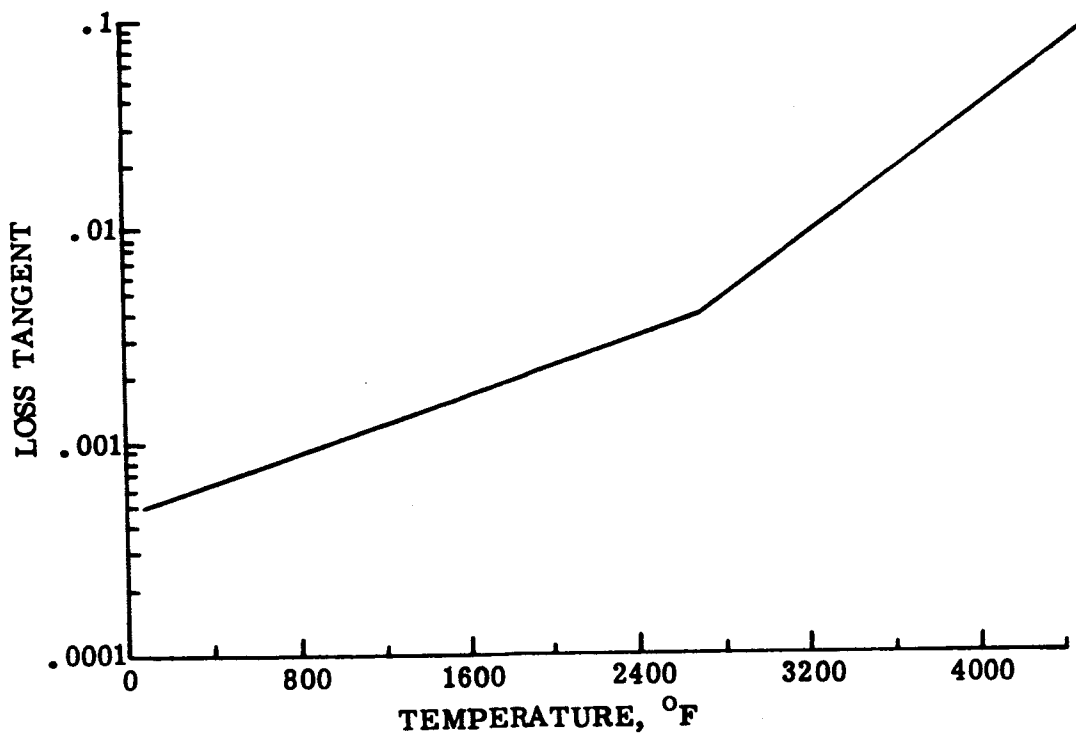
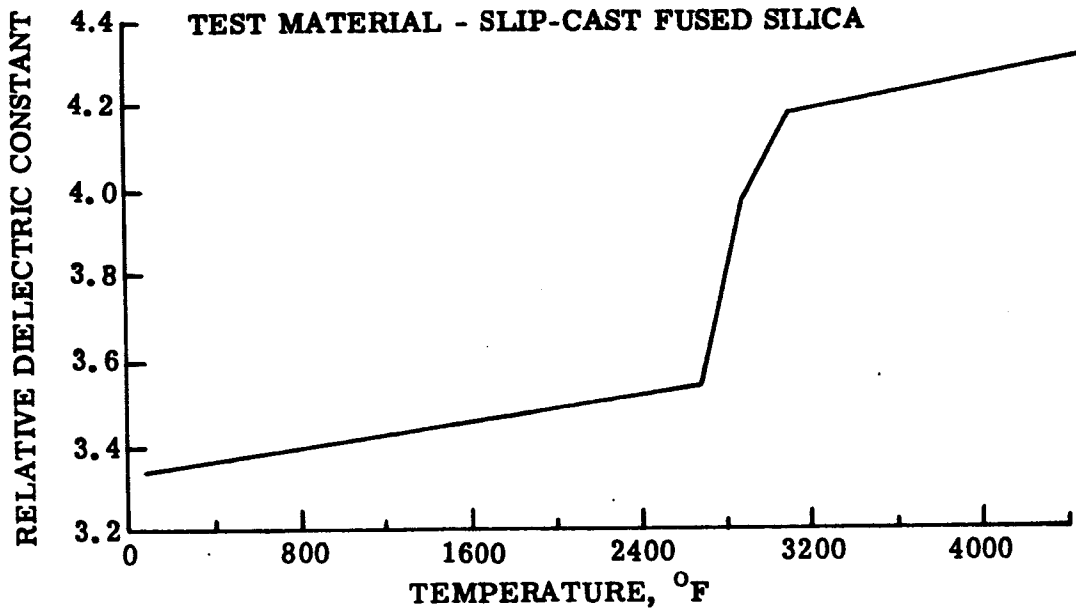




GEORGIA TECH HIGH TEMPERATURE FACILITY

## **DIELECTRIC PROPERTY MEASUREMENTS PERFORMED AT GEORGIA TECH**

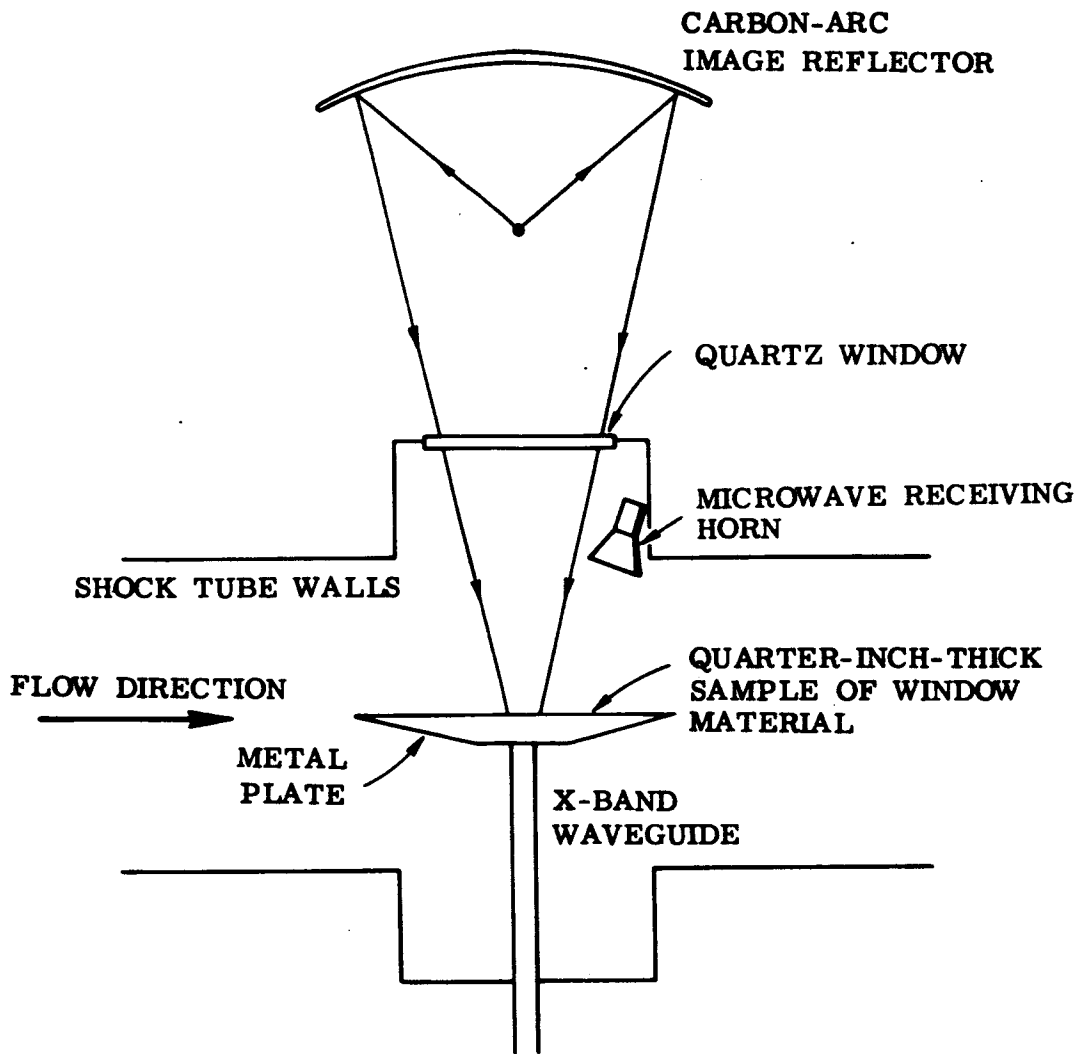
**The dielectric constant and loss tangent of slip-cast fused silica were measured from ambient to approximately 4400° F by using the Georgia Tech free-space technique. These data are typical of those that will be obtained for the candidate materials being considered, except that the maximum temperature will be approximately 2400° F.**



DIELECTRIC PROPERTY MEASUREMENTS PERFORMED AT GEORGIA TECH

## SCHEMATIC PRESENTATION OF APPARATUS FOR MEASUREMENTS IN SHOCK TUBE

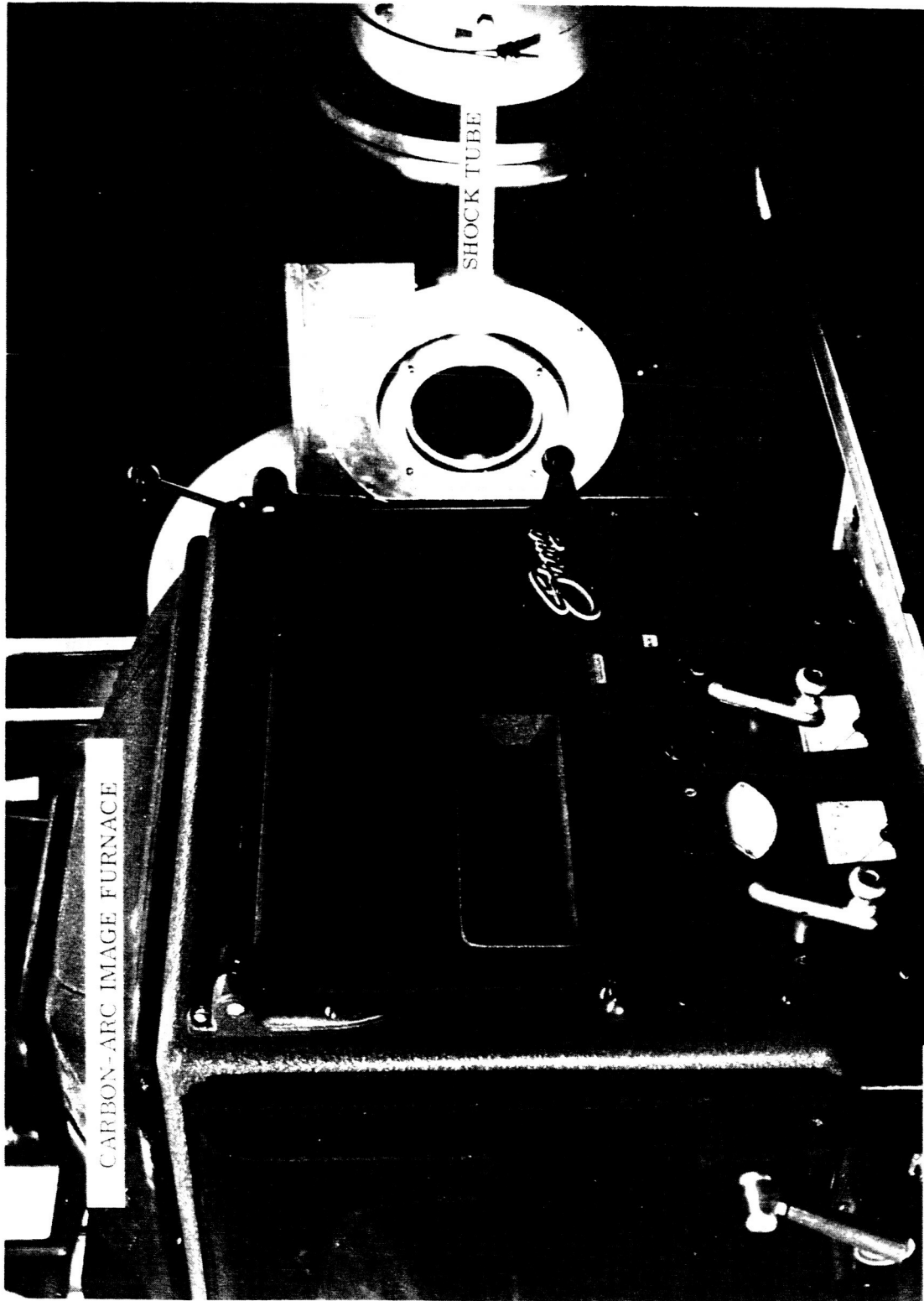
Because of the possibility that high transmitted power levels will be needed for some of the many communications and guidance functions on the shuttle vehicle, a program was conducted at SRI during which a technique was developed for evaluating candidate RF window and TPS materials during exposure to high surface temperatures and high RF power levels. The tests were performed in the SRI 12-inch shock tube facility by using an externally mounted carbon-arc image furnace as the heat source. The tube was used both to serve as a pressure vessel and to furnish a plasma over the samples where breakdown at the plasma/sample interface was investigated. The measurements were performed at X-band.



**SCHEMATIC PRESENTATION OF APPARATUS FOR MEASUREMENTS  
IN SHOCK TUBE**

## STANFORD RESEARCH INSTITUTE HIGH TEMPERATURE FACILITY

The carbon-arc image furnace used for producing the 2200° F surface temperatures on the various test materials is shown with the shock tube facility. The quartz window through which the samples mounted in the shock tube were heated is also visible.



STANFORD RESEARCH INSTITUTE HIGH TEMPERATURE TEST FACILITY

### **SAMPLE HOLDER AND TEST ANTENNA**

Shown are the stainless steel test sample holder with test material and horn test antenna used for the SRI shock tube tests. Thermocouples were imbedded in the test samples to determine surface temperatures. A mass spectrometer was also used to investigate material outgassing. The horn antenna used had a 0.90-inch-square aperture, and the test sample diameter was 1.4 inches. Test sample thickness was 0.25 inch.





MASS SPECTROMETER  
INTAKE TUBE

DIELECTRIC TEST SAMPLE

THERMOCOUPLES

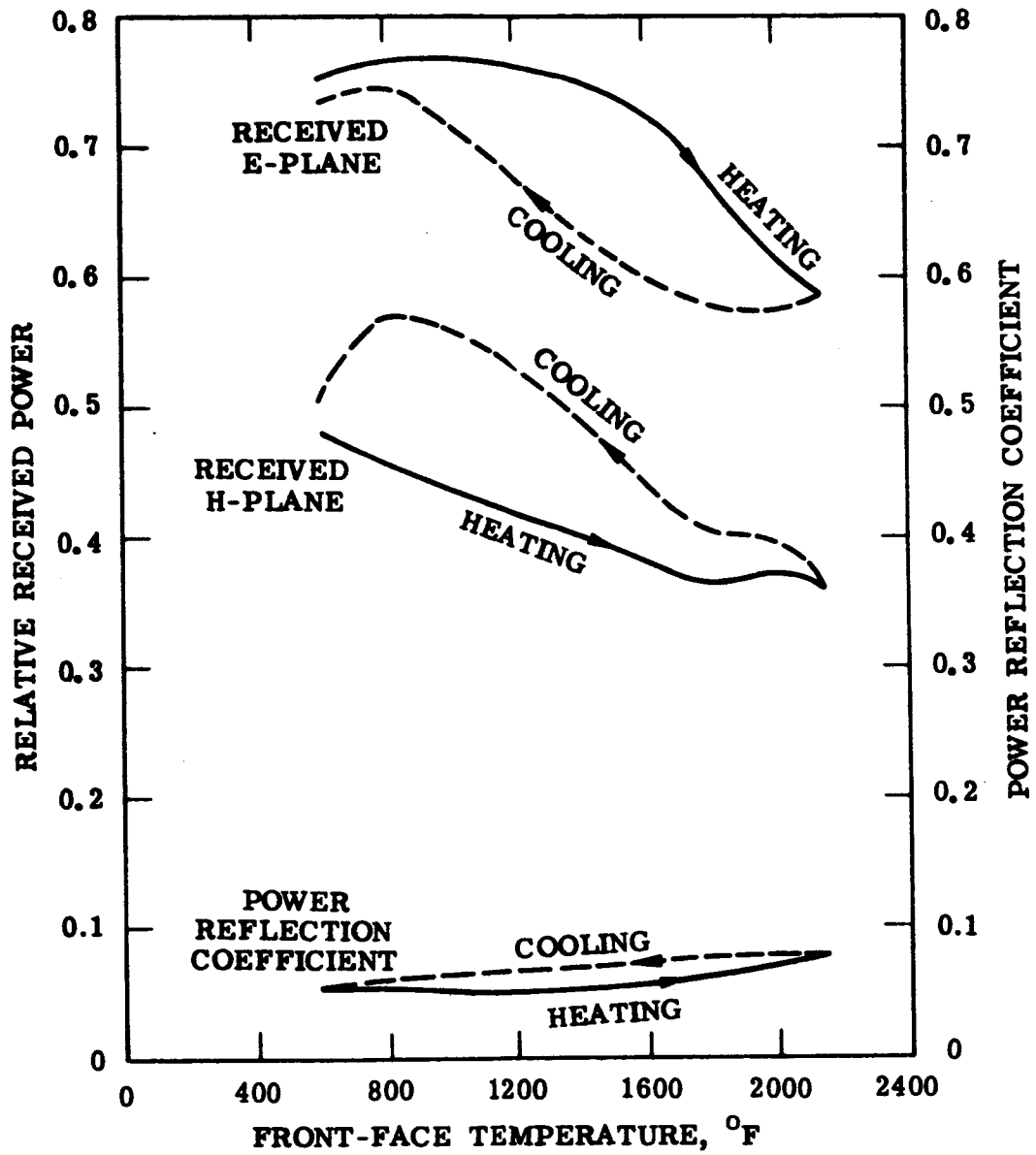
SAMPLE HOLDER AND TEST ANTENNA

## MICROWAVE MEASUREMENTS DURING HEATING AND COOLING CYCLES

### TEST MATERIAL AS-3DX

Transmission and reflection data similar to those presented here were obtained for six different test materials as a function of surface temperature. Both the E-plane and the H-plane transmitted levels were monitored by using horns located at a 45° angle with the center line (such as to be out of the focused beam of the carbon arc) and 6.5 inches from the sample. Apparently, the differences measured for the two polarizations were caused by pattern effects.

The results of the SRI tests indicated that none of those materials considered showed any evidence of material breakdown. These results were obtained from one test per sample. If it is determined from the Georgia Tech recycling tests that the loss tangent of a particular material increases considerably as the number of cycles increases, additional breakdown testing in the SRI facility may be necessary.



MICROWAVE MEASUREMENTS DURING HEATING AND COOLING CYCLES.  
 TEST MATERIAL AS-3DX

ANTENNA TECHNOLOGY - ANTENNA  
DESIGN AND SCALE MODEL TECHNIQUES

W. F. Croswell

NASA-Langley Research Center  
Hampton, Virginia

ANTENNA DESIGN AND SCALE MODEL TECHNIQUES

OBJECTIVE: TO DEVELOP PROTOTYPE ANTENNA DESIGNS AND METHODS OF MEASURING AND PREDICTING ANTENNA CHARACTERISTICS WHEN MOUNTED ON LARGE COMPLEX SHAPES SUCH AS SPACE SHUTTLE.

APPROACH: . CHOOSE TYPICAL ANTENNA TYPES THAT MEET SHUTTLE REQUIREMENTS

. DEVELOP ANALYTICAL METHODS FOR COMPUTER-AIDED DESIGN OF SUCH ANTENNAS

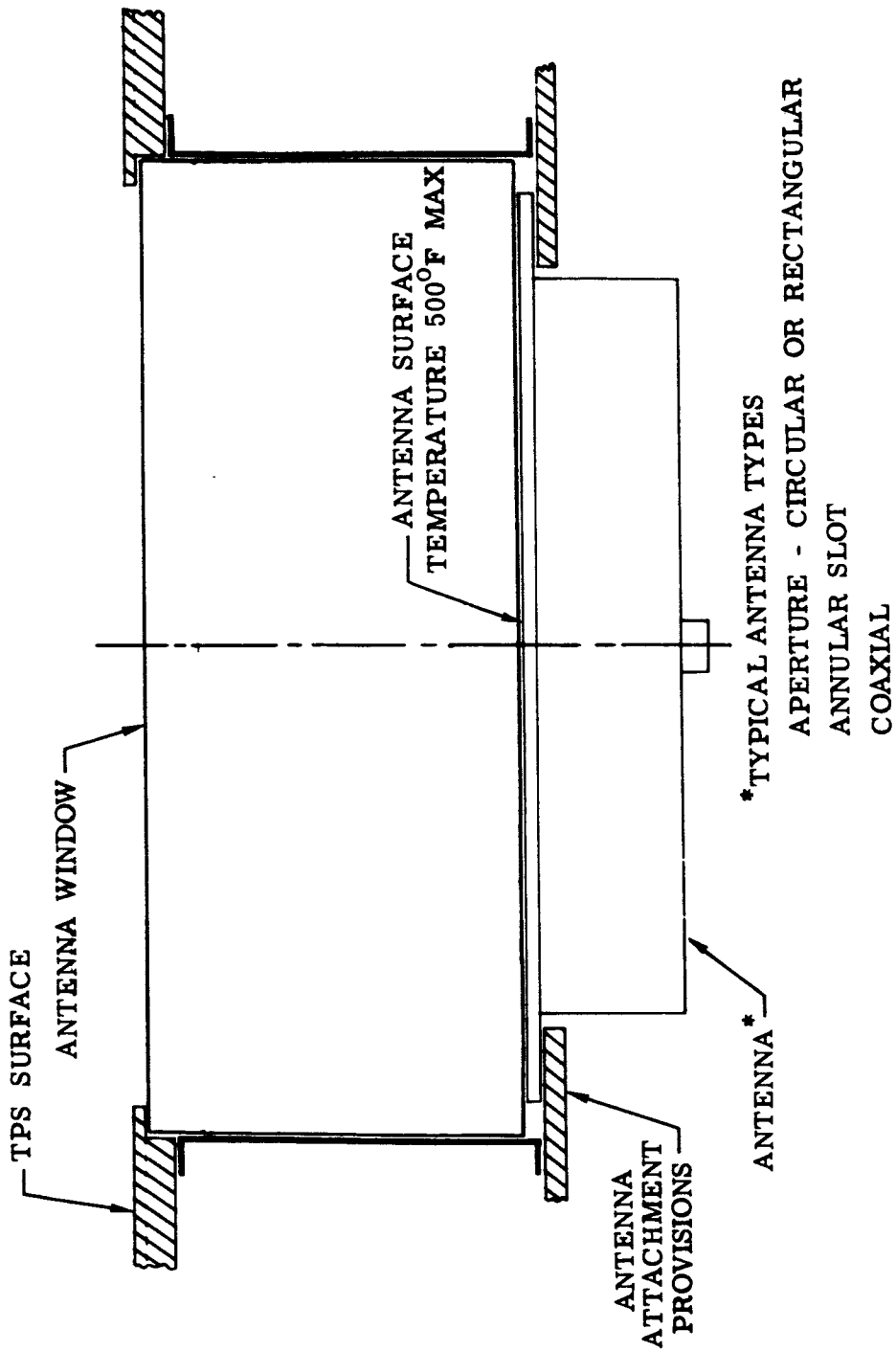
. CHECK DESIGN METHODS BY USE OF SCALE MODELS OF SPACE SHUTTLE SHAPES

## **ANALYTICAL METHODS**

- **APERTURE FIELDS OF PROTOTYPE ANTENNAS**
- **EFFECTS OF EDGES ON ANTENNA PATTERNS**
- **EFFECTS OF CURVATURE ON ANTENNA PATTERNS**
- **SCALE MODEL ANTENNA MEASUREMENTS**

#### ANTENNA WINDOW CONFIGURATION

This slide is an outline sketch showing a typical Space Shuttle antenna installation. It is proposed that all antennas for Space Shuttle use be recessed under a dielectric layer or be plugged to reduce the operational reentry temperature of the antenna metallic structure. Such a design is particularly important for extending the reuse capability of operational antenna systems. Several types of antenna configurations have been chosen as typical for meeting Space Shuttle electronic systems requirements. These antenna types are the annular slot, waveguide, or slot fed horn antennas. All of these antennas are being analyzed to determine the aperture fields and admittance as a function of operating frequency, plug thickness and dielectric constant, and the external dielectric insulation or antenna window properties. The aperture fields are then used to determine the radiation pattern of the typical antenna types mounted on Space Shuttle vehicle shapes. Parts of this analytical work have been completed and computer programs have been written and are operating.

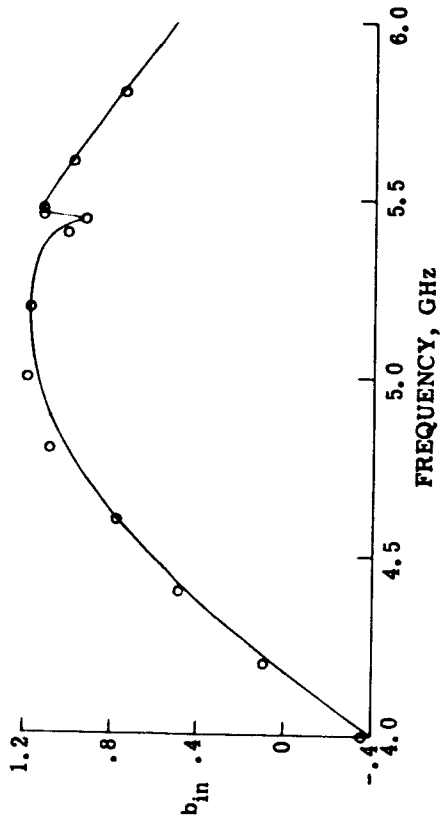
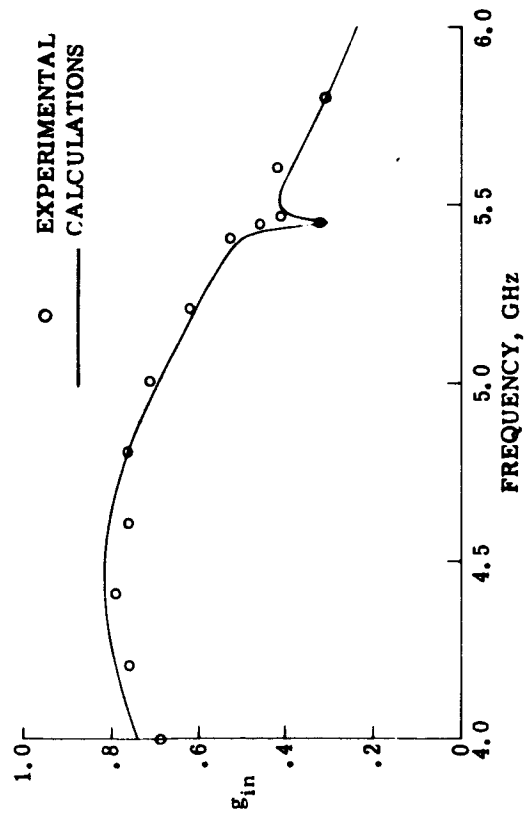


ANTENNA/WINDOW CONFIGURATION



ADMITTANCE OF A RECTANGULAR WAVEGUIDE ANTENNA LOADED  
WITH A QUARTZ DIELECTRIC PLUG

One type of waveguide antenna that has a plug in the aperture has already been analyzed. It has been determined that resonances can occur which are dependent upon the dielectric constant dimensions of the plug and waveguide and the operating frequency. An example of the effect on the input admittance is given in this slide. The resonance is the bump in the corresponding curves of aperture conductance  $g_{in}$  and aperture susceptance  $b_{in}$ . In other antennas having larger apertures, the resonances produce even larger admittance changes. It is to be noted that if the resonances can be avoided, the plugged antennas can be designed to have good admittance characteristics.



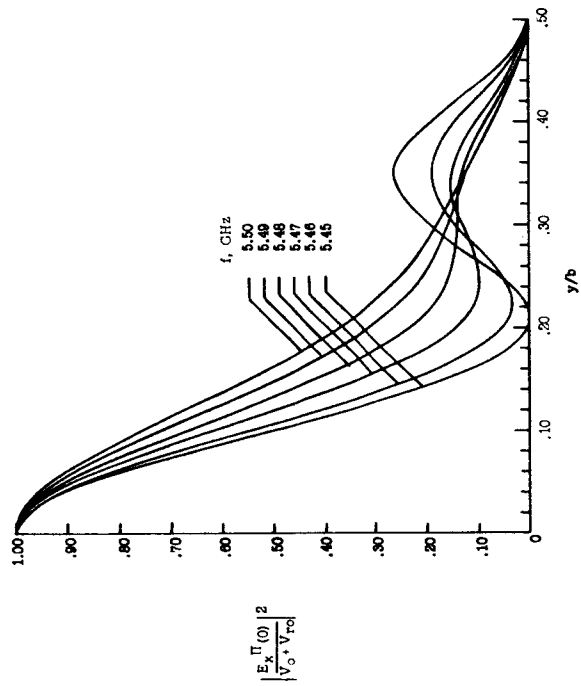
### INPUT ADMITTANCE OF A RECTANGULAR WAVEGUIDE

### LOADED WITH A QUARTZ PLUG

APERTURE FIELD DISTRIBUTIONS IN THE RESONANCE REGION  
OF A QUARTZ PLUGGED RECTANGULAR WAVEGUIDE

In the vicinity of the resonance region, shown in the previous slide, there are large changes in the aperture field of the plugged waveguide antenna. These changes, which are shown in this slide as a function of the normalized waveguide half dimension  $y/b$ , should be compared to a cosine distribution normally produced in the aperture.

These large changes in the aperture field can produce unexpected nulls in an otherwise smooth antenna pattern. Indeed, such nulls have been observed in the resonance region of a number of different types of plugged reentry antennas.

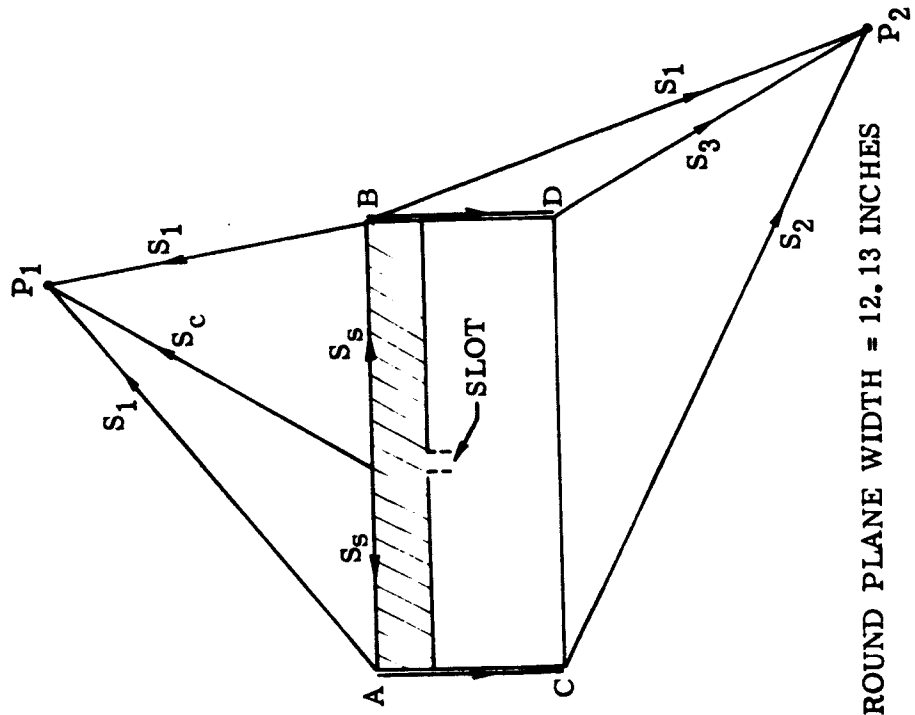


**PLOTS OF THE APERTURE ELECTRIC FIELD DISTRIBUTION**

## DIELECTRIC COATED GROUND PLANE

Knowing the aperture fields of a dielectric plugged or coated antenna mounted on a flat ground plane, it is sometimes possible to predict the pattern of such an antenna when it is mounted on a complex shaped surface. Of particular importance to pattern shape are the effects of edges or sharp corners.

An example of treating such edge problems has been worked out by Ohio State University using a modified form of the geometrical theory of diffraction. Depicted in this slide are the equivalent ray produced fields in the region above the ground plane at  $P_1$  and below the ground plane at  $P_2$ . For example, the field observed at  $P_1$  is the sum of the direct slot field  $S_c$  and the two surface ray  $S_s$  fields diffracted and radiated at points A and B.



GROUND PLANE WIDTH = 12.13 INCHES

GROUND PLANE HEIGHT = 1.71 INCHES

SLOT WIDTH = 0.062 INCH

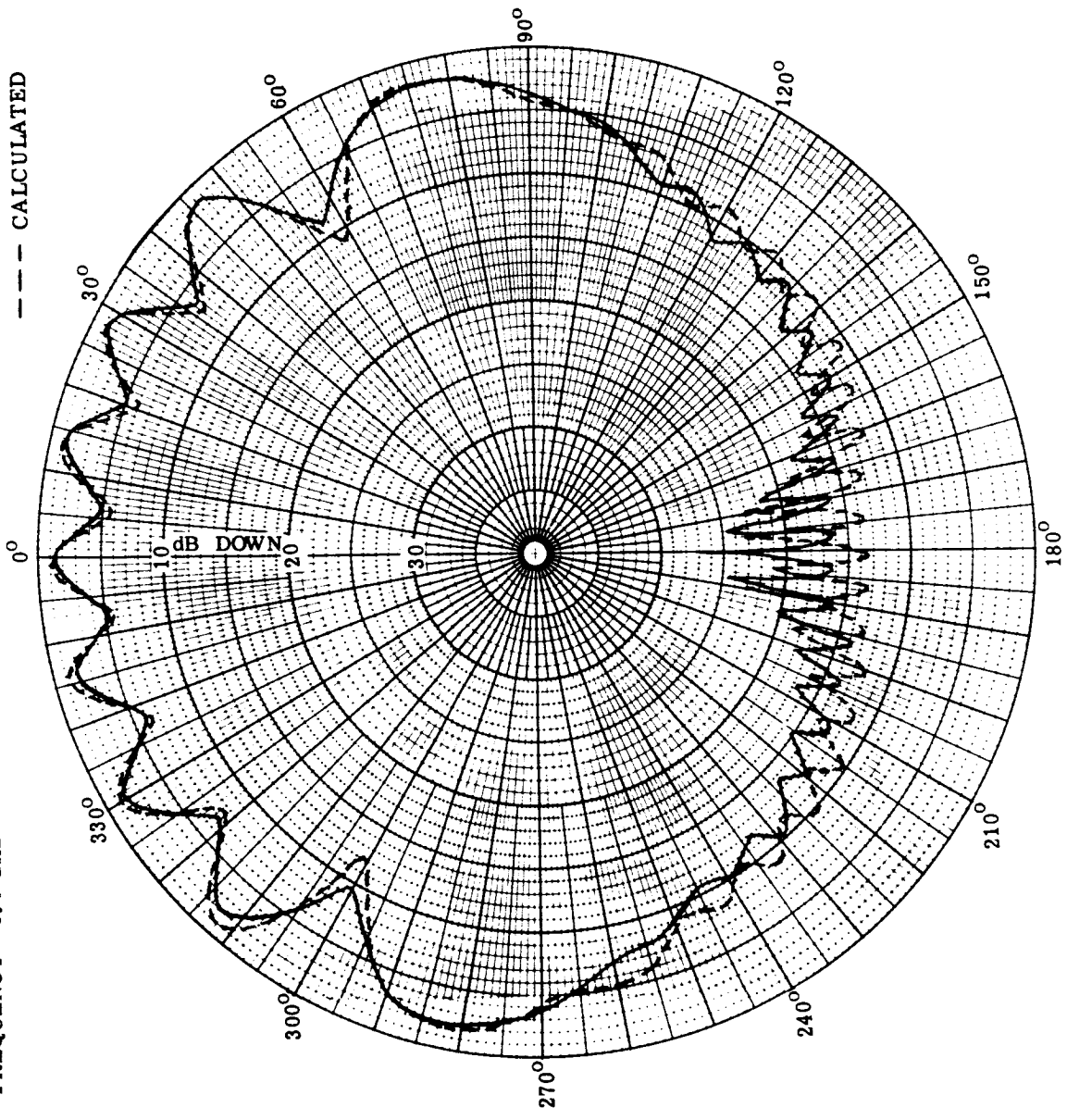
RAY'S EMANATING FROM A SLOT IN A DIELECTRIC CLAD GROUND PLANE.

PATTERN OF A SLOT IN A DIELECTRIC COVERED GROUND PLANE

Using the dimensions given in the previous slide, a ground plane was constructed and a dielectric cover ( $\epsilon = 2.57$ ) placed over it. Patterns for various thickness covers were measured and computed. A typical result is given in this slot where  $O^0$  represents the direction directly above the slot in the ground plane. Notice that these results compare favorably. It was found that detailed agreement of a points of the pattern is precluded by tolerances of construction in the experimental models. This is the first time such a theoretical solution has been accomplished.

DIELECTRIC COVER = 0.110 INCH PLEXIGLAS  
FREQUENCY = 8.0 GHZ

— EXPERIMENTAL  
- - - CALCULATED



PATTERN OF A SLOT IN A DIELECTRIC COVERED GROUND PLANE

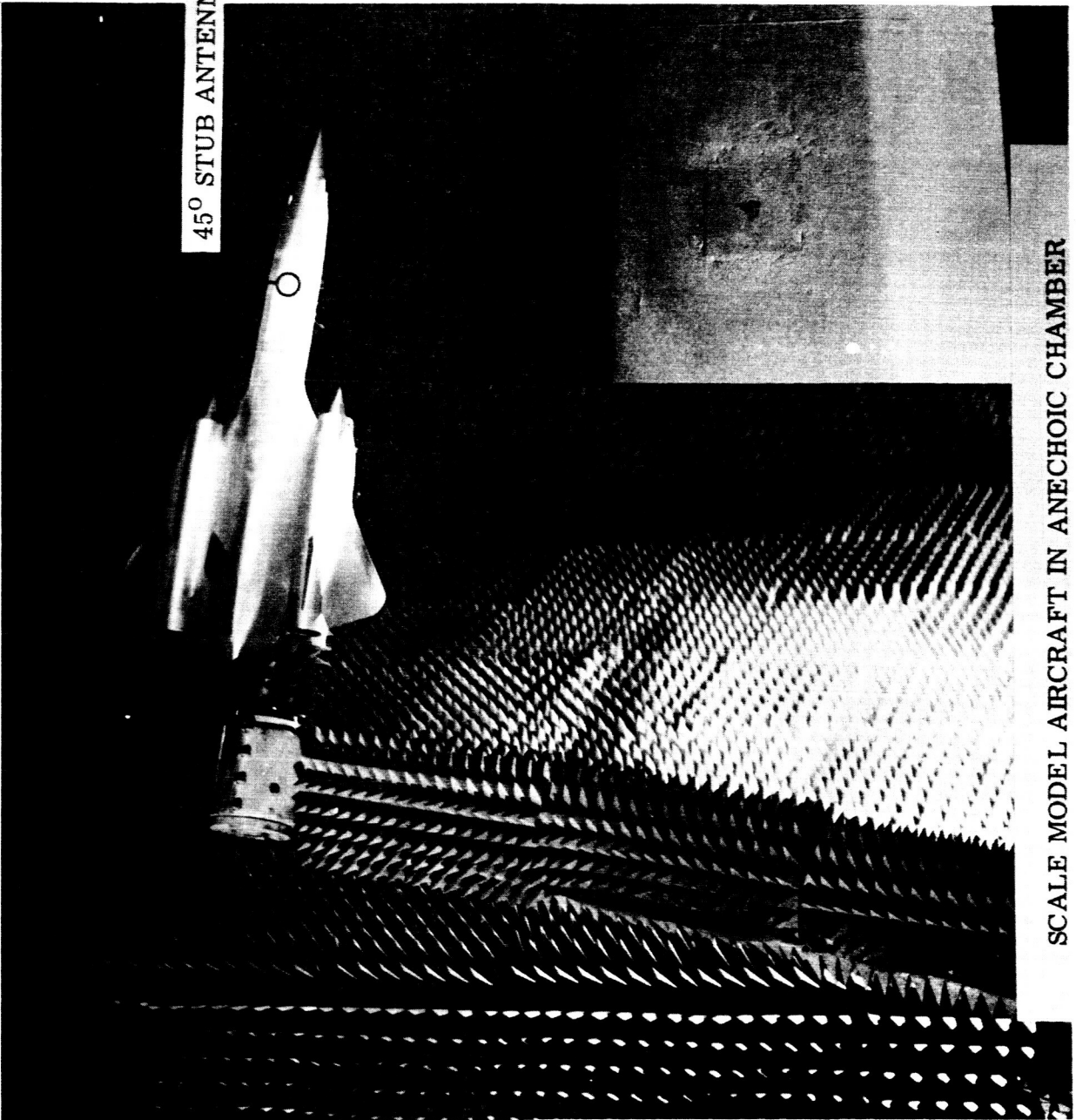


### 1/2<sup>nd</sup> SCALE MODEL AIRCRAFT

This slide shows a photograph of a scale model of an aircraft being used for antenna design studies in the antenna chamber at LRC. This antenna design study is being conducted for FRC at Edwards Air Force Base. The insert shows the scale model antenna at 35 GHz which is being used to determine the effects of the aircraft structure on two antenna excitation modes.

45° STUB ANTENNA

SCALE MODEL AIRCRAFT IN ANECHOIC CHAMBER

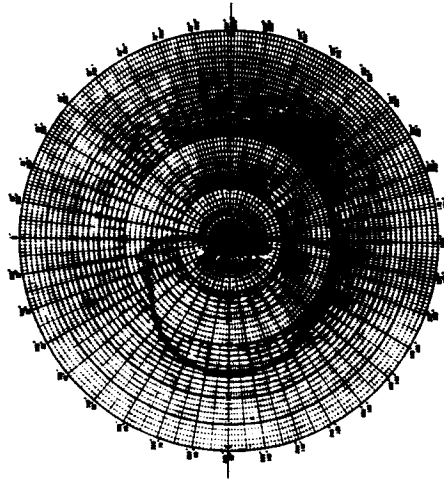


## RADIATION PATTERNS MEASURED AT 35 GHz USING A ONE TWENTY-FOURTH SCALE MODEL AIRCRAFT

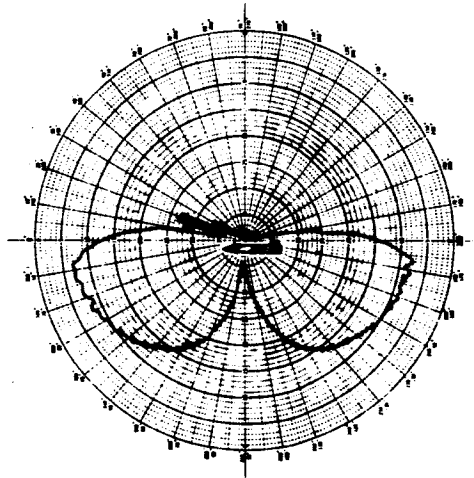
In order to demonstrate some of the problems associated with designing antennas on large spacecraft and the usefulness of scale model measurements, three patterns are presented in a series of slides. All of these patterns are principal plane cuts through the axis of a small stub antenna mounted on the bottom of the 1/24th scale model aircraft shown in the previous slide or in one instance an equivalent flat plate. For example, consider the middle pattern which is one of a short vertical stub on the aircraft. Notice the null directly below the aircraft and the fine ripple structure as we approach the nose or tail region. Now compare this middle pattern with the one on the left of the same small vertical stub mounted at the same point on a flat metal plate the same width and length as the aircraft fuselage. Notice that the overall shape of this pattern is similar to that of the aircraft mounted antenna except for the large ripple structure near the equivalent nose and tail region. This comparison gives an indication of the effects of sharp edges and of the importance of using accurate scale models to obtain detailed patterns.

By bending the stub to a 45 degree angle, one can fill in the pattern underneath the aircraft as shown in the third pattern at the sequence. Consequently, most commercial aircraft use a bent stub or blade antenna on the top and bottom of the airplane for communication purposes. For Space Shuttle applications, such external antennas are not suitable; however, by a combination of the flush mounted types of aperture antennas discussed earlier in this paper, similar patterns can be produced on Space Shuttle shaped vehicles.

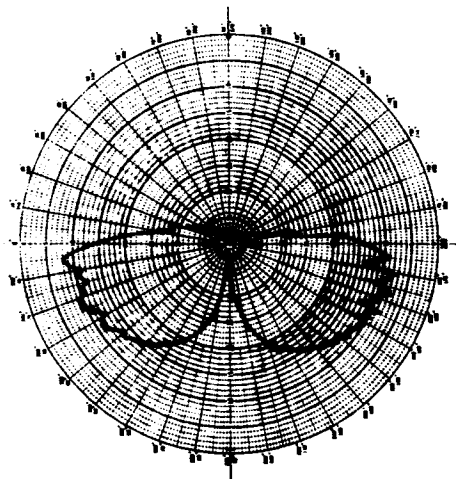
60° STUB MOUNTED ON THE BOTTOM OF A ONE TWENTY-FOURTH SCALE MODEL AIRCRAFT



STUB MOUNTED ON THE BOTTOM OF A ONE TWENTY-FOURTH SCALE MODEL AIRCRAFT.



STUB MOUNTED OF FLAT GROUND PLANE



## BLACKOUT CALCULATIONS

**OBJECTIVE:** TO DEFINE THE BLACKOUT BOUNDARIES FOR  
VARIOUS ANTENNA LOCATIONS ON SPACE  
SHUTTLE VEHICLES

**APPROACH:**

- DEVELOP ANALYTICAL METHODS WHICH EXTEND APOLLO  
DEVELOPED COMPUTER PROGRAMS TO SPACE SHUTTLE  
CONFIGURATIONS AND CONDITIONS
- CHECK ANALYTICAL METHODS BY PREDICTING MEASURED  
PLASMA PROPERTIES FOR RAM C VEHICLES
- PERFORM PARAMETRIC CALCULATIONS ON SPACE SHUTTLE  
SHAPES WITH TYPICAL TRAJECTORIES

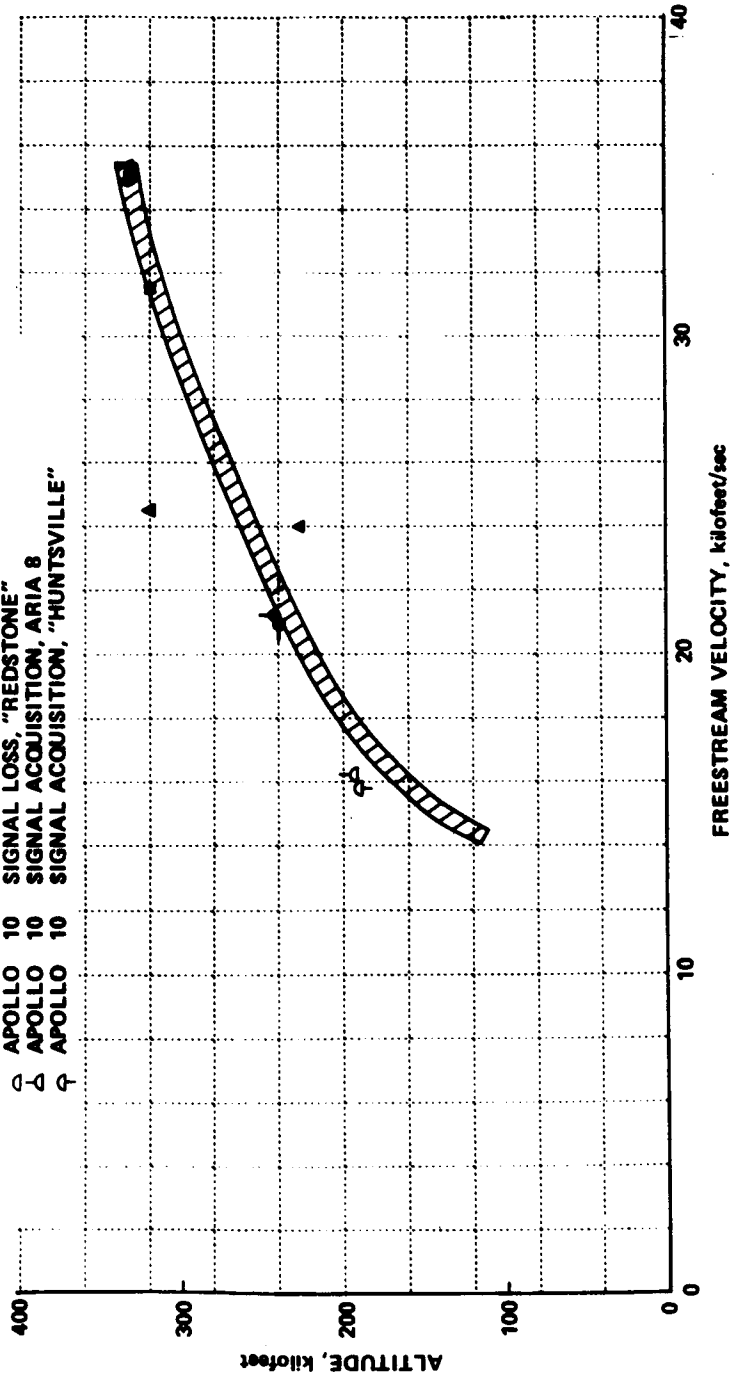
COMPARISON BETWEEN PREDICTED AND FLIGHT  
DATA BLACKOUT BOUNDARIES

This slide presents the available measured blackout conditions for Apollo reentry along with predictions run by Cornell Aeronautical Laboratory. Further discussion of these results is available in NASA SP-252 published in February 1971.

CORNELL AERONAUTICAL LABORATORY PREDICTION,  
PURE-AIR

KEY TO CALCULATED TRAJECTORY POINTS

- ▨ BLACKOUT, NASA 432 AIRCRAFT
- APOLLO 4 SIGNAL ACQUISITION, ARIA 5
- APOLLO 4 SIGNAL LOSS, ARIA 5
- ◐ APOLLO 6 BLACKOUT, NASA 427 AIRCRAFT, "WATERTOWN"
- △ APOLLO 7 SIGNAL LOSS, ARIA 5
- ▲ APOLLO 7 SIGNAL LOSS, NASA 427, GROUND STATIONS
- ◆ APOLLO 8 SIGNAL LOSS, ARIA 1
- ◇ APOLLO 10 SIGNAL LOSS, "REDSTONE"
- ◒ APOLLO 10 SIGNAL ACQUISITION, ARIA 8
- ◓ APOLLO 10 SIGNAL ACQUISITION, "HUNTSVILLE"



COMPARISON BETWEEN PREDICTED AND FLIGHT DATA BLACKOUT BOUNDARIES

**AUTOMATIC ANTENNA SWITCHING  
TECHNIQUES**

**H. DEAN CUBLEY**

**MANNED SPACECRAFT CENTER  
HOUSTON, TEXAS**



# **TABLE OF CONTENTS**

- **SHUTTLE COMMUNICATIONS REQUIREMENTS**
- **SHUTTLE ANTENNAS**
- **POSSIBLE SHUTTLE ANTENNA CONTROL TECHNIQUES**
- **MSC SYSTEM TEST PROGRAM DESCRIPTION**
- **MSC SYSTEM TEST DATA**
- **CONCLUSIONS**

AUTOMATIC ANTENNA SWITCHING TECHNIQUES

H. Dean Cubley

NASA-Manned Spacecraft Center  
Houston, Texas

SUMMARY

A development program is described that has as its purpose the optimization of the communications antenna performance of the orbiter portion of the Shuttle vehicle. The basic configuration of the communications antennas on the Shuttle is discussed in view of the presently anticipated communications requirements. The design problems associated with the placement of Shuttle antennas and the possible effects of interference between antennas are explored. A proposal is made that some type of switching system for antenna control must be a basic part of any Shuttle design. The basic types of antenna control systems are reviewed with emphasis on their applicability to the Shuttle requirements. The results of an extensive comparative analysis of all of these basic systems and certain of their hybrid combinations are presented. The development of engineering models of some of the most interesting of these antenna control systems is discussed in relation to their adaptation to the Shuttle requirements. The present MSC in-house test program being conducted on these engineering models is discussed, and some of the results of these tests are presented. A summary of the additional planned development and testing objectives of this program is presented.

## INTRODUCTION

The design of the Shuttle orbiter stage communications system must contain a sufficient number of antennas to provide the necessary pattern coverage to fulfill the Shuttle mission without constraints on the orientation of the vehicle. Because of the thermal heating of the Shuttle during reentry and the requirement for multiple mission usage, the placement of these antennas is not optimum from a coverage standpoint. The result of these conflicting requirements is a Shuttle antenna system that requires some means of logical selection of the best set of spacecraft antennas at each point in the Shuttle mission. The means of this antenna selection can take various forms depending on the mission requirements and the degree of sophistication available in the antenna selection system. The most basic selection system is manual selection by a Shuttle crew member. However, this technique will require an excessive amount of crew time. The more sophisticated techniques range from semi-automatic and automatic RF tracker techniques to complete antenna control by an onboard computer.

## SHUTTLE BASIC COMMUNICATIONS REQUIREMENTS

The basic communications requirements of the first generation of Shuttle vehicles will consist of three separate phases. The first phase will consist of the relatively short range communications between the launch site and the orbiter and booster stages during and shortly after launch. The second phase of communications will consist of those transmissions between the orbiter and booster and down-range ground stations prior to the attainment of orbit. The final phase of communications will consist of transmissions between the orbiter stage and the various global ground stations after attainment of orbit. Because of the very low orbits planned for the orbiter stage, a large range of look angles to the various ground stations will be encountered. This variation in look angles will require repeated selection of the appropriate communications antenna in order not to have loss of communications.

# SHUTTLE BASIC COMMUNICATIONS REQUIREMENTS

ATMOSPHERIC COMM ORBITER AND BOOSTER TO GROUND



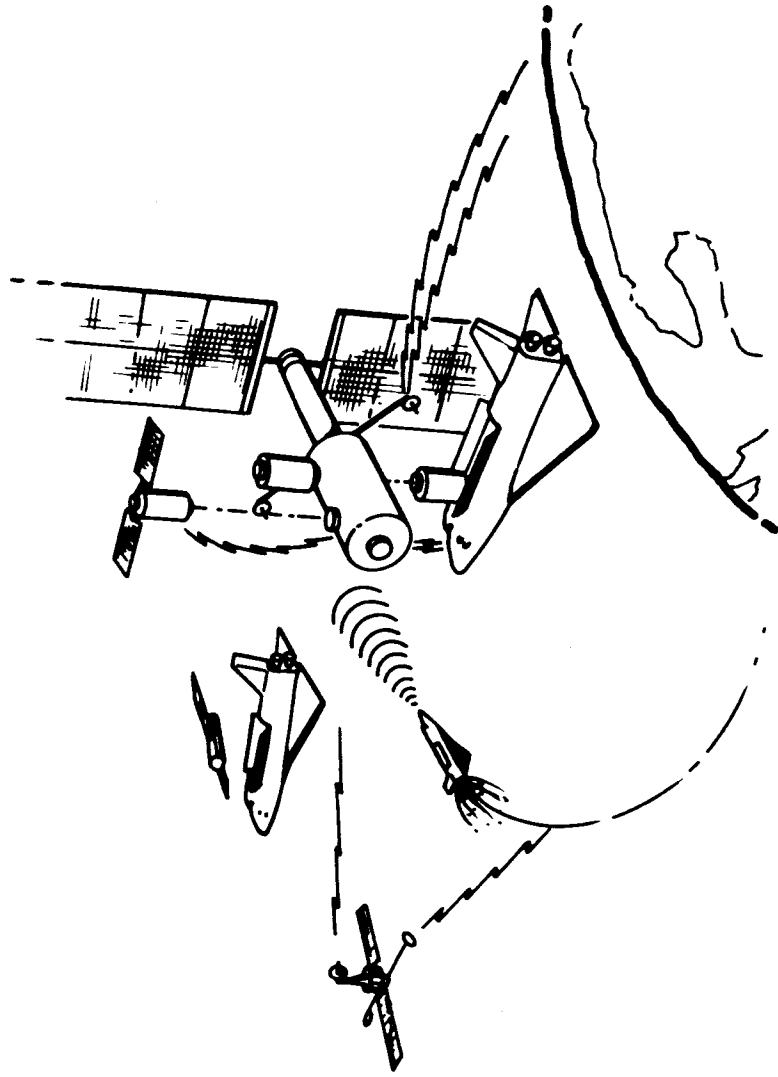
LAUNCH COMM ORBITER AND BOOSTER TO GROUND

ON-ORBIT COMM ORBITER TO GROUND

#### SHUTTLE ADVANCED COMMUNICATIONS REQUIREMENTS

The more advanced Shuttle missions will encounter the same basic problems of antenna selection as those of previous missions. However, for Shuttle missions supporting other manned vehicles such as the space base, additional antenna selection requirements are encountered. Because of the more complex look-angle geometry between a Shuttle vehicle, a space base, and several ground stations, the selection of the appropriate antennas for all the required communications links will consume a large portion of the time of one Shuttle crew member if accomplished manually. In addition, as logistic requirements for the space base become greater, there is the likelihood that even more than one Shuttle may be in orbit at a given time. This will undoubtedly necessitate even more communications requirements, with the resultant increase in antenna switching operations.

# SHUTTLE ADVANCED COMMUNICATIONS REQUIREMENTS



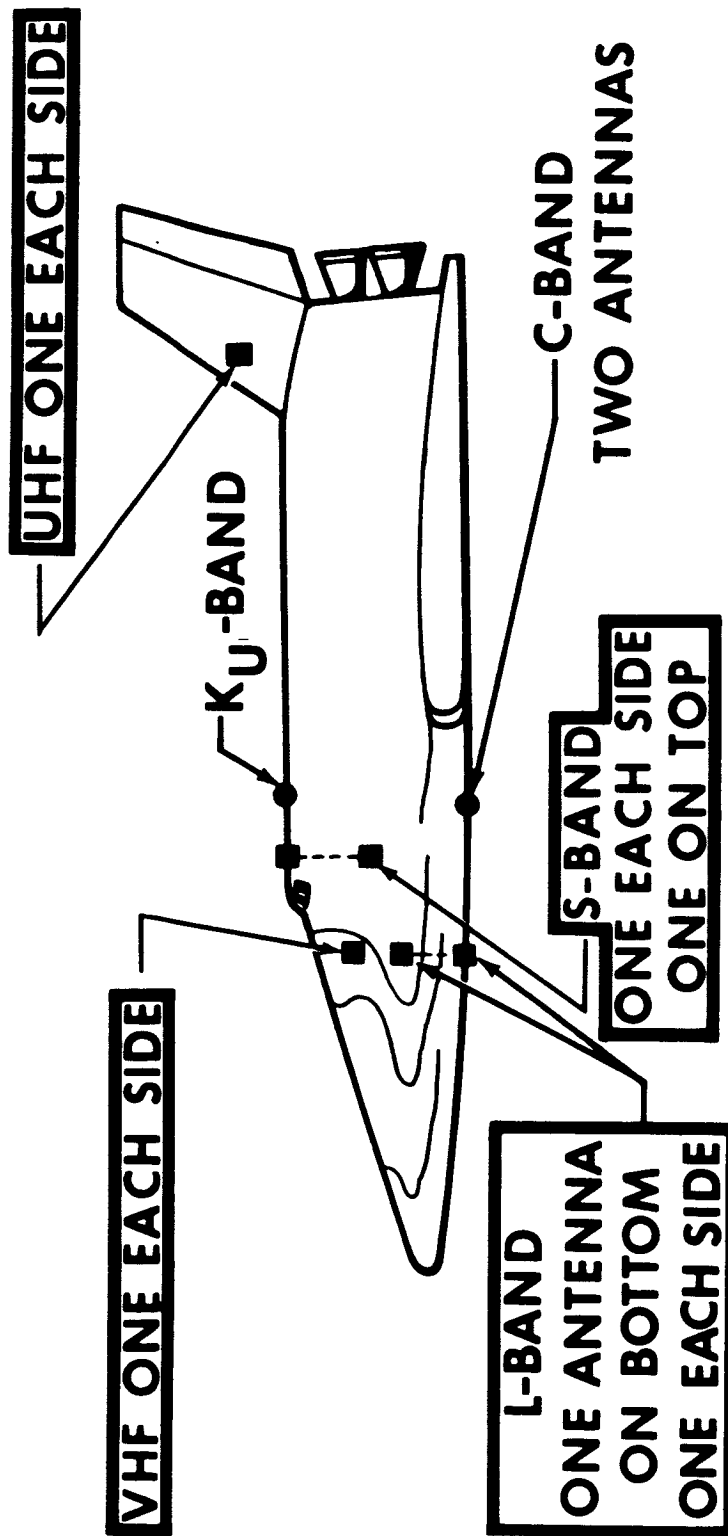
#### SHUTTLE COMMUNICATIONS ANTENNA LOCATIONS

The obvious solution to the Shuttle antenna selection problem is to design a Shuttle communications antenna system with the minimum number of antenna elements. The nature of the Shuttle communications requirements necessitates almost complete coverage in the plane perpendicular to the longitudinal axis of the vehicle. Two antennas located on opposite sides of the Shuttle forward of the crew compartment represent the best choice for all the communications requirements. Unfortunately, this location also imposes severe heating levels on the antenna elements. The most logical choice for a compromise antenna location is shown in the accompanying figure. The basic communications frequencies are S-band, VHF, and UHF. The S-band antenna system consists of three antennas located directly behind the crew compartment. One of these S-band antennas is located centrally on the top of the vehicle to provide coverage above the Shuttle. The other two S-band antennas are located on opposite sides of the Shuttle to provide coverage both below and to each side of the vehicle. The VHF system consists of one antenna located on each side of the vehicle slightly forward of the crew compartments. The UHF antenna system consists of one antenna located on each side of the Shuttle vertical stabilizer tail assembly.

# ANTENNA LOCATIONS

**SWITCHABLE**

**NOTE:  
ALL SHUTTLE ANTENNAS  
NOT SHOWN**



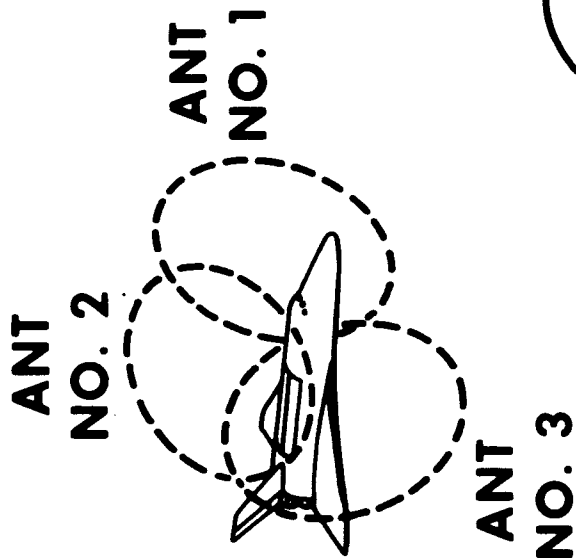


#### SHUTTLE ANTENNA INTERFERENCE PATTERNS

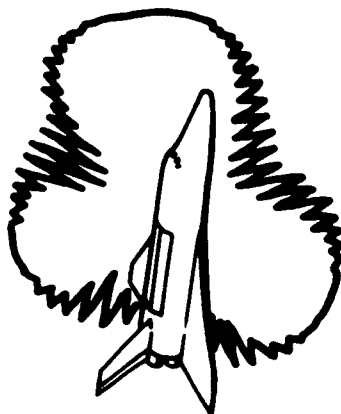
As an example of the type of pattern coverage expected from the Shuttle antenna system, consider the various antenna configurations shown in the accompanying figure. The S-band antennas previously described are the basis for this figure. The first part of this figure illustrates the typical shape of each of the individual S-band antenna patterns in the plane perpendicular to the Shuttle longitudinal axis. It should be noted that these patterns provide a large amount of overlapping coverage. This particular type of antenna pattern is required in order to minimize the total number of antennas required for complete coverage. One method that has been proposed to provide the required coverage is to connect all three antennas in parallel and thus eliminate the need for antenna switching. The result of such an arrangement is shown in the second part of the figure. One can see that the interference between the various antennas results in very deep nulls over a major portion of the composite pattern. By contrast, the composite pattern obtained by the use of any automatic switching system is shown in the third portion of the figure.

# SHUTTLE ANTENNA INTERFERENCE PATTERNS

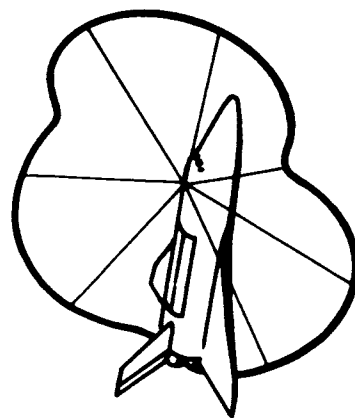
## A. INDIVIDUAL ANTENNAS



## B. ANTENNAS IN PARALLEL



## C. ANTENNAS AUTOMATICALLY SWITCHED



#### POSSIBLE SHUTTLE ANTENNA CONTROL TECHNIQUES

The possible antenna selection and switching techniques available to the Shuttle designer range from a simple mechanical switch to a system completely controlled by an onboard computer. The mechanical system consists of a switch that allows a crewman to select any one of the Shuttle antennas. The basis for his selection may be a preplanned sequence or a general knowledge of the look angles to the receiving station. A degree of sophistication may be added to the selection process if the switching is accomplished automatically, based on some knowledge of the signal strength being received from the remote station. All such switching systems may be termed RF track control systems. The most simple of the RF track control systems is the phase quadrature tracking system. This system may be used to phase the signal arriving from the various Shuttle antennas such that they may be connected in parallel without experiencing the interference nulls. A slightly more sophisticated RF system is the cochannel switching system. This system periodically connects the various antennas to the receiver and samples and compares the signal strength. The antenna with the strongest signal strength is then connected to the receiver until the selection process is repeated at the next sampling time. One disadvantage to this system is that the received signal must be periodically disconnected from the receiver in order to permit the required sampling. The most sophisticated RF system is the separate channel switching system. This system is the same as the cochannel system, except that the sampling is accomplished in a parallel fashion through the use of a secondary receiver. The ultimate in antenna control may be accomplished through the use of a small computer to select the proper antenna based on either a pre-programmed trajectory or possibly on inputs from the Shuttle guidance system.

# **POSSIBLE SHUTTLE ANTENNA CONTROL TECHNIQUES**

- **MANUAL CONTROL BY CREWMAN**
- **RF TRACK CONTROL SYSTEMS**
  - **PHASE QUADRATURE TRACKING SYSTEM**
  - **COCHANNEL SWITCHING SYSTEM**
  - **SEPARATE CHANNEL SWITCHING SYSTEM**
- **COMPUTER CONTROLLED SELECTION BASED  
ON GUIDANCE SYSTEM INFORMATION**

### PHASE QUADRATURE TRACKING SYSTEM

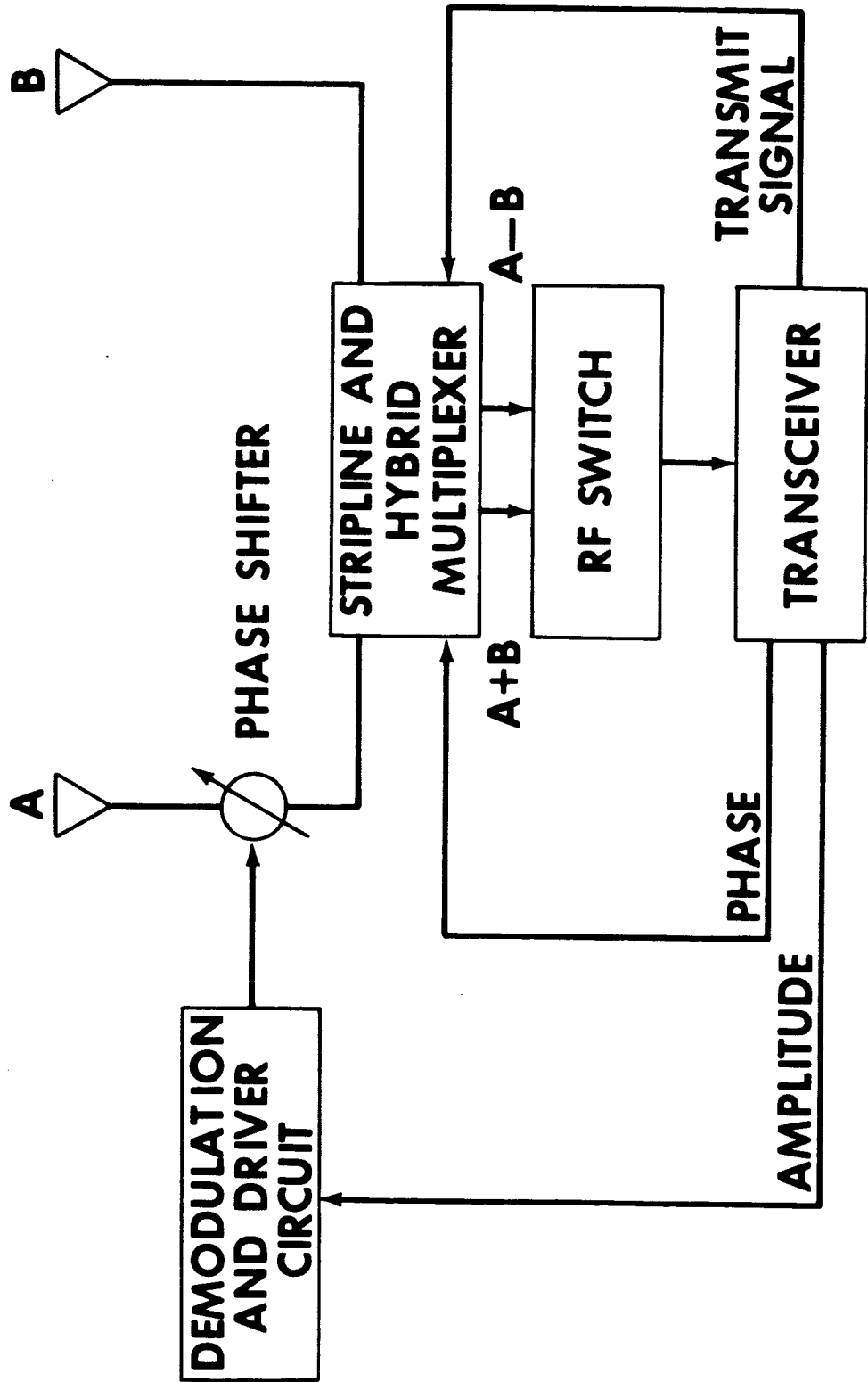
An antenna-array, phase quadrature tracking system automatically adjusts the phase relationship between the input signals appearing on two widely spaced parallel-connected antenna elements in the array. An optimum signal is delivered to a transceiver in the control system when a quadrature-phase relationship is achieved between the two input signals.

In the basic system, the two input signals in a single array are combined to form the absolute sum and difference values of the signals. The sum and difference signals are then time multiplexed through an RF switch at 10-millisecond intervals and processed to form a single multiplexed output which is applied to an amplitude detector in the receiver. The detector senses amplitude variations in the multiplexed signal and generates an output control voltage proportional to the deviation from the ideal quadrature-phase condition. The control voltage is applied to a feedback loop in a variable phase shifter circuit that automatically adjusts the relative phase of the two antenna signals until amplitude modulation ceases in the multiplexed signal (i.e., until the two antenna signals are locked in phase quadrature). The control loop continuously adjusts the relative phase of the two antenna signals to maintain the optimized signal input condition.

The RF switching operating in the multiplexing stage creates a phase modulation of the two input signals which is dependent upon the relative amplitude of the signals received on each of the antenna elements. The signal combining and multiplexing operations, including the RF switching, are accomplished by means of a stripline hybrid circuit which reduces the number of components in the antenna system.

When the antenna tracking system operates in the transmitting mode, power is delivered to the antenna element which will provide the maximum gain between the transmitting array and the receiving station. The automatic selection of the antenna element with the proper phase relation provides a substantially omnidirectional antenna coverage with a minimum number of antenna elements. The complete system is lightweight and sufficiently compact to permit its use in a Space Shuttle communications system.

# PHASE QUADRATURE TRACKING SYSTEM



## COCHANNEL SWITCHING SYSTEM

The operation of the system is based on fixed sampling and dwell periods generated by timing circuits in the switch logic. During the sampling period, each antenna is connected in sequence to the receiver. The AGC samples are held in the logic, and at the end of the sampling period, the logic switches to the antenna which provided the largest signal for the dwell period of communication on the selected antenna. In a marginal gain situation, information may be lost during three-fourths of the sampling period. For comparison with other sampling methods, an equation may be written for the information transfer efficiency in percent when at least one antenna is capable of reception is

$$I_1 = 100 \times [1 - K_1 t_s / (t_s + t_d) - t_r / t_R], \text{ percent}$$

$K_1$  = a dimensionless constant = 0.750

$t_s$  = sampling period, seconds

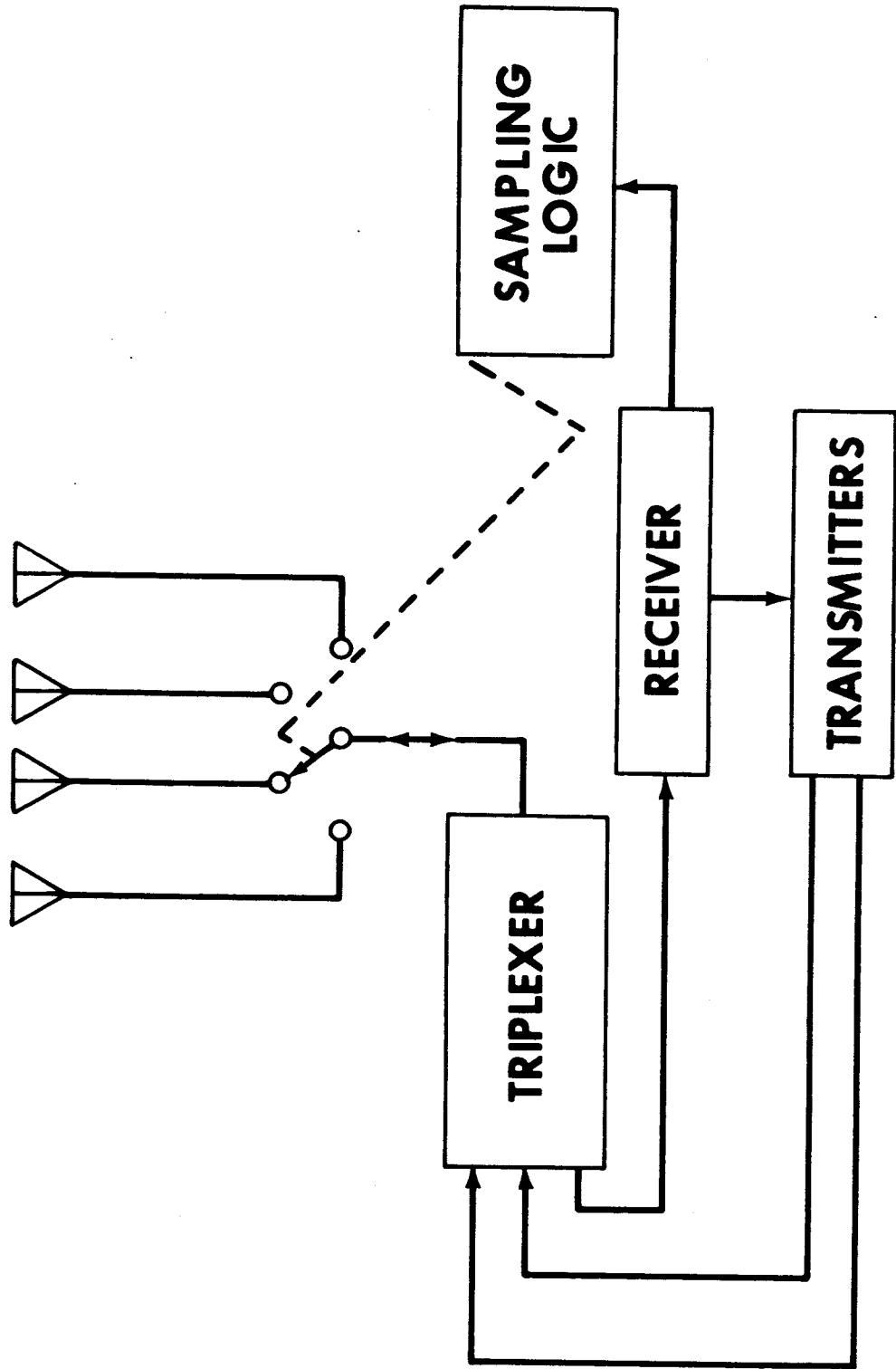
$t_d$  = dwell period, seconds

$t_r$  = time during dwell period in which signal is lost due to rotation

$t_R$  = seconds per revolution

$K_1$  is determined by the gain margin and antenna directivity.  $t_r$  is a function of gain margin, antenna directivity, and roll rate. Additional refinement may be added to this system by including threshold and/or rate logic such that the sampling period becomes a function of the signal strength and/or the rate of change of signal strength.

# COCHANNEL SWITCHING SYSTEM





### SEPARATE CHANNEL SWITCHING

In separate channel switching, the sampling process is continuous in the sampling and control channel. The optimum antenna can be selected during each sampling period. If at least one antenna is capable of reception, information will be lost only during the marginal crossover period. The loss will occur four times per revolution of the spacecraft and have a maximum duration of  $0.75t_s$ . The loss of information can then be expressed as

$$\text{Fraction of information lost} = 4(0.75t_s/T_1)$$

$$T_1 = \text{roll period, seconds}$$

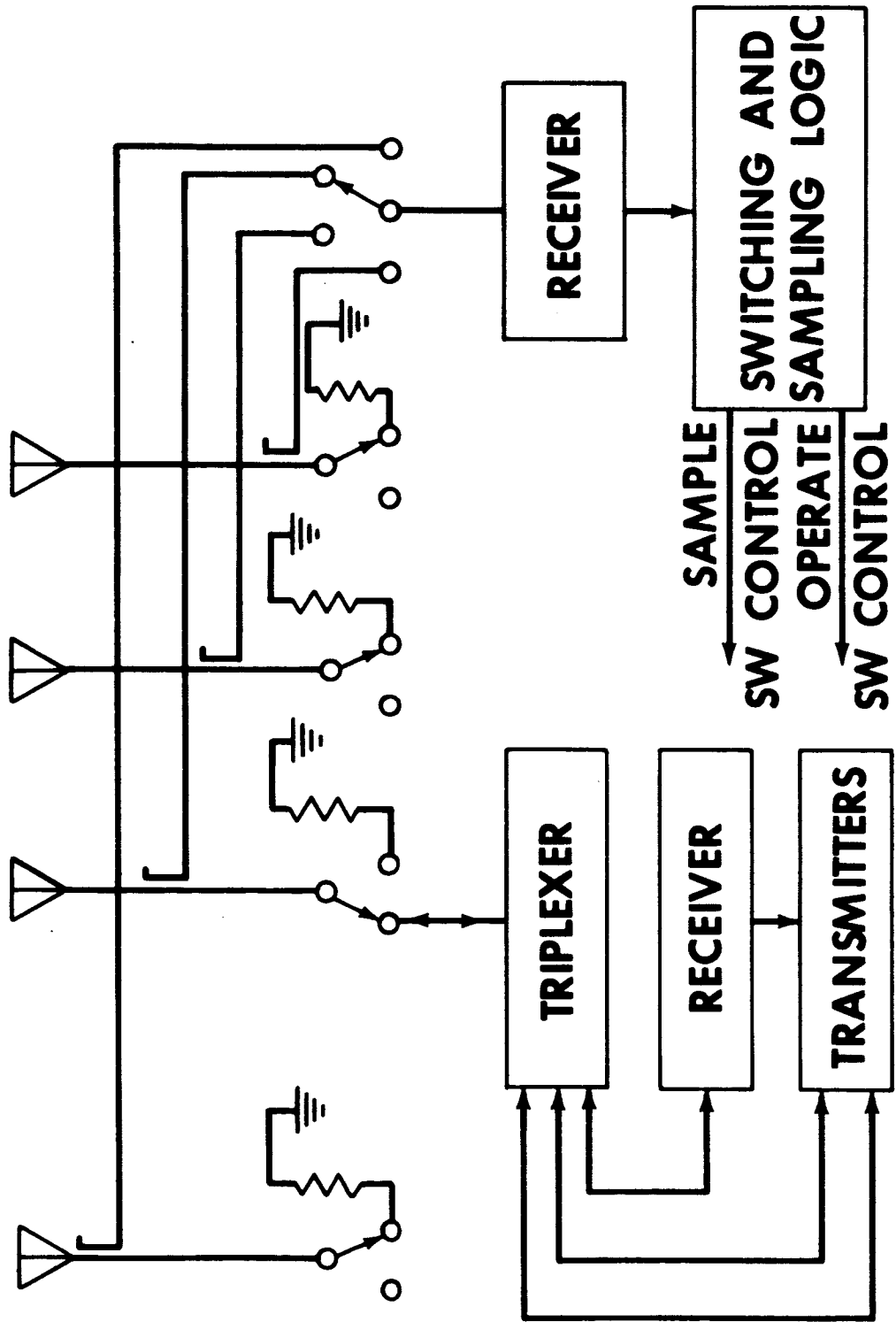
The intelligence transmission efficiency is then

$$I_2 = 100(1 - 3t_s/T_1) \text{ percent}$$

Practically speaking, in comparison to the cochannel switching system, the intelligence transmission efficiency can be taken as 100 percent, except for submarginal transmission conditions.

Part of the received signal is diverted to the sampling receiver. The transmission loss can be kept less than 1 dB. The nominal gain with respect to the cochannel system for the ground-to-air link can then be taken as -1 dB.

# SEPARATE CHANNEL SWITCHING



## COMPARISON OF POSSIBLE SHUTTLE AUTOMATIC ANTENNA SWITCHING SYSTEMS

An analytical comparison of the various candidate Shuttle antenna control systems was conducted to assess the various operational parameters of each such system. In addition, several hybrid systems were investigated to provide a better understanding of the various system tradeoffs. In general, this analysis revealed that the simple and adaptive switching techniques provide the highest percentage of coverage using the 3-dB pattern level as a basis for comparison. These particular systems also have the lowest rotational losses and the highest relative gain factors. However, the information transfer efficiency of these basic cochannel type of switching systems is quite low because of the requirement of periodic interruption of information flow to accomplish the antenna selection process. The separate channel switching system has a somewhat lower receive gain than the cochannel systems as a result of the need for part of the signal to be coupled to the second receiver. The percent coverage for this system is very high, and the rotational losses are quite small since antenna comparison may now be conducted on an almost continual basis. The most interesting parameter for the separate channel switching system is the information transfer efficiency which is essentially 100 percent regardless of the vehicle rotational rate. Unfortunately, the price that must be paid for the use of the separate channel switching system is the added weight, power, and complexity of the second receiver. The various phasing systems that were considered have in general a somewhat lower gain than the switching systems due to the fact that all of the antennas are always connected to the receiver in parallel. Also, the 3-dB coverage for these systems is somewhat lower than the switching systems. The information transfer efficiency of the phasing systems can be made very good with the proper choice of phasing angle depending on the particular application required.

# RF AUTOMATIC ANTENNA SWITCHING TECHNIQUES

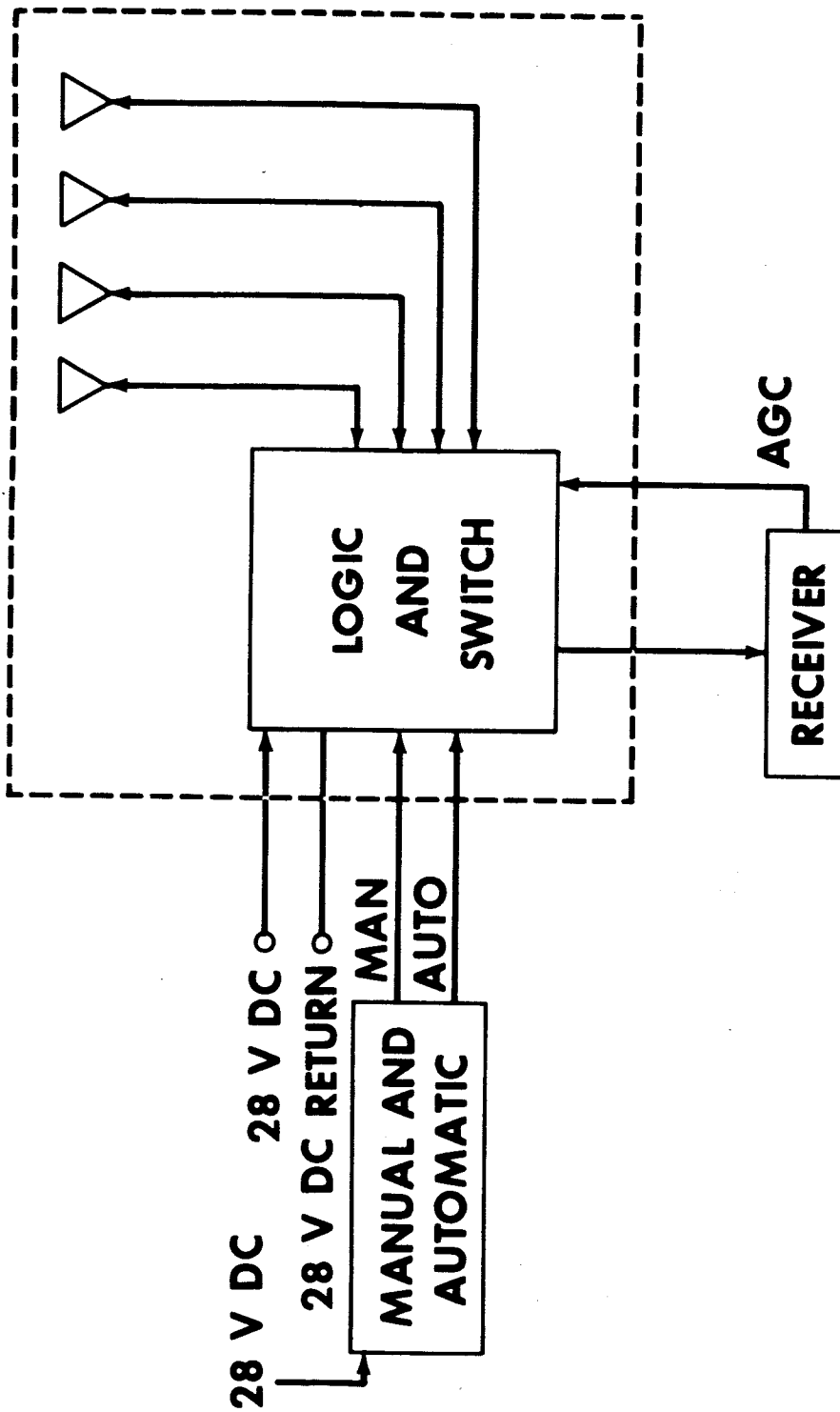
SYSTEM	THRES- HOLD	RECEIVE GAIN	TRANSMIT GAIN	COVER- AGE	TRANSMIT NULL DEPTH	ROTAT- IONAL LOSS 9 DEG/ SEC	ROTAT- IONAL LOSS 36 DEG/ SEC	MAX XMSN LOSS	INFORMATION TRANSFER EFFICIENCY												SIZE AND WEIGHT	MTBF	
									9 DEG/SEC				18 DEG/SEC				36 DEG/SEC						RELATIVE UNITS
									MARGIN		PERCENT		MARGIN		PERCENT		MARGIN		PERCENT				
									3 dB	6 dB	12 dB	PERCENT	3 dB	6 dB	12 dB	PERCENT	3 dB	6 dB	12 dB	PERCENT			RELATIVE UNITS
SIMPLE SWITCHING	NO	0	-0.7	100	-2.5	-1.5	-6.7	-9.2	95	95	95	95	0	0	0	95	1.0	1000					
SIMPLE SWITCHING	YES	0	-0.7	100	-2.5	-1.5	-6.7	-9.2	95	95	100	0	95	100	0	100	1.05	950					
ADAPTIVE SWITCHING	NO	0	-0.7	100	-2.5	-1.5	-6.7	-9.2	97	98.5	99.5	94	97	98.5	89.5	94.5	1.2	830					
ADAPTIVE SWITCHING	YES	0	-0.7	100	-2.5	-1.5	-6.7	-9.2	97	98.5	100	94	97	100	89.5	94.5	1.25	800					
SEPARATE CHANNEL SWITCHING	--	-1	-0.7	100	-2.5	-0.4	-1.7	-5.2	100	100	100	100	100	100	100	100	2.2	450					
0 DEG PHASING SIMPLE SWITCH	YES	.6	-3.4	71	-12	0	0	-12	95	95	95	95	95	95	95	95	2.05	490					
0 DEG PHASING ADAPTIVE SWITCH	YES	.6	-3.4	71	-12	0	0	-12	100	100	100	100	100	100	100	100	2.25	440					
90 DEG PHASING SIMPLE SWITCH	YES	-2.5	-3.2	78	-8.5	-0.5	-5	-13.5	95	95	95	0	95	95	0	95	2.05	490					
90 DEG SEPARATE SWITCH	--	-3.5	-3.2	78	-8.5	0	-5	-14.5	100	100	100	100	100	100	0	100	3.2	310					
90 DEG PHASING ADAPTIVE SWITCH	YES	-2.5	-3.2	78	-8.5	-0.5	-5	-13.5	95	100	100	0	95	100	0	95	2.25	440					
135 DEG PHASING SIMPLE SWITCH	YES	-7.5	-3.1	95	-7.5	-8.5	-8.5	-16	0	0	95	0	0	95	0	0	2.05	490					
135 DEG PHASING ADAPTIVE SWITCH	YES	-7.5	-3.1	95	-7.5	-8.5	-8.5	-16	0	0	100	0	0	100	0	0	2.25	440					

MSC SYSTEMS EVALUATION HARDWARE - BLOCK DIAGRAM

The automatic system presently being tested consists of a cochannel sampling system based on fixed sampling and dwell periods generated by timing circuits in the switch logic. During any one sampling period, AGC samples are stored in the logic circuits, and at the end of the sampling period, the logic switches to the antenna which provided the largest signal.

The system known as the OR logic cochannel logic commutation system (OLCLCS) performs the function of automatically selecting the antenna with the strongest signal input regardless of roll, turns, or other spacecraft maneuvers. Very basically, the OLCLCS consists of (1) a sampling circuit which samples the signal level of each antenna, (2) digital logic which performs the decision as to which one of the four antennas sampled has the strongest input signal, (3) and digital control circuitry which sets the RF switch to that antenna.

# MSC SYSTEMS EVALUATION HARDWARE - BLOCK DIAGRAM



MSC SYSTEM EVALUATION HARDWARE - SYSTEM DESCRIPTION

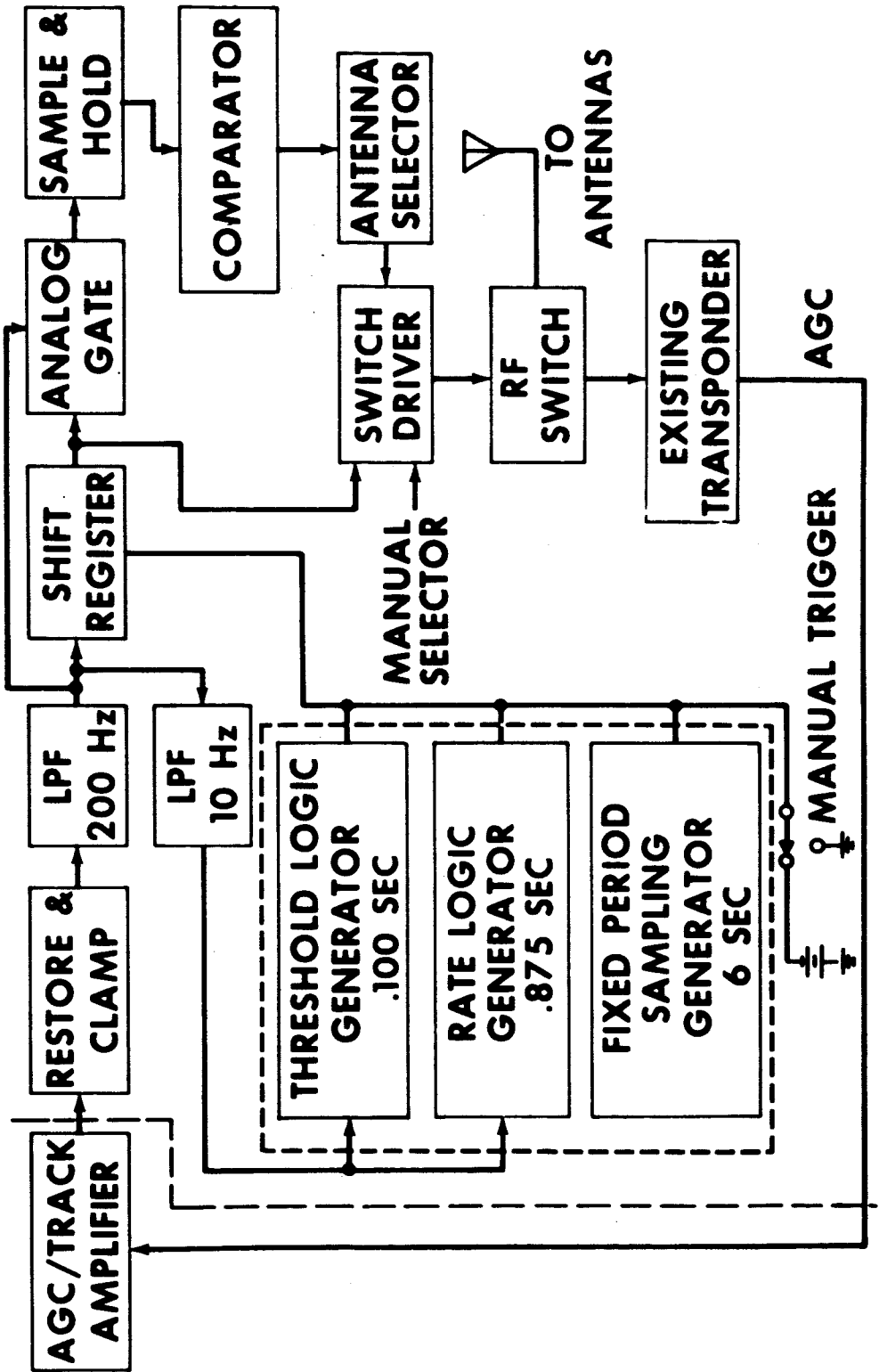
Initiation of sampling is caused by three timing circuits. The rate timing circuit is a function of the rate of decrease of the signal level on the selected antenna. A rate of voltage decrease of 0.042 volts/second will cause sampling every 0.875 seconds. This corresponds to a 6-RPM rotational rate. The level logic circuit causes sampling to occur at a maximum rate of 0.1-second intervals if the coherent amplitude detector voltage falls below a predetermined threshold. The fixed-time-interval logic causes sampling every 6 seconds.

In general, if the vehicle is not rotating, the fixed-time-interval logic causes fixed period sampling every 6 seconds. If the input signal is above the threshold setting and the vehicle is rotating at such a rate to cause a voltage decrease of 0.042 volts/second, then the rate timing circuit initiates sampling at 0.1-second intervals.

In addition, provisions are incorporated for a manual over-ride function to allow an operator to manually select the desired antenna.

# MSC SYSTEM EVALUATION HARDWARE

## SYSTEM DESCRIPTION





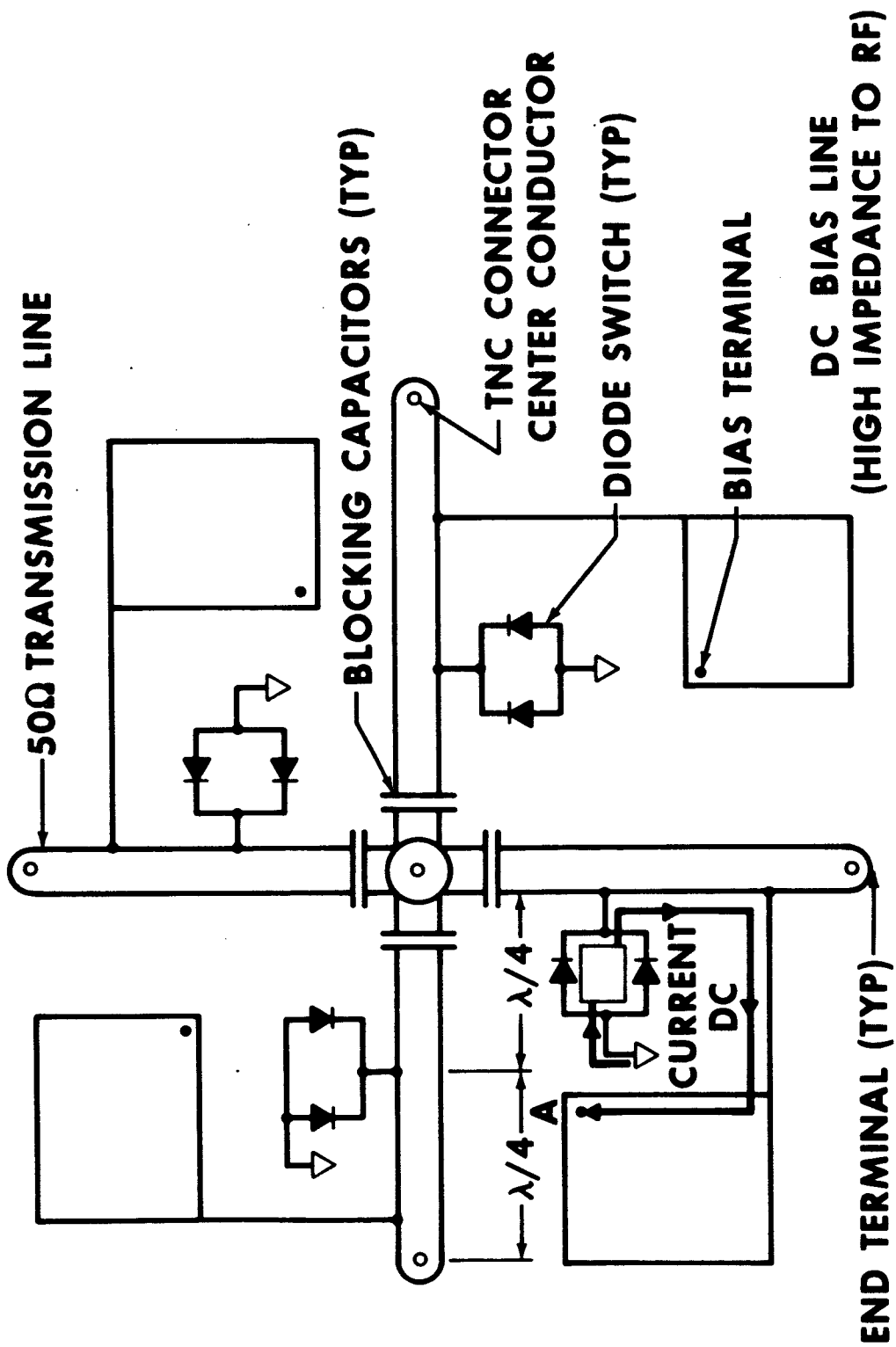
MSC SYSTEM HARDWARE - ANTENNA SWITCH

The antenna switch that is being evaluated for all Shuttle switching systems under consideration is a stripline device printed on dielectric boards and sandwiched between parallel conductive plates. It is composed of four orthogonal 50Ω transmission lines joined at a common junction. Attached to each transmission line is a switching diode, a high-RF impedance DC bias line, and an in-line blocking capacitor in front of the junction. The switching diodes are placed 90 electrical degrees from the common junction and the END terminal.

If a negative DC bias is applied at point A, DC current is from ground, through the forward biased diodes, to point A. If the diodes are of high quality and driven with sufficient current, they present a very low impedance shunt across the 50Ω line. Theoretically, if the shunt impedance of the diode can be driven to zero, an infinitely high impedance will be reflected to both the junction and the end of the line. A positive bias placed at point A causes the diode to appear as a very high impedance shunt to any incident RF energy. The blocking capacitor blocks the DC current from the RF junction.

In normal operation, three of the bias points of the switch have a negative bias, and one (the switched port) has a positive bias. Thus, on the three arms with a negative bias, a high impedance is reflected to both the END terminal and the common junction, while the positively biased port is essentially a 50Ω transmission line.

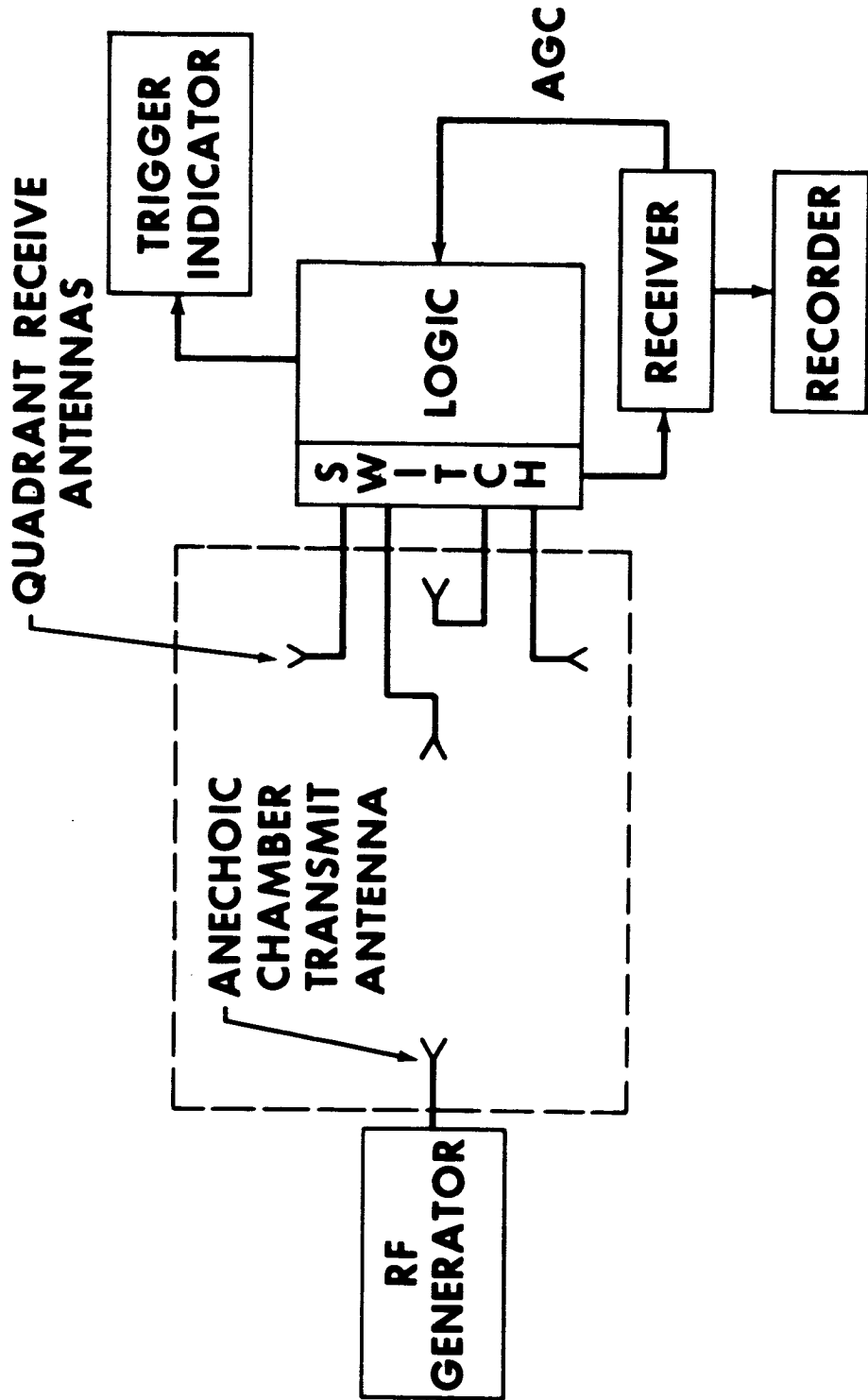
# MSC SYSTEM EVALUATION HARDWARE - ANTENNA SWITCH



MSC SYSTEMS TEST PROGRAM - BLOCK DIAGRAM

All of the system evaluation tests being conducted at MSC on possible Shuttle candidate antenna control systems are being conducted in Building 14, anechoic chamber test facility. Each of the antenna switching systems is connected to the appropriate antenna configuration mounted on a positioner in the anechoic chamber, and complete radiation distribution plots of the composite antenna patterns are recorded for each test condition. The transmitter source antenna is located at such a position in the chamber that far field requirements are met for each test configuration. During the initial test phase of this evaluation, all the test configurations are at full scale, with the Shuttle antennas mounted on a wooden platform with only the essential parts of the Shuttle structure mocked up. Later tests will be conducted at 1/10 scale on a completely structured Shuttle orbiter mockup.

# MSC SYSTEM TEST PROGRAM BLOCK DIAGRAM



MSC SYSTEM TEST PROGRAM - TEST DATA

The MSC System Test Program is primarily devoted to accomplishing those data recording tasks that will identify the candidate systems of Shuttle antenna control systems that warrant further development. With this purpose in mind, all of the systems tests have been specifically tailored to Shuttle applications.

To date, a considerable amount of data has been recorded on the cochannel switching system, with somewhat more limited data on the other candidate systems. The reason for this situation is that a cochannel switching system had been already developed under a previous development contract. This system was easily modified to fit Shuttle requirements and was a logical choice for the initial testing. Work is presently underway in the development of test units of the other candidate systems, and similar testing will subsequently be accomplished.

Data tasks that are presently being planned include the testing of scale models of the cochannel, separate channel, and phase quadrature control systems on a 1/10 scale model of the Shuttle orbiter. Also, the operation of the solid state switch design at all the frequencies and power levels of interest will be investigated. Lastly, the candidate systems will be investigated to determine the effects of each candidate system on the operation of the communications system as a whole.

## **MSC SYSTEM TEST PROGRAM**

- **DATA TASKS ACCOMPLISHED TO DATE**
  - **PATTERN DATA FOR COCHANNEL SYSTEM AT S-BAND**
  - **EVALUATION OF SAMPLING RATE REQUIREMENTS IN COCHANNEL SYSTEM**
  - **EVALUATION OF SOLID STATE SWITCH OPERATION AT S-BAND**
  - **EVALUATION OF RATE EFFECTS ON COCHANNEL SYSTEM OPERATION**
  - **EVALUATION OF MULTIPLEXER DESIGN FOR PHASE QUADRATURE SYSTEM**
  - **PATTERN DATA FOR PHASE QUADRATURE SYSTEM AT S-BAND**

## **MSC SYSTEM TEST PROGRAM (CONT)**

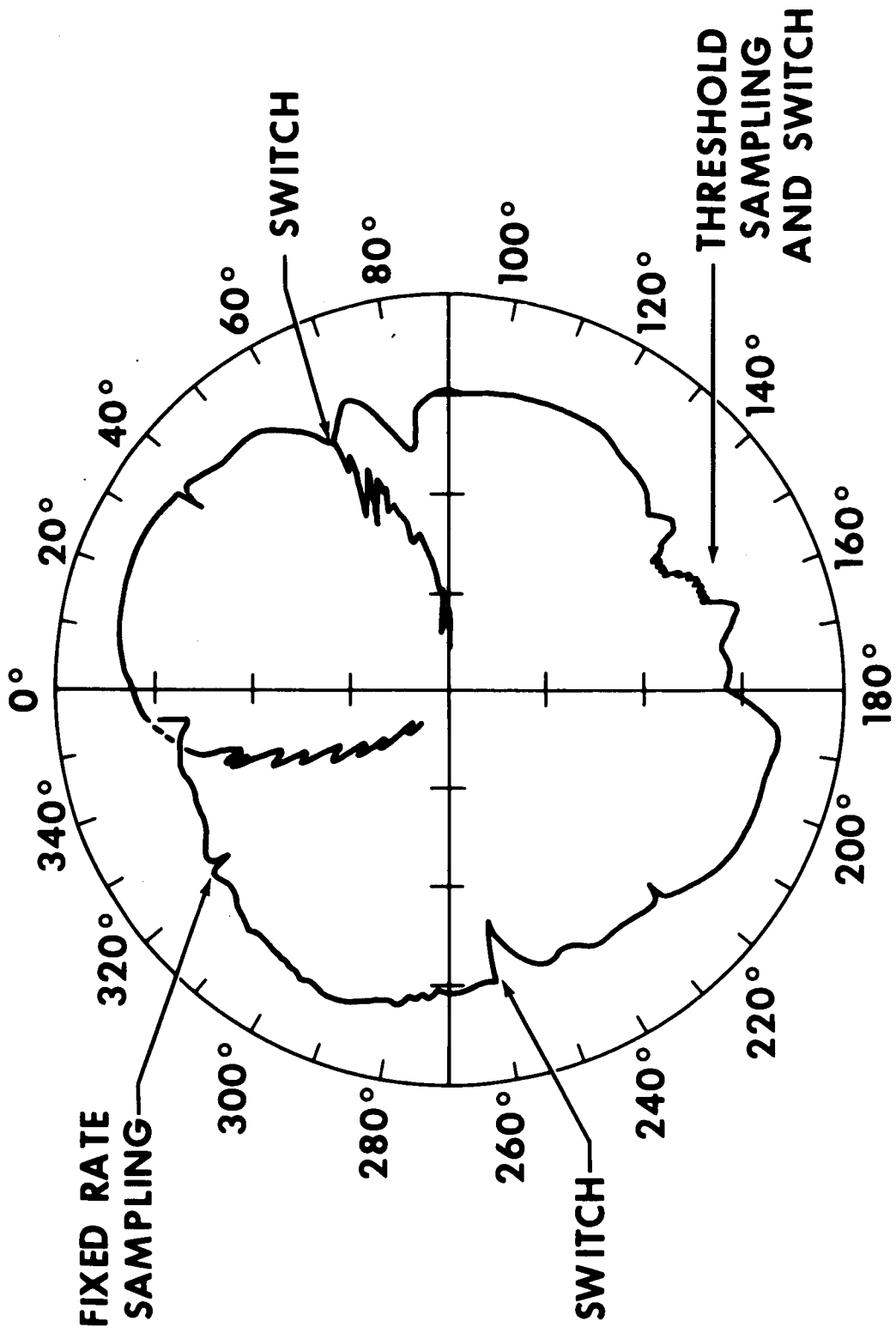
- **TEST RESULTS SUMMARY**
  - **COCHANNEL SYSTEM PROVIDES ADEQUATE PATTERN COVERAGE BUT RESULTS IN A REDUCED COMMUNICATIONS TRANSFER EFFICIENCY COMPARED TO THE SEPARATE CHANNEL SYSTEM**
  - **SAMPLING RATES IN COCHANNEL SYSTEM MAY BE GREATLY REDUCED AND STILL SATISFY SHUTTLE PATTERN REQUIREMENTS**
  - **SOLID STATE SWITCH DESIGN APPEARS FEASIBLE FOR SHUTTLE APPLICATIONS**
  - **PHASE SHIFTER CHARACTERISTICS MUST BE FURTHER EVALUATED FOR THE BASIC PHASING SYSTEMS**

## **MSC SYSTEM TEST PROGRAM (CONCL)**

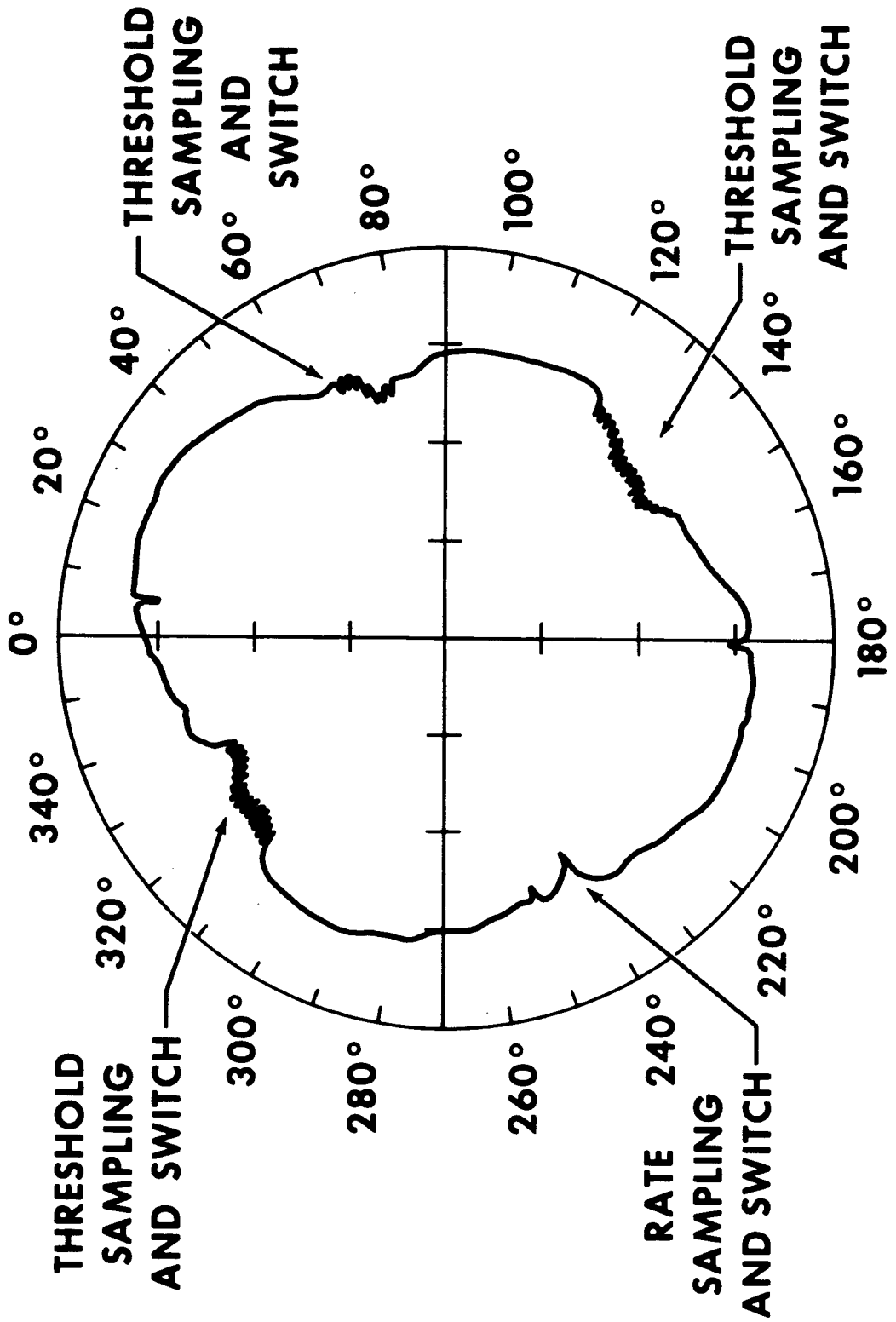
- **PLANNED TASKS**
  - **PATTERN DATA FOR COCHANNEL, SEPARATE CHANNEL, AND PHASE QUADRATURE SYSTEM AT 1/10 SCALE S-BAND ON SHUTTLE MOCKUP**
  - **EVALUATION OF THE EFFECTS OF THE ANTENNA SYSTEM ON THE COMMUNICATIONS SYSTEM AS A WHOLE**
  - **EVALUATION OF THE SOLID STATE SWITCH OPERATION AT HIGH POWER LEVELS AND AT LOWER FREQUENCIES**
  - **COMPLETE EVALUATION OF FACTORS SUCH AS WEIGHT, VOLUME, POWER CONSUMPTION, COMPLEXITY, MANUFACTURABILITY**



# MSC SYSTEM TEST PROGRAM - TEST DATA



# MSC SYSTEM TEST PROGRAM - TEST DATA



### CONCLUSIONS

The work that has been conducted to date indicates that the Shuttle requirements dictate some type of antenna control system to relieve the crew operational requirements. The preliminary analysis and testing indicate that several different control systems meet the basic Shuttle requirements. The desirability of one system over another will depend on the results of detailed testing of the complete Shuttle antenna system. Detailed testing of the Shuttle antenna system will be conducted on breadboard hardware as this hardware becomes available.

## SPACECRAFT INTEGRATED PARAMETRIC

### AMPLIFIER DEVELOPMENT

P. H. Dalle Mura

NASA-Goddard Space Flight Center  
Greenbelt, Maryland

#### SUMMARY

An integrated, all-solid-state paramp for utilization aboard the Space Shuttle has been developed through the initial prototype phase. The paramp is tunable over the entire 3.7 GHz to 4.2 GHz commercial satellite communications band, has an instantaneous bandwidth of 100 MHz minimum when tuned over the band, a gain of 17 dB, and a noise figure ranging from 104°K at the low end to 150°K at the high end of the band. The paramp utilizes a combination of microstrip, coax, and waveguide circuitry in an extremely compact and lightweight package. The paramp weighs seven ounces and has a volume of less than six cubic inches. It is completely operational when supplied with seven volts d.c. at 0.6 ampere. A comparison of the development of this second generation unit with a first generation S-Band paramp is presented. Measured test results of the two units are analyzed to show how deficiencies in the first generation paramp were eliminated in the second development. A prototype K<sub>u</sub>-Band Spacecraft Paramp being developed for the TDRS Program is described.

# SPACECRAFT INTEGRATED PARAMETRIC

## AMPLIFIER DEVELOPMENT

### INTRODUCTION

At the Space Shuttle Technology Symposium in 1970, the development of a completely integrated, all-solid-state S-Band prototype paramp was reported.<sup>1</sup> That effort was the successful first step in establishing the feasibility of compact, lightweight, low noise paramps for utilization in spacecraft applications. Microminiature and hybrid integrated circuit techniques were employed, in conjunction with the technology of recently perfected solid state microwave power sources to produce an advanced paramp design. This design removed the obstacles previously preventing the development of a paramp having the potential suitability for use in an orbiting spacecraft.

The experience acquired during this first generation development has led to the successful completion of a second generation integrated C-Band paramp<sup>2</sup> for use in the Space Shuttle communications receiver. This latest prototype unit embodies improved packaging and performance characteristics which are a direct outgrowth of techniques developed during the first generation program. Areas which improved measurably are microstrip circulator design, solid state Gunn oscillator design, varactor mounting and broadband resonating, and integrated packaging design. These improvements have produced a paramp with improvements in noise figure, tunability, stability, and packaging.

A second phase of the current program is now under way. During this phase, the prototype paramp will undergo extensive re-design and testing with the purpose of producing a completely space-qualified paramp which is suitable for use aboard the Space Shuttle vehicle.

Also, a companion program to develop a prototype spacecraft paramp operating at K<sub>u</sub>-Band is in progress. Some preliminary test results obtained thus far will be presented later in this paper.

### REFERENCES:

1. NASA Technical Memorandum, NASA TMX-52876, Volume VI, Integrated Electronics, pp. 289.
2. This work was performed under Contract NAS5-21527 by Airborne Instruments Laboratory, Melville, Long Island, New York.

## DESCRIPTION

### S-Band Paramp

A brief review of the first generation S-Band integrated paramp will be presented in order to demonstrate how the second generation C-Band paramp resulted in greatly improved performance.

Originally, it was intended that the entire paramp be formed in microstrip circuitry in order to minimize the weight and volume characteristics. This approach was abandoned when it became evident that a stable, low noise pump oscillator could not be achieved using low-Q microstrip resonators. In addition, surface wave interaction between the pump and the varactor circuitry was found to be intolerable. Accordingly, it was decided upon an optimum compromise of waveguide for the pump components and microstrip for the circulator and varactor circuitry. Figure 1 is a photograph of the S-Band paramp showing the circulator-varactor portion in microstrip and the solid state pump source in  $K_u$ -Band waveguide. The microstrip utilizes thin film deposited copper conductors on a twenty-three mil thick glazed alumina substrate. All critical electrical connection points such as the circulator-paramp junction and the OSM coax-to-microstrip junctions are reinforced by small sections of gold ribbon parallel-gap-welded across the junction.

The circulator is a three port design consisting of a one inch diameter ferrite disc cemented into a one inch diameter hole in the alumina substrate with the "Wye" junction and matching transformers deposited on top of the ferrite-alumina combination. A one and one-quarter inch diameter permanent magnet having a field strength of 400 Gauss is cemented to the ground plane side of the circulator "Wye" junction.

A Sylvania Type 5147E varactor is employed in a single-ended circuit. Figure 2 depicts the method of shunt mounting the varactor through the microstrip substrate and shows how contacting to the varactor is effected by means of low temperature indium solder and a welded gold ribbon. Both the signal and idler circuits are composed of distributed element resonators in microstrip circuitry. A novel parallel-pair open-stub configuration is employed to achieve signal circuit broadbanding.

The pump source consists of a commercially available, gallium arsenide Gunn Effect Device mounted in a high-Q,  $K_u$ -Band waveguide cavity. The Gunn Oscillator has an RF power output capability of 100 milliwatts at 14 GHz. The d.c. power requirement is 7.7 volts at 0.5 ampere. The Gunn oscillator consists of a Varian VSU-9202D Gunn-Effect device post-mounted in a three-quarter wavelength resonant cavity. The output is coupled through a circular waveguide

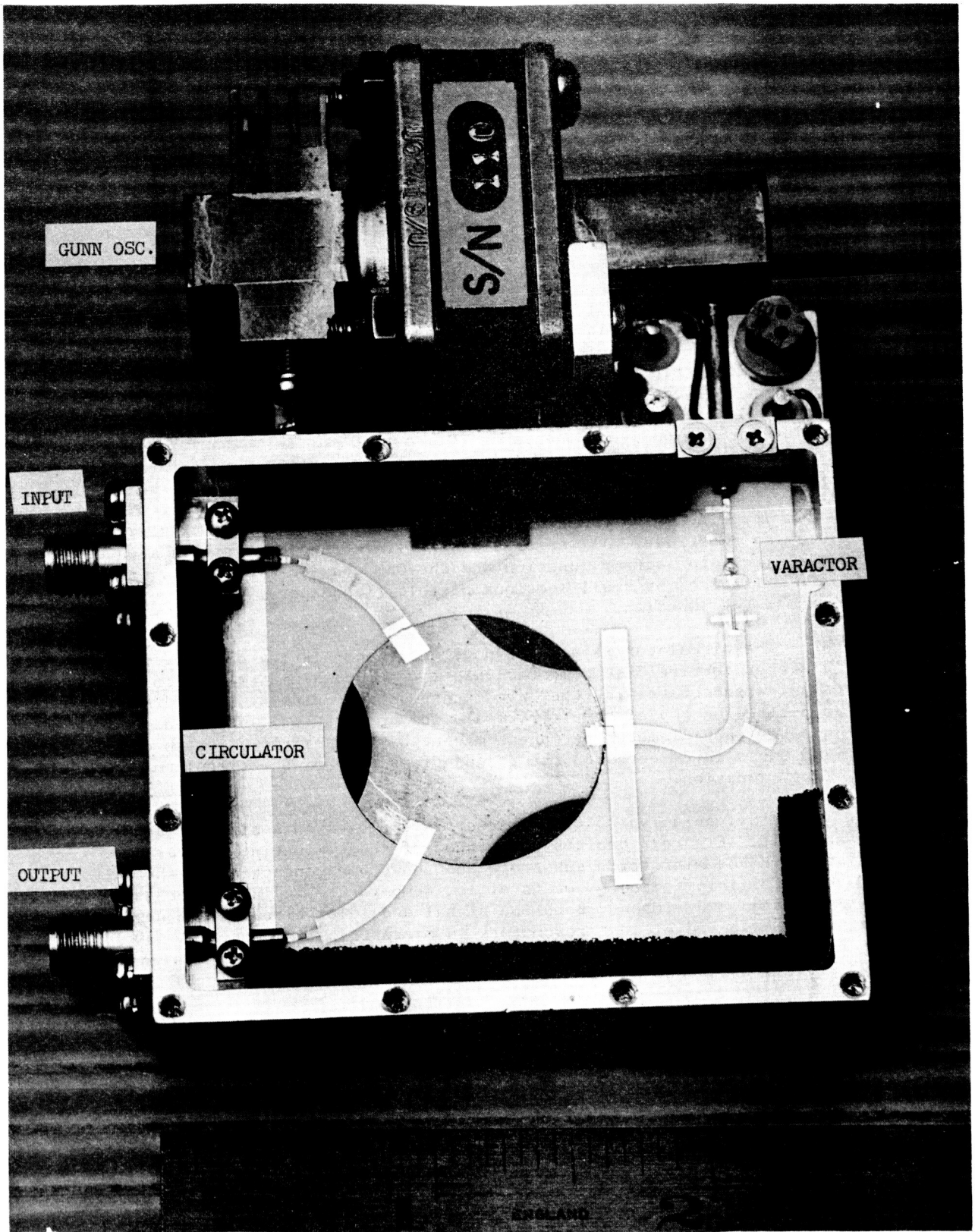
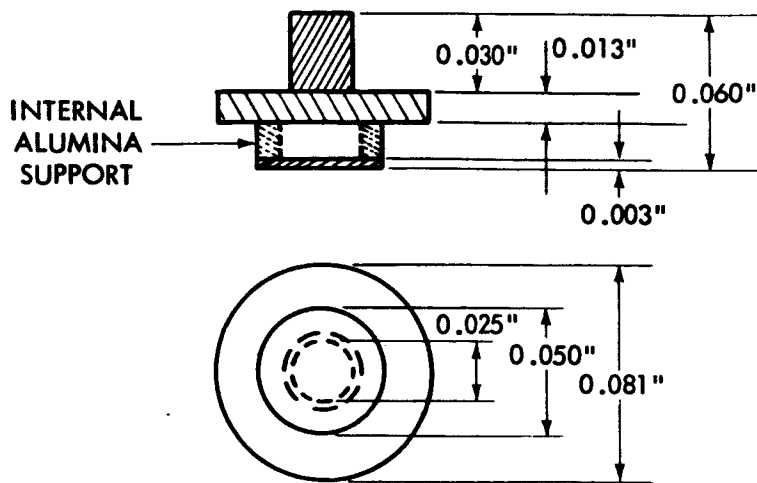
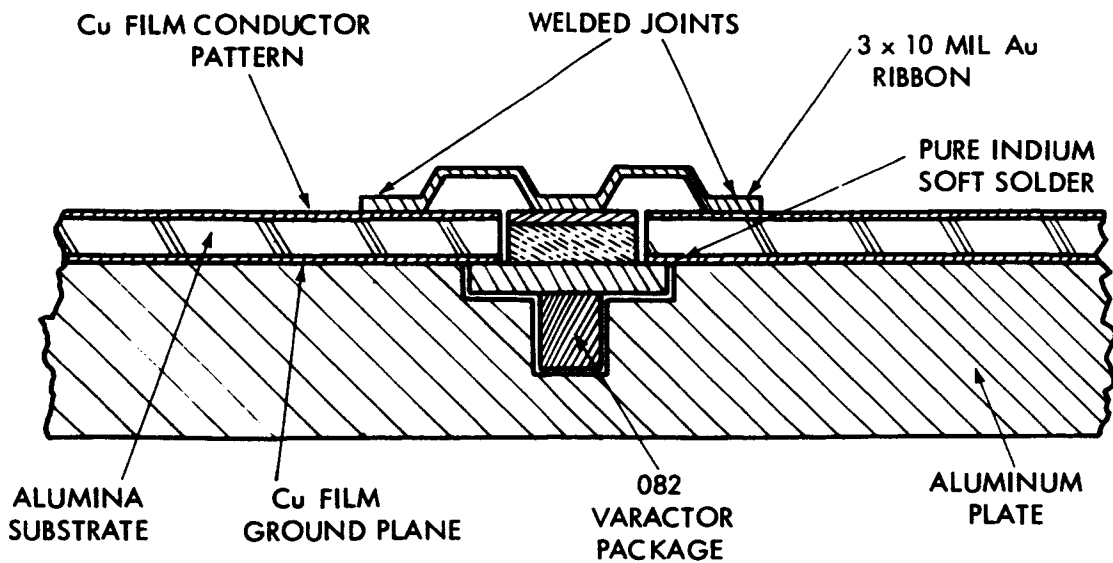


FIGURE 1



A - MICRO PILL (082) VARACTOR PACKAGE OUTLINE



B - SHUNT MOUNTING CONFIGURATION IN MICROSTRIP

FIGURE 2



iris, then through a commercial miniature waveguide ferrite isolator, and finally to the microstrip mounted varactor by means of a waveguide-to-coax probe adapter.

The mechanical package consists of a 2.5 inch by 2.25 inch aluminum frame which supports the microstrip board and the standard  $K_u$ -Band waveguide pump oscillator components which are attached to the aluminum frame along one of its edges. The package occupies a volume of approximately 6 cubic inches and weighs a little more than 9 ounces.

### C-Band Paramp

The C-Band prototype paramp represents a true second generation development, inasmuch as the only major design changes from the S-Band unit were those which either corrected earlier deficiencies or improved the performance of the C-Band paramp or both. The areas in which these design changes were effected are; (1) the input-output circulator, (2) the varactor circuit configuration, (3) the varactor mechanical configuration, (4) the pump circuitry; and (5) the overall integrated packaging design.

To avoid the input VSWR problem encountered on the S-Band paramp and to improve the overall gain stability, a decision was made early in the design to employ a 5-port ferrite circulator composed of three 3-port units in cascade. Figure 3 is a photograph of the C-Band prototype paramp with its top cover removed. Clearly visible are the three "Wye" junction ferrite discs with interconnecting matching transformers. The metal dividers separating the three junctions serve both to prevent electrical interaction and to provide more rigid mechanical support for the microstrip boards. The basic circulator design is similar to the S-Band unit with improvements in insertion loss and isolation resulting from the use of unglazed alumina substrate and more homogeneous magnetic fields. The first and third junctions serve as input and output isolators, respectively, by having their third ports terminated by means of 50 ohm beam lead resistances.

The varactor circuit configuration is a combination of microstrip, coax, and waveguide circuitry. A balanced pair of Sylvania 5147E varactors is employed in order to achieve wide tuning and instantaneous bandwidth and to insure a rugged and stable mounting structure. A two-stage signal circuit transformer and a pair of parallel broadbanding resonators are formed in microstrip and connect the second stage circulator to the varactor waveguide mount. Figure 4 shows a cross section of the mounting of the balanced varactor pair in the waveguide mount. The center point of the varactor pair is coupled to the microstrip by a short length of high impedance coax transmission line that conveniently serves as the signal tuning inductance.

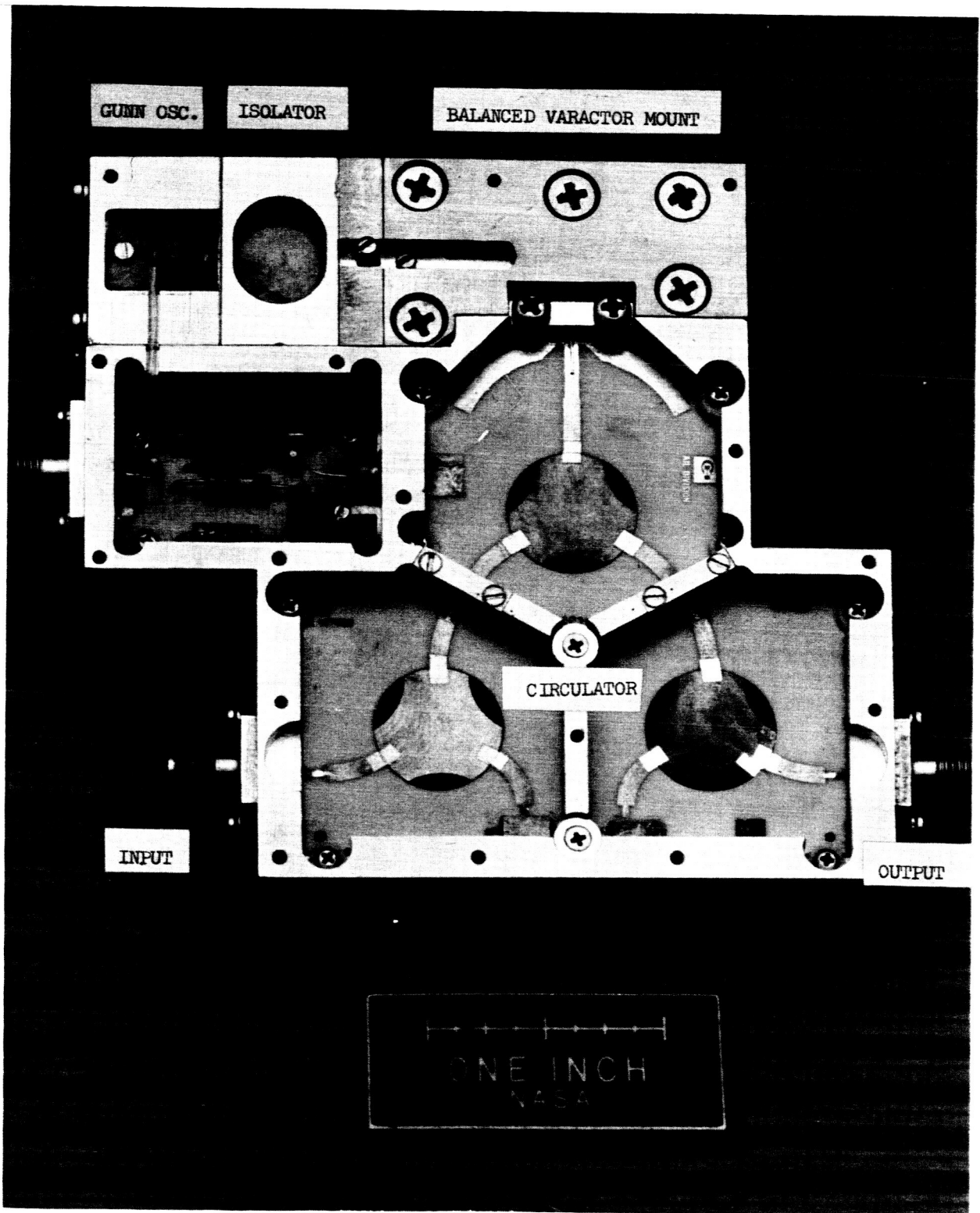


FIGURE 3

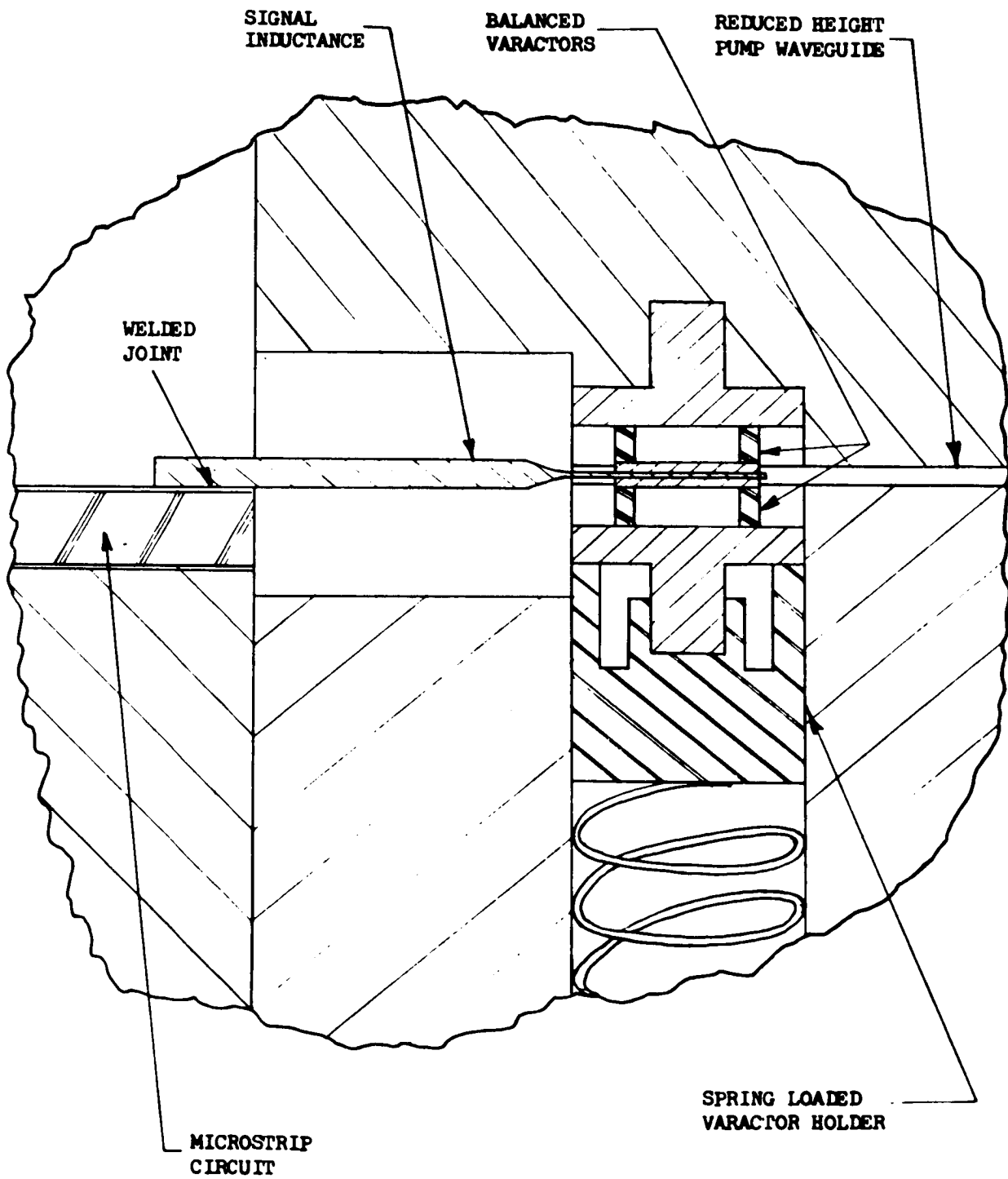


FIGURE 4 BALANCED VARACTOR MOUNTING CONFIGURATION

The back-to-back mounted varactors are operated so that their series self resonance form the idler circuit resonator required for parametric amplification. The pump waveguide is selected so that the idler frequency is below the cutoff of the guide, thereby confining the idler currents to the vicinity of the varactors. This enhances the bandwidth and eliminates the requirement of a lossy filter in the input line as is the case in a single ended configuration.

The pump section is composed of a cavity-mounted Gunn Effect oscillator, a coupling iris, a ferrite isolator, and a waveguide matching section. The Gunn oscillator is similar to the S-Band paramp oscillator except that the circuit is more simply tuned and consequently better behaved during initial turn-on. The commercially available Gallium Arsenide Gunn device used is supplied by Nippon Electric Company. The oscillator operates at 23.8 GHz which puts the idler frequency in the 20 GHz region. The selection of a higher pump frequency improves both the theoretical noise figure and bandwidth of the C-Band paramp as will become evident later.

The overall mechanical and electrical packaging represents a truly integrated design. Each component was designed to meet the required electrical performance while embodying a high degree of miniaturization and mechanical compatibility with the interrelated components. The basic unit is a milled-out aluminum frame with the varactor mount and pump components (also aluminum) attached along one edge of the frame. One-thirty-second inch thick aluminum plates cover both top and bottom to make a completely enclosed unit.

#### TEST RESULTS

The test results for the most important characteristics of the C-Band paramp are presented in Table 1. For the purpose of comparison, the S-Band paramp test results are also listed. The noise temperature measurement for both paramps was obtained by means of a very accurately calibrated hot and cold input termination setup. As can be seen from the table, the C-Band paramp meets or exceeds every major specification. Especially interesting is the 104°K noise temperature measured at 3.7 GHz. The theoretically minimum noise temperature contribution from a lossless varactor operating at a signal frequency of 3.7 GHz and an idler frequency of 20.1 GHz is

$$T = T_D \frac{F_S}{F_I}$$

where

$T_D$  = varactor physical temperature

$F_S$  = signal frequency

$F_I$  = idler frequency

	<u>C-BAND</u>		<u>S-BAND</u>
	SPECIFICATION	MEASURED	
GAIN	17 DB	17 DB	15 DB
3 DB BANDPASS	75 MHZ	100 MHZ	120 MHZ
TUNING RANGE	3.7 GHZ - 4.2 GHZ	3.7 GHZ - 4.2 GHZ	2.25 GHZ FIXED
NOISE TEMP.	170 °K	104 °K at 3.7 GHZ 150 °K at 4.2 GHZ	139 °K
INPUT VSWR	1.5 to 1	1.3 to 1	4 to 1
1 DB COMPRESSION	-50 DBM	-35 DBM	- 38 DBM
GAIN STABILITY	+ 1.0 DB/ 8 HRS.	+ 0.1 DB/ 8 HRS.	+ 0.2 DB/ 8 HRS.
WEIGHT	12 OUNCES	7 OUNCES	9 OUNCES
VOLUME	6 CUBIC INCHES	6 CUBIC INCHES	6 CUBIC INCHES
POWER CONSUMPTION	-----	4 WATTS	4 WATTS

TABLE 1  
TEST RESULTS FOR C-BAND AND S-BAND SPACECRAFT PARAMS

Inserting  $T_D = 293^{\circ}\text{K}$ ,  $F_S = 3.7 \text{ GHz}$ , and  $F_I = 20.1 \text{ GHz}$ ,

$$T = 54^{\circ}\text{K}$$

Using a circulator loss of 0.2 dB per pass or 0.4 dB total loss through 2 passes, the theoretically minimum paramp noise temperature calculates out to be  $88.8^{\circ}\text{K}$ . The measured value of  $104^{\circ}\text{K}$  compares quite favorably with the theoretical value with the difference due to finite losses in the varactor and some heating of the varactor by pump power.

The areas of major improvement of the C-Band paramp over the S-Band paramp are lower noise temperature, greatly improved input VSWR, improved stability, and lower volume and weight. The improved mechanical packaging is depicted in Figure 5 which is a photograph of the C-Band paramp and the S-Band paramp side-by-side.

#### CONCLUSION

The C-Band Spacecraft prototype paramp represents a significant improvement over the first generation S-Band paramp. The performance deficiencies of the latter have been entirely eliminated in the former by both electrical and mechanical redesign of several critical areas. The C-Band paramp program has now entered its second phase. This phase will extend the prototype design to the development and testing of a space qualified unit.

A program under TDRS funding for the development of a  $K_u$ -Band prototype spacecraft paramp is now nearing completion. Preliminary test results thus far indicate the following performance can be expected:

Gain	- 17 dB
3 dB BW	- 500 MHz
Bandpass	- 14.7 GHz to 15.2 GHz
Noise Figure	- 4 dB
Volume	- 6 cubic inches
Weight	- 12 ounces
Power	- 5 watts

This unit will be extended to a completely space qualified unit under Space Shuttle programming.

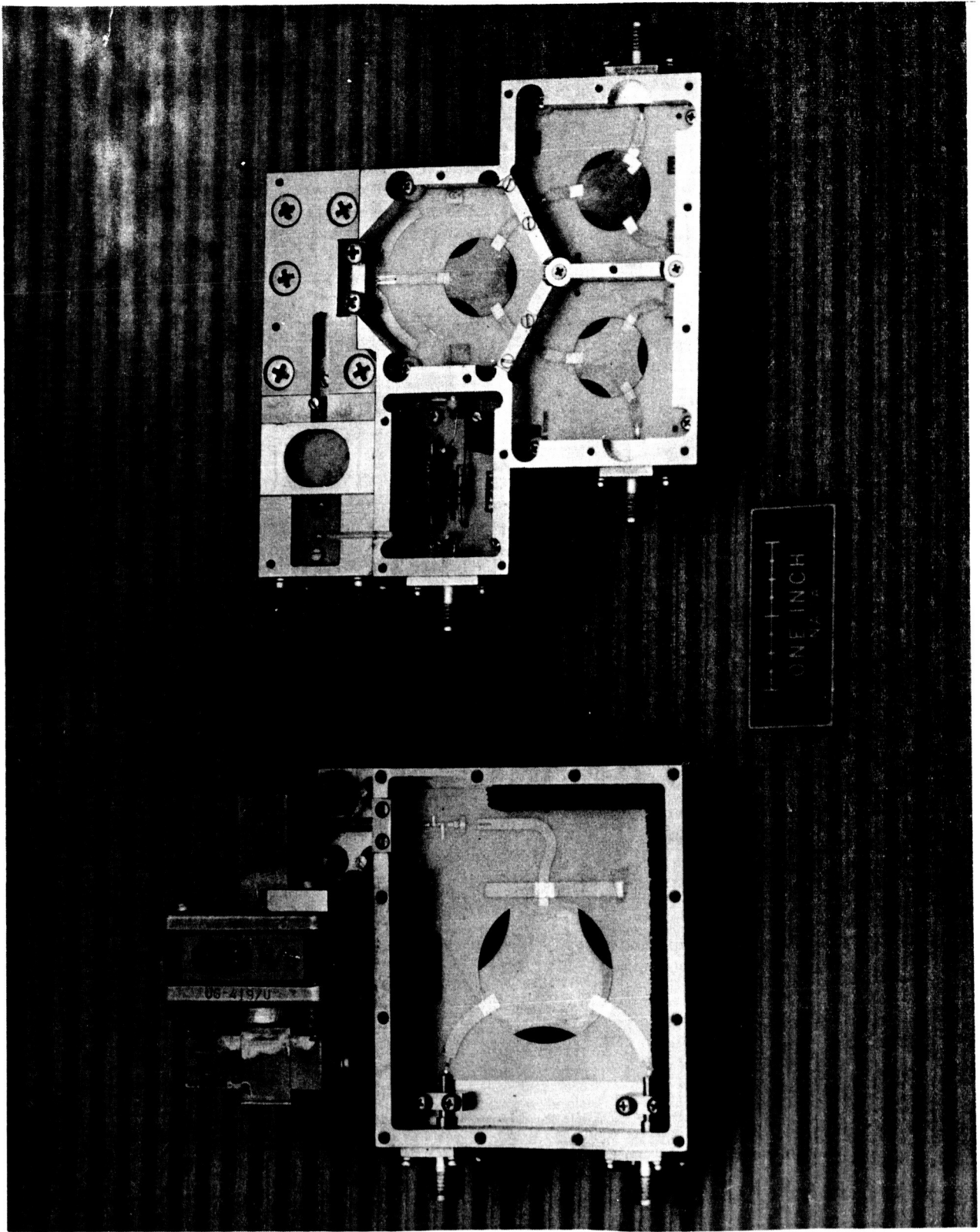


FIGURE 5

**LOW - RATE COMMUNICATIONS  
UTILIZING DIGITAL CODING  
AND  
MODULATION**

**B. H. BATSON, C. K. LAND, AND R. W. MOOREHEAD**

**MANNED SPACECRAFT CENTER  
HOUSTON, TEXAS**



## SUMMARY

A highly efficient all-digital communications signal design employing convolutional coding and optimum (PSK) modulation is described for two-way transmission of voice and low-rate (several kbps) data between the space shuttle and ground. Variable-slope delta modulation is selected for analog/digital conversion of the voice signal. A convolutional decoder based on the Viterbi decoding algorithm is selected for use at the receiving terminal. Performance predictions (both theoretical and experimental) are presented for transmission via the Intelsat IV relay satellite system, with application of state-of-the-art technology to the space shuttle RF system. Hardware estimates are provided for an actual flight-qualified communications system employing the coded digital signal design.

## INTRODUCTION

It will be possible to maintain almost continuous communications between the space shuttle and ground by utilizing a system of two or more relay satellites and perhaps no more than a single ground station. However, launch vehicle constraints will limit the allowable relay satellite size and weight and, therefore, its antenna sizes and transmitter powers. The capabilities of existing (and currently conceived) relay satellites are such that the links between the space shuttle and satellite will be extremely power-limited. Consequently, it will be important to utilize highly efficient communications signal designs which minimize the required shuttle transmitter power and transmit/receive antenna gains, and which minimize the requirement for very low noise receivers on the shuttle.

All-digital communications signal designs have appeared increasingly attractive in recent years for applications in which maximum link efficiency is an important design goal. One favorable characteristic of all-digital designs is that error control encoding/decoding can be applied to achieve significant improvements in overall link performance. The introduction of coding into a digital link allows, for a fixed transmitted (or received) power level and for an allowable bit error probability, transfer of more information per unit time. Alternately, for a fixed information rate, the introduction of coding can provide a reduction in the transmitted (or received) power level required to maintain a specified error probability. The exact increase in information rate which can be achieved, or the amount of coding gain (allowable reduction in power level) which is realizable depends on the particular class of encoding/decoding technique employed and on various encoder and decoder parameters which must be selected by the communications system design engineer.

## **INTRODUCTION**

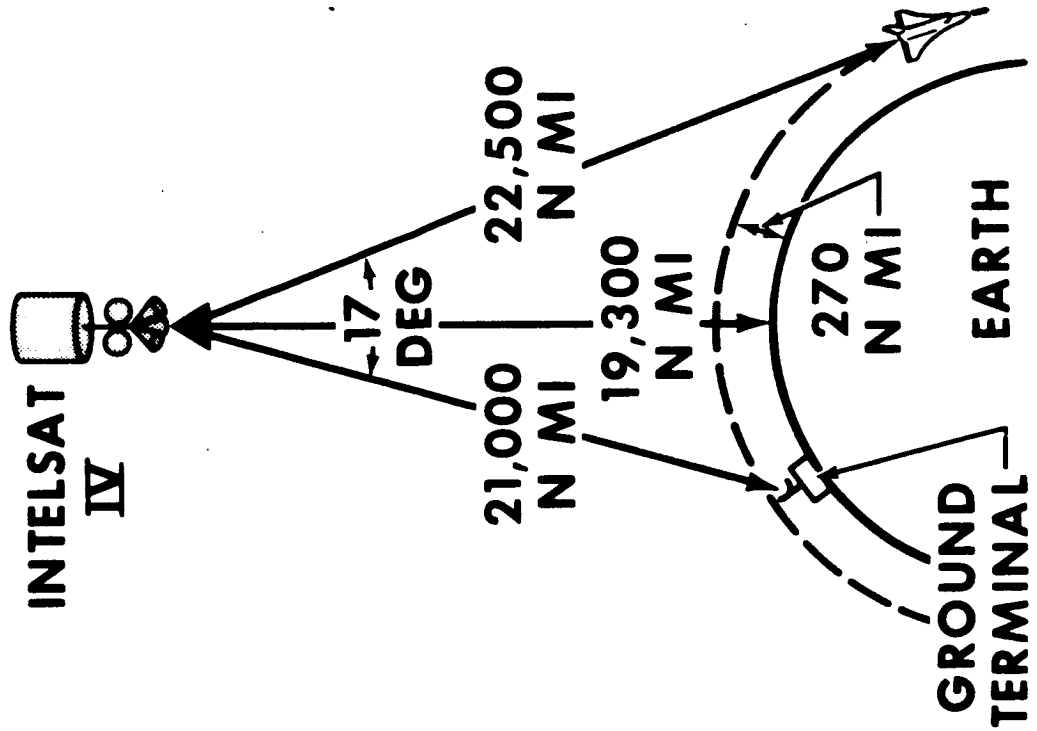
- **INCREASED COMMUNICATIONS COVERAGE POSSIBLE  
USING SYSTEM OF RELAY SATELLITES**
- **LIMITED CAPABILITIES OF RELAY SATELLITES RESULT  
IN POWER-LIMITED LINKS**
- **CURRENT TECHNOLOGY IN SIGNAL PROCESSING  
TECHNIQUES CAN BE APPLIED TO IMPROVE  
LINK EFFICIENCIES**
- **EXAMPLE: TWO-WAY TRANSMISSION OF VOICE  
AND DATA BETWEEN SHUTTLE AND GROUND  
VIA INTELSAT IV**
  - **ANALOG (DUAL-SUBCARRIER) SYSTEM**
  - **ALL-DIGITAL SYSTEM**

#### SHUTTLE COMMUNICATIONS VIA INTELSAT IV

Consideration will be given to two-way transmission of a single voice channel and a low-rate data channel between the space shuttle and an earth-based terminal, with relay through the Intelsat IV series of communications relay satellites. Intelsat IV is assumed as an example because it is already in existence and thus potentially represents a minimum-cost relay satellite system for manned space flight use. Also, because Intelsat IV is a very low-capability relay device for such applications, the resulting constraints on the shuttle communications system are more severe and point out more emphatically the need for application of the latest technological advances in RF equipment and in signal processing techniques.

The Intelsat IV transmit and receive antenna gains (16.5 dB and 16.7 dB, respectively) are relatively low at the C-band operating frequencies (4 GHz and 6 GHz). It is primarily because of these relatively low antenna gains that Intelsat IV is a low-capability relay device for applications typical of manned space flight.

# SHUTTLE COMMUNICATIONS VIA INTELSAT IV



## INTELSAT IV PARAMETERS

TRANSMIT POWER	6.3 WATTS
TRANSMIT ANTENNA GAIN	16.5 dB
RECEIVE ANTENNA GAIN	16.7 dB
SYSTEM NOISE TEMPERATURE	1160° K
TRANSMIT/RECEIVE LOSSES	2 dB
TRANSMIT FREQUENCY	4 GHZ
RECEIVE FREQUENCY	6 GHZ

SPACE SHUTTLE

GROUND TERMINAL  
EARTH

#### PROJECT SHUTTLE RF CAPABILITIES

Should it be necessary to communicate between the space shuttle and ground via the Intelsat IV series of relay satellites, a directional antenna will be required on the shuttle. Minimization of the physical dimensions of such an antenna becomes a problem of major importance. It is, therefore, desirable to incorporate a high-power transmitter and a low-noise receiver at the shuttle terminal. Fortunately, technological advances are presently being made by NASA in both of these areas.

A high-efficiency C-band power amplifier now under development by the Langley Research Center will provide a 100-watt transmitter capability for the space shuttle. This power amplifier will provide a gain of more than 33 dB and will have an efficiency of nearly 50%. Development of this device is scheduled for completion by the fall of 1971, and the production of a flight-qualified version could be completed in 1972.

A wideband (100 MHz) low-noise (1.5-dB noise figure) C-band parametric amplifier now under development by the Goddard Space Flight Center is also expected to be available for the space shuttle program. Development of this device is scheduled to be completed by early 1972, and it is anticipated that flight-qualified hardware could be available later in 1972.

# PROJECTED SHUTTLE RF CAPABILITIES

## C-BAND POWER AMPLIFIER DEVELOPMENT - LANGLEY RESEARCH CENTER

POWER OUTPUT \_\_\_\_\_ **100 WATTS**  
EFFICIENCY \_\_\_\_\_ 45 PERCENT - 50 PERCENT  
GAIN \_\_\_\_\_ >33 dB  
WEIGHT \_\_\_\_\_ <20 POUNDS  
SIZE \_\_\_\_\_ 4 IN. x 7 IN. x 12 IN.  
AVAILABILITY \_\_\_\_\_ **1972**

## C-BAND PARAMETRIC AMPLIFIER DEVELOPMENT - GODDARD SPACE FLIGHT CENTER

NOISE FIGURE \_\_\_\_\_ **1.5 dB**  
GAIN \_\_\_\_\_ 17 dB  
BANDWIDTH \_\_\_\_\_ 100 MHZ  
WEIGHT \_\_\_\_\_ 7 OUNCES  
SIZE \_\_\_\_\_ 3.5 IN. x 3.5 IN. x 0.5 IN.  
AVAILABILITY \_\_\_\_\_ **1972**

#### SHUTTLE ANTENNA REQUIREMENTS FOR ANALOG TRANSMISSION SYSTEM (INTELSAT IV RELAY)

The information to be transmitted between the space shuttle and ground via Intelsat IV will be assumed to consist of a single voice channel and a 19.2-kbps data channel. In order to meaningfully assess the value of a coded digital transmission system, performance predictions will first be presented for a conventional Apollo-type (dual subcarrier) analog transmission system with optimized modulation parameters. The voice signal is assumed to frequency modulate one subcarrier, while the data signal phase modulates the second subcarrier, and a linear combination of the two modulated subcarriers phase modulates the main carrier. The performance criteria for the two channels are assumed to be the same as for the Apollo Program, i.e., 90% word intelligibility (corresponding to a 14-dB output signal-to-noise ratio) for the voice channel and 10<sup>-4</sup> bit error probability for the data channel. The system parameters assumed for the shuttle are based on incorporation of the new C-band RF technology (high-power transmitters and low-noise receivers) considered earlier.

For the analog transmission system considered, the shuttle antenna diameter required to provide a 3-dB performance margin in each information channel is 4.5 feet for the downlink and 6.3 feet for the uplink. In order to provide the required two-way communications capability, then, the required shuttle antenna diameter is 6.3 feet.

# SHUTTLE ANTENNA REQUIREMENT FOR ANALOG TRANSMISSION SYSTEM

## INTELSAT IV RELAY

- INFORMATION CHANNELS
  - 1 FM VOICE CHANNEL
  - 1 DATA CHANNEL (19.2 KBPS)
- PERFORMANCE CRITERIA
  - 90-PERCENT WORD INTELLIGIBILITY
  - $10^{-4}$  BIT ERROR PROBABILITY
- ASSUMED SHUTTLE PARAMETERS
  - TRANSMIT POWER \_\_\_\_\_ 100 WATTS
  - TRANSMIT LOSSES \_\_\_\_\_ 2 dB
  - SYSTEM TEMPERATURE \_\_\_\_\_ 180° K
  - RECEIVE LOSSES \_\_\_\_\_ 1 dB
- REQUIRED ANTENNA DIAMETERS FOR 3-dB PERFORMANCE MARGINS
  - DOWNLINK \_\_\_\_\_ 4.5 FT
  - UPLINK \_\_\_\_\_ 6.3 FT



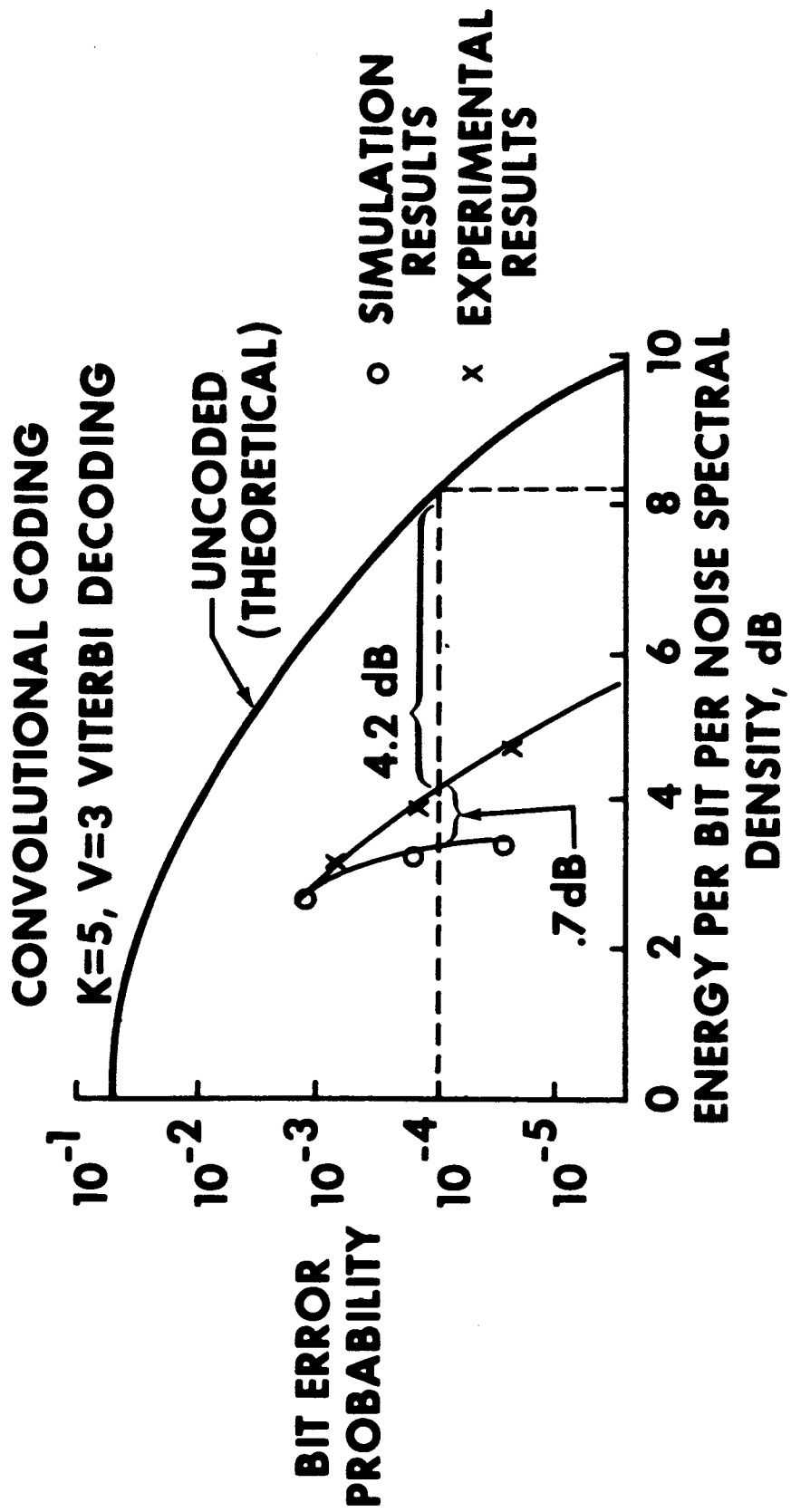
#### PERFORMANCE OF DIGITAL SYSTEMS UTILIZING ERROR CONTROL CODING

After reception and demodulation of a digital communications signal, it is necessary to decide which digital level was actually transmitted over each signaling interval. Because of the presence of noise, there is always a finite probability of error associated with these decisions. The probability of error is directly related to the amount of signal energy ( $E_b$ ) contained in each bit at the input to the bit detector, and to the noise spectral density ( $N_0$ ) at the receiver.

Several error correction encoding and decoding techniques are available for incorporation into a digital transmission system. As previously noted, the amount of coding gain which is realizable depends on the particular combination of encoding and decoding techniques which is employed. A characteristic common to all such techniques, however, is that redundancy is added on a controlled basis to the transmitted signal. That is, the number of bits transmitted per second over the channel is increased. Therefore, for fixed power levels, the introduction of coding results in a decrease in the available energy per bit at the bit detector input. The bit error probability at the bit detector output is thus greater with coding than with no coding. By applying a clever encoding/decoding scheme which makes efficient use of the controlled redundancy present in the encoded data, it is possible to reconstruct the original information signal with a lower bit error probability than before the introduction of coding.

Several recent studies have indicated that convolutional encoding, used in conjunction with Viterbi algorithm decoding, provides a good trade-off between performance gain and hardware complexity. Computer simulations performed at MSC predicted that a coding gain of about 4.9 dB should be achievable at an information bit error probability of  $10^{-4}$ , for Viterbi decoding of a convolutional code with a constraint length ( $K$ ) of 5 and a rate ( $1/V$ ) of  $1/3$ . The parameter  $K$  is the length of the shift register which is used to generate the convolutional code, while  $V$  is the number of channel bits transmitted for each information bit. A  $K = 5$ ,  $V = 3$  encoder and a Viterbi decoder were designed, fabricated, and tested in 1970; and the experimental coding gain provided by these devices is within 0.7 dB of these predictions. (0.3 dB of this variation from predicted performance was due to non-ideal operation of the bit detector.)

# PERFORMANCE OF DIGITAL SYSTEMS UTILIZING ERROR CONTROL CODING



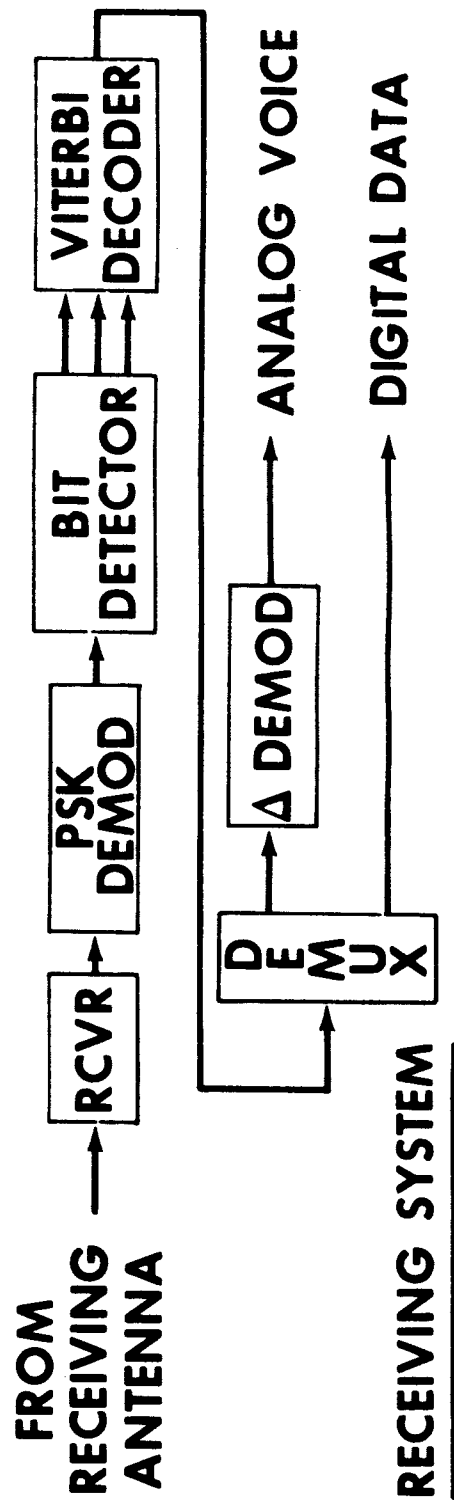
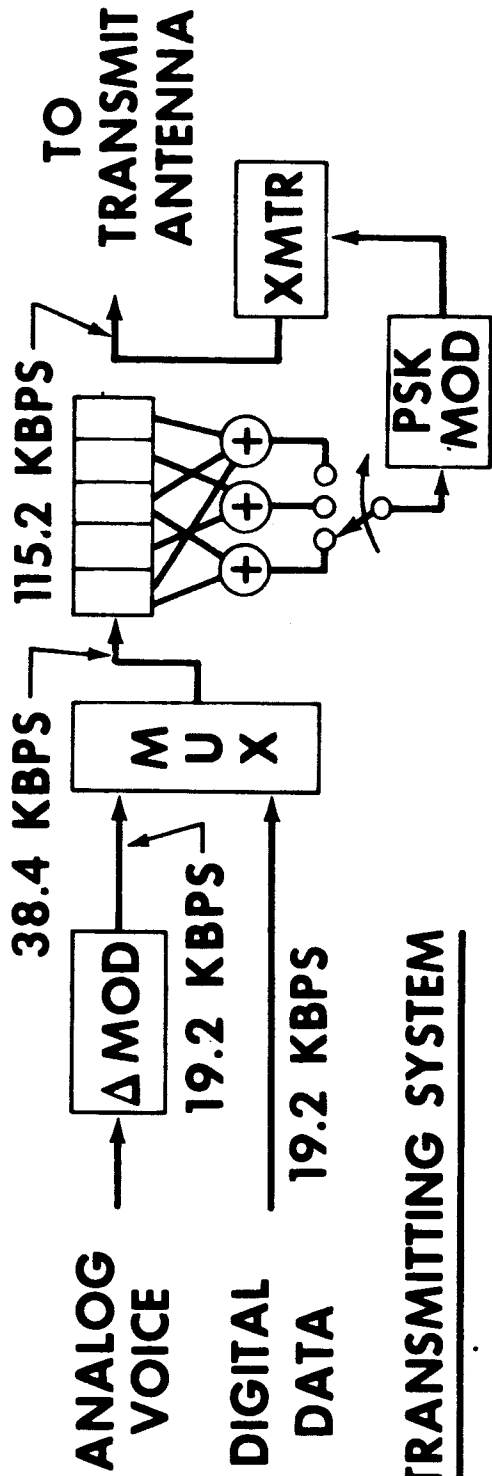
### CODED DIGITAL TRANSMISSION OF VOICE AND DATA

The performance of an all-digital system for transmission of a voice channel and a 19.2-kbps data channel will now be contrasted with that of the Apollo-type analog transmission system considered earlier. Variable-slope delta modulation is chosen as the analog-to-digital conversion technique for the voice signal. The required sampling rate for delta modulation is higher than for PCM, but only one bit is required to represent each sample. For some classes of information signals (such as voice), the bit transmission rate required for a given measure of channel performance (such as 90% word intelligibility) is significantly lower for delta modulation. Additionally, tests at MSC indicate that delta modulation is much less sensitive to bit errors than PCM. Both of these factors (lower transmit bit rates and higher allowable error rates) allow reductions in transmit power levels for delta modulation systems. The voice channel transmit bit rate assumed for this example is 19.2-kbps.

The delta-modulated voice signal and the 19.2-kbps data signal, after being time-multiplexed are encoded by a rate  $1/3$  convolutional encoder. The channel bit rate at the encoder output is, therefore,  $19.2 \times 2 \times 3 = 115.2$  kbps. The coded bit stream is used to phase-shift-key (PSK) a carrier, and this PSK signal is power amplified and transmitted over the relay link.

After reception and demodulation of the digital signal, the noisy channel bits are input to an optimum (integrate-and-dump) bit detector. Rather than utilize "hard" bit decisions which indicate merely that the integrator contents were positive or negative at the end of a bit period, use is made of "soft" bit decisions which indicate both the sign and magnitude of the integrator contents. Soft decisions are implemented by quantizing the bit detector output voltages into three-bit words. These three-bit words, which represent estimates of the channel bits, are input to the decoder for error correction. After decoding, the delta-modulated voice and data are demultiplexed and converted to forms suitable for the final users.

# CODED DIGITAL TRANSMISSION OF VOICE AND DATA



SHUTTLE ANTENNA REQUIREMENT FOR CODED DIGITAL TRANSMISSION SYSTEM (INTELSAT IV RELAY)

The parameters assumed for the shuttle are again based on incorporation of the expected C-band technological advances in high-power transmitters and low-noise receivers. The performance criterion for the digital transmission system is a  $10^{-4}$  bit error probability at the output of the Viterbi decoder. This error probability exactly satisfies the performance criterion for the data channel and, according to tests performed at MSC, more than satisfies the 90% word intelligibility requirement for the voice channel.

The coded digital transmission system provides a 9.2-dB improvement in link performance over the Apollo-type analog transmission system considered. This improvement can be realized as a decrease in the required shuttle antenna size. For the digital system, the shuttle antenna diameter required to provide a 3-dB performance margin is 1.5 feet for the downlink and 2.2 feet for the uplink. The required two-way communications can, therefore, be maintained with a 2.2-foot shuttle antenna.

# SHUTTLE ANTENNA REQUIREMENTS FOR CODED DIGITAL TRANSMISSION SYSTEM

## INTELSAT IV RELAY

- INFORMATION CHANNELS
  - 1 DELTA MODULATED VOICE CHANNEL (19.2 KBPS)
  - 1 DATA CHANNEL (19.2 KBPS)
- PERFORMANCE CRITERIA
  - $10^{-4}$  OUTPUT INFORMATION BIT ERROR PROBABILITY
- ASSUMED SHUTTLE PARAMETERS
  - TRANSMIT POWER \_\_\_\_\_ 100 WATTS
  - TRANSMIT LOSSES \_\_\_\_\_ 2 dB
  - SYSTEM TEMPERATURE \_\_\_\_\_ 180° K
  - RECEIVE LOSSES \_\_\_\_\_ 1 dB
- REQUIRED ANTENNA DIAMETERS FOR 3-dB PERFORMANCE MARGIN
  - DOWNLINK \_\_\_\_\_ 1.5 FT
  - UPLINK \_\_\_\_\_ 2.2FT

FLIGHT HARDWARE ESTIMATES FOR CODED DIGITAL TRANSMISSION SYSTEM

Implementation of the digital transmission techniques considered earlier is entirely feasible at this time. Delta modulators and demodulators have been in field use by the military for several years, and various types of coding and decoding have been utilized in the unmanned deep-space programs. Breadboard versions of the delta modulator and demodulator and the convolutional encoder and Viterbi decoder have been fabricated and tested in MSC laboratories. Additionally, Viterbi decoders have recently been fabricated and tested independently by several industrial organizations. The present technology in digital logic is such that all of these devices could be available as flight-qualified hardware in 1972. The estimated power requirements, weights, and sizes of the flight hardware make these digital transmission techniques appear to be compatible with manned space flight applications. The hardware estimates are based on utilization of medium-scale integration. Large-scale integration could be applied to further reduce size and weight, but with a probable increase in cost.

## FLIGHT HARDWARE ESTIMATES FOR CODED DIGITAL TRANSMISSION SYSTEM

DEVICE	COMPLEX- ITY, IC'S*	POWER REQMT, WATTS	WEIGHT, OZ	VOLUME, CU IN.	AVAIL- ABILITY
VARIABLE-SLOPE DELTA MODULATOR	40	6	5	12	1972
VARIABLE-SLOPE DELTA DEMODULATOR	40	6	5	12	1972
CONVOLUTIONAL ENCODER	10	1.5	2	3	1972
VITERBI DECODER	60-65	9	8-10	40	1972

\* Integrated Circuits



### CONCLUSIONS

The digital transmission techniques which have been considered represent state-of-the-art technology in communications signal processing. These techniques, when incorporated into flight systems, provide a significant improvement in overall link efficiency. If state-of-the-art RF technology (high-power transmitters and low-noise receivers) is applied to the space shuttle communications system, then this improvement in efficiency is realizable as a decrease in the required shuttle antenna size. A smaller shuttle antenna is desirable because of the reduced penalty in weight and because of the reduced physical and mechanical penalties associated with storing, deploying, and positioning a smaller antenna. In addition, at a given frequency, beamwidth varies inversely with antenna diameter. The larger beamwidths associated with smaller antennas are desirable because the requirements on tracking accuracy can be relaxed.

It should be noted that, for the case of transmission of one voice channel and one low-rate data channel via the Intelsat IV relay satellite system, not even application of the latest technology in RF equipment and signal processing techniques can remove the requirement for a tracking antenna on the shuttle. In fact, if the communications requirement could be reduced to only a single voice channel (no data), a tracking antenna would still be required. If it is desired to operate without a tracking antenna on the shuttle, then it will be necessary to utilize a relay satellite system other than Intelsat IV.

## **CONCLUDING REMARKS**

- **DIGITAL TRANSMISSION TECHNIQUES WITHIN EXISTING TECHNOLOGY**
- **REAL AND SIGNIFICANT IMPROVEMENTS IN LINK EFFICIENCY ARE POSSIBLE**
- **IMPROVED LINK EFFICIENCY CAN DECREASE SIZE OF SHUTTLE TRACKING ANTENNA (OR INCREASE DATA RATE CAPABILITY)**
- **TRACKING ANTENNA ALWAYS REQUIRED IF INTELSAT IV IS USED**

• •

• •

COMPRESSION AND ERROR CORRECTION FOR TV

R. B. Blizard, W. A. Stevens, J. L. McKinney, H. M. Gates, W. B. Anthony, D. L. Manion, and C. C. Korge†

Martin Marietta  
Denver, Colorado

## COMPRESSION AND ERROR CORRECTION FOR TV

The objective of this study was to determine the feasibility of digital transmission of real-time, standard format TV, together with voice and all the other data that must be returned from the Apollo spacecraft. The principal benefit offered by a digital system is a reduction in the RF power required to transmit a good picture and reliable data. To achieve this improvement it is necessary to use two techniques, always considered together, made possible by converting to an all-digital system: error-correcting codes and data compression. Data compression makes each transmitted bit more important so that fewer errors can be tolerated, and error correction gives more improvement at low error rates.

Two reports were written:

"Potential Applications of Digital Techniques to Apollo Unified S-Band Communications System. Final Report." Martin Marietta Corporation MCR-70-34 February 1970.

"Study of Potential Applications of Digital Techniques to the Apollo Unified S-Band Communications System Phase 2 - Final Report". Martin Marietta Corporation MCR-70-419, November 1970.

## COMPRESSION AND ERROR CORRECTION FOR TV

MARTIN MARINETTA  
DENVER DIVISION

### OBJECTIVES:

Good Picture.

Low SNR Requirement.

Reasonable Bandwidth.

SIMULTANEOUS STUDY OF COMPRESSION AND CODING.

ANALYSIS OF CODE PERFORMANCE.

SIMULATION OF COMPRESSION AND CODING.

HARDWARE DESIGN.

BREADBOARD.

Contract NAS9-9852 - Study of Potential Applications of Digital Techniques to  
the Apollo Unified S-Band Communication System.

July 1969-November 1970.

### COMPRESSION ALGORITHMS

The delta modulators, though easy to implement at the source, still will require some memory for buffering data during frame and line retrace, and for the multiplexing of other data. The predictors and interpolators make more efficient use of available memory.

The statistics of pictures is not favorable for delta modulators compared to algorithms that have a large buffering capability. Pictures typically have broad dull regions with patches of detail. The eye focuses on the detail and demands that it be reproduced sharply, if not with perfect brightness fidelity. It is impossible for a system without a buffer to encode this type of source efficiently, and therefore concentration on polynomial algorithms began early in the study.

We recommended the zero order interpolator (ZOI) algorithm, but results do not show much difference between the ZOI and the zero order predictor (ZOP). Both algorithms are fairly simple to implement, and our design studies show that operation at  $5 \times 10^6$  pixels/sec is feasible (pixel: picture element). The first order interpolator (FOI) gives pictures without contouring, but it is more difficult to implement because it requires taking the quotient of two numbers.

**COMPRESSION ALGORITHMS**

**MARTIN MARIETTA**  
**DENVER DIVISION**

- I. DELTA MODULATION
- II. POLYNOMIAL - Zero and First Order Predictors and Interpolators.

(ZOP, ZOI, FOP, FOI)

FOI - Best Pictures, No Contouring.

Requires Division.

ZOP } Good Pictures, Simple Computation  
ZOI }

Require Memory Buffer. Buffer Permits Use of Retrace Time.

### ZOI COMPRESSION VARIABLE TOLERANCE

The game is to draw horizontal lines that approximate, within a given tolerance, the actual sampled and quantized data points, represented by X's.

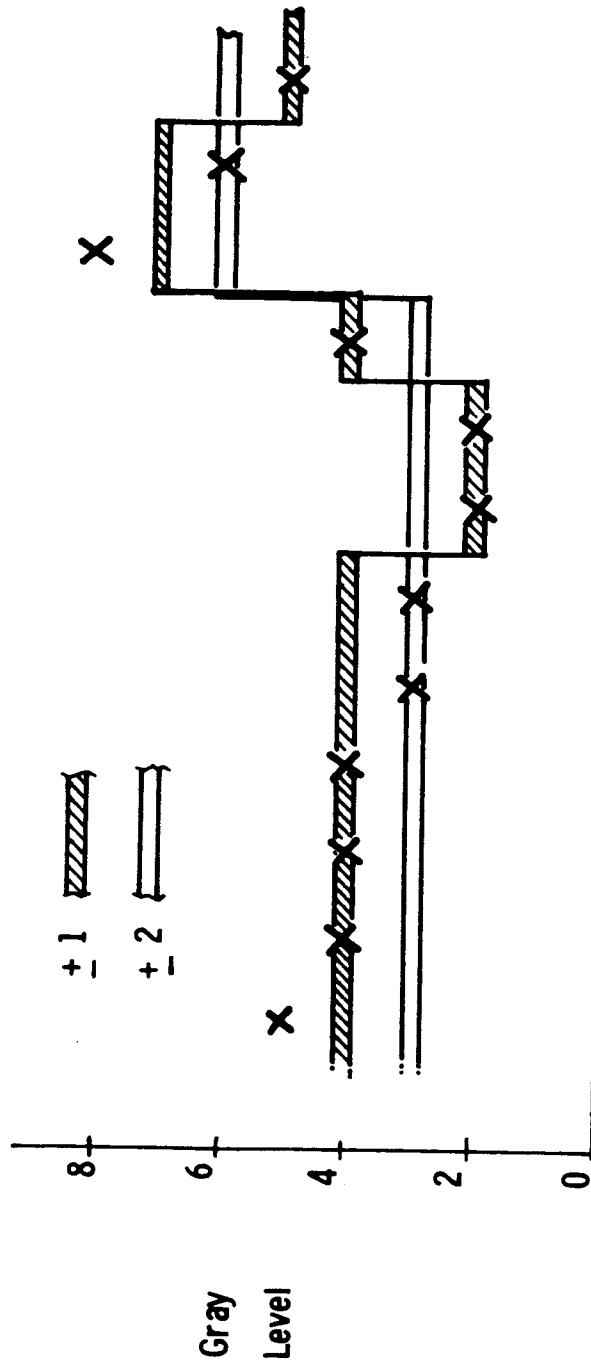
With a tolerance of +1, the transmitted message would be "gray level 4, 6 times; gray level 2, 2 times; gray level 4, 1 time; gray level 7, 2 times; gray level 5, 1 time." Relaxing the tolerance to +2 permits a much briefer message "gray level 3, 9 times; gray level 6, 3 times."

The average bit rate of the message is made to fit the channel rate by adjusting the tolerance.



# ZOI COMPRESSION, VARIABLE TOLERANCE

MARTIN MATHIE LTD  
 GEMER DIVISION



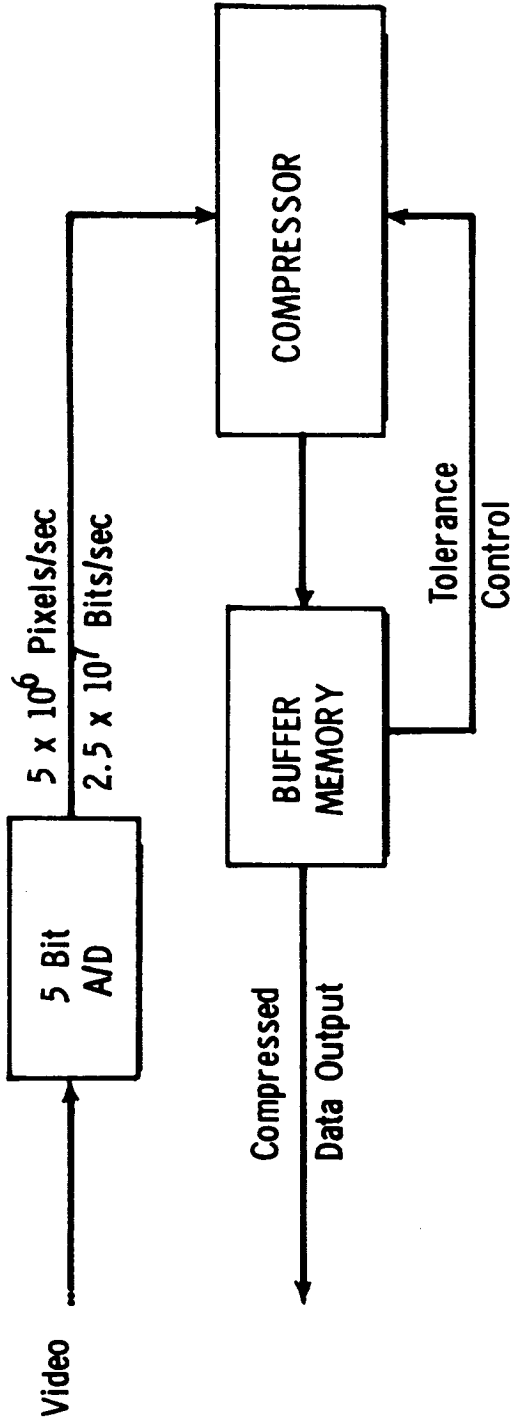
### COMPRESSOR BLOCK DIAGRAM

The video signal is sampled 5 times each microsecond and digitized to 5 bits. The compressor converts these data to gray-level and run-length form. The amount of data stored in the buffer is controlled by adjusting the compression tolerance. As the buffer nears overflow, the tolerance is increased in steps to + 8 and finally the run-length is forced to a large value. When the buffer contents decrease, the tolerance is reduced, and as a final measure to prevent underflow, the compressor is forced to transmit every pixel.

The average number of bits transmitted per pixel is 1.8.

# COMPRESSOR BLOCK DIAGRAM

MARTIN MARIETTA  
DEWEER DIVISION



## DATA CODING

The transmitted information is encoded into words of variable length. The first five bits (in the selected version) indicate one of 32 possible gray levels and the remaining bits indicate how many successive picture elements or "pixels" are to be given that gray level. This number is called the run length, and the code for the run length is of variable length, three bits for 1 through 4, four bits for 5 through 8, and so forth up to length 20. The last bit of each word is a 0, called a comma, to indicate to the reconstructing system that the word is terminated.

With such a system, unless precautions are taken, a single bit in error can upset a large part of the picture that is being transmitted. An error in the gray level code will persist for a run length. An error in the run length code will displace all subsequent pixels. An error in a comma, or an error that inserts a comma where none should be, completely upsets reconstruction of the line from that point on. To limit propagation of the effects of errors, a special code is used at the end of each line that cannot be mistaken for any segment of ordinary code words. Therefore no matter how badly the timing of a line is upset, the reconstruction system will recover on the first end-of-line code that it receives correctly. Other special orders signify the ends of field and frame.

**DATA CODING**

**MARTIN MARIE TTTA**  
**DENVER DIVISION**

**GRAY LEVEL CODE -- 5 BIT BINARY**

**RUN LENGTH CODE -- VARIABLE LENGTH WORD:**

**1 000 5 0010**

**2 010 11 10110**

**3 100 14 011110**

**4 110 20 1111110**

**END OF LINE 11111111111100**

**END OF FIELD 11111111111101**

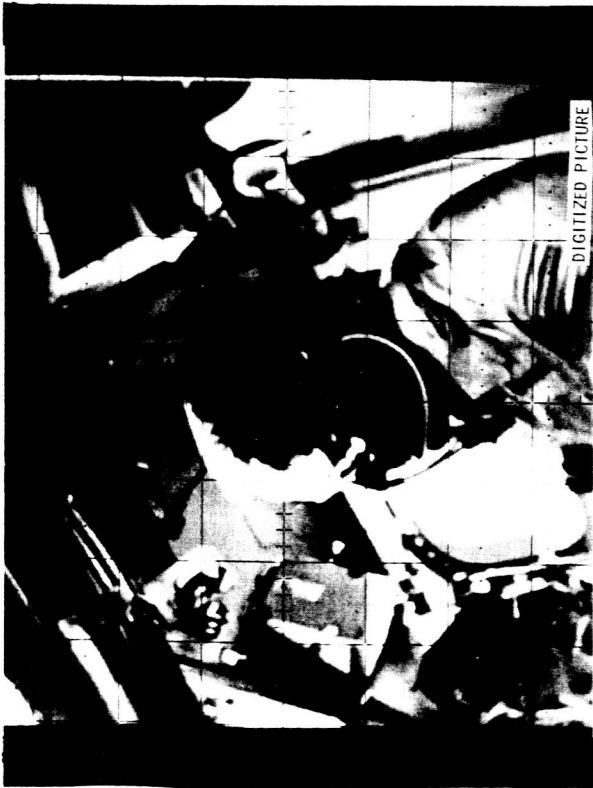
**END OF FRAME 11111111111110**

## SIMULATION OF A SINGLE TV FRAME

Slide 6 shows the original digitized picture with 64 gray levels and 512 x 512 pixels.

Slide 7 shows the same pattern with half the pixels ignored (in a checkerboard pattern) and the remaining pixels transmitted with an average of 1.8 bits per remaining pixel. Slides 3 and 9 show the effect of the kind of noise that would be seen in a channel using a convolutional code with constraint length 5 and rate  $\frac{1}{2}$  at signal-to-noise ratios per bit ( $E_b/N_0$ ) of 3.0 and 4.0 dB.

It is obvious that the end of line codes are effective in getting reconstruction back on the track. The frequency of these special codes is a parameter of the system that may be adjusted for optimum performance. If middle-of-line codes were also used, the error streaks would only be half as long, but signal energy would be diverted from the main data and there would be more errors. Similarly, signal energy could be saved by inserting the special code words only after every other line, thus making half the streaks extend into the next line. The choice of this parameter is not critical, but the optimum seems to be near 1 per line, and this is a convenient arrangement.



### CODING COMPARISON

Two types of convolutional decoders were seriously considered for this application: a hard-decision Fano decoder like the one that the Codex Corporation had built for the Army, and a Viterbi decoder for constraint length 5 and rate  $\frac{1}{2}$ . As the slide shows, their signal requirements are nearly identical for an error rate equal to  $10^{-5}$  (a good error rate for compressed pictures), but the Viterbi gives better performance at lower signal-to-noise ratios.

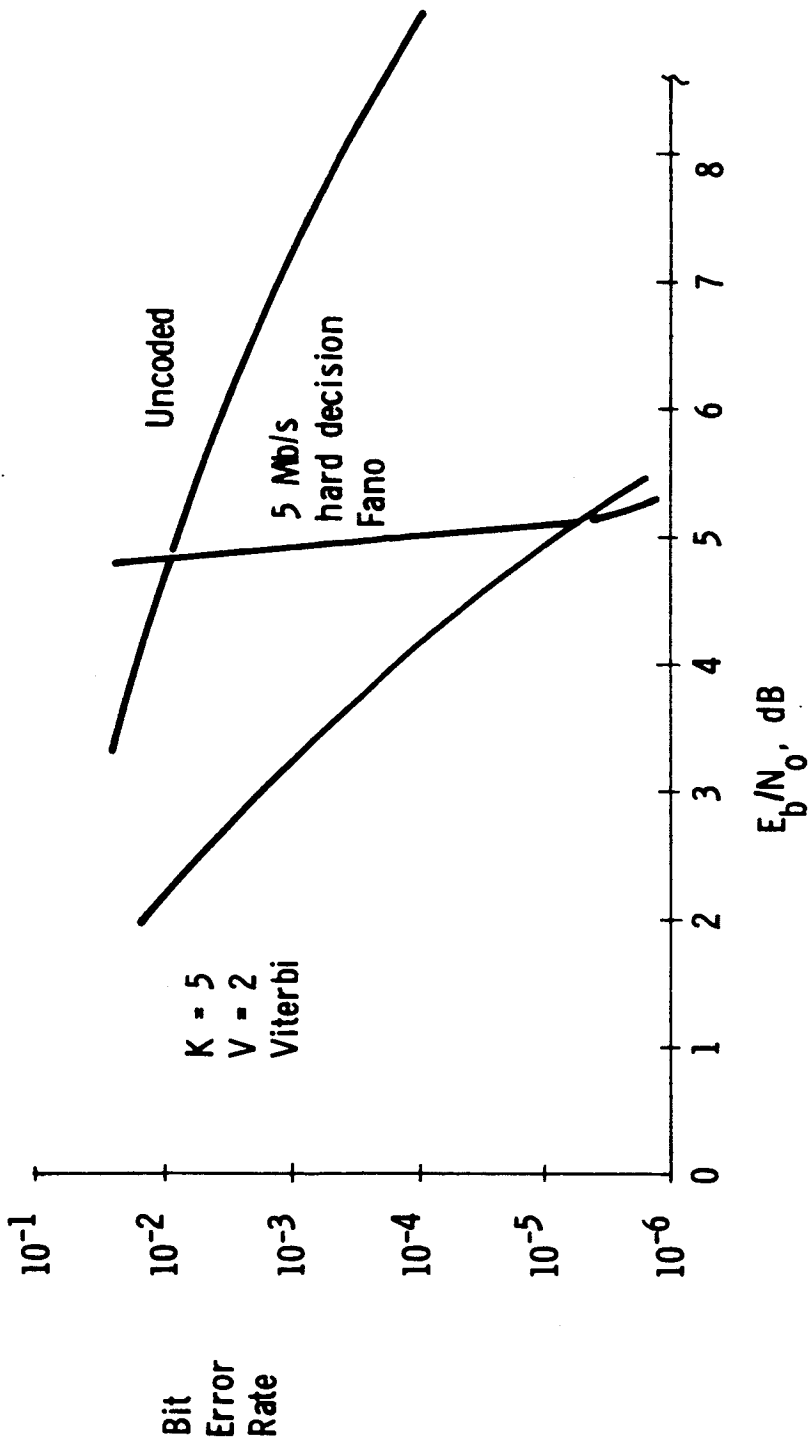
We designed a Viterbi decoder that we were confident would run at 7.5 Mb/s, the speed needed for TV. A parts count showed that it needed about the same number of integrated circuits as the Codex machine but did not need a core memory as did the latter. Furthermore, the speed of the Codex machine (5 Mb/s) was a little lower than we wanted. For these reasons we recommended the Viterbi decoder.

A reevaluation at this time should take account of recent developments including our new algorithm.



# CODING COMPARISON

MARTIN MARIETTA  
DENVER  
DIVISION



## NEW DECODING ALGORITHM

As part of the contract we originated, developed, and demonstrated a new decoding algorithm that can operate at very low signal-to-noise ratios and is practical at high as well as low data rates. It uses a systematic code and solves the decoding equations by successive approximations. Large constraint lengths are practical -- current work is with a length of 220, and we have used lengths as high as 958. Analysis shows that, in the limit of large constraint length and large band expansion, channel capacity can be approached. Unlike sequential decoding, the new algorithm is self-starting, and it is not necessary to insert periodic sequences of known bits to assure recovery after decoding failure.

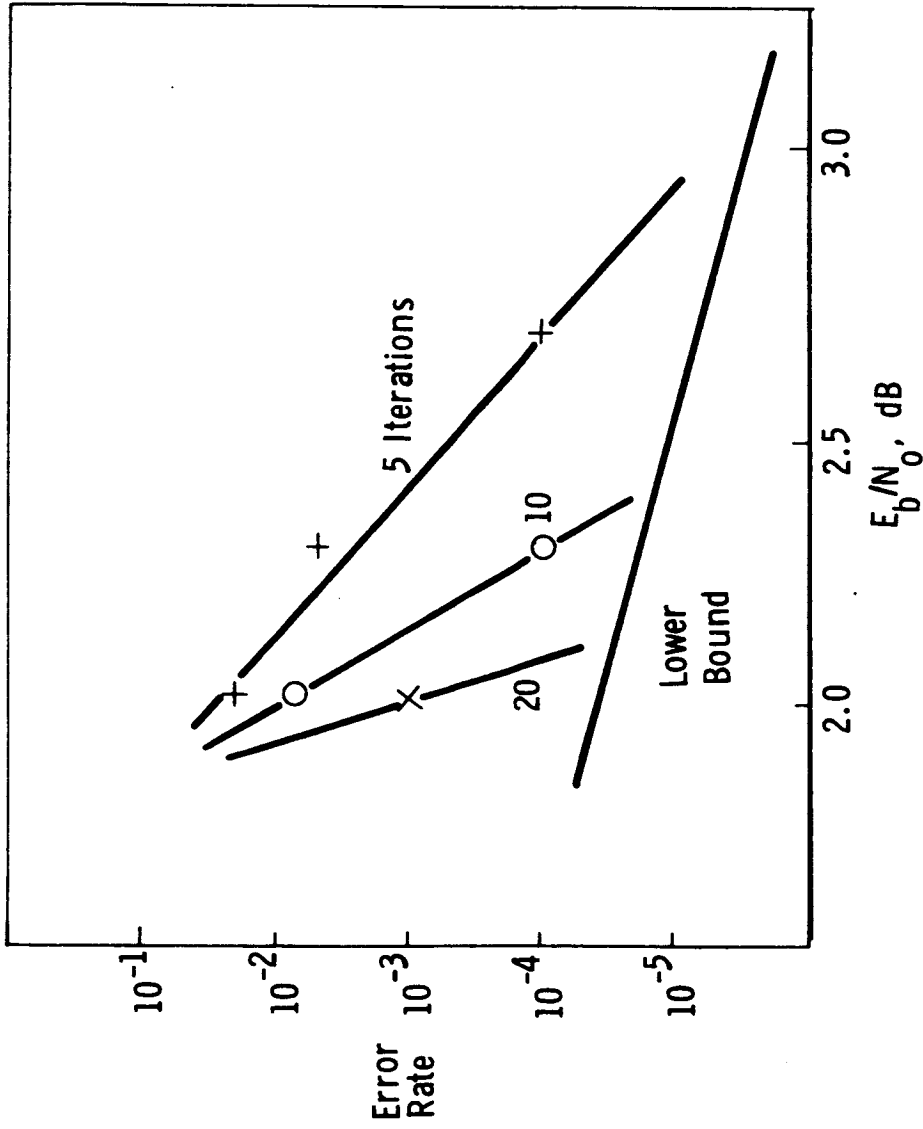
To demonstrate the feasibility of operation at high speed, we built a breadboard that operates at 11 Mb/s with TTL MSI.

Since the completion of the contract, we have continued to develop the algorithm and have achieved substantial improvements for rate 1/2 codes. The slide shows current performance results for a code of constraint length 220 for 5, 10, and 20 iterations of the decoding process. The lower bound on error probability is based on the minimum code word weight, and it could be reduced at the cost of some increase in the amount of computation that the decoder must perform. With the present code, 20 iterations requires slightly more arithmetic operations than does the Viterbi algorithm with a constraint length of 9.

The recent improvements have not been applied to rate 1/3 codes, but we speculate that it should be quite feasible to operate at  $E_b/N_0 = 1.0$  dB.

NEW ALGORITHM.  $K = 220$ ,  $V = 2$ .

MARTIN MARIETTA  
DENVER DIVISION



INTEGRATION OF RF FUNCTIONS FOR NAVIGATION,  
VOICE AND DATA COMMUNICATION

T. S. Bettwy

TRW Systems Group  
Redondo Beach, California

The advent of the Space Shuttle Project has produced requirements for both communication and navigation functions that were non-existent for the Apollo project. These functions are associated with landing at an airport. Although the new functions can readily be accomplished with traditional (FAA type) systems, a much more cost effective approach is proposed. This technique, called USCANS for Unified S-Band Communication and Navigation System, makes maximum use of existing NASA equipment, can be employed on other NASA projects such as Skylab, Space Station, and FFP and increases shuttle system performance during on-orbit phases. The proposed system is also compatible with the Air Force's Satellite Control Network.

## SHUTTLE RF FUNCTIONS

The RF functions for NASA missions are comprised of voice transmission, data transmission and navigation. These functions must be intervehicular as well as between space vehicles and ground. On Apollo, the voice and data transmission was done principally with S-band and VHF. Navigation data was obtained at S-band with MSFN. A VHF ranging link between CSM and LM was also employed. Onboard radars were used during both the rendezvous phase and lunar landing phase of the mission.

In the USCANS concept, all functions are performed at S-band. Multilateration to ground transponders is employed for navigation in the terminal region. Ranging between shuttle and target satellite is accomplished with the same shuttle equipment as used with the ground transponders. If the target satellite is compatible with MSFN, no additional on-board equipment is needed for communication or navigation.

With the USCANS concept, all functions shown on the attached chart can be performed by an integrated set of S-band equipments.

SHUTTLE RF FUNCTIONS

TERMINALS	FUNCTION	VOICE	DATA	NAVIGATION
	BOOSTER - LAUNCH SITE	P	N	N
	BOOSTER - MSFN	N	N	N
	BOOSTER - LANDING SITE	P	N	P
	BOOSTER - ORBITER	P	N	N
	ORBITER - LAUNCH SITE	P	N	D
	ORBITER - MSFN	P	P	P
	ORBITER - TARGET SATELLITES	P	D	P
	ORBITER - LANDING SITES	P	N	P

P - MUST BE PROVIDED

N - NO REQUIREMENT DEFINED

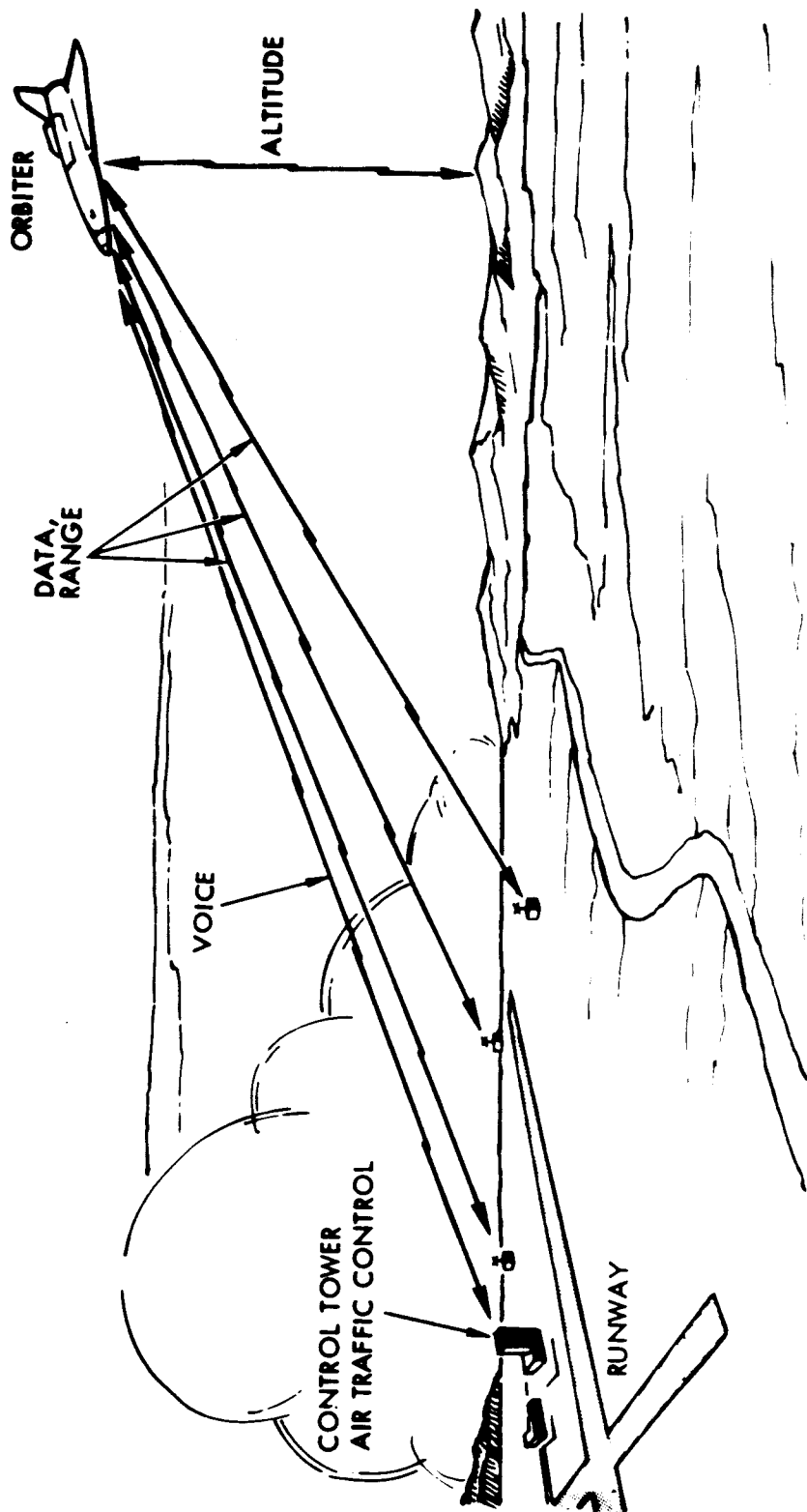
D - DESIRABLE

## CRUISE AND LANDING SCENARIO

The USCANS system is conceived as operating with ground transponders located at the designated booster and orbiter landing sites. Location of the transponders in the terminal area will be optimized to provide the best navigation data. Since multiple transponder locations are required for navigation accuracy, redundancy is achieved if more than three locations are used. It is anticipated that the transponders will be dual redundant at each location. All ground transponders are similar except each has its own location code. The receivers are always operating. The ground transponders transmit only when called by means of the location code. To minimize cost, the control tower is tied to only two dual redundant transponders for voice purposes. Meteorological data on ground equipment health status could be sent to the vehicle on the data link.

The booster or orbiter sequentially interrogates the ground transponders, thus obtaining range (and possibly range rate) information. This data is filtered onboard the vehicle for navigation and guidance purposes.

# CRUISE AND LANDING SCENARIO





## ON ORBIT

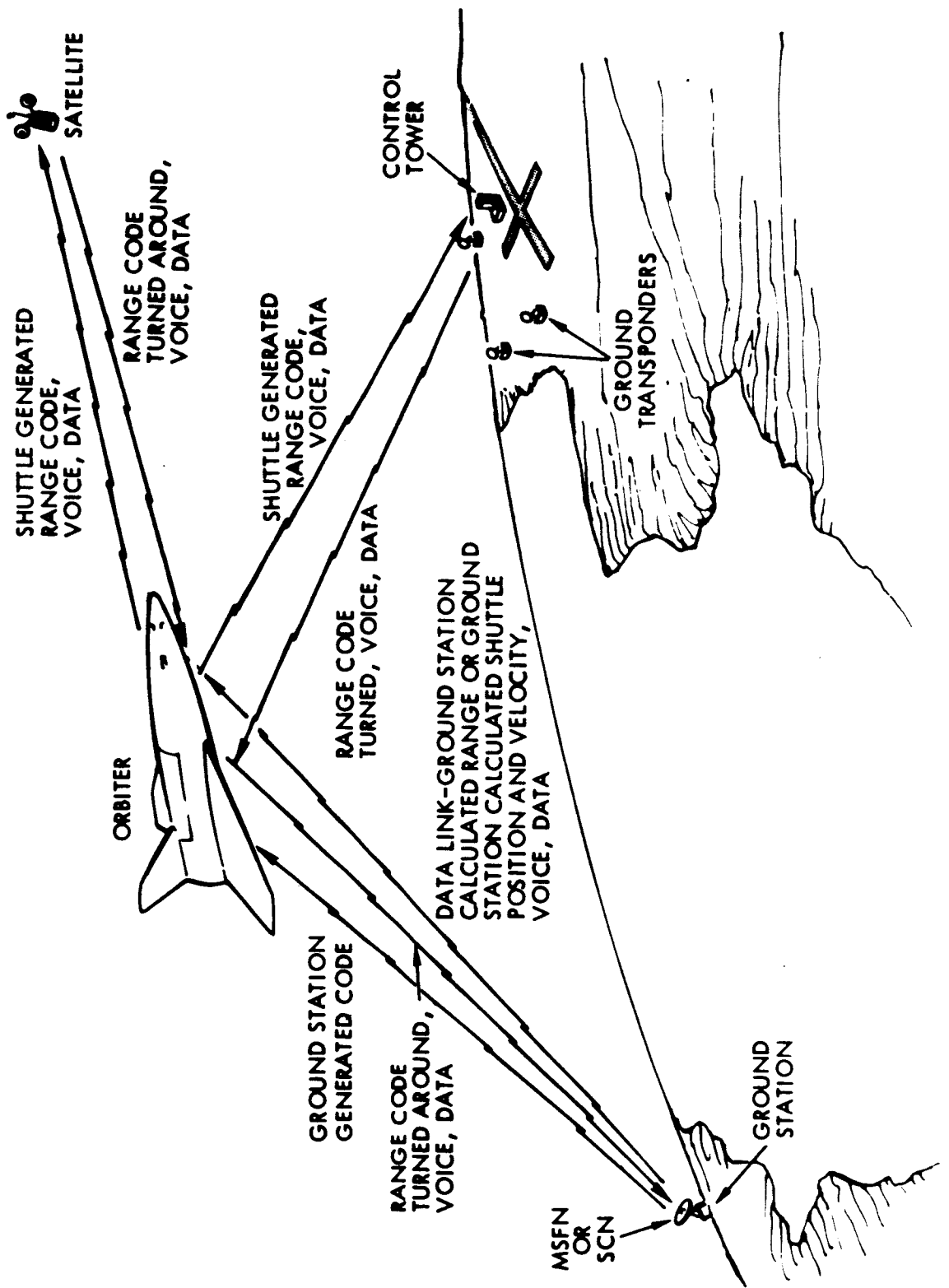
On orbit operations with MSFN are the same as on the Apollo project. For navigation, a MSFN generated range code is received by the orbiting vehicle and returned to the MSFN. A ground computed vehicle state vector can be sent to the orbiter on the data link. As an alternate mode, MSFN determined range and range rate can be transmitted via the data link for use in the onboard navigation filter. Voice and data links are the same as presently used.

334

Additional navigation data (also voice and data if desired) can be obtained from the transponders located at the landing sites. By interrogating one of the transponders, range to the known transponder location can be accurately obtained and on orbit navigation updated.

Communication with a MSFN compatible satellite is the same as to a ground transponder or MSFN. Both voice and data can be transmitted. For navigation, the orbiter generates and transmits a range code which is subsequently turned around by the MSFN compatible satellite. Relative navigation is performed onboard the orbiter.

ON ORBIT

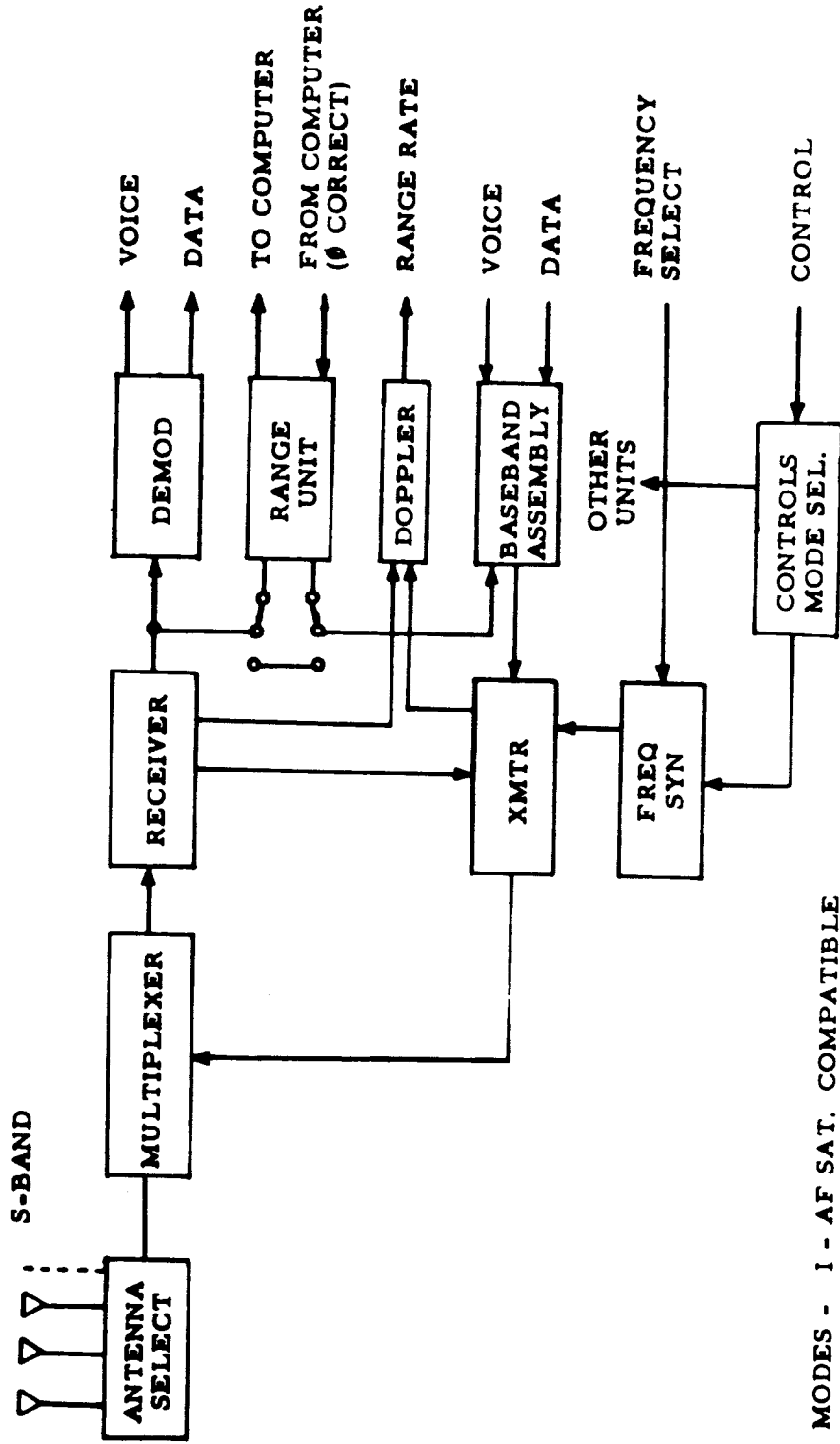


PROPOSED SYSTEM - VEHICLE EQUIPMENT

The onboard S-band equipment required is very similar to the Unified S-Band Equipment used on Apollo. In effect, only the addition of a range code generator and frequency synthesizer is required. The former is for ranging to target satellites and ground transponders while the latter is to provide compatibility with MSFN, MSFN compatible satellites, SCN, and SCN compatible satellites. A switch is included to eliminate the range unit so that the equipment will be compatible with MSFN by merely turning around the range code.

As presently conceived the ranging is achieved with a sequential binor code. This is in contrast to the tones used on Apollo and the PRN used on MSFN. Sequential binor has been selected because of its rapid acquisition characteristics as well as receiver simplicity.

PROPOSED SYSTEM - VEHICLE EQUIPMENT

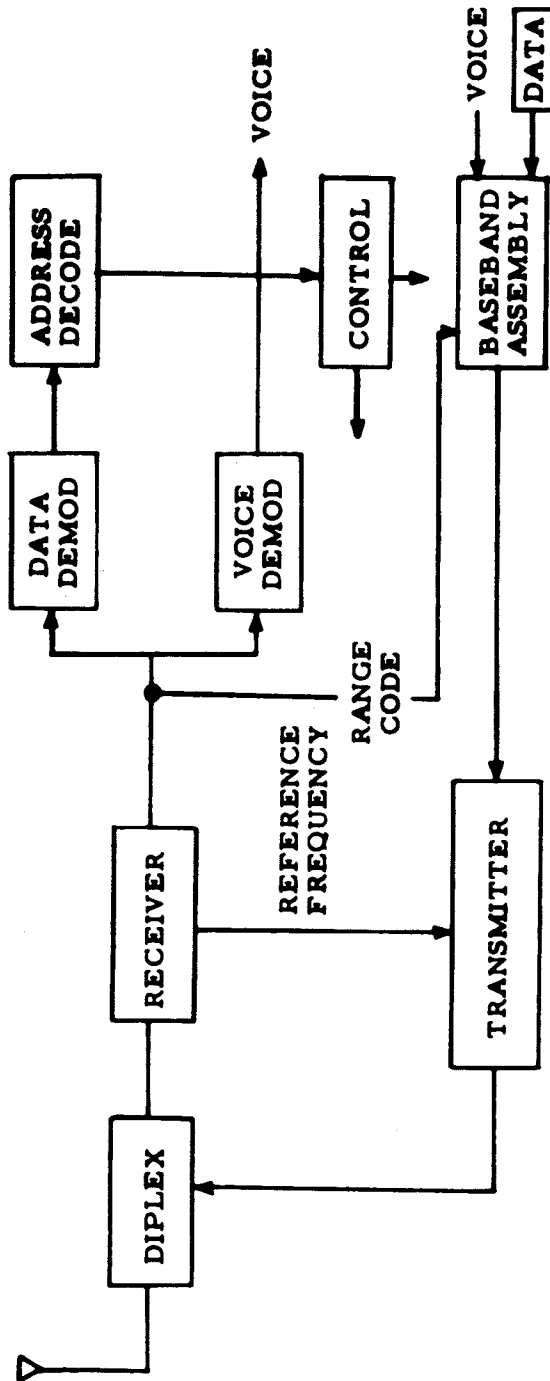


- MODES - I - AF SAT. COMPATIBLE  
 II - SPACE STATION COMPATIBLE  
 III - MSFN COMPATIBLE  
 IV - SCF COMPATIBLE

PROPOSED SYSTEM - LANDING SITE TRANSPONDER BLOCK DIAGRAM

The ground transponder (as well as the target satellite transponder) is also very similar to the Unified S-Band Equipment onboard the Apollo. Since each transponder is to contain its own location code and transmit only when that code is received, a technique is provided to recognize the location code and turn on the transmitter.

PROPOSED SYSTEM - LANDING SITE TRANSPONDER BLOCK DIAGRAM



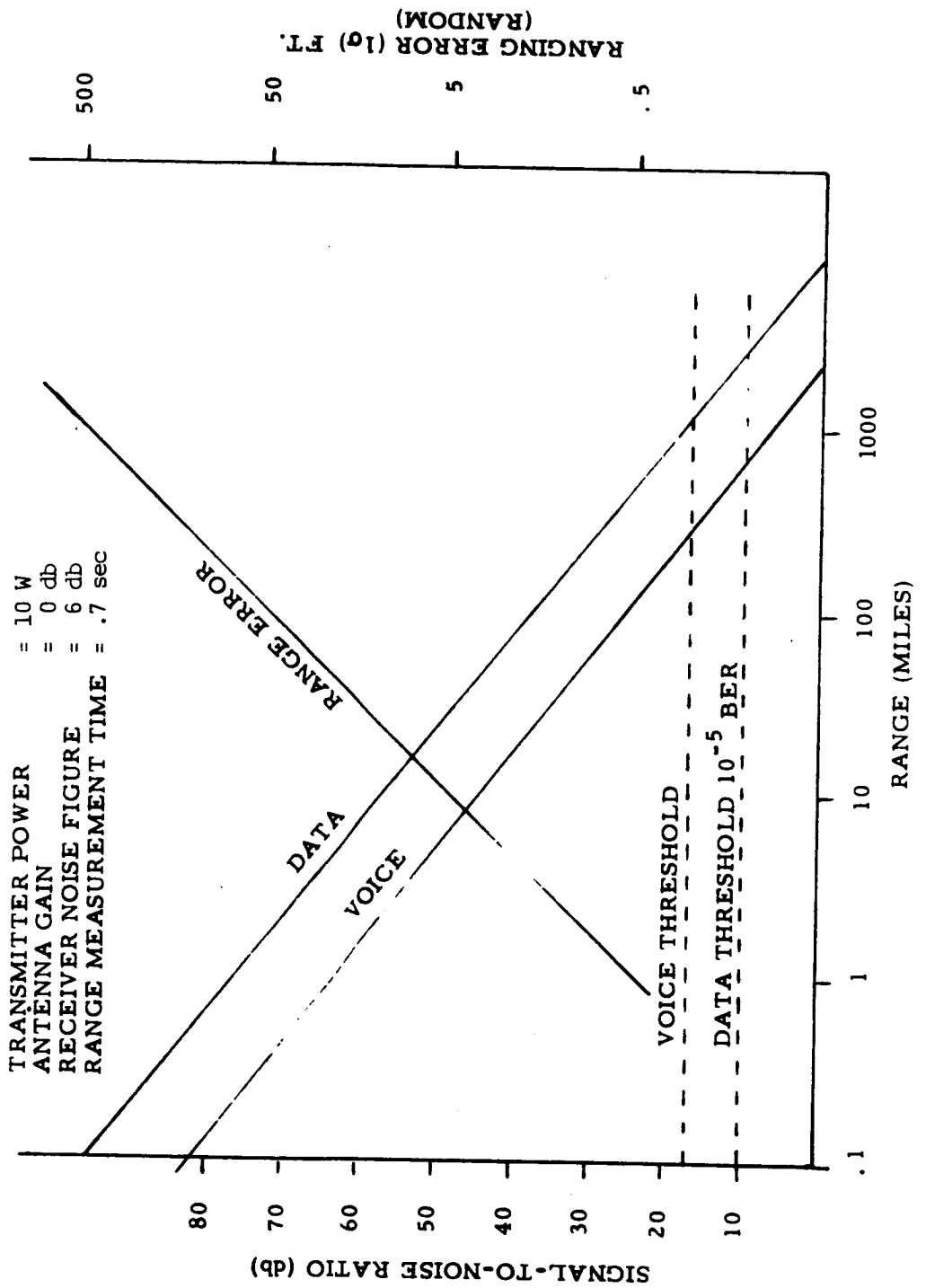
### USCANS LINK PERFORMANCE

USCANS link performance is shown on the following chart. As shown, the data link has a signal to noise ratio of greater than 10 db to ranges greater than 1000 miles. The 10 db threshold corresponds to a bit error rate (BER) of  $10^{-5}$ .

The voice threshold shown of 16 db corresponds to an articulation index of approximately 0.4. This provides 82% intelligibility of isolated words and 97% for sentences.

Range error is a function of range measurement time (as well as range). Thus, range error can be decreased by increasing the measurement time if desired.

USCANS LINK PERFORMANCE



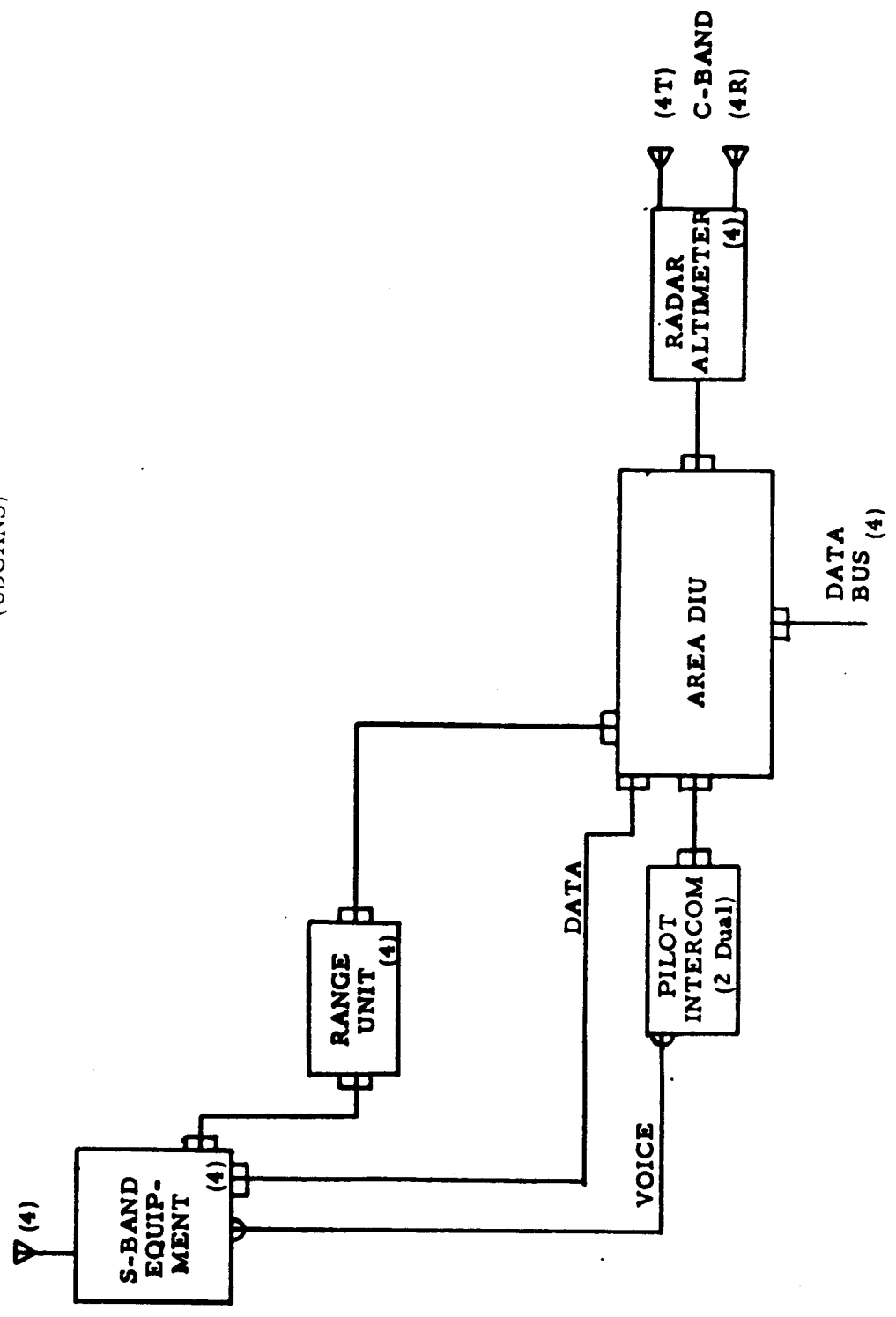


ONBOARD COMMUNICATION AND NAVIGATION EQUIPMENT  
(USCANS)

Several communication and navigation subsystem configurations are now considered to form the basis of a cost analysis. These configurations all conform to the NASA Level 1 failure operational, fail operational, fail safe redundancy requirement.

The basic configuration is that of USCANS. All communication and navigation functions, as described above, are at S-band. C-band radar altimeters are shown in the figures. However, requirements for their use are in question. The numbers in parentheses indicate the number of units onboard to satisfy the redundancy requirements.

ONBOARD COMMUNICATION AND  
NAVIGATION EQUIPMENT  
(USCANS)



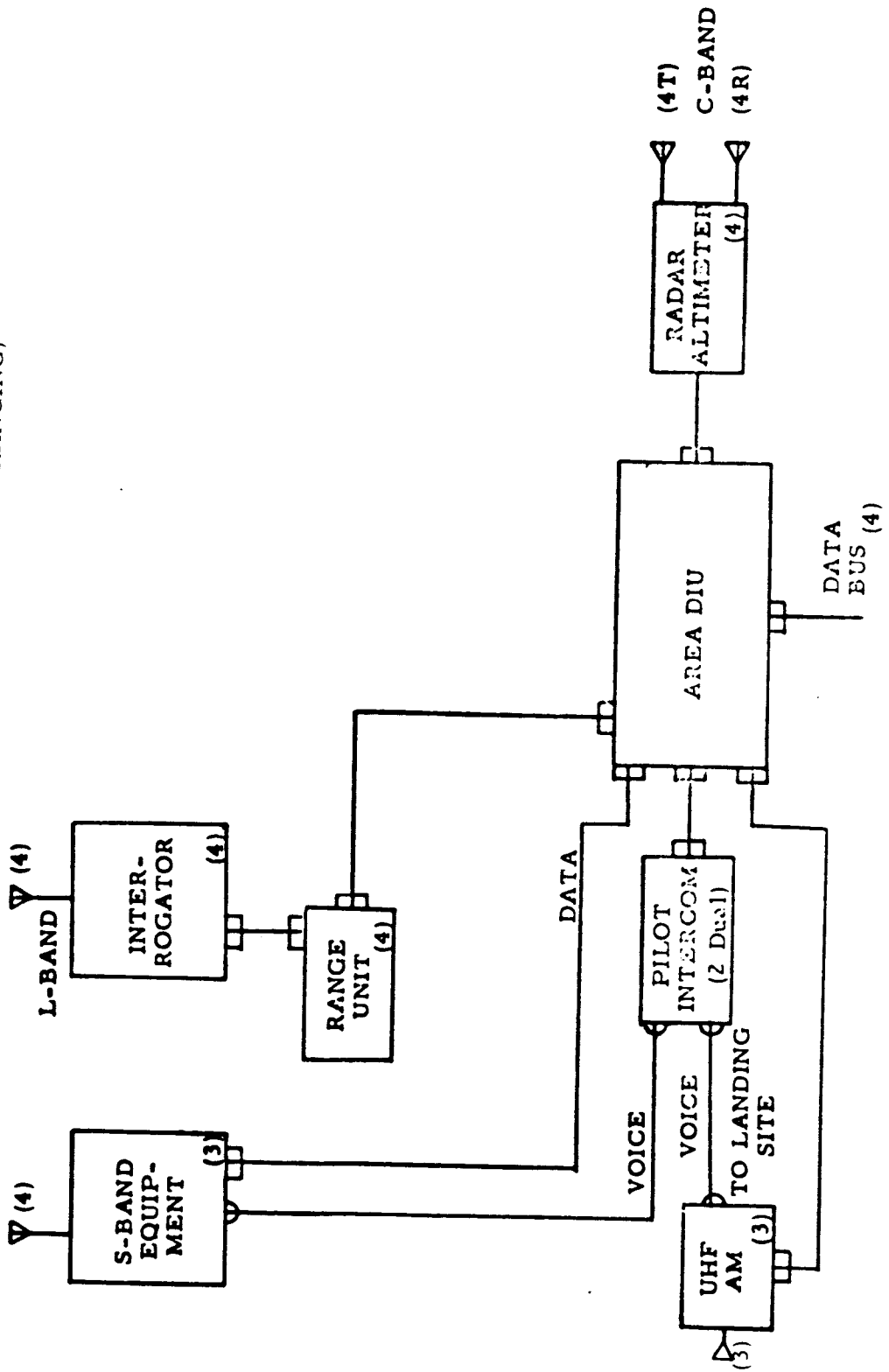
ONBOARD COMMUNICATION AND NAVIGATION EQUIPMENT  
(S-BAND AND SEPARATE RANGING)

The first alternative to USCANS is to perform the ranging function at a different frequency (say L-band) than S-band. In this case the ranging unit would interconnect to the L-band interrogator rather than the S-band equipment as shown. This configuration has been proposed since some existing multilateration systems operate at L-band.

Utilization of L-band ranging suffers from several deficiencies:

1. Additional antennas (L-band) are required on the shuttle (as well as on the target vehicle).
2. Voice to the control tower must be achieved in some manner such as on the L-band or on UHF in which case more antennas are required or on S-band where the voice link already exists for compatibility with MSFN (S-band antennas and L-band antennas then needed at the landing site).

ONBOARD COMMUNICATION AND  
 NAVIGATION EQUIPMENT  
 (S-BAND AND SEPARATE RANGING)



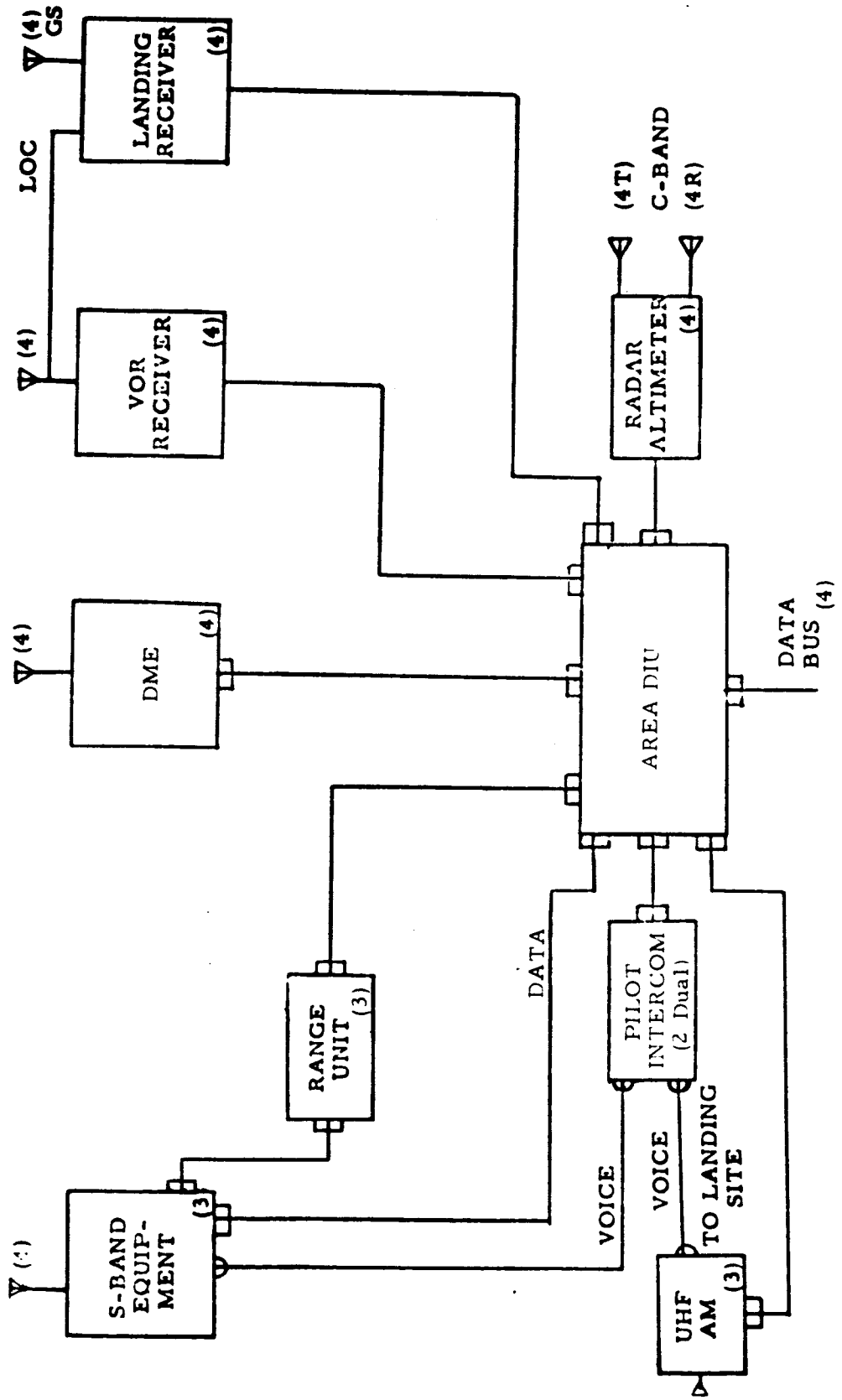
ONBOARD COMMUNICATION AND NAVIGATION EQUIPMENT

(FAA COMPATIBLE)

A third alternative is to be compatible with the FAA existing or proposed terminal area and approach navigation equipment. This requires additional onboard equipment as shown. Ranging and voice over the S-band link are still retained for operation with the target satellite.

This configuration has been proposed because of the availability of landing sites around the world with the required equipment installed.

ONBOARD COMMUNICATION AND  
 NAVIGATION EQUIPMENT  
 (FAA COMPATIBLE)



SYSTEM CONFIGURATIONS AND COST ELEMENTS

Three systems are configured for cost comparison. This chart shows the equipment used in each configuration. Both orbiter and booster equipment are considered. The cost elements are considered to be conservative estimates based upon experience and informal data from vendors. Antenna costs are considered to be very conservatively estimated.

SYSTEM CONFIGURATIONS AND COST ELEMENTS

ITEM	USCANS	FAA COM- PATIBLE	S-BAND # SEPARATE RANGING	COST \$M		WEIGHT (LBS/SET)
				RDT&E	RECUR- RING	
S-BAND EQUIPMENT	4/4	3/0	3/0	6.0	.21	17
ALTIMETER	4/4	4/4	4/4	6.0	.08	21
RANGING UNIT	4/4	3/0		1.0	.03	7
INTERCOM	2/2	2/2	2/2	3.0	.08	5
UHF TRANSCEIVER		3/3	3/3	6.0	.13	30
ILS		4/4		4.0	.07	11
VOR		4/0		3.0	.04	10
DME		4/4		4.0	.08	30
L-BAND VEHICLE EQUIPMENT			3/3	4.0	.20	10
L-BAND GROUND TRANS- PONDERS			24	1.0	.26	
USCANS GROUND TRANS- PONDERS	24			1.0	.42	

ANTENNA COST:

RDT&E \$.5M EACH TYPE  
 ACQUISITION \$.05M EA.  
 ORBITER/BOOSTER



### COST COMPARISON

Analysis of the data on this chart indicates a significant cost savings if the USCANS concept is employed. This result occurs because the USCANS equipment is employed in all configurations to achieve compatibility with MSFN. Several costs were not estimated as indicated. Each of these items would tend to favor the USCANS (and the S-band and separate ranging) configuration. The conservative 27% cost savings shown makes USCANS a very attractive candidate.

COST COMPARISON

ITEM OF COST	USCANS	FAA COM-PATIBLE	S-BAND & SEPARATE RANGING
DEVELOPMENT COST	\$17 M	36 M	27 M
VEHICLE EQUIPMENT	1	0	1
GROUND EQUIPMENT	1	2.0	1
GSE			
ACQUISITION COST			
VEHICLE EQUIPMENT	17.1M	24.94M	23.48M
GROUND EQUIPMENT	10.2	0	6.3
GSE	2.0	4.0	2.0
TOTAL	48.3 M	66.94M	66.78M
WEIGHT SAVINGS			
ORBITER Δ COST	3.3 M		2.6 M
BOOSTER Δ COST	1.35		.85
Δ TOTAL	4.65M		3.45M

COSTS NOT CONSIDERED:

- POWER SAVINGS
- FUEL DUE TO IMPROVED ACCURACY
- STRUCTURES
- DISPLAYS
- FAA GROUND INSTALLATIONS

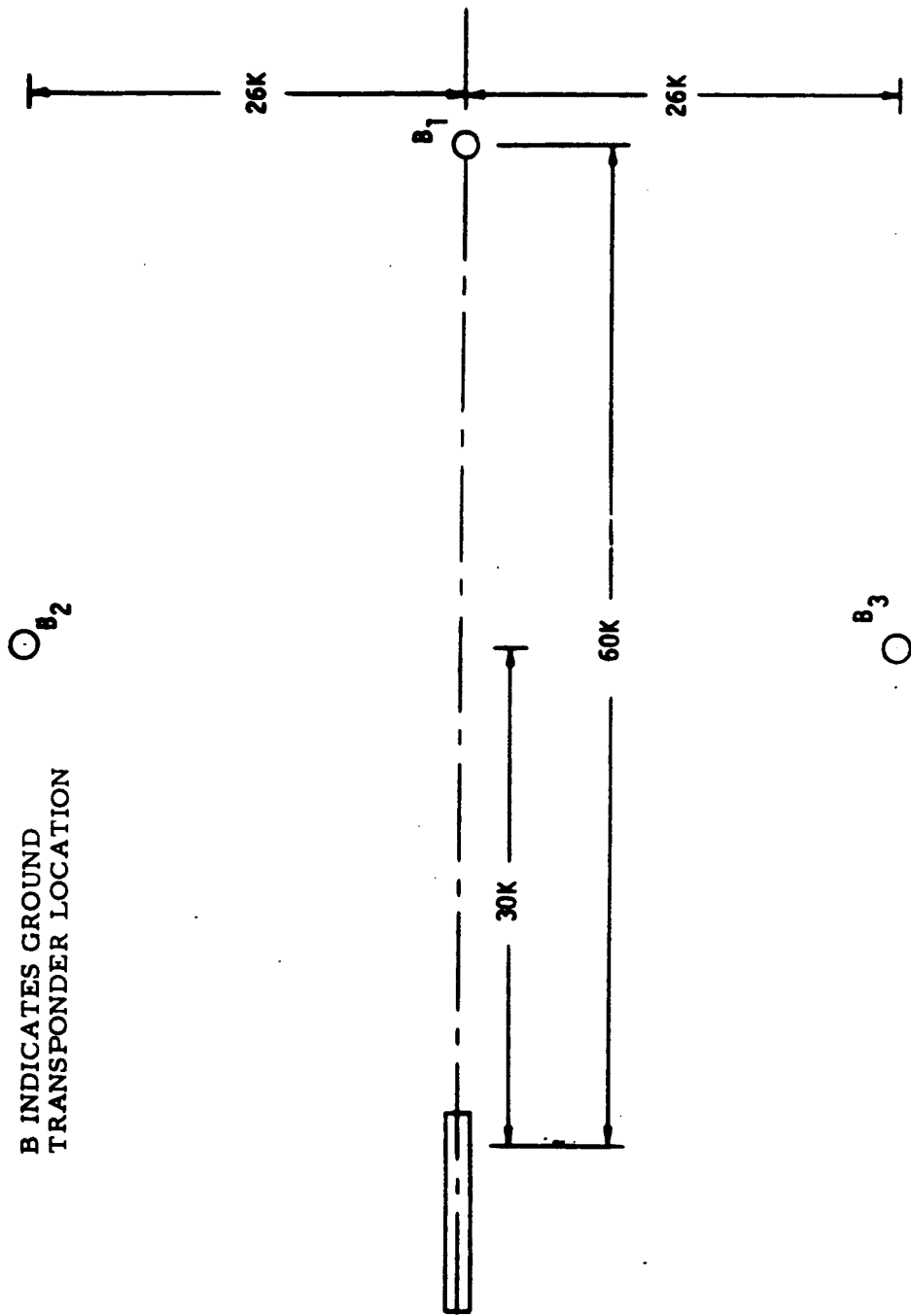
### PERFORMANCE

As an indication of the performance achievable with multilateration systems, several cases of landing navigation accuracy are presented. In addition, results of using the ground transponders for aiding the inertial navigation system during ascent into orbit are also presented. This latter capability may be necessary for specific Air Force missions that require high accuracy orbit insertion.

### GROUND TRANSPONDER LOCATIONS IN VICINITY OF LANDING SITE

In the landing navigation analysis, three ground transponders were located as shown. In addition to the ground transponders, an IMU and altimeter were employed. The shuttle vehicle was lined up with runway and flew directly over ground transponder B<sub>1</sub> at an approximate altitude of 8000 feet. Landing velocity was approximately 320 feet/second.

GROUND TRANSPONDER LOCATIONS IN VICINITY OF LANDING SITE



APPROACH AND LANDING ERROR MODEL AND ASSUMPTIONS

Results of two cases are being presented. The error models are presented in the attached chart. To perform the navigation analysis, a 19 state variable recursive filter was employed. The state variables are:

- 3 Position
- 3 Velocity
- 3 Gyro Bias
- 3 Accelerometer Bias
- 1 Altimeter Bias
- 3 Platform Misalignment
- 3 Range Biases

APPROACH AND LANDING ERROR  
MODEL AND ASSUMPTIONS

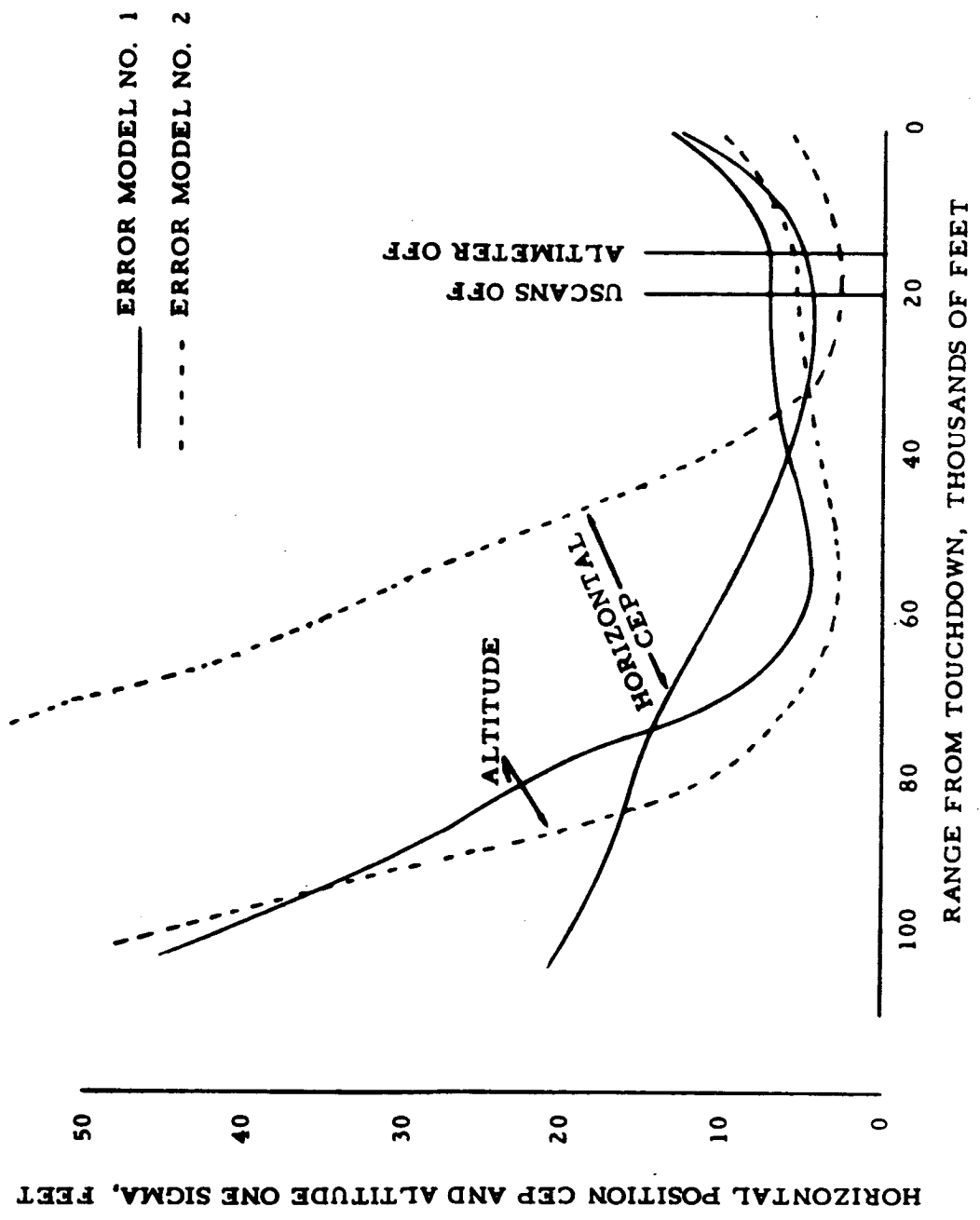
GYRO DRIFTS:  $0.1^\circ/\text{HR.}$ , ( $.05^\circ/\text{HR.}$ ) 3600 SEC. CORRELATION TIME  
ACCELEROMETER BIASES:  $100 \mu\text{g}$  ( $50 \mu\text{g}$ )  
BAROMETRIC ALTIMETER: 50 FT. BIAS, 0.5% RANDOM WHITE  
RANGE MEASUREMENTS: 10 (50) FT. BIAS, 5 (1.6) FT. RANDOM WHITE  
UPDATE RATE: 1/SEC.  
INITIAL HORIZONTAL POSITION UNCERTAINTIES: 1 N. MI.  
INITIAL ALTITUDE UNCERTAINTY: 1000 FT.  
INITIAL VELOCITY UNCERTAINTIES: 10 FPS ALL AXES  
INITIAL HORIZONTAL PLATFORM TILT UNCERTAINTIES: 0.25 DEG.  
INITIAL AZIMUTH UNCERTAINTY: 1 DEG.

\*NUMBERS IN PARENTHESES INDICATE ERROR MODEL NO. 2

POSITION ESTIMATION ERROR HISTORY  
(TRANSPONDER CONFIGURATION B)

Position errors are as shown in the following chart. To test the system severely, no information was obtained from the multilateration system within 20,000 feet of the runway. This was done for illustration purposes only and does not reflect an operational restriction. The altimeter was also turned off at 18,000 feet so that from this point on the navigation was performed with the IMU only. Final velocity errors were approximately 0.2 feet/second. It is anticipated that optimum ground system configuration and operational utilization would enable removal of the radar altimeter used for landing flare.

POSITION ESTIMATION ERROR HISTORY  
(TRANSPONDER CONFIGURATION B)





## ASCENT NAVIGATION ANALYSIS

To achieve very precise orbit insertion cutoff conditions (as required on some Air Force missions), range measurements from the ground transponders may be used to update the inertial navigation system. An analysis has been conducted using the following models to evaluate the navigation improvement potential.

406 second ascent trajectory into a 50 x 100 n. mi. orbit

39 degree orbit inclination

IMU system characterized by 0.05°/hr gyros (1σ)

Ranging system noise

1.6 Ft. (1σ)

Ranging system bias

50 Ft. (1σ)

Tropospheric refraction

5 N units (1σ)

Transponder location error  
(Cherry Point and Wallops Island only)

30 Ft. (1σ)

Navigation update rate

1 range measurement/  
10 seconds

Four different cases were considered which are distinguished by the number of ground transponders employed. Information from ground transponders was not used when the elevation angle was less than 5 degrees. The navigation accuracy presented is valid at thrust termination. As anticipated, little aid in cross range navigation is obtained from one transponder located at the launch site. Use of out of plane transponders significantly reduces the navigation errors. Utilization of radio aided inertial navigation in this manner during the launch phase implies that IMU quality will be dictated by other phases or operations during the mission.

ASCENT NAVIGATION ANALYSIS

NAVIGATION SYSTEM	ONE SIGMA STATE ERRORS AT THRUST TERMINATION								
	POSITION (FT)			VELOCITY (FT/SEC)			UP		
	DR	CR	UP	DR	CR	UP	DR	CR	UP
INERTIAL NAVIGATION ONLY	420	1310	730	2.5	7.9	5.8			
INERTIAL NAVIGATION AND TRANSPONDER AT CAPE KENNEDY	50	1300	240	0.4	7.9	1.9			
INERTIAL NAVIGATION AND TRANSPONDERS AT CAPE KENNEDY AND CHERRY POINT	50	140	140	0.3	1.0	1.1			
INERTIAL NAVIGATION AND TRANSPONDERS AT CAPE KENNEDY, CHERRY POINT, CARTER CAY AND WALLOPS ISLAND	40	60	60	0.2	0.6	0.7			

TRACKING COULD CONTINUE AFTER INSERTION FROM CHERRY POINT AND WALLOPS ISLAND.

## OBJECTIONS TO USCANS

The following objections to USCANS have been voiced. Comments for these objections are presented.

1. Use of USCANS implies landing at a limited number of sites. This objection arises because commercial aviation landing fields do not use multilateration systems for landing or S-band for voice. Thus, in the event of an emergency, such fields could not be used for automatic landing or voice communication.  
  
Considerable amounts of money will be spent on the Shuttle to provide the desired redundancy and reliability levels to obviate such emergencies. To further penalize the shuttle system to be compatible with FAA facilities is not cost effective. Compromise positions do exist, however, such as using multilateration for landing navigation and UHF for voice. This technique does not show all the cost advantages indicated above but is an attractive alternative.
2. Special equipment or procedures must be employed for ferry operations. This objection is similar to the first one in that automatic landing and voice will, in general, not be available at the airports used for ferrying if USCANS is employed. In response, it is suggested that strap-on equipment be employed for this mode just as other equipment (air breathing engines) will be employed. This approach is consistent with not penalizing or compromising the operational system because of the ferry requirements.
3. Time and operations required to qualify a new landing system (multilateration) may be incompatible with the Shuttle Program.  
  
This objection is currently being investigated and preliminary results indicate that no problems exist. It should be noted that, currently, landing tests with a multilateration system are being conducted at NASA Ames.

OBJECTIONS TO USCANS (CONTINUED)

4. System is potentially incompatible with TDRS. USCANS has been defined based upon current operational concepts. It is true that, if TDRS is employed and USCANS is not compatible with it, a better solution to the problem may exist. On the other hand, it may be that USCANS is still the best answer. These items will not be resolved until the TDRS concept is more fully defined and the design definitized.

OBJECTIONS TO USCANS

- USE OF USCANS IMPLIES LANDING AT A LIMITED NUMBER OF SITES
- SPECIAL EQUIPMENT OR PROCEDURES MUST BE EMPLOYED FOR FERRY OPERATIONS
- TIME AND OPERATIONS REQUIRED TO QUALIFY A NEW LANDING SYSTEM (MULTILATERATION) MAY BE INCOMPATIBLE WITH SHUTTLE PROGRAM
- SYSTEM IS POTENTIALLY INCOMPATIBLE WITH TDRS

## SUMMARY

An S-band system has been proposed for all voice, data, and RF navigation functions. This system is compatible with the MSFN and SCN. High performance is achievable with this system, and inherent advantages of redundancy and all runway landing capability are obtained. The most significant feature of this approach is the program cost savings obtained primarily from reducing the amount of onboard equipment and antennas.

## SUMMARY

- ALL S-BAND - VOICE, DATA, NAVIGATION
- COST EFFECTIVE SYSTEM
- HIGH PERFORMANCE - INHERENT REDUNDANCY
- COMPATIBLE WITH EXISTING MSFN AND SCN

**MICROWAVE TRAVELING WAVE TUBE AMPLIFIERS  
FOR SPACE COMMUNICATIONS SYSTEMS \***

Bruce M. Kendall

NASA-Langley Research Center  
Hampton, Virginia

**INTRODUCTION**

The need has become apparent for efficient and reliable high power microwave amplifiers for the Space Shuttle communications and tracking subsystems. Microwave output powers on the order of several tens of watts are required to reduce vehicle communications antenna size and achieve the most desirable subsystem configuration. Since microwave traveling wave tube amplifiers (TWTAs) have not only demonstrated high power capability for space application but also have the inherent characteristic of wide bandwidth, their selection to meet the need was in order. The wide bandwidth capability is most desirable for high data rate transmission of information. An additional factor, most important in the selection of a spacecraft amplifier, was that considerable improvement in the overall dc to rf conversion efficiency had been made under NASA sponsorship. The conversion efficiency is important to the spacecraft battery and/or solar panel requirements. The development of microwave traveling wave tube amplifiers specifically designed for Space Shuttle communications with Intelsat IV satellites could be accomplished utilizing presently available technology. Much of this technology is the result of several NASA-Langley sponsored programs to improve the conversion efficiency of space-type S-band traveling wave tubes and develop X-band traveling wave tubes for the international space research band as 8.4 GHz.

NASA studies on advanced data relay and tracking satellites have shown that improved communications performance can be obtained by extension of present microwave tube technology to  $K_u$ -band. Increasing the frequency of communications from C-band to  $K_u$ -band allows for an even wider bandwidth to permit the use of increased data rate transmission.

\*This report was not presented at the conference.

## BACKGROUND

The state-of-the-art traveling wave tubes which are presently available for spacecraft application have all evolved either directly or indirectly from NASA-Langley sponsored research programs and are summarized in table I. Initial improvement in the overall conversion efficiency of an S-band traveling wave tube (TWT) produced the WJ-274. This improvement was obtained by use of the overvoltage condition and by a tighter control on fabrication techniques and materials. The WJ-274, which achieved an efficiency generally in excess of 35 percent, represented quite an improvement at that time over other space-type TWT's whose efficiencies were in the 25-percent range. Its application to the Saturn program was achieved by NASA-Huntsville. Further improvement in the efficiency of the WJ-274 TWT was achieved under an additional research program resulting in efficiencies on the order of 42 percent using a positive tapered helix. Utilization of this improvement by Huntsville and JPL produced higher power versions of the WJ-274 with efficiencies greater than 40 percent at 50 watts (WJ-448) and greater than 45 percent at 100 watts (WJ-395). These tubes were developed as an advanced version of the Saturn TWT and the relay communications amplifier for Voyager, respectively. Designation of the space research band at 8.4 to 8.5 GHz prompted the development of a 20-watt X-band traveling wave tube amplifier for communications and telemetry use by NASA and other qualified users. The TWT (219-H) of the amplifier package has an efficiency of 35 percent. A list of the important characteristics of the complete TWTA (1153-H) unit is given in table II, and a photo of the amplifier package is shown in figure 1. The 1153-H X-band TWTA is presently on life test at NASA-Langley and has currently accumulated in excess of 9600 hours operation time with no change in output power.

## DEVELOPMENT PROGRAM

### Objectives

The objective of the Langley program is to develop microwave traveling wave tube amplifiers for the communications subsystem of the Space Shuttle vehicle utilizing presently available techniques and tube designs.

### Approach

An engineering model (breadboard) of a C-band 100-watt traveling wave tube amplifier will be developed for the Space Shuttle communications subsystem and will be compatible with Intelsat IV. The main specifications of this tube are given in table III. This initial phase (phase I) will also produce firm specifications for amplifier design and assure compatible transmitter and antenna requirements. These specifications will also be used to generate the second phase of the development program (phase II), which will be the fabrication of

units for flight qualification and life testing. Upon completion of the C-band TWTA development phases, the same technology will be used to develop TWTA's at  $K_u$ -band for utilization of the Tracking Data Relay Satellite. This development will also involve subsequent qualification and life testing of flight units.

#### Current Status

Phase I of the C-band TWTA development program is presently being pursued. NASA-Langley contract number NAS1-10417 was awarded to the Hughes Electron Dynamics Division on November 10, 1970, to develop the engineering model of the 100-watt C-band TWTA. The TWT has been designated the 279 H, and the TWTA package is identified as the 1222 H. The unit will operate at approximately 100-watt rf output with less than 270-watt dc input and 42-percent efficiency over the band of 5.925 to 6.425 GHz. A hybrid cooling system consisting of heat pipes backed by a parallel conduction path for most efficient performance and maximum reliability will be used. Also the use of multi-stage depressed collectors is being investigated. At the present time, the electrical design of the first two tubes is complete, and the mechanical design is near completion. Their construction will be accomplished in the near future. The program schedule calls for all the experimental TWT's to have been built and tested by September 1971. Delivery of the complete TWTA package is expected near the end of 1971. However, final specification for the TWTA will be available before that time to allow the initiation of phase II of the development program for the fabrication of flight hardware for qualification and life testing.



TABLE I

STATE-OF-THE-ART SPACE TWT'S\*

<u>TWT</u>	<u>FREQUENCY</u>	<u>POWER</u>	<u>EFFICIENCY</u>	<u>PROGRAM</u>
WJ - 274	S-BAND	20 WATTS	35 PERCENT	SATURN
WJ - 448	S-BAND	50 WATTS	40 PERCENT	SATURN
WJ - 395	S-BAND	100 WATTS	45 PERCENT	VOYAGER
219 - H	X-BAND	20 WATTS	35 PERCENT	X-BAND TELEMETRY

\* CONDUCTION COOLED

TABLE II

X-BAND 20W TWTA SPECIFICATIONS

20-WATT RF OUTPUT POWER

8400 - 8500 MHz

30-dB MIN. RF POWER GAIN

10-MHz B. W.

35-PERCENT MIN. EFF. (TWT)

85-PERCENT MIN. EFF. (PS)

TUBE WT.: 2-LB MAX.

TUBE SIZE: 80-IN<sup>3</sup> MAX.

PS WT: 5-LB MAX.

PS SIZE: 130-IN<sup>3</sup> MAX.

TABLE III

C-BAND TWT SPECIFICATIONS

<b>FREQUENCY RANGE</b>	- 5.925 TO 6.425 GHz
<b>SATURATED OUTPUT POWER</b>	- 100 ± 10 WATTS
<b>RF GAIN</b>	- > 33 dB AT SATURATION
<b>EFFICIENCY</b>	- TO BE MAXIMIZED
<b>COOLING</b>	- CONDUCTION
<b>LIFE</b>	- > 14,000 HOURS

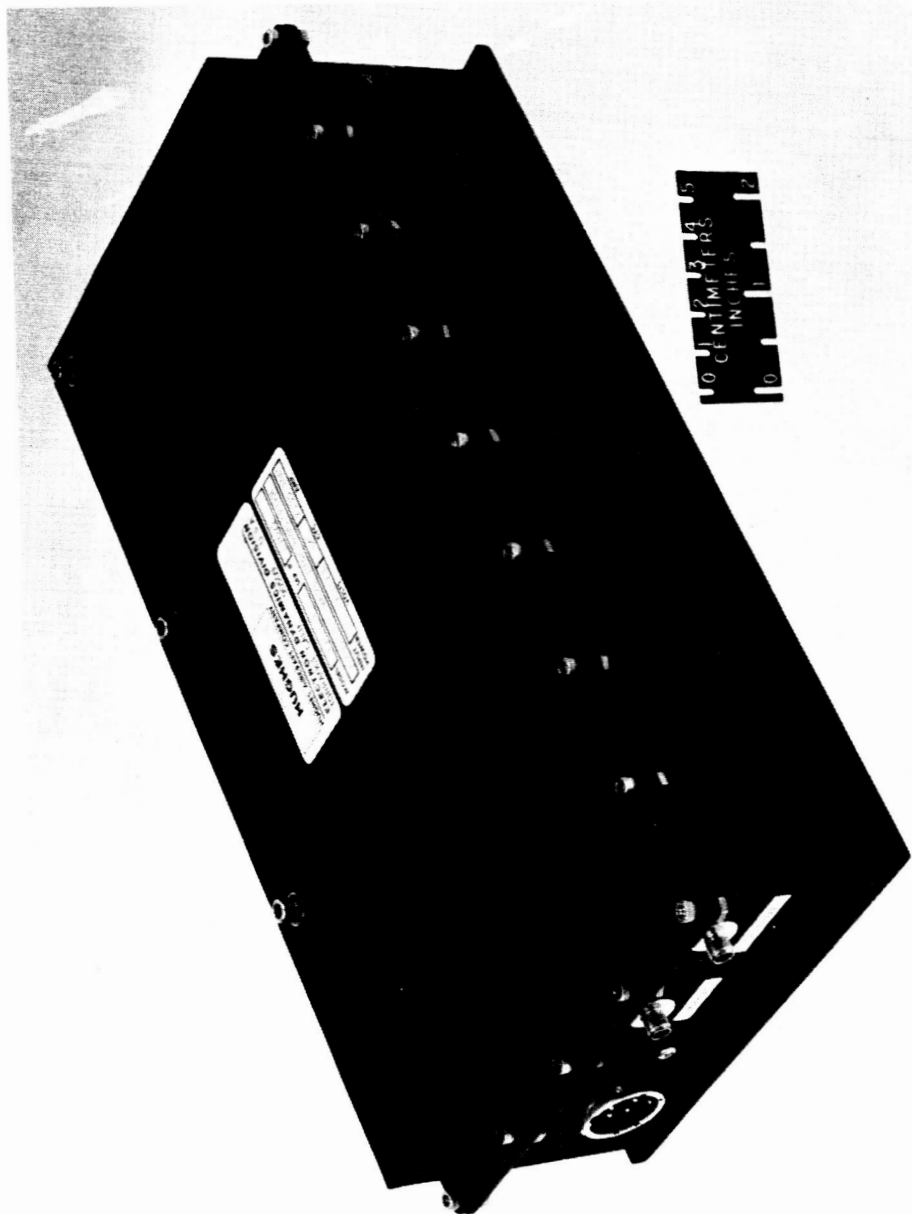


Figure 1. - The X-band 20-watt traveling wave tube amplifier.